



**“Development Of Three-Dimensional Liver
Models For Drug Development And
Therapeutical Applications.”**

**“Entwicklung eines dreidimensionalen Lebermodells
für Wirkstoffentwicklung und therapeutische
Anwendungen”**

Doctoral thesis for a doctoral degree
at the Graduate School of Life Sciences,
Julius-Maximilians-Universität Würzburg,
Section: Biomedicine

submitted by

Sarada Devi Ramachandran

from

Salem, India

Würzburg 2015



Submitted on: February 19th 2015

Office stamp

Members of the *Promotionskomitee*:

Chairperson: Prof. Dr. Thomas Dandekar

Primary Supervisor: Prof. Dr. Heike Walles

Supervisor (Second): Prof. Dr. Frank Edenhofer

Supervisor (Third): Dr. Joris Braspenning

Supervisor (Fourth): Dr. Bernhard Müntst

Date of Public Defence: May 05th 2015

Date of Receipt of Certificates:

Abstract

Primary human liver cells such as hepatocytes when isolated and cultured in 2D monolayers, de-differentiate and lose their phenotypic characteristics. In order to maintain the typical polygonal shape of the hepatocytes and their polarization with respect to the neighbouring cells and extra cellular matrix (ECM), it is essential to culture the cells in a three-dimensional (3D) environment. There are numerous culturing techniques available to retain the 3D organization including culturing hepatocytes between two layers of collagen and/or Matrigel™ (Moghe et al. 1997) or in 3D scaffolds (Burkard et al. 2012).

In this thesis, three different 3D hepatic models were investigated.

1. To reflect the *in vivo* situation, the hepatocytes were cultured in 3D synthetic scaffolds called Mimetix®. These were generated using an electrospinning technique using biodegradable polymers. The scaffolds were modified to increase the pore size to achieve an optimal cell function and penetration into the scaffolds, which is needed for good cell-cell contact and to retain long-term phenotypic functions. Different fibre diameters, and scaffold thicknesses were analyzed using upcyte® hepatocytes. The performance of upcyte® hepatocytes in 3D scaffolds was determined by measuring metabolic functions such as cytochrome P450 3A4 (CYP3A4) and MTS metabolism.

2. Apart from maintaining the hepatocytes in 3D orientation, co-culturing the hepatocytes with other non-parenchymal cell types, such as liver sinusoidal endothelial cells (LSECs) and mesenchymal stem cells (MSCs), better reflects the complexity of the liver. Three different upcyte® cell types namely, hepatocytes, LSECs and MSCs, were used to generate 3D liver organoids. The liver organoids were generated and cultured in static and dynamic conditions. Dynamic conditions using *Quasi-vivo*® chambers were used to reflect the *in vivo* blood flow. After culturing the cells for 10 days, the structural orientation of cells within the organoids was analyzed. Functional integrity was investigated by measuring CYP3A4 activities. The organoids were further characterized using *in situ* hybridization for the expression of functional genes, albumin and enzymes regulating glutamine and glucose levels.

3. An *ex vivo* bioreactor employing a decellularized organic scaffold called a “Biological Vascularized Scaffold” (BioVaSc) was established. Jejunum of the small intestine from pigs was chemically decellularized by retaining the vascular system. The vascular tree of the

BioVaSc was repopulated with upcyte[®] microvascular endothelial cells (mvECs). The lumen of the BioVaSc was then used to culture the liver organoids generated using upcyte[®] hepatocytes, LSECs and MSCs. The structural organisation of the cells within the organoids was visualized using cell-specific immunohistochemical stainings. The performance of liver organoids in the BioVaSc was determined according to metabolic functions (CYP3A4 activities).

This thesis also addresses how *in vitro* models can be optimized and then applied to drug development and therapy.

A comprehensive evaluation was conducted to investigate the application of second-generation upcyte[®] hepatocytes from 4 donors for inhibition and induction assays, using a selection of reference inhibitors and inducers, under optimized culture conditions. CYP1A2, CYP2B6, CYP2C9 and CYP3A4 were reproducibly inhibited in a concentration-dependent manner and the calculated IC₅₀ values for each compound correctly classified them as potent inhibitors. Upcyte[®] hepatocytes were responsive to prototypical CYP1A2, CYP2B6, CYP2C9 and CYP3A4 inducers, confirming that they have functional AhR, CAR and PXR mediated CYP regulation. A panel of 11 inducers classified as potent, moderate or non-inducers of CYP3A4 and CYP2B6 were tested. Three different predictive models for CYP3A4 induction, namely the Relative Induction Score (RIS), AUC_u/F₂ and C_{max,u}/Ind₅₀ were analyzed. In addition, PXR (rifampicin) and CAR-selective (carbamazepine and phenytoin) inducers of CYP3A4 and CYP2B6 induction, respectively, were also demonstrated.

Haemophilia A occurs due to lack of functional Factor VIII (FVIII) protein in the blood. Different types of cells from hepatic and extrahepatic origin produce FVIII. Supernatants harvested from primary LSECs were evaluated for the presence of secreted functional FVIII. In order to increase the FVIII production, different upcyte[®] endothelial cells such as blood outgrowth endothelial cells (BOECs), LSECs and mvECs were transduced with lentiviral particles carrying a FVIII transgene. Also, to reflect a more native situation, primary mvECs were selected and modified by transducing them with FVIII lentivirus and investigated as a potential method for generating this coagulation factor.

Zusammenfassung

Primäre humane Leberzellen wie beispielsweise Hepatozyten de-differenzieren und verlieren ihre phänotypischen Eigenschaften, wenn man sie isoliert und in 2D Monoschicht kultiviert. Um die typische, polygonale Form der Hepatozyten und ihre Polarisation gegenüber den benachbarten Zellen und der extrazellulären Matrix (EZM) zu erhalten, ist es essentiell die Zellen in einer dreidimensionalen (3D) Umgebung zu kultivieren. Es sind zahlreiche Techniken verfügbar, um die 3D-Organisation zu erhalten wie beispielsweise die Kultur von Hepatozyten zwischen zwei Schichten von Kollagen und/oder MatrigelTM (Moghe et al. 1997) oder in einem 3D Gerüst (Burkard et al. 2012).

In dieser Arbeit wurden 3 verschiedene, hepatische 3D Modelle untersucht.

1. Um die *in vivo* Situation widerzuspiegeln, wurden die Hepatozyten in einer synthetischen 3D Matrix namens Mimetix[®] kultiviert. Diese wurde aus biologisch abbaubaren Polymeren elektrogenesponnen. Die Matrix wurde modifiziert indem die Poren vergrößert wurden, um eine optimale Besiedlung des Zellgerüsts und dadurch eine gesteigerte Zellfunktionalität zu erreichen. Dies wird sowohl für die Ausbildung von Zell-Zell-Kontakten wie auch für den Erhalt der phänotypischen Funktionen über einen längeren Zeitraum hin benötigt. Unterschiedliche Faserdurchmesser und Matrixschichtdicken wurden mittels upcyte[®] Hepatozyten analysiert. Die Leistungsfähigkeit der upcyte[®] Hepatozyten wurde durch die Messung metabolischer Funktionen bestimmt, wie beispielsweise Cytochrom P450 3A4 (CYP3A4) und MTS Metabolismus.

2. Abgesehen vom Erhalt der 3D Orientierung der Hepatozyten, hilft eine Ko-Kultur der Hepatozyten mit anderen nicht-parenchymalen Zelltypen wie beispielsweise lebersinusoidalen Endothelzellen (LSECs) und mesenchymalen Stammzellen (MSCs) die Komplexität der Leber darzustellen. Drei unterschiedliche upcyte[®] Zelltypen, das heißt Hepatozyten, LSECs und MSCs wurden eingesetzt, um 3D Leberorganoide zu generieren. Die Leberorganoide wurden in statischen Zellkulturbedingungen generiert und dynamischen Bedingungen kultiviert. Durch den *Quasi-vivo* Bioreaktor als dynamisches Zellkultursystem wurde der Blutstrom *in vivo* wiedergespiegelt. Nach einer Kulturdauer von 10 Tagen wurde die strukturelle Organisation der Zellen innerhalb der Organoide analysiert. Die Funktionalität wurde durch Messungen der CYP3A4 Enzymaktivitäten untersucht. Darüber hinaus wurden

die Organoide mittels *in situ* Hybridisierung auf die Expression von funktionalen Genen, Albumin sowie Glutamin- und Glukose-regulierende Enzyme hin analysiert.

3. Es wurde ein *ex vivo* Bioreaktor etabliert, dessen Grundlage ein dezellularisiertes Zellgerüst namens ‚Biological Vascularized Scaffold‘ (BioVaSc) bildet. Hierfür wurde das Jejunum vom Dünndarm des Hausschweins chemisch dezellularisiert, wobei gleichzeitig das vaskuläre System erhalten wurde. Dieses Gefäßsystem wurde dann mit upcyte[®] humanen dermalen mikrovaskulären Endothelzellen (HDMECs) besiedelt. Das Lumen der BioVaSc wurde anschließend benutzt, um darin die Leberorganoide, die aus den upcyte[®] Hepatozyten, LSECs und MSCs generiert wurden, zu kultivieren. Die strukturelle Organisation der Zellen innerhalb der Organoide wurde mittels zell-spezifischer, immunhistochemischer Färbungen visualisiert. Die Funktionalität der Leberorganoide in der BioVaSc wurde anhand von metabolischer Aktivität (CYP3A4 Enzymaktivität) bestimmt.

Diese Arbeit beschäftigt sich auch mit der Fragestellung, wie *in vitro* Modelle optimiert werden können, um sie schlussendlich für die Wirkstoffentwicklung aber auch zelltherapeutische Anwendungen einsetzen zu können.

Eine umfassende Untersuchung wurde durchgeführt, um zu untersuchen inwiefern 4 Donoren der zweiten upcyte[®] Hepatozyten Generation für Inhibitions- und Induktionsstudien geeignet sind. Hierfür wurde eine Auswahl an Referenzinhibitoren und – induktoren unter optimierten Kulturbedingungen eingesetzt. CYP1A2, CYP2B6, CYP2C9 und CYP3A4 konnten durch den Einsatz von Inhibitoren reproduzierbar, konzentrationsabhängig inhibiert werden und die berechneten IC₅₀-Werte klassifizierte jede Substanz korrekt als potenten Inhibitor. Upcyte[®] Hepatozyten reagierten auf proto-typische CYP1A2-, CYP2B6-, CYP2C9- und CYP3A4-Induktoren, wodurch eine funktionale AhR-, CAR- und PXR-vermittelte Regulation der jeweiligen CYP Enzymaktivität bestätigt werden konnte. Eine Sammlung von 11 Induktoren, die für CYP2B6 sowie CYP3A4 als potent, moderat potent und nicht potent klassifiziert sind wurden analysiert. Drei unterschiedliche Vorhersage-Modelle für die Induktion von CYP3A4 wurden analysiert, der (I) ‚Relative Induction Score (RIS)‘, (II) AUC₀/F₂ und (III) C_{max,u}. Darüber hinaus wurden PXR-selektive (Rifampicin) und CAR-selektive (Carbamazepin und Phenytoin) Induktoren für eine CYP3A4- und CYP2B6-Induktion gezeigt.

Hämophilie A tritt aufgrund eines Mangels an funktionalem Faktor VIII protein (FVIII) im Blut auf. Verschiedene Zelltypen hepatischen und extra-hepatischen Ursprungs produzieren FVIII. Zellkulturüberstände von primären LSECs wurden abgenommen und hinsichtlich des Vorhandenseins von sekretiertem FVIII untersucht. Um die FVIII-Produktion zu steigern, wurden unterschiedliche upcyte[®] Endothelzellen, wie beispielsweise ‚blood outgrowth endothelial cells‘ (BOECs), LSECs und HDMECs, mit lentiviralen Partikeln, die ein FVIII Transgen tragen transduziert. Um eine nativere Situation widerzuspiegeln, wurden primäre HDMECs ausgewählt, um sie mittels Transduktion von FVIII lentiviralen Partikeln zu modifizieren, zu selektionieren und im Anschluss hinsichtlich ihres Potentials zur Bildung des Koagulationsfaktors FVIII zu untersuchen.

List of abbreviations

°C	Degrees Celsius
Fig	Figure
AB	Antibody
BioVaSc	Biological Vascularized Scaffold
BOEC	Blood outgrowth endothelial cells
BSA	Bovine serum albumin
CYP	Cytochrome
DAPI	4',6-Diamidino-2-Phenylindole, Dilactate
DMEM	Dulbecco's modified Eagle medium
DMSO	Dimethyl sulfoxide
DNA	Deoxyribonucleic acid
dNTP	Deoxynucleotide Triphosphates
EC	Endothelial cells
ECGM	Endothelial cell growth medium
ECM	Extra Cellular Matrix
EDTA	Ethylenediaminetetraacetic acid
FBS	Fetal bovine serum
fc	Final concentration
FVIII	Factor VIII
h	Hour
HE	Hematoxylin -eosin
HGF	Hepatocyte growth factor
HGM	Upcyte [®] hepatocyte growth medium
HPM	Upcyte [®] hepatocyte high performance medium
HSA	Human serum albumin
HSC	Hepatic stellate cell
HUVEC	Human umbilical
IgG	Immunoglobulin G
iPSC	Induced pluripotent stem cell
kGr	Kilo Gray
KHB	Krebs-Henseleit buffer
LB	Luria Bertani
LSEC	Liver sinusoidal endothelial cell

M	Molar
min	Minute
mM	Millimolar
mm	Millimeter
ml	Milliliter
MOI	Multiplicity of infection
mvEC	Microvascular endothelial cells
MTS	3 - (4,5- Dimehtylthiazol -2-yl) -2,5- diphenyl- -tetrazolium bromide
μ	Microns
NaCl	Sodium chloride
PBS	Phosphate buffer saline
PCR	Polymerase chain reaction
PD	Population doubling
PLLA	Poly(L-lactic acid)
rFVIII	Recombinant FVIII
RNA	Ribonucleic acid
rpm	Rounds per minute
RT	Room temperature
SDS	Sodium dodecyl phosphate
SOC	Super Optimal broth with Catabolite repression
VEGF	Vascular endothelial growth factor
vWF	Von Willebrand factor
e.g.	Example
2D	Two-dimensional
3D	Three-dimensional

Table of content

I. Abstract	III
II. List of Abbreviations.....	VIII
1. Introduction	1
1.1 Structure and physiology of the liver	1
1.2 Hepatic cells and their function	2
1.2.1 Hepatocytes	2
1.2.2 Liver sinusoidal endothelial cells	3
1.2.3 Microvascular endothelial cells	4
1.2.4 Mesenchymal stem cells	5
1.3 <i>In vitro</i> hepatic models	6
1.3.1 Advantages and disadvantages	6
1.3.2 Upcyte [®] technology.....	7
1.4 Co-culture	9
1.5 Development of 3D models (2D vs 3D).....	10
1.6 Tissue Engineering	10
1.6.1 Cells used for bioreactors	11
1.6.2 Scaffolds used for bioreactors	11
1.6.3 Bioreactors	14
1.7 Application of hepatic models	14
1.7.1 Drug metabolism and drug-drug interactions	14
1.7.2 Use of upcyte [®] hepatocytes for CYP induction and inhibition assays.....	16
1.8 Therapy- Hemophilia A	17
1.8.1 Hemophilia A	17
1.8.2 Factor VIII.....	18
1.8.3 Biosynthesis of FVIII	20
1.8.4 Blood coagulation.....	20
1.8.5 Current treatment for haemophilia A	21
1.8.6 Other treatments	22
1.9 Aim of the thesis	24

2. Materials & Methods	25
2.1 Materials	25
2.1.1 Disposable material	25
2.1.2 Chemicals	25
2.1.3 Solutions and buffers.....	28
2.1.4 Cells and cell culture medium	30
2.1.5 Antibodies	31
2.1.6 Kits	31
2.1.7 Primers.....	31
2.1.8 General technical equipment and devices	32
2.2 Methods.....	34
2.2.1 Cell culture techniques	34
2.2.1.1 Incubation conditions	34
2.2.1.2 Thawing and plating of cryopreserved cells	34
2.2.1.3 Subculturing of cells	35
2.2.1.4 Cell counting and viability determination	35
2.2.1.5 Cryopreservation	36
2.2.2 Hepatic models – 3D Mimetix [®] scaffolds	36
2.2.2.1 Upcyte [®] hepatocyte in Mimetix [®] scaffolds	36
2.2.2.2 Confocal analysis	37
2.2.2.3 Metabolic activity in Mimetix [®] scaffolds	37
2.2.2.4 Upcyte [®] hepatocyte culture viability and protein content	37
2.2.3 Hepatic models – Liver organoids.....	37
2.2.3.1 Generation of liver organoids	37
2.2.3.2 Liver organoids in <i>Quasi-vivo</i> [®] System	38
2.2.3.3 Scalability to different well formats	39
2.2.3.4 Immunocytochemistry in 2D monolayer.....	39
2.2.3.5 Immunohistochemistry of 3D organoid	39
2.2.3.6 <i>In situ</i> hybridization	40
2.2.4 Hepatic models – Liver organoids/BioVaSc	40
2.2.4.1 Explantation of BioVaSc	40
2.2.4.2 Decellularization of BioVaSc	41
2.2.4.3 Colonization of the BioVaSc	42
2.2.4.4 Liver organoids in BioVaSc	43

2.2.5 Application of hepatic models - inhibition/induction study	43
2.2.5.1 Pre-culture conditions for inhibition/induction study	43
2.2.5.2 Upcyte [®] hepatocyte inhibition assays	44
2.2.5.3 Upcyte [®] hepatocyte induction assays measuring CYP activities	44
2.2.5.4 Calculation and curve fitting	45
2.2.5.5 Metabolite analysis by HPLC	46
2.2.6 Application of hepatic models - Haemophilia Therapy	47
2.2.6.1 Cloning of FVIII gene	47
2.2.6.2 Generation of entry clones	48
2.2.6.3 Transformation and plasmid extraction	48
2.2.6.4 Double restriction hydrolysis of entry clone	49
2.2.6.5 Generation of expression clones	49
2.2.6.6 Double restriction hydrolysis of expression clone	50
2.2.6.7 Midi preparation and sequencing of FVIII transgene	50
2.2.6.8 Lentiviral production and Transduction	51
2.2.6.9 Titration of virus supernatant	52
2.2.6.10 Transduction	53
2.2.6.11 Cytotoxicity curve analysis	53
2.2.6.12 Tube formation assay	54
2.2.6.13 FVIII analysis from different cell cultures	54
3. Results	56
3.1 Hepatic models – 3D Mimetix[®] scaffolds.....	56
3.1.1 Effect of scaffold fibre thickness on cell penetration.....	56
3.1.2 Viability and growth of upcyte [®] hepatocytes in 3D scaffolds.....	57
3.1.2.1 Scaffold thickness: 100 µm vs 50 µm	57
3.1.2.2 Fibre thickness: 4 µm vs 6 µm	58
3.1.3 Functionality of upcyte [®] hepatocytes in Mimetix [®] scaffolds.....	59
3.1.3.1 Scaffold thickness: 100 µm vs 50 µm	60
3.1.3.2 Fibre thickness: 4 µm vs 6 µm	60
3.1.4 Viability: donor-to-donor variation	61
3.1.4.1 Functionality: donor-to-donor variation	62
3.2 Hepatic models – Liver organoids	63
3.2.1 Generation of liver organoids using upcyte [®] and primary cells.....	63

3.2.2	Generation of liver organoids using only upcyte [®] cells	65
3.2.3	Histology of organoids maintained in static culture.....	66
3.2.4	Scalability	66
3.2.5	Adaptation of liver organoid in dynamic culture	67
3.2.6	Histology of liver organoids maintained in dynamic culture	67
3.2.7	Immunocytochemistry in 2D monolayers	68
3.2.8	Immunohistochemistry of 3D organoid	68
3.2.9	<i>In situ</i> hybridizations	70
3.2.10	Liver organoid architecture	71
3.2.11	Metabolic activity	72
3.3	Hepatic models – BioVaSc/Organoids.....	73
3.3.1	Liver organoids in BioVaSc	73
3.3.2	Immunostaining of organoids in BioVaSc	74
3.3.3	Immunostaining for BioVaSc/organoid vascularization	75
3.4	Application of hepatic models - CYP inhibition.....	76
3.4.1	Culture optimisation for inhibition studies	76
3.4.2	CYP inhibition studies.....	80
3.5	Application of hepatic models - CYP induction studies.....	82
3.5.1	CYP induction responses in upcyte [®] hepatocytes	82
3.5.2	Prediction models for <i>in vivo</i> CYP3A4 induction.....	83
3.5.3	CAR and PXR selective induction of CYPs	85
3.6	Application of hepatic models – Haemophilia Therapy	88
3.6.1	FVIII expression in primary LSECs	89
3.6.2	Generation of lentiviral FVIII construct	89
3.6.2.1	Cloning of FVIII gene	89
3.6.2.2	Cloning of expression clone	90
3.6.2.3	Sequencing of FVIII gene	91
3.6.3	Viral titer determination	91
3.6.4	FVIII expression in upcyte [®] mvECs	91
3.6.5	Transduction of primary mvECs	92
3.6.5.1	Characterization of primary mvECs	93
3.6.5.2	FVIII expression in primary mvECs	94

4. Discussion	95
4.1 Hepatic models – 3D Mimetix[®] scaffolds	96
4.1.1 Confocal analysis of upcyte [®] hepatocytes.....	96
4.1.2 Scaffold thickness and fiber diameter	96
4.1.3 Donor-to-donor variation	97
4.2 Hepatic models – Liver organoids and in BioVaSc	99
4.2.1 3D liver model- Liver organoid.....	99
4.2.2 Generation of liver organoid	100
4.2.3 Organoids cultured in a dynamic system	101
4.2.4 Immunostainings of liver organoid and in BioVaSc	102
4.2.5 Liver organoid architecture	104
4.2.6 Metabolic activity.....	105
4.2.7 Vascularization.....	105
4.3 Application of hepatic models - CYP inhibition	106
4.3.1 Culture optimisation	106
4.3.2 CYP activities in different donors of upcyte [®] hepatocytes	107
4.3.3 Inhibition and induction studies	108
4.3.4 Prediction models for <i>in vivo</i> CYP3A4 induction.....	109
4.3.5 CAR and PXR selective induction of CYPs	109
4.4 Application of hepatic models – Haemophilia Therapy	110
4.4.1 Calculation for FVIII dosage.....	111
4.4.2 Proof-of-Principle.....	111
4.4.3 Cloning of FVIII gene	112
4.4.4 Lentiviral Transduction	113
4.4.5 FVIII production in upcyte [®] cells	113
4.4.6 FVIII production in primary mvECs	115
5. Summary	117
6. Appendix	117
6.1 Sequence of FVIII	117
6.2 References	119
6.3 Figures	138
6.4 Tables	140

6.5 Publications.....	141
6.6 Curriculum Vitae	143
6.7 Affidavit.....	144
6.8 Acknowledgement	145

INTRODUCTION

1. Introduction

1.1 Structure and physiology of the liver

The liver is a multifunctional organ that plays a vital role in removing harmful chemicals/xenobiotic compounds from the body and is therefore often the first organ to suffer potentially adverse consequences. The liver is organized into irregular polygonal lobules, 60% of which are composed of parenchymal cells arranged in cords (hepatocytes) and 20% are sinusoidal cells such as LSECs and Kupffer cells (hepatic macrophages). The remaining 8-10% of the liver contain perisinusoidal cells (hepatic stellate cells) (Gu & Manautou, 2012) Portal triads are situated between the adjacent lobules at the corners (Figure 1). Each of the portal triads are comprised of hepatic portal vein, hepatic artery and bile duct. Approximately 75% of the liver is vascularized with blood derived from the hepatic portal vein and the remaining is from the hepatic artery. The hepatic portal vein carries deoxygenated/venous blood from spleen, gastrointestinal tract and other associated organs into the liver lobules (Godoy et al. 2013).

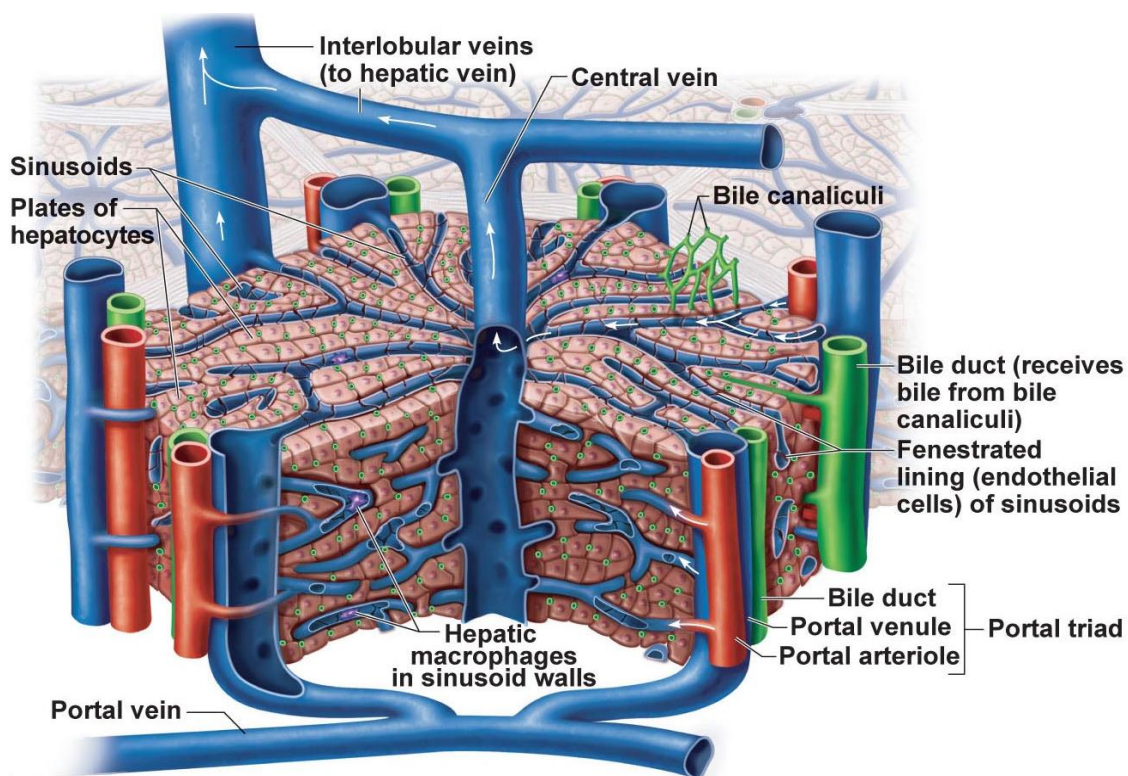


Figure 1: Portal triads comprised of the bile duct (green), hepatic portal vein (blue) carrying the deoxygenated blood from intestinal tract and hepatic artery (orange) supplying oxygenated blood. The central vein runs through the centre of lobules and drains blood from the lobules (Picture source: Pearson Education Inc.)

INTRODUCTION

1.2 Hepatic cells and their function

1.2.1 Hepatocytes

The liver is made of structural subunits called liver lobules. Liver lobules are composed of hepatocyte cords or also known as cords. Hepatocytes are the epithelial cells of the liver that are cuboidal in shape with 20-30 μm in diameter. The average life span of a hepatocyte is five months. Hepatocytes contain a large proportion of rough endoplasmic reticulum and mitochondria. Binucleated hepatocytes are common in adult hepatocytes but tetraploidy or polyploidy is also a common feature of hepatocytes (Elaut et al. 2006). Hepatocytes arranged in plates are exposed to vascular channels (sinusoids) to facilitate the exchange of various compounds. The surface that contacts adjacent hepatocytes is termed as lateral face. Bile canaliculi are formed between two adjacent hepatocytes joined by tight junctions. The thin capillaries of bile canaliculi merge to form bile ducts that transport bile secreted by hepatocytes. The space of Disse separates the hepatocytes from the sinusoids. Microvilli on the hepatocytes extend into space of Disse to increase the absorption of components from the plasma. Hepatic plates radiate from the central vein towards the periphery and they are organized in three different zones, namely the periportal, transitional and perivenous zones. Based on their location, there is a microdiversity in the hepatocytes, which can be detected using *in situ* hybridization (Gebhardt 1992; Jungermann & Kietzmann 1996).

Hepatocytes play a key role in the metabolism and elimination of xenobiotic and endogenous compounds. Therefore, the function of hepatocytes has strong influence on the pharmacokinetics and toxicity of drugs (Boyer, Wright and Manns 2011). Cultures of isolated primary human hepatocytes contain a broad complement of CYPs and transporter proteins. Hepatocytes are the main site of glycogen storage, from where it is broken down into glucose and released directly into the blood stream. Hepatocytes play an important role in gluconeogenesis (formation of glucose from non-carbohydrate substrates) and in the deamination of amino acids to urea. Hepatocytes produce the majority of circulating plasma proteins (e.g. albumin), lipoproteins, non-immune alpha and beta-globulins and glycoproteins, including fibronectin. Hepatocytes also synthesize protease inhibitors (e.g. α_1 -antitrypsin, antithrombin), blood coagulation factors (e.g. fibrinogen, factor V, VII and VIII), modulators of immune complexes and inflammation (e.g. complement C3) (Boyer, Wright and Manns 2011). Hepatocytes also synthesize the lipid portion of lipoprotein and cholesterol. Lipids are also stored in the liver and are present in various sizes of lipid droplets.

INTRODUCTION

1.2.2 Liver sinusoidal endothelial cells

The physiology of the liver is maintained by a special category of endothelial cell called liver sinusoidal endothelial cells (LSECs (Aird 2007)). Nearly 50% of the non-parenchymal hepatic cells are comprised of LSECs. Hepatocytes are separated from the circulating blood by LSECs and the latter are responsible for hepatic microcirculation (Oda et al. 2003). LSECs from the liver form a fenestrated monolayer but they do not possess a basement membrane (Braet & Wisse 2002). The main function of LSECs is to control the exchange of materials between liver parenchyma and blood. LSECs also express a variety of scavenger receptors and as a result, constitute the most important scavenger system in the body (Smedsrød et al. 1990). Together with hepatocytes, these cells play a vital role in the uptake, metabolism and elimination of xenobiotic compounds; therefore, these cells are also termed “scavenger endothelial cells”. LSECs are also antigen-presenting cells because they take up antigens by receptor-mediated endocytosis and/or phagocytosis. These antigens are presented to lymphocytes by a similar mechanism to that of dendritic cells. LSECs suppress selectively the proliferation of cells by producing interferon-gamma. This activity promotes the outgrowth of Th2 cells to express interleukin-4 (Klugewitz et al. 2002). LSECs play a vital role in immune tolerance of the liver without activating T-cells (Limmer et al. 2000). Regulatory T-cells producing interleukin-4 and interleukin-10 develop, when T-cells interact with LSECs (Bertolino et al. 2002; Limmer & Knolle 2001).

LSECs secrete a coagulation factor, FVIII that plays a vital role in the intrinsic coagulation pathway (Do et al. 1999). LSECs are one of the most difficult cells to maintain *in vitro* whilst retaining their phenotypic character. Upon isolation of LSECs from liver, they lose their typical phenotypic function (Smedsrød et al. 1994). Rat LSECs, when cultured alone, lose the expression of SE-1 antigen (biomarker) and the expression of CD31 is increased. Increased expression of CD31 in LSECs indicates the cells have low proliferation capacity and reach senescence (DeLeve et al. 2004). However, co-culture of LSECs with primary hepatocytes suppresses CD31 expression (DeLeve et al. 2004) and enhances SE-1 expression (Hwa et al. 2007). Optimal configuration of LSECs was retained for 2 weeks when they were co-cultured with hepatocytes and fibroblasts (March et al. 2009).

INTRODUCTION

1.2.3 Microvascular endothelial cells

The lumen of blood vessels is lined with endothelial cells (ECs), which helps to maintain the vessel wall permeability. ECs exhibit cobblestone-like morphology when cultured in collagen-coated plates in 2D. ECs also play an important role in maintaining the blood pressure by vasodilation or vasoconstriction (Cosentino & Volpe 2005). These cells also contribute to blood coagulation processes such as thrombosis and fibrinolysis (Wiel et al. 2006; Chen & López 2005). ECs harbour Weibel palade bodies that store growth factors, cytokines and hormones (Hannah et al. 2002; Michaux & Cutler 2004; van Mourik et al. 2002). Under physiological conditions, ECs play a vital role in vascular biology (Wiel et al. 2006) and angiogenesis i.e. sprouting of new blood vessels from an already existing vessel system. Receptors present on the surface of the cells are activated by angiogenic growth factors such as vascular endothelial growth factor (VEGF). The ECs degrade the underlying basement membrane and migrate through it. This migration and invasion is one of the characteristic features of endothelial cells. The migrated ECs proliferate into the surrounding extracellular matrix to form vascular sprouts (Brown et al. 1998; Bergers & Benjamin 2003). The specialized ECs that are present in the edge of vascular sprouts form a vascular network by connecting to the adjacent sprouts (Gerhardt & Betsholtz 2005; Szekanecz & Koch 2005).

ECs are highly heterogeneous, for example: the gene expression between the human umbilical vein endothelial cells (HUVECs) and mvECs differ markedly. Likewise, the ECs that line arterial blood vessels differ significantly from those that line the veins. Like other cell lines, ECs isolated from tumours differ significantly from healthy ECs with regards to the marker profile (Charalambous et al. 2005). ECs isolated from different locations of the body express different surface proteins such as von Willebrand factor (vWF) (Turner et al. 1987). mvECs isolated from organs, such as the brain and lungs, also express different cell surface markers (Grau et al. 1997). The availability of a pure population of human mvECs is always a rate-limiting step (Scott & Bicknell 1993) and they tend to lose the phenotypic markers when placed into culture (Unger et al. 2002). In addition, mvECs have a low proliferating potential (Kim & von Recum 2008) which underlines the need for alternative cell sources.

INTRODUCTION

1.2.4 Mesenchymal stem cells

Mesenchymal stem cells (MSCs) are a type of adult stem cell that has a self-renewal capacity (Williams et al. 2011) and a wide differentiation potential (Meirelles et al. 2009). The major cell types derived from MSCs include osteogenic or bone cells (Brighton et al. 1992; Marsell & Einhorn 2011), cartilage cells or chondrocytes (Brighton & Hunt 1991) and adipocytes or fat cells. MSCs can also differentiate into neuron-like cells (Jiang et al. 2002), muscle cells and skin cells (Figure 2). Amniotic fluid is a rich source of MSCs. Among the cells collected during amniocentesis, 1 in 100 cells are MSCs. Morphologically; the MSCs resemble fibroblasts, that is they have long and thin cell bodies with prominent nuclei. MSCs can be obtained from the stroma of bone marrow, as well as non-marrow tissues such as fat tissue, adult stroma, corneal tissue (Branch et al. 2012) and from the deciduous pulp of teeth (Batouli et al. 2003). Isolated MSCs are easy to culture as they adhere to standard plastic culture plates. Bone deterioration is one of the challenging steps with aged patients (Smith et al. 2011; Wang et al. 2013). As MSCs have the potential to differentiate into osteoblasts, these cells are used for bone regeneration (Wang et al. 2013). Fat tissue is easily obtained from patients, and thus naturally lends itself as a source of autologous cells, especially since it has a low risk of tumorigenesis (Cao et al. 2005; Kuo et al. 2008) and can overcome immune-rejection. MSCs express specific antigen expressing markers on their cell surface, such as CD73, CD90 and CD105 (M et al. 2011).

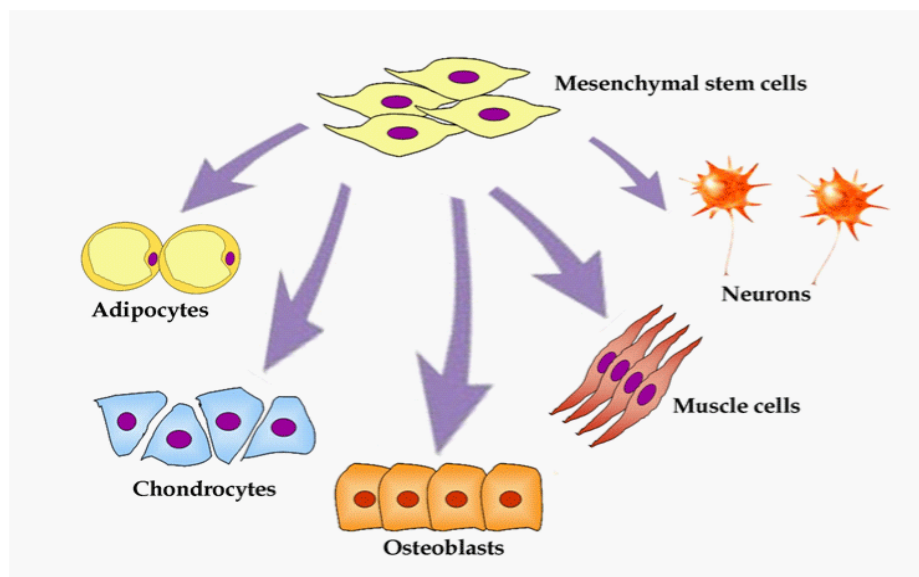


Figure 2: Differentiating ability of MSCs includes adipocytes, chondrocytes, bone cells or osteoblast, muscle cells and neurons (Picture- Meregalli et al., 2011)

INTRODUCTION

1.3 *In vitro* hepatic models

1.3.1 Advantages and disadvantages

There are numerous cell types that have been used as an alternative to primary human hepatocytes. These, together with their advantages and disadvantages, are summarized in Table 1. One of the most important disadvantages, especially relevant to screening assays, is the lack of a sufficient source of cells.

Table 1. Summarizes *in vitro* hepatic models, its advantages and disadvantages.

Hepatic model(s)	Advantages	Disadvantages
Primary human hepatocytes	<ul style="list-style-type: none">- Gold standard for the evaluation of human-specific drug properties such as metabolic fate, drug-drug interactions and drug toxicity (Hewitt et al. 2007; Li & Jurima-Romet 1997).	<ul style="list-style-type: none">- Bulk availability is rate limiting and the cells are mostly derived from non-healthy donor.- Donor-to-donor variability.- Limited life span and difficulties in maintaining a differentiated phenotype in <i>in vitro</i> culture.- Results in reduced expression of some of the transporters (Guguen-Guillouzo & Guillouzo 2010).
Immortalized cell line (HepG2, Hep3B, Huh7, Fa2N4, HepaRG)	<ul style="list-style-type: none">- Unlimited life span provides high availability.- Stable phenotype, logistically easy to culture and maintain, serves as alternative <i>in vitro</i> models for screening purposes (Godoy et al. 2013).- In Fa2N4 cells, the induction response to major CYPs is high (Youdim et al. 2007).- In HuH7 cells, increased level of CYP3A4 activity after treatment for several weeks is observed (Sivertsson et al. 2010).	<ul style="list-style-type: none">- Represent only a single donor and some may lack sufficient responsiveness to CYP3A4 inducers (Westerink & Schoonen 2007).- In Fa2N4, basal enzyme activities are low (Sinz et al. 2008) and CAR expression is lacking (Hariparsad et al. 2008).- In HuH7 cells, phenotypic changes occur in the absence of DMSO (Sivertsson et al. 2010).- In HepaRG cells, CYP expression is generally lower than freshly isolated primary cells, except CYP3A4 (Kanebratt & Andersson 2008).

INTRODUCTION

<p>iPS derived hepatocytes</p>	<ul style="list-style-type: none"> - iPS cells can be expanded and directly differentiated into hepatocytes in <i>in vitro</i> cultures. - Positive for many hepatic functions such as albumin secretion, glycogen storage, drug metabolism, drug transportation and lipogenesis (Rashid et al. 2010; Si-Tayeb et al. 2012). - Used to study familial hereditary cholestasis, α1-antitrypsin deficiency and glycogen storage disease type 1a (Ghodsizadeh et al. 2010). 	<ul style="list-style-type: none"> - Large quantities of iPS-derived hepatocytes are required for large scale toxicity screening. - Variability in functionality and gene expression between batches (Godoy et al. 2013). - Variability in iPS differentiation procedures such as differences in iPS reprogramming (Kim et al. 2010) and epigenetic cell memory (Ohi et al. 2011; Ruiz et al. 2012).
<p>Embryonic stem cell-derived hepatocytes</p>	<ul style="list-style-type: none"> - Secrete albumin, store glycogen, uptake low-density lipoprotein, and possess inducible CYP activity. - Express adult liver cell markers tyrosine aminotransferase, CYPs (7A1, 3A4 and 2B6) (Cai et al. 2007). 	<ul style="list-style-type: none"> - Cells possess high levels of telomerase activity and, when injected in mice, they generate teratoma and eventually teratocarcinoma (Przyborski 2005).
<p>Animal hepatocytes model (mouse, rat and dog)</p>	<ul style="list-style-type: none"> - Bulk availability. - Used for <i>in vitro</i> toxicological studies. 	<ul style="list-style-type: none"> - Species-dependent metabolism and physiology prevents an accurate prediction of toxicity to humans for many drugs (Martignoni et al. 2006). - Rat hepatocytes lose Ntcp mRNA expression and taurocholate uptake capacity on collagen-coated plates (Liang et al. 1993) and Oatp transporters (Rippin et al. 2001).

An ideal *in vitro* model would possess the advantages of both cell lines and primary cells: easy access and availability, the ability to proliferate, a consistent response to inducers with the ability to study donor variation, and expression of cell-specific enzymes and drug transporters that most closely resemble fresh primary cells (Sinz et al. 2008).

INTRODUCTION

1.3.2 Upcyte[®] technology

The proliferative capacity of hepatocytes differs under different conditions, such that they do not proliferate *in vitro* but they do have significant proliferative capacity *in vivo*, particularly after partial hepatectomy. A technology called “upcyte[®]” technology has been developed to address the gap between the primary cells and cell lines. Human upcyte[®] cells are derived from primary human cells by transducing them with proliferation inducing genes through lentiviral transduction (Patent WO 2009/030217) (Burkard et al. 2012). The proliferating cells are referred to as “upcyte[®]” cells. The upcyte[®] cells have the potential to undergo a finite number of cell divisions i.e. 20-40 population doublings, without losing adult primary cell phenotype (e.g. adult cell markers). After this additional number of population doublings, upcyte[®] cells enter into senescence (Scheller et al. 2012). The extended proliferation capacity between primary cells (up to 10-25 population doublings) and cell lines (> 60 population doublings) represent that they are not immortalized.

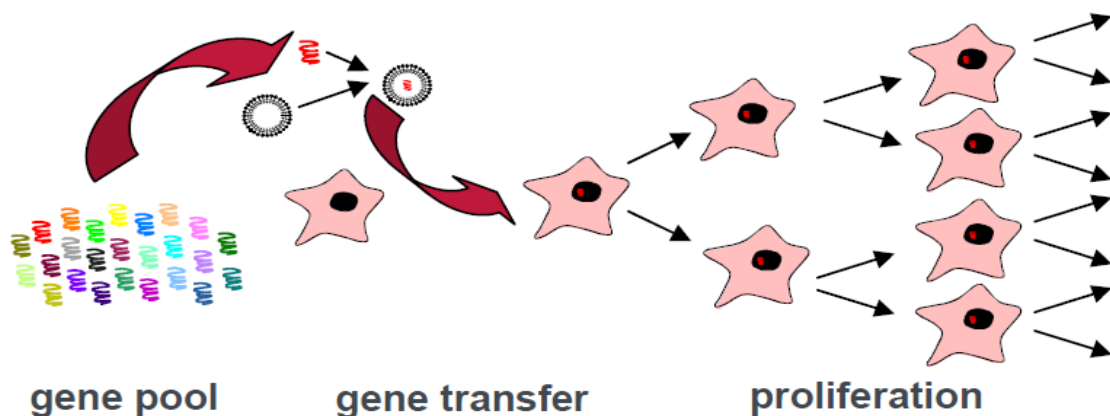


Figure 3: Primary human cells are induced to proliferate by a pool of cellular and viral genes using upcyte[®] technology. This circumvents the cell cycle control mechanism, which results in controlled cell growth without immortalising them. The proliferating cells are selected and referred to as “upcyte[®]” cells.

After application of the upcyte[®] process to primary cells, they are seeded at a low density which allows the cells to proliferate. The non-transduced cells have a limited lifespan and eventually detach from the culture dish culture, so a selection process is not necessary. When the upcyte[®] technology is applied to single vial of primary human hepatocytes, more than 12 billion upcyte[®] hepatocytes can potentially be generated. Using the upcyte[®] technology, first and second generation upcyte[®] hepatocytes were generated. Second generation upcyte[®] hepatocytes were generated by refining the upcyte[®] process (Levy et al-Manuscript submitted) enabling the cells for higher CYP activities compared with the first generation

INTRODUCTION

hepatocytes. These upcyte[®] hepatocytes also exhibit a primary cell phenotype such as adult cell markers, albumin production, phase 1 and 2 activities (Burkard et al. 2012). Upcyte[®] technology can be applied to different cells types e.g. mvEC (Scheller et al. 2012), LSECs (Nörenberg 2013) etc. and to different batches of cells, so that a range of primary cells from multiple donors can exhibit an extended lifespan. The cells are simple to use and offer the possibility of generating large amounts of cells from a single donor. Thus the upcyte[®] technology allows for sufficient quantities of different cell types to be produced for human-based cell screening studies and are particularly suitable for the standardization of *in vitro* test systems and in tissue engineering (Scheller et al. 2012).

1.4 Co-culture

The liver is one of the most complex organs of the body and is composed of different cell types. Therefore, co-culturing hepatocytes with other hepatic cell types will better reflect the *in vivo* cellular composition than cultures containing only hepatocytes. In line with this, it has been shown that adult primary rat hepatocytes co-cultured with fibroblasts or other liver epithelial cells increase their function, such as albumin secretion (Guguen-Guillouzo et al. 1983).

LSECs and hepatocytes arrange themselves in close proximity in the liver. Cross talk between these two cell types plays an important role in their function and differentiation. For example, hepatocytes co-cultured with endothelial cells at a high concentration of vascular endothelial growth factor (VEGF) stimulated cell migration and neoangiogenesis (Shimizu et al. 2005). Cell polarization is important for hepatocytes to retain the correct distribution of transporters in the sinusoidal, basolateral and canalicular membranes (Berthiaume et al. 1996). Therefore, an *in vitro* liver model employing the co-culture of hepatocytes with endothelial cells is supposed to be beneficial. Hepatocytes co-cultured with MSCs derived from bone marrow have been shown to maintain their proliferative capacity and metabolic function (Shi et al. 2011). Co-culture with more than one cell type has also been investigated to develop 3D liver organoid-like structures. In these studies, human derived induced pluripotent stem cells (iPSCs), MSCs and human umbilical vein endothelial cells (HUVECs) were co-cultured on Matrigel[™] and subsequently self-organized to form liver bud-like structures (Takebe et al. 2013). Co-cultures with more than two cell types coupled with 3D environments offers a promising model for many applications e.g. for toxicology tests (Godoy et al. 2013).

INTRODUCTION

1.5 Development of 3D models (2D vs 3D)

Although there are numerous advantages of using 2D cultures, the cells cultured in conventional monolayer (2D) are not reflective of the physiological situation. This is because the organization of cells *in vivo* is 3D. When cells are cultured over a long time in conventional 2D monolayers on a rigid surface, they do not accurately recapitulate the structure of the cells *in vivo*. In addition, many of the *in vivo* functions and physiology of living tissues are lost in 2D cultures, making it difficult to evaluate key cellular and molecular events. One such example is hepatocytes: hepatocytes cultured in 2D lose their skeletal integrity, which results in a flattening of their morphology. They also tend to de-differentiate and lose their phenotypic characters (Gómez-Lechón et al. 1998) that results in down-regulation of phase I and II enzymes (Clayton & Darnell 1983). Ideally, the polygonal shape of the hepatocytes should be retained in addition to their polarization with respect to their neighbouring cells to maintain optimal parenchymal functions (Bissell et al. 1987). The 3D orientation of the hepatocyte can be retained *in vitro* using a number of culturing techniques (Pampaloni et al. 2009). When hepatocytes are cultured using a sandwich technique in which the cell monolayer is overlaid with an extra cellular matrix e.g. collagen, CYP activities and culture viability were reported to be increased (Dunn et al. 1991). Other 3D formats include the use of hydrogels such as MatrigelTM (Moghe et al. 1997), ExtracelTM (Ranucci et al. 2000), synthetic scaffolds (Burkard et al. 2012; Bokhari et al. 2007) and biological scaffolds (Mertsching et al. 2005).

1.6 Tissue Engineering

The term “tissue engineering” was introduced in 1987 during a meeting of the National Science Foundation. Tissue engineering has evolved from the collaborative application of life science and engineering to understand the fundamental relationship of structure and function of the biological substitutes (Bell et al. 1981). The main aim of tissue engineering is to overcome the disadvantage of conventional treatment for organ transplantation or tissue repair. When there is an essential need to replace an organ, the major challenge is the availability of a suitable organ donor. Therefore, the application of the principles of tissue engineering to synthesize an organ or tissue *ex vivo* using patients’ cells (autologous) will reduce the dependency of supplementary therapies (Patrick, C. W., Jr., Mikos, A. G., and McIntire, L. 1998). Products of tissue engineering are not only interesting as grafts but also can provide a test system for validating drugs.

INTRODUCTION

The main essential components of tissue engineering are cells, scaffolds and bioreactors.

1.6.1 Cells used for bioreactors

Tissue engineering offers the advantage of generating donor specific grafts; however, the availability of cells required to develop such organs grafts is difficult. There are numerous cell types and techniques that have been explored in order to meet the demand for bulk supplies of cells (Parenteau & Hardin-Young 2002; Germain et al. 2002; Faustman et al. 2002). These include adult, embryonic and foetal stem cells, as well as cells modified with nuclear transplantation. The major problem with progenitor cells was the absence of specific adult cell markers (Faustman et al. 2002). Autologous cells naturally offer a big advantage (Germain et al. 2002) over cells from a different donor. External organs such as skin can easily be treated with skin substitutes using autologous cells, which is minimally invasive. Also, such skin grafts integrate with the host tissue (Parenteau & Hardin-Young 2002). By contrast, it is not possible to obtain a sufficient quantity of autologous cells from internal organs (liver) from small biopsies. Allogeneic and xenogeneic cells can be used as an alternative source; however, both can cause problems such as disease transmission (Germain et al. 2002) and adverse immune responses (Germain et al. 2002; Faustman et al. 2002). Despite these difficulties, tissue engineering has been shown to be successful in certain cases such as generation of cardiac tissue (Sefton 2002; Taylor 2002). Isolation of cells and their expansion has been achieved *ex vivo* with subsequent *in vivo* differentiation. However, the process of developing an entire organ under laboratory conditions using bioreactor is still difficult (Hirschi et al. 2002; Niklason et al. 2002).

1.6.2 Scaffolds used for bioreactors

1.6.2.1 Electrospinning scaffolds

The electrospinning technique consists of three main components: a pipette tip or extruder, a high voltage power supply and a collecting plate. The biodegradable polymer solution is extruded at a constant rate through the pipette tip or nozzle at high DC voltage (10 to 100 kV) at room temperature under atmospheric conditions (Liang et al. 2007). The voltage is applied to the dissolved polymer solvents, which induce a charge on the surface of the liquid droplet. When the voltage is high enough, the hemispherical surface of the fluid elongates due to the electric field and a “Taylor cone” is established. On increasing the applied voltage further, a jet of whipping polymer solution is ejected from the Taylor cone (Bhardwaj & Kundu 2010). The charged liquid jet is attracted to the earthed collector, which is positioned at a fixed

INTRODUCTION

distance from the needle. During this process the solvent evaporates from the polymer solution, leaving dry polymer fibres on the collector. As a result, fibrous scaffold with varying pore size (in microns) and large surface area-to-volume ratio is obtained (Figure 4).

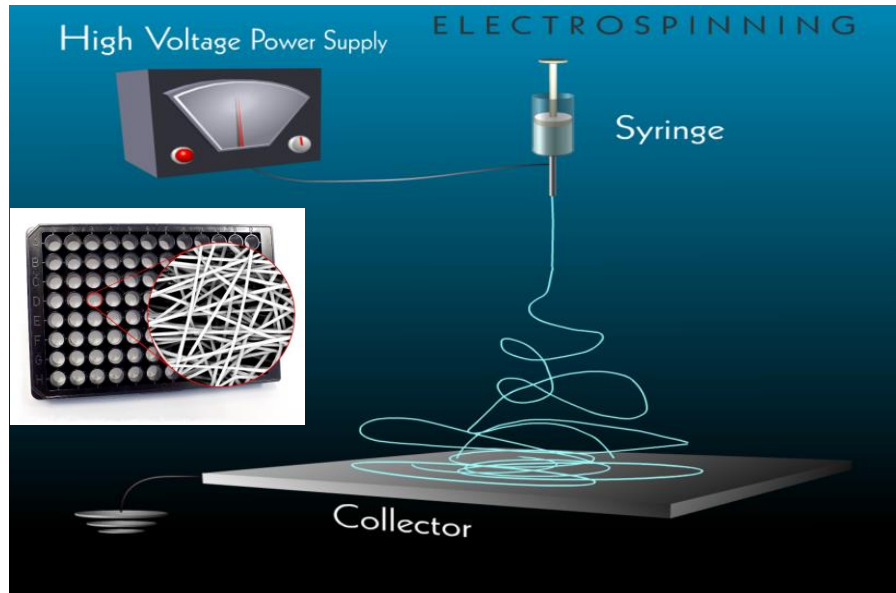


Figure 4: Schematic diagram of the set up of electrospinning apparatus representing the polymer solution extruded through spinneret by a high voltage power supply and a collecting plate at the bottom (Picture source: The Electrospinning company, UK)

Scaffolds generated using this electrospinning technique have advantages in disciplines such as tissue engineering or in regenerative medicines (Wang et al. 2011). Electrospinning is ideal for the preparation of fibrillar networks with controlled diameters of down to tens or hundreds of nanometers (Reneker & Chun 1996) and 3D organization, which resembles that of the natural ECM. Culturing the cells in these types of scaffolds provides a 3D architecture, which resembles the physiological situation (Singh et al. 2011). Electrospun scaffolds are spun with nano or micrometer fibres. Electrospun fibres are composed of natural or synthetic biodegradable polymers such as poly-L-lactic acid (PLLA) or poly-L/D- lactic acid (PLDLA). When the microenvironment of each cell type is considered, the spinning conditions such as voltage, flow rate and polymer concentration can be altered to produce scaffolds with appropriate different fibre diameters/pore sizes (Liang et al. 2007). In order to increase the cell adherence to the scaffolds, they have been modified to carry negatively charged groups such as (COOH) (Lin et al. 2004). Other surface functionalization of scaffolds with sugar residues, such as galactose, can also enhance cell growth and functionality (Yin et al. 2003).

INTRODUCTION

1.6.2.2 Biological Vascularized Scaffold

Scaffolds have also been derived from natural materials and used to culture cells to retain their 3D architecture. For example, rat liver lobes have been decellularized and subsequently used to culture hepatocytes on heparin layers (Bao et al. 2011). A similar model has been developed using the jejunum of the small intestine from pigs. In this technique, a 10 to 15 cm length of “biological vascularized matrix (scaffold)” (BioVaSc) is chemically decellularized without disrupting the vascular system (capillaries, arterial inflow and venous outflow) lined with collagen I (Mertsching et al. 2005). The vascular system and the lumen portion of the BioVaSc are sterilized by gamma irradiation. Colonization of the vascular system can be achieved using mvECs (Scheller et al. 2012). Together with the vascular system, the lumen of the BioVaSc can also be populated with cells (Mertsching et al. 2005; Mertsching et al. 2009). As the vasculature in the BioVaSc is preserved, it provides a physiologically relevant model for optimized nutrient and mass transfer, which supports better viability and functionality of the cells.

When more than one cell type was co-cultured in the BioVaSc, it was possible to generate vascularized tissue models (Schanz et al. 2010). As graft rejection is a major problem in organ transplantation, it is possible to generate such organ models using autologous cells. This will also obviate the need for long-term immune-suppressive drugs to prevent rejection. A BioVaSc populated with upcyte[®] mvECs was able to pre-vascularize the decellularized matrix (Scheller et al. 2012). During transplantation, vasculature of BioVaSc can be connected to the existing vasculature of the patient to prevent necrosis. Decellularized BioVaSc seeded with autologous muscle cells and fibroblasts were shown to successfully repair a tracheal defect in 58-year old man (Macchiarini et al. 2004). In addition to this, the BioVaSc has also been used as a tumour test system (Moll et al. 2013; Thude et al. 2008); a model for pharmacological, toxicological, cosmetic screening (Mertsching & Walles 2009); heart valves (Bader et al. 1998); as well as blood vessels (Robotin-Johnson et al. 1998) and trachea models (Schanz et al. 2009). These multiple applications of the BioVaSc emphasises the increasing the demand for vascularized test system.

INTRODUCTION

1.6.3 Bioreactors

Bioreactors have been used in many fields, such as in fermentation, effluent treatment and food processing industries (Martin & Vermette 2005). In the early 1980s, bioreactors were used to produce vaccines and drugs using animal cell culture. More sophisticated bioreactors are computer-controlled to regulate the physiological conditions (Hutmacher & Singh 2008; Mertsching & Hansmann 2009). The bioreactors used in tissue engineering today were evolved from these early models.

The main aim of using bioreactors in tissue engineering is to:

- Enhance uniform distribution of cells throughout the 3D scaffolds (Holy et al. 2000). The cells that are cultured in 3D scaffolds, harbours fewer cells at the centre of the scaffolds. Due to non-uniform distribution of cells in the scaffolds, development of 3D tissue-like structures *in vitro* is challenging (Cartmell et al. 2003). Also, cells in the middle of these scaffolds enter apoptosis or senescence because they are devoid of nutrients. The cells are further encouraged to produce ECM (Freed & Vunjak-Novakovic 1997), which further blocks the flow of nutrients to the cells in the centre.
- Ensure optimal concentration of gas and nutrient circulation (Sutherland et al. 1986). The nutrient gradient is higher in the periphery of scaffolds than the centre, which influences the cells to move away from the centre (Goldstein et al. 2001).
- Provide mass transport to the tissue and mechanical stimulus to encourage cell differentiation e.g. MSCs (Altman et al. 2002).

The main aim of using bioreactors in tissue engineering is not only to develop implantable grafts using autologous cells but also to develop *ex vivo* devices in case of non-availability of autologous cells or compatible organ (Mazariegos et al. 2001). Also as these 3D grafts reflect the *in vivo* situation, they can be used for drug research (Griffith & Naughton 2002).

1.7 Application of hepatic models

1.7.1 Drug metabolism and drug-drug interactions

When a drug is administered orally, it enters the portal circulation into liver. These xenobiotic chemical substances will undergo biotransformation - a process in which insoluble parent compounds are converted to excretable water-soluble metabolites by xenobiotic metabolizing enzymes (XMEs). Although CYP enzymes represent more than 50 isozymes, 90% of marketed drugs are metabolized by six different CYPs, namely CYP1A2, CYP2C19, CYP2C9, CYP2D6, CYP2E1, and CYP3A4. Among these, the two CYPs that play a vital

INTRODUCTION

role in drug metabolism are CYP3A4 and CYP2D6 (Ogu & Maxa 2000). In this thesis, four CYP isoforms (CYP1A2, CYP2C9, CYP3A4, CYP2B6) and their inducers and inhibitors for 4 donors of upcyte[®] hepatocytes have been characterized. CYP2D6 was not analyzed as the upcyte[®] hepatocytes express negligible amount of CYP2D6 to be detected by HPLC analysis. Drugs and other xenobiotics may be metabolized by phase I and phase II enzymes before they are eliminated from the body. CYPs are responsible for major phase I reactions that biotransform the parent compound via oxidation or reduction or hydrolysis into hydrophilic compounds or reactive metabolite (Figure 5). Kidneys will excrete the resulting hydrophilic metabolites. Reactive metabolites that are not cleared from the circulation can be further metabolized by phase II enzymes via conjugation reactions (mostly by transferase enzymes).

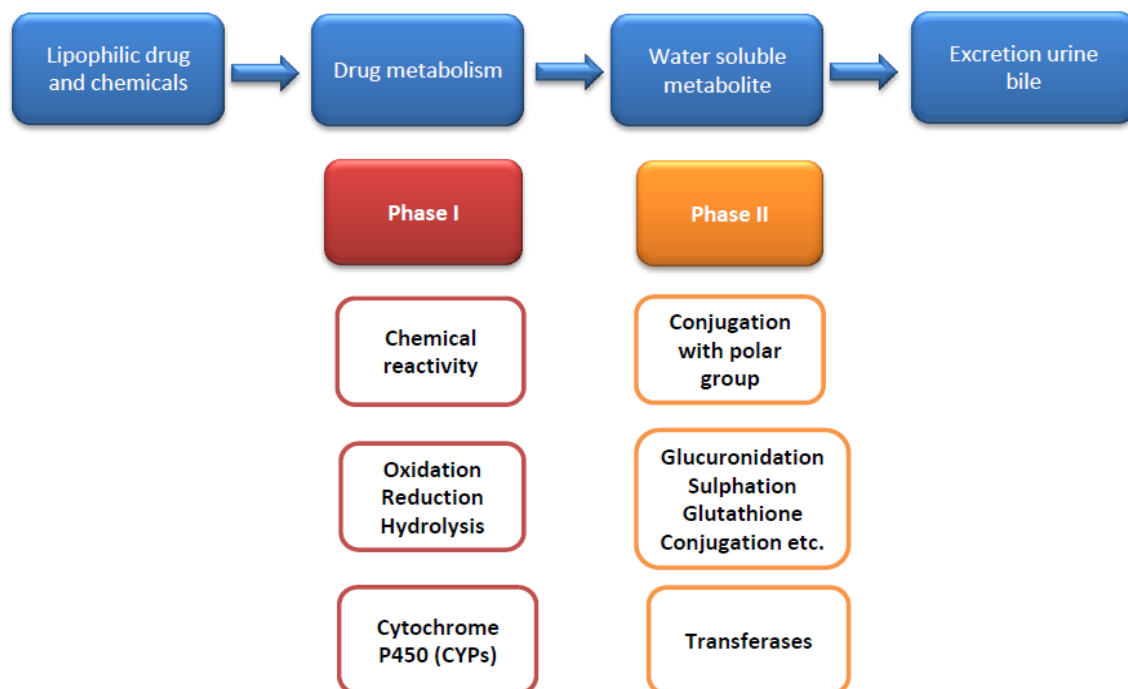


Figure 5: Schematic representation of phase I und phase II metabolism.

Most fatal drug-drug interactions are due to XME inhibition (Zhou et al. 2007). As a result, drugs that inhibit XMEs are a major concern in drug development and in the clinic such that potent inhibitor drugs are either de-selected from development or require labelling once on the market. In addition to inhibition, drugs that induce XMEs are also avoided in drug development since increased levels of XMEs increase the metabolic clearance of drugs, causing the plasma levels to drop below the therapeutic threshold. A well-known example of this is the rejection of organs in recipient patients also taking rifampicin in combination with the CYP3A4 metabolized immunosuppressant, cyclosporine (Zylber-Katz 1995). Therefore, it is important to identify potential CYP inducers at an early stage in drug screening.

INTRODUCTION

1.7.2 Use of upcyte[®] hepatocytes for CYP induction and inhibition assays

The upcyte[®] hepatocytes generated using the refined technology were tested to determine whether they could be used in drug-drug interaction screening assays. Although first generation upcyte[®] hepatocytes exhibited phase 2 activities that were comparable to those in freshly isolated human hepatocytes, the levels of CYP activities were present at levels of primary hepatocytes after 5 days in culture (i.e. not freshly isolated levels) (Burkard et al. 2012). This may be expected since the primary cells are not transduced until 24 h after plating, after which time the levels of CYPs are known to be markedly lower than initial levels (Liddle et al. 1998). This meant that in order to be used in metabolism or inhibition studies, upcyte[®] hepatocytes need to express higher CYP activities. The upcyte[®] process was therefore refined to generate upcyte[®] hepatocytes (second generation) with significantly higher CYP activities than was previously achieved. In addition, the culture conditions were altered to determine whether they could be optimized to favour higher CYP activities.

Having established the second generation upcyte[®] hepatocytes, it was investigated whether they could be used in classical CYP inhibition assays using known potent CYP inhibitors. The inhibitors, α -naphthoflavone, miconazole and ketoconazole, were selected as potent competitive inhibitors of CYP1A2, CYP2C9 and CYP3A4, respectively (Mao et al. 2012; Moeller et al. 2013). Ticlopidine was used as an inhibitor of CYP2B6 activities since this is known to be one of the most potent inhibitors of this CYP (Turpeinen et al. 2006). In addition, ticlopidine is a mechanism based inhibitor of CYP2B6 such that its metabolism by CYP2B6 (and not other CYPs) leads to a reactive metabolite that inhibits the enzyme (Richter et al. 2004).

First generation upcyte[®] hepatocytes are responsive to CYP inducers and for CYP3A4, the extent of induction of in upcyte[®] hepatocytes generally reflected that in the paired primary cells (Burkard et al. 2012). Prototypical inducers at the mRNA level induced all CYP1A2, CYP2B6 and CYP3A4; however, CYP2B6 activities were not significantly induced by phenobarbital. The responsiveness to all three CYPs was markedly improved by placing upcyte[®] hepatocytes into 3D culture using alvetex[®] polystyrene scaffolds (Burkard et al. 2012), and the regulatory genes for these CYPs were up-regulated (data not shown). Having refined the upcyte[®] technology, it was investigated whether this improved the responsiveness of the second-generation cells to inducers in 2D cultures, as well as increasing the basal CYP activities.

INTRODUCTION

AhR, CAR and PXR mediated induction was measured using prototypical inducers recommended by the FDA: omeprazole (AhR mediated induction of CYP1A2), phenobarbital (CAR mediated induction of CYP2B6) and rifampicin (PXR and CAR mediated induction of CYP2C9 and CYP3A4) (Food and Drug Administration 2012). CYP induction was monitored by measuring CYP selective substrate metabolism (i.e. activities), rather than changes in mRNA expression since the whole pathway of induction (from AhR/CAR/PXR activation, mRNA expression and subsequent synthesis of active enzyme proteins) can be shown to be functional. To this end, the compounds that were known to induce activities but were not potent mechanistic inhibitors were selected.

The *in vitro-in vivo* CYP3A4 induction correlation has been modelled using predictions based on the maximum fold induction (Ind_{max}), the concentration causing 50% maximal induction (Ind_{50}) or the concentration causing a 2-fold induction (the “F2”). The Ind_{max} and Ind_{50} can be related to the unbound plasma concentration of the drug ($C_{max,u}$) using the Relative Induction Score (RIS) and compared to the *in vivo* induction of CYP3A4 by each drug (measured as the percentage decrease in the midazolam AUC). Data generated from CYP3A4 induction studies using upcyte[®] human hepatocytes were applied to three models recommended by PhARMA (Chu et al. 2009) to determine whether they can mimic the correlations already established for human hepatocytes (Fahmi et al. 2008).

1.8 Therapy- Hemophilia A

1.8.1 Hemophilia A

Hemophilia A is an X-linked recessive disorder that affects 1 in 5000 males (Antonarakis et al. 1995). This is caused by a deficiency of functional FVIII in the blood plasma. The lack of sufficient production of FVIII may be due to spontaneous mutation in the gene that codes for FVIII, which is responsible for blood clotting. Between 5 to 10% of Haemophilia A occurs is due to a qualitative deficiency i.e. the production of a dysfunctional version of FVIII. The remaining 85-90% of patients have an insufficient amount of FVIII in the blood plasma (Meili 2004). The normal concentration of FVIII in the blood plasma is 1 IU/ml of blood, equivalent to 200 ng of FVIII per ml. Both quantitative and qualitative deficiencies occur due to different mutations. Therefore, a general classification of haemophilia A is made depending on the amount of FVIII in the blood plasma. Hemophilia A is classified into three main categories. Patients with a FVIII plasma level less than 1% of normal level are categorized as severe hemophiliacs. Severe hemophilia is the most complicated condition because spontaneous

INTRODUCTION

bleeding occurs in joints, soft tissues, and vital organs (Figure 6). Patients with levels of FVIII of more than 1% but less than 5% are categorized as moderate hemophiliacs. Patients with FVIII levels above 5% but less than 49% of normal levels are classified as mild hemophiliacs. For mild hemophiliacs, it is often difficult to diagnose the condition until a severe bleeding or surgery occurs. In addition to these categories, development of inhibitory antibodies to FVIII can result in acquired hemophilia A or can complicate the treatment of genetic cases.

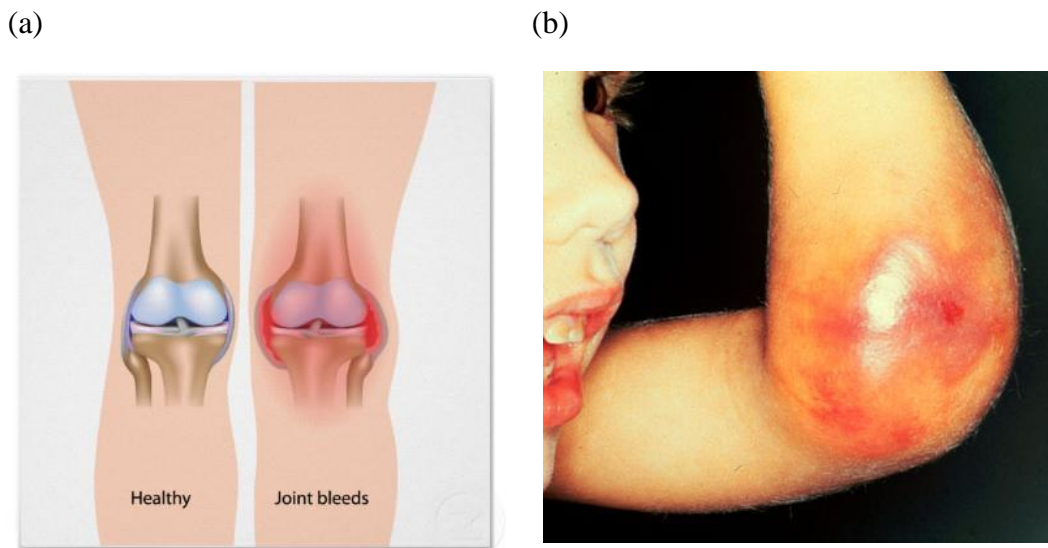


Figure 6: a. Spontaneous bleeding occurs in joints and soft tissues of severe hemophilia-A patients, b. Haemarthrosis of the elbow joints (picture source: shsgdp.wikispaces.com)

1.8.2 Factor VIII

FVIII is a single chain glycoprotein encoded by the F8 gene (Toole et al. 1984; Truett et al. 1985) on the X chromosome (Xq28) (Levinson et al. 1990). Transcription of FVIII molecules takes several hours and the gene is comprised of 26 exons, which encode a polypeptide chain of 2351 amino acids. The molecular weight of pre-mature FVIII at the time of synthesis is 320 kDa. However the majority of FVIII is cleaved during expression and the molecular weight of mature FVIII ranges between 200 to 280 kDa, equal to 2332 amino acids. FVIII is also known as anti-hemophilic protein and is composed of two homologous groups, a heavy chain and a light chain, which are separated by third segment. The FVIII domain structure is organized as A1-A2-B-A3-C1-C2 (Vehar et al. 1984) (Figure 7). Heavy chain and light chains are cleaved intracellularly into two heterodimer chains. The domain of the light chain is organized as A3-C1-C2 and has a molecular weight of 80 kDa. The molecular weight of the heavy chain ranges from 90 to 200 kDa. The heavy chain is highly heterogeneous and is composed of an A1-A2-B domain. The heterogeneity is due to varying degrees of posttranslational modification, such as glycosylation (Manning et al. 1993).

INTRODUCTION

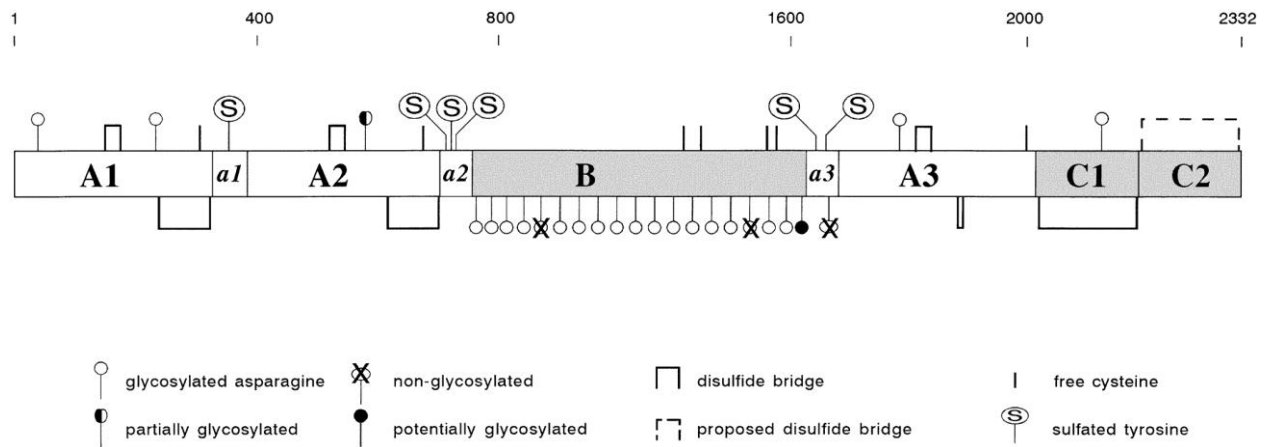


Figure 7: Organization of FVIII domain. Light chain A1-A2-B and heavy chain A3-C1-C2 are intercellularly bonded using disulphide bridges. (Picture source: Lenting et al. 1998).

FVIII circulates as inactive protein in the blood. The inactive form of FVIII molecule forms stable non-covalent bonds with another protein called the vWF (Kaufman et al. 1988; Legaz et al. 1973). The binding of FVIII to vWF occurs via the light chain (Saenko et al. 1994). The molecular weight of vWF is 226 kDa and serves as a carrier protein to FVIII molecule. vWF predominantly occurs as multimeric forms that are linked by disulphide bridges (Kaufman et al. 1989). Failure to bind to the vWF protein will result in the FVIII molecule being highly unstable. Thus, the association of vWF with FVIII stabilizes the bonding between the light and heavy chains (Kaufman 1992; Wise et al. 1991; Fay 1988). FVIII is released from the vWF molecule via proteolytic cleavage by thrombin. A series of proteolytic degradation occurs that result in the release of FVIII from vWF molecule, thus resulting in activation of FVIII (Vehar et al. 1984). The activated form of FVIII is known as FVIIIa and composed of the A1-A2 domain of the heavy chain and the A3-C1-C2 of the light chain. FVIIIa is highly unstable as it is deactivated due to dissociation of the A2 domain (Pipe & Kaufman 1997). The activated form of FVIIIa functions as a cofactor and plays a vital role in the coagulation pathway (Fay et al. 1991). During the activation of FVIII molecule, the B domain from heavy chain is lost and it does not play any role in coagulation activity (Toole et al. 1986; Fulcher et al. 1983). Therefore, the B domain deleted (BDD) version of FVIII transgene has been used to clone the FVIII construct.

INTRODUCTION

1.8.3 Biosynthesis of FVIII

Hepatic source

Research on the *in vivo* production of FVIII in liver is ambiguous, with contrasting findings being reported. For example, liver transplantation (Marchioro et al. 1969; Bontempo et al. 1987) and liver perfusion (Shaw et al. 1979; Owen et al. 1979) in hemophiliac patients resulted in increased amount of FVIII levels in blood. Results showed that FVIII mRNA was detected in hepatocytes rather than in LSECs (Karen L. Wion et al. 1985) and the response element in the FVIII promoter region was also found to be hepatocyte-specific (Figueiredo & Brownlee 1995). However, histochemical analysis detected FVIII in LSECs (Stel et al. 1983; van der Kwast et al. 1986; Kadhon et al. 1988). Although it has not been conclusively shown whether hepatocytes and/or LSECs produce FVIII, it is clear that liver is the major FVIII-producing site.

Extra hepatic source

Although the liver (hepatocytes or LSECs) is the major site for production of FVIII, the FVIII gene has also been expressed in several non-hepatic tissues such as in kidney and lymph nodes (K L Wion et al. 1985; Levinson et al. 1992; Elder et al. 1993). Transplantation of spleens into hemophiliac animals resulted in the detection of FVIII in their blood (Veltkamp et al. 1974). Studies using perfused *ex vivo* human lungs also show that FVIII is produced in the lung (Jacquemin et al. 2006; Groth et al. 1974). Likewise, human adult pulmonary mvECs have also been shown to produce FVIII (Jacquemin et al. 2006).

1.8.4 Blood coagulation

Blood coagulation is an important response of the body for survival when there is a vascular injury. The process of blood clotting (Figure 8), followed by dissolution of the clot leading to the repair of damaged vascular damage or tissue injury, is termed "haemostasis".

INTRODUCTION

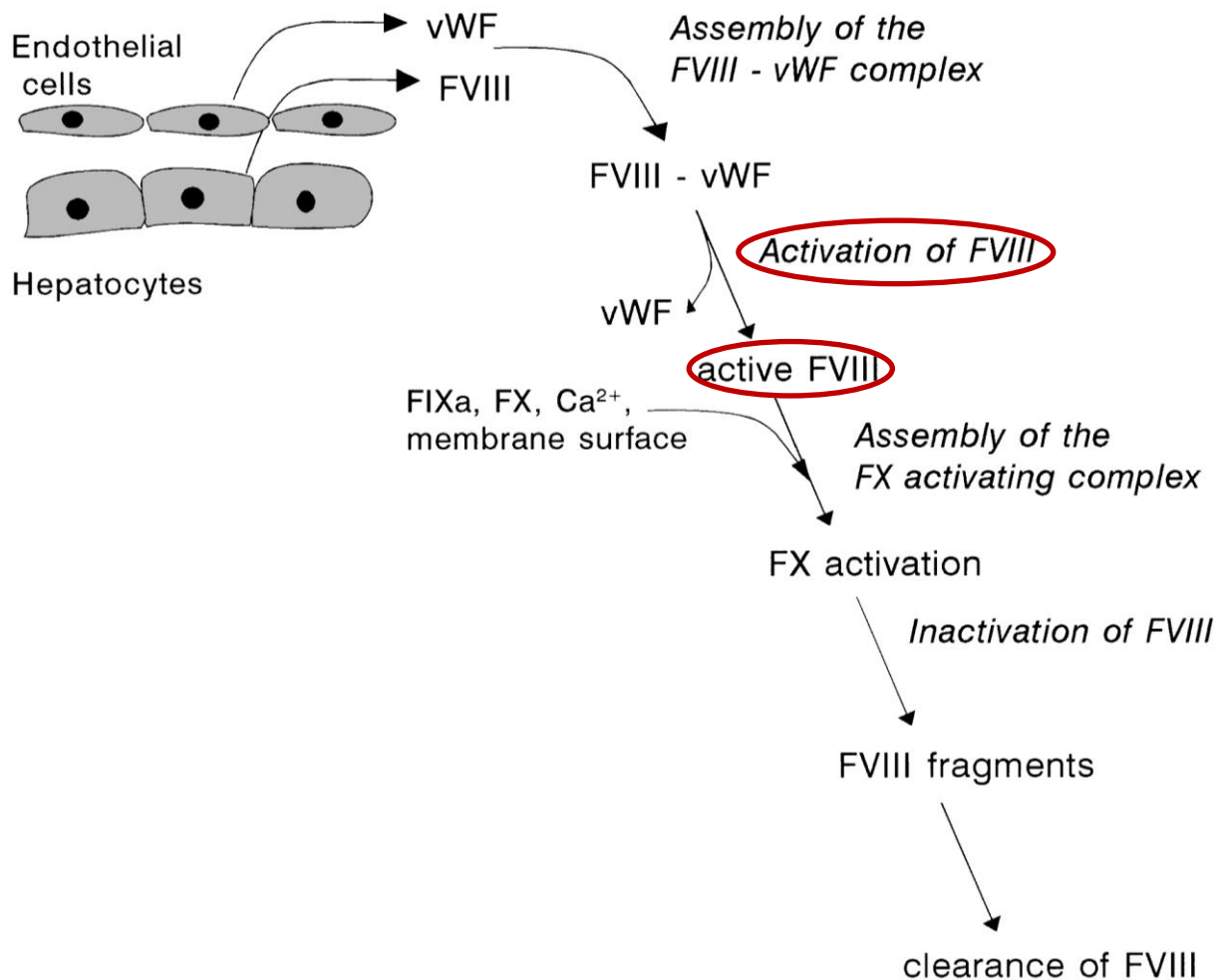


Figure 8: Schematic representation of coagulation cascade involving FVIII molecule (Picture source: Lenting et al. 1998).

1.8.5 Current treatment for haemophilia A

Fundamental treatment to prevent the hemophilia A to bleed continuously is to infuse them with the missing clotting factor concentrate (FVIII) by intravenous injection. However the problem with FVIII is its stability: its half-life in the blood is between 7.4 h and 20.4 h. Therefore, treatment for hemophilia A patients has to be carried out three times a week (van Dijk et al. 2005).

Factor replacement therapy

FVIII concentrate is obtained from two main sources:

1. Plasma derived
2. Recombinant derived

INTRODUCTION

Plasma derived

Plasma derived FVIII concentrate is prepared from human blood. Pooled plasma is fractionated into different components, such as FVIII and albumin. However, plasma derived FVIII concentrate had many disadvantages in early 1980s. One of the most serious was that nearly half of the hemophiliacs infused with plasma derived FVIII concentrates were infected with HIV and hepatitis C.

Recombinant derived

Recombinant derived FVIII concentrates can be achieved by genetic engineering. Using transgenic technology, the FVIII gene is incorporated into the host genome in cells such as Chinese hamster ovary cells (CHOs), baby hamster kidney cells, HEK 293 F cells (Casademunt et al. 2012) for the production of FVIII in cell culture. As FVIII is stabilized by vWF (Kaufman 1992; Wise et al. 1991; Fay 1988), co-expression of vWF with FVIII increases the stability of FVIII in cell culture (Pipe & Kaufman 1997). Failure to co-express vWF results in the secretion of FVIII as inactive separate chains (Kaufman et al. 1989; Wise et al. 1991). Recombinant FVIII (rFVIII) has an effective pathogen safety profile but post-translational modification of the FVIII shows non-human patterns (Burnouf 2011). Incorrect post-translational modification of FVIII triggers an immune response in hemophiliacs, which results in the production of natural FVIII inhibitors. The percentage of hemophiliacs developing inhibitors due to recombinant FVIII is relatively high; 34.5% (Iorio et al. 2010). In order to treat the hemophiliacs by the healthcare systems, the cost ranges from 1.800€ to 2.500€ / dose, with an average of 220.000€ /year/haemophiliac. This means that this is one of the most expensive diseases (Manco-Johnson 2007; Nichols et al. 2009).

1.8.6 Other treatments

Desmopressin

Desmopressin or DDAVP (1-desamino-8-D-arginine vasopressin) is a synthetic drug, which is a modified version of arginine vasopressin. vWF is stored in weibel palade bodies (WPB) present in endothelial cells that lines the blood vessels (Rosenberg et al. 2000; Yarovoi et al. 2003; Wilcox et al. 2003; Shi et al. 2006). Administrating DDAVP stimulates WPB to release stored vWF into the blood stream, which binds to the FVIII molecule and stabilizes it.

INTRODUCTION

Antifibrinolytic treatment

An antifibrinolytic medicine, such as tranexamic acid and epsilon aminocaproic acid, is used as a supplement to replacement therapy (Tengborn 2012). This prevents the degradation of blood clots. This medication was very often used in order to do the dental work on hemophiliacs or to treat intestinal bleeding in mild hemophiliacs.

Gene therapy

All the above-mentioned standard treatments for hemophilia A patients involve infusing patients with clotting factors for a prophylactic regime, which usually takes place between 2 to 3 times a week. Although this is a temporary remedy, the quality of life is poor and a lot of care is involved in planning daily activities. The goal of researchers is to analyze a definitive cure that can permanently convert a patient from a severe to a mild or moderate stage i.e. correction through gene transfer (Youjin & Jun 2009). Successful results have been obtained from hemophilia animal models with gene transfers (Pfeifer & Verma 2001; Kelley et al. 2002). However, this procedure has certain disadvantages, such as transient and therapeutically inadequate levels of clotting factors in blood (Powell et al. 2003). Other side effects such as induced host immune responses, insertional mutagenesis and random integration of gene resulting in oncogenesis, has decreased the drive for such remedies (High 2007). Other gene therapies investigated have included the modification of cells such as platelets or endothelial cells to produce FVIII (Yarovoï et al. 2003; Shi et al. 2006).

Cell therapy

Implantation of *ex vivo* modified primary fibroblasts that have been transfected by receptor-mediated adenovirus allowed the *in vivo* production of FVIII in mice (Zatloukal et al. 1994). Autologous primary fibroblasts that were genetically modified *ex vivo* and subsequently implanted in the greater omentum region resulted in the detection of FVIII in the blood (Roth et al. 2001).

INTRODUCTION

1.9 Aims of the thesis

This thesis addresses optimization of *in vitro* hepatic models and application of these hepatic models for drug development and therapy.

- The penetration of upcyte[®] hepatocytes in 3D scaffolds (namely Mimetix[®]) was optimized using confocal microscopy. The growth, viability and metabolic functions of upcyte[®] hepatocytes were optimized using different formats of 3D scaffolds.
- Upcyte[®] hepatocytes, LSECs and MSCs were used to generate liver organoids. The structural organisation of the cells within the organoids and functionality of the organoid (CYP3A4 activity) were investigated after culture in static conditions or in dynamic, long-term conditions using a *Quasi-vivo*[®] chamber system.
- An *ex vivo* bioreactor employing a decellularized organic scaffold (BioVaSc) to culture liver organoids was established. The vascular tree of the decellularized BioVaSc was first populated with upcyte[®] mvECs. The structural orientation and functionality (CYP3A4) of the liver organoids were analyzed after 30 days dynamic culture.
- The application of upcyte[®] hepatocytes to drug development was investigated by measuring CYP inhibition and induction. In order to achieve the optimal levels required for CYP inhibition, the culture conditions were optimized.
- The therapy of hemophilia is currently lacking a suitable source of FVIII. Therefore, the application of mvECs and their modification by transducing them with FVIII lentivirus was investigated as a potential method for generating this coagulation factor.

MATERIALS & METHODS

2. Materials & Methods

2.1 Materials

2.1.1 Disposable Material

Falcon tubes	BioCoat™ BD (Heidelberg, Germany)
Pipette	Eppendorf (Hamburg, Germany)
Tips	Greiner (Frickenhausen, Germany)
Multiwell plates - collagen coated	BD (Heidelberg, Germany)
Tissue culture dishes - collagen coated	BD (Heidelberg, Germany)
Multiwell plates - non-coated	Greiner (Frickenhausen, Germany)
Tissue culture dishes - non-coated	Greiner (Frickenhausen, Germany)
Freezing tubes	Greiner (Frickenhausen, Germany)
Disposable gloves	Diagonal (Münster, Germany)
Petri dishes, 60 mm	Greiner (Frickenhausen, Germany)
Pressure dome	Memscap AS (Skoppum, Norway)
Sterile filter, 0.2 micron	Whatman (Dassel, Germany)
Sterile filter, 0.45 micron	Whatman (Dassel, Germany)
Scalpels	Aesculap AG (Tuttlingen, Germany)
Screw caps with septa 100/pk	Agilent (Karlsruhe, Germany)
Screw vials, 2 ml clear 100/pk	Agilent (Karlsruhe, Germany)
Spin-X UF 20 ml Concentrator, 100K cutoff	Corning (Kaiserslautern, Germany)
Precolumns Eclipse XDB-C18 4.6x12.5, 5mm	Agilent (Karlsruhe, Germany)
100 ml glass inserts	Agilent (Karlsruhe, Germany)
Oasis® µElution Plate Oasis® HLB (30mm)	Waters (Eschborn, Germany)
10 ml x 24 Collection plate	Waters (Eschborn, Germany)
µElution Spacer	Waters (Eschborn, Germany)
Gene Pulser/MicroPulser Cuvettes	Bio-Rad (Munich, Germany)

2.1.2 Chemicals

Chemical/supplements	Supplier	Cat#
α-Naphthoflavone	Sigma-Aldrich (Deisenhofen, Germany)	N5757
Acetaminophen (APAP)	Sigma-Aldrich (Deisenhofen, Germany)	A7085
Acetonitrile, CHROMASOLV®	Sigma-Aldrich (Deisenhofen, Germany)	34998-2.5L
Agarose	AppliChem (Darmstadt, Germany)	A0949
Albumin fraction V	AppliChem (Darmstadt, Germany)	A1391

MATERIALS & METHODS

4-Androstene-3,17-dione (ASD) VETRANAL [®]	Sigma-Aldrich (Deisenhofen, Germany)	46033-250MG
Blasticidin S HCl	Invitrogen (Karlsruhe, Germany)	R210-01
Bupropion-HCl	Sigma-Aldrich (Deisenhofen, Germany)	B102
Carbamazepine	Sigma-Aldrich (Deisenhofen, Germany)	C4024
CellTiter [®] 96 AQueous non- radioactive cell proliferation assay	Promega (Mannheim, Germany)	G5421
Chlorpropamide	Sigma-Aldrich (Deisenhofen, Germany)	C1290
DAPI	Sigma-Aldrich (Deisenhofen, Germany)	32670
Dexamethasone	Sigma-Aldrich (Deisenhofen, Germany)	D4902
Diethyl ether, CHROMASOLV [®] , for HPLC = 99.9%, inhibitor-free	Sigma-Aldrich (Deisenhofen, Germany)	309966-1L
Dispase	Sigma-Aldrich (Deisenhofen, Germany)	D4818
Distilled water HPLC grade	GE Healthcare (Munich, Germany)	S31-012
DMSO	Applichen (Darmstadt, Germany)	A3672
DMEM	GE Healthcare (Munich, Germany)	P-04-03600
Ethanol (99.8 % p.a)	AppliChem (Darmstadt, Germany)	20.821.330
FBS Gold Eu approved	PAN (Aidenbach, Germany)	P40-38500
Flumazenil	Sigma-Aldrich (Deisenhofen, Germany)	F6300
Formic acid 98%	Sigma-Aldrich (Deisenhofen, Germany)	6440
Isopropanol	Applichem (Darmstadt, Germany)	A1592,2500
Ketoconazole	Sigma-Aldrich (Deisenhofen, Germany)	K1003
Krebs-Henseleit buffer	Sigma-Aldrich (Deisenhofen, Germany)	K3753
L-Glutamine	PAN (Aidenbach, Germany)	P04-80100
Lipofectamin 2000	Invitrogen (Karlsruhe, Germany)	11668-019
hHGF	Pepro Tech Inc. (Hamburg, Germany)	100-39
4-Hydroxybupropion	Santa Cruz Biotechnology (Heidelberg, Germany)	sc-211604
4-Hydroxymethyltolbutamide	Santa Cruz Biotechnology (Heidelberg, Germany)	Sc-218585
6b-Hydroxytestosterone	Sigma-Aldrich (Deisenhofen, Germany)	H2898
Na-Butyrate	Sigma-Aldrich (Deisenhofen, Germany)	B-5887
NaOH	Sigma-Aldrich (Deisenhofen, Germany)	S5881

MATERIALS & METHODS

Nifedipine	Sigma-Aldrich (Deisenhofen, Germany)	N7634
Matrigel™ growth factor reduced	BD (Heidelberg, Germany)	356230
MEM non-essential aminoacid	GE Healthcare (Munich, Germany)	P08-36500
Methanol, CHROMASOLV®	Merck (Darmstadt, Germany)	34860
(±)Miconazole nitrate salt	Sigma-Aldrich (Deisenhofen, Germany)	M3512
MTS	Promega (Mannheim, Germany)	G5421
Oligo Dt primer	BioSpring (Frankfurt am Main, Germany)	-
Omeprazole	Sigma-Aldrich (Deisenhofen, Germany)	O104
Opti-MEM I	Gibco® Life Technologies (Darmstadt, Germany)	31985-047
Oncostatin M	Pepro Tech Inc. (Hamburg, Germany)	300-10T-B
PBS w/o Mg ²⁺ w/o Ca ²⁺ (PBS ⁻)	PAN (Aidenbach, Germany)	P04-36500
Penicillin-Streptomycin	PAN (Aidenbach, Germany)	P06-07001
Phenacetin	Sigma-Aldrich (Deisenhofen, Germany)	77440
Phenobarbital sodium salt	Sigma-Aldrich (Deisenhofen, Germany)	P1636
Phenytoin	Sigma-Aldrich (Deisenhofen, Germany)	PHR1139
Pioglitazone	Sigma-Aldrich (Deisenhofen, Germany)	E6910
Polybrene (hexadimethrinebromide)	Sigma - Aldrich (Steinheim, Germany)	H9268
Poly-D-lysine	Sigma - Aldrich (Steinheim, Germany)	P7280
Potassium phosphate monobasic (KH ₂ PO ₄)	Sigma - Aldrich (Steinheim)	P5655
Quinidine, anhydrous	Sigma-Aldrich (Deisenhofen, Germany)	Q3625
Sulfaphenazole	Sigma-Aldrich (Deisenhofen, Germany)	S0758
Reichstein's substance (Cortexolone)	Sigma-Aldrich (Deisenhofen, Germany)	R0500
RNase A	Sigma-Aldrich (Deisenhofen, Germany)	R5125
Rifampicin	Sigma-Aldrich (Deisenhofen, Germany)	R3501
Testosterone C-III	Sigma-Aldrich (Deisenhofen, Germany)	T6147
Ticlopidine hydrochloride	Sigma-Aldrich (Deisenhofen, Germany)	T6654
Tolbutamide	Sigma-Aldrich (Deisenhofen, Germany)	T0891

MATERIALS & METHODS

Triton X	Sigma-Aldrich (Deisenhofen, Germany)	X100
Troglitazone	Sigma-Aldrich (Deisenhofen, Germany)	T2573
Trypan blue 0.4 %	Sigma - Aldrich (Steinheim, Germany)	T8154
Trypsin /EDTA	PAN (Aidenbach, Germany)	P10-024100
Versene	Invitrogen (Karlsruhe, Germany)	15040033
VEGF	Sigma - Aldrich (Steinheim, Germany)	V7259

* All used chemicals were of analytical grade, unless otherwise stated, and were of the highest purity. For cell culture methods, chemicals that were appropriate for cell culture were chosen. All water used was free of ionic and organic compounds and was from a Milli-Q water conditioning system.

2.1.3 Solutions and Buffers

Krebs-Henseleit-buffer (KHB)

The contents of the Sigma KHB (K3753) and following chemicals were dissolved in 900 ml distilled water:

NaHCO ₃	2.1 g
CaCl ₂ 2H ₂ O	0.175 g
HEPES	5.958 g

The pH was adjusted to 7.4 and then made up to 1l.

Protein lysis buffer

The following were combined:

NaCl	4.38 g
MgCl ₂ x 6H ₂ O	0.1 g
Tergitol [®] Type NP-40S	5 ml
Tris-HCl (1 M)	25 ml

The volume was made up to 500 ml with distilled water.

Decellularization solution

Sodium deoxycholate	20 g
Gentamycin	

The volume was made up to 500 ml with distilled water.

HPLC internal standards

Chlorpropamide solution	1 mg/ml in 100% methanol
5 mM Cortisolone stock solution	1.73 mg/ml in 100% methanol
0.5 mM Cortisolone working solution	The stock solution was diluted 1:10 in 100% methanol

MATERIALS & METHODS

HPLC solvents:

2% Formic acid in methanol	1 ml formic acid was added to 49 ml 100% methanol
1:1 methanol:water	25 ml 100% methanol was mixed with 25 ml distilled water

Standard metabolites

1 mM 4-Hydroxytolbutamide	0.29 mg/ml in 100% methanol
1 mM 4-Hydroxybupropion	0.26 mg/ml in 100% methanol
1 mM 6 β -Hydroxytestosterone	0.304 mg/ml in 100% methanol
25 mM Acetaminophen (APAP)	3.78 mg/ml in 100% DMSO

Mobile Phases

All mobile phases were degassed using vacuum filter before use.

For tolbutamide and bupropion:

Mobile phase A	1.36 g KH ₂ PO ₄ in 800 ml cell culture grade distilled water made up to 1 l (pH 4.6). 52.6 ml 100% acetonitrile
Mobile phase B	500 ml acetonitrile 500 ml water

Testosterone

Mobile phase A	390 ml methanol 600 ml distilled water 10 ml acetonitrile
Mobile phase B	800 ml methanol 180 ml distilled water 20 ml acetonitrile

Phenacetin

Mobile phase A	17 ml isopropanol 1 ml formic acid
Mobile phase B	1000 ml distilled water (purest quality) 100 ml methanol

MATERIALS & METHODS

2.1.4 Cells and cell culture medium

Cells

293 FT	Invitrogen (Karlsruhe, Germany)
Primary* mvECs	Medicyte (Heidelberg, Germany)
Upcyte [®] mvECs	Medicyte (Heidelberg, Germany)
Upcyte [®] LSECs	Medicyte (Heidelberg, Germany)
Upcyte [®] Hepatocytes	Medicyte (Heidelberg, Germany)
Upcyte [®] MSCs	Medicyte (Heidelberg, Germany)
Primary* MSCs	Fraunhofer IGB (Stuttgart)

*All human cells offered by Medicyte are derived from donors who have signed an informed consent form. This donor consent form outlines in detail the purpose of the donation and the procedure for processing the tissue. Medicyte is not accepting or using any human cells without signed donor consent documents.

Cell culture medium

upcyte [®] Hepatocyte Thawing medium	Medicyte (Heidelberg, Germany)
upcyte [®] Hepatocyte Growth Medium (HGM)	Medicyte (Heidelberg, Germany)
upcyte [®] Hepatocyte High Performance medium (HPM)	Medicyte (Heidelberg, Germany)
upcyte [®] LSECs Growth Medium	Medicyte (Heidelberg, Germany)
upcyte [®] mvECs Thawing Medium	Medicyte (Heidelberg, Germany)
vericyte [®] Endothelial Cell Growth Medium	Medicyte (Heidelberg, Germany)

Upcyte[®] MSC Growth Medium

DMEM High Glucose (4,5g/l) W/O L-Glutamine PAN (Aidenbach)
W/O sodium pyruvate (E15-011)

+ FBS

final concentration 10%

Liver organoid growth medium

upcyte[®] LSECs Growth Medium
upcyte[®] Hepatocyte Growth Medium (HGM)-Mixed in 1:1 ratio

MATERIALS & METHODS

Freezing medium

Growth Medium	70%
DMSO	10%
FBS	20%

2.1.5 Antibodies

Antibodies for immunostaining

Antibody (1st or 2nd)	Supplier	Cat#
Mouse anti-Ck 8 (C51)	Santa Cruz Biotech (Heidelberg, Germany)	Sc-8020
Mouse anti-Ck 18(DC-10)		Sc-6259
Mouse anti human CD31	Dako (Hamburg, Germany)	M0823
Mouse anti human vWF	Dako (Hamburg, Germany)	M0616
Vimentin	Santa Cruz Biotech (Heidelberg, Germany)	Sc-373717

2.1.6 Kits

Kits	Supplier
QIAquick [®] PCR Purification Kit	Qiagen (Hilden, Germany)
RNeasy [®] Mini Kit	Qiagen (Hilden, Germany)
RNeasy [®] Micro Kit	Qiagen (Hilden, Germany)
SuperScript [®] III First beach synthesis kit	Invitrogen (Karlsruhe, Germany)
ViraPower [™] Lentiviral Packaging Mix	Invitrogen (Karlsruhe, Germany)
Gateway [®] LR Clonase [®] II Enzyme mix	Invitrogen (Karlsruhe, Germany)
Gateway [®] BP Clonase [®] II Enzyme mix	Invitrogen (Karlsruhe, Germany)
ElectroMAX [™] Stbl4 [™]	Invitrogen (Karlsruhe, Germany)
Mega DH10B [™] T1 ^R	Invitrogen (Karlsruhe, Germany)

2.1.7 Primers

Name	Sequence
FVIII-pENTR FWD	ACAAGTTTGTACAAAAAAGCAGGCT
FVIII-pENTR REV	ACCACTTTGTACAAGAAAGCTGGGT
pENTR11-R	ACGGGCCAGAGCTGCAGC
FVIII-FOR_601-1200	TTGAATTCAGGCCTCATTGG
FVIII-FOR_1201-1800	CCTTCCTTTATCCAAATTCGC
FVIII-FOR_1801-2400	TTGAGGATCCAGAGTTCCAA
FVIII-FOR_2401-3000	GCCATCAACGGGAAATAACT
FVIII-FOR_3001-3600	GAAAAAGATGTGCACTCAGGC
FVIII-FOR_3601-4200	GACAGTGGGCCCCCAAAGC

MATERIALS & METHODS

FVIII-FOR_4201-4416	GGGAGTAAAATCTCTGCTTACCA
pEXP_Lenti6_FVIII_V5_CMV FWD1	CATAATGATAGTAGGAGGC
pEXP_Lenti6_FVIII_V5_CMV FWD2	CGCAAATGGGCGGTAGGCGTG
LTR -143 FWD	TGTGTGCCCGTCTGTTGTGT
LTR -143 REV	GAGTCCTGCGTCGAGAGAGC
KRT18 FWD	GGTCAGAGACTGGAGCCACTT
KRT18 REV	CCAGCTTGACCTTGATGTTTCAGCAG
Albumin FWD	GGTGAGACCAGAGGTTGATGTGATG
Albumin REV	CACACATAACTGGTTCAGGACCACG
Glutaminase2 FWD	GTGTGTGAGCAGCAACATTGTGCTC
Glutaminase2 REV	GATGGCTCCTGATACAGCTGACTTG
Glutamine synthetase FWD	GTTGCCTGAGTGGAATTCGATGGC
Glutamine synthetase REV	CGGTTTCATTGAGAAGACACGTGCG
HIF1 α FWD	CATGGAAGGTATTGCACTGCACAGG
HIF1 α REV	CAGCACTACTTCGAAGTGGCTTTGG
G6P FWD	GTGGCGTATCATGCAAGTGCTATGC
G6P REV	GAGGCTGAGACATGAGAATCGCTTG

* - All the primer sequence were bought from Biospring (Frankfurt Am Main, Germany)

2.1.8 General technical equipment and devices

Equipment	Type	Manufacturer / Headquarters
Analytical balance	BP 211D	Sartorius (Göttingen, Germany)
Autoclave	5075 ELV	Systec (Wettenberg, Germany)
Automated cell counter	Scepter™ 2.0	Millipore, Germany
Centrifuge	Biofuge Pico	Heraeus (Hanau, Germany)
Centrifuge	Biofuge stratos	Heraeus (Hanau, Germany)
Confocal microscope	ZEISS Axiovert 200M	Zeiss (Neuenheim, Germany)
Cryo 1 °C Freezing Container	5100	Nalgene Nunc International (Wiesbaden, Germany)
Erlenmeyer flasks and beakers	-	Schott (Mainz, Germany)
Fluorescence microscope	Axio Observer.Z1	Zeiss (Heidelberg, Germany)
Freezer (-20° C)		PKM (Moers, Germany)
Freezer (-80° C)	Hera freeze	Heraeus (Hanau, Germany)
HPLC	1200 Infinity	Agilent Technologies (Waldbronn, Germany)
Ice machine	MF 26	Scotsman (Milan, Italy)
Incubator	NU- 5500E	Integra Bioscience GmbH (Fernwald, Germany)
Laboratory Bottles	-	Simax (Trutnov, Czech Republic)

MATERIALS & METHODS

Laminar Flow	Hera Safe	Kendra (Hanau, Germany)
Magnetic stirrers with heating	Mr 3001 K	OMNILAB (Bremen, Germany)
Measuring cylinders, various Sizes	-	Duran (Wertheim, Germany)
Microscope	DMIL	Leica Microsystems GmbH (Wetzlar, Germany)
Microplate Reader	Fluostar	BMG labtech (Virginia, US)
Microplate Reader	Sunrise	Tecan (Crailsheim, Germany)
MicroPulser™ Electroporator	165-2100	Bio-Rad (Munich, Germany)
Microcentrifuge	5804R	Eppendorf (Hamburg, Germany)
Milli-Q water conditioning system	NanoPure Infinity	Werner Reinstwassersysteme (Leverkusen, Germany)
Mimetix® plates	-	The Electrospin Company Ltd. (Didcot, UK)
NanoDrop	2000	Thermo Scientific (Schwerte, Germany)
Neubauer counting chamber		NeoLab (Heidelberg, Germany)
Nitrogen tank	CryoPlus 1	Thermo Scientific (Schwerte, Germany)
PCR device	PTC -200	MJ Research (St.Bruno, Canada)
Pipetboy	Pipetboy acu	Integra Biosciences (Fernwald, Germany)
Pipettes	10 µl , 200µl , 1000µl SL PetteXE	Nichiryo (Maryland heights, US)
pH Meter	-	INO-Lab Servos (Singapore)
<i>Quasi-vivo</i> ® System	-	Kirkstall Ltd. (Sheffield, UK)
Real-time PCR instrument	Rotor-Gene Q	Qiagen (Hilden, Germany)
Refrigerator	-	Liebherr (Biberach an der Riss, Germany)
Shaker	DRS -12	NeoLab (Heidelberg, Germany)
SunFire IS column	C18 2.5µm 3.0 x 20mm	Waters (Eschborn, Germany)
Universal oven	Function line	Heraeus (Hanau, Germany)
Vacuum pump	VacuSafe	Integra Biosciences (Fernwald, Germany)
Vortex	Vortex Genie -2	Scientific Industries (Karlsruhe, Germany)
Water bath	GFL	M & S Lab Equipment GmbH (Wiesloch, Germany)

MATERIALS & METHODS

2.2 Methods

2.2.1 Cell culture techniques

2.2.1.1 Incubation conditions

The entire cell culture work was performed under sterile conditions under laminar flow. Morphology was examined daily via light microscope. All cells were cultured under standard culture conditions i.e. at 37°C, under an atmosphere of 5% CO₂ and 95% humidity. The medium was refreshed twice a week using medium which had been pre-warmed at 37°C for 10-15 min before use.

2.2.1.2 Thawing and plating of cryopreserved cells

The cryovial containing the frozen cells were rapidly thawed in a water bath maintained at 37°C. The cells were then transferred directly by pouring the entire content into a falcon tube containing 50 ml of thawing medium. The tube was gently inverted to achieve a homogenous cell suspension. The cells were then centrifuged for 5 min at RT to pellet the cells using the appropriate speed, as shown in Table 2.

The appropriate speed for centrifugation for different cell types were shown in Table 2.

Table 2: Centrifugation parameters used for different cell types.

Cell Type	Centrifugal force
Upcyte [®] hepatocytes	90 ×g
Upcyte [®] /primary mvECs	260 ×g
Upcyte [®] LSECs	720 ×g
Upcyte [®] / primary MSC	260 ×g

The supernatant was discarded and the pellet was suspended in cell-specific Growth Medium (GM) (2.1.4). The cell density was counted using Millipore Scepter™- handheld automated cell counter (2.2.1.4). The cells were subsequently seeded and cultured in fully supplemented GM. The seeding density for different cell types was shown in Table 4. For the induction/inhibition experiments only, the upcyte[®] hepatocytes were cultured at a seeding density of 5000 cells/cm² and cultured in upcyte[®] hepatocyte growth medium (HGM) containing 0.5% DMSO for 3 to 5 days.

MATERIALS & METHODS

2.2.1.3 Subculturing of cells

The cells were subcultured when they reached a confluence of 75-80 %. The cells were rinsed with PBS⁻ to remove the GM, which can inhibit trypsin. Pre-warmed trypsin/EDTA solution was added (50 $\mu\text{l}/\text{cm}^2$) and incubated under standard culture conditions for 3-5 min to detach the cells. This reaction was stopped with three times the volume of stop solution (See Table 3 for cell-specific stop solutions). The entire content of the flask was transferred to a sterile 50 ml tube. The cells were then centrifuged at an appropriate speed (See Table 2). The supernatant was aspirated, the pellet was suspended in cell-specific culture medium, and the cells were seeded in a culture format according to the experiment and cell type. The seeding density for different cell types was shown in table 4. Remaining cells were cryopreserved (see Section 2.2.1.5). The growth of the cells was determined according to the number of population doublings (PD) they had undergone.

Table 3. Cell-specific stop solutions

Cell Type	Stop solution
upcyte [®] hepatocytes	upcyte [®] Hepatocyte Thawing Medium
upcyte [®] /primary mvECs	Trypsin Neutralising Solution
upcyte [®] LSECs	upcyte [®] LSECs Medium + 10% FBS
upcyte [®] /primary MSC	DMEM High Glucose (4,5g/l) W/O L-Glutamine W/O sodium pyruvate + 10% FBS

Table 4. Cell-specific seeding density.

Cell Type	Optimal seeding densities	
	After thawing	After subculturing
Upcyte [®] hepatocytes	10,000-20,000 cells/cm ²	5,000 cells/cm ²
Upcyte [®] /primary mvECs	5000-10,000 cells/cm ²	5000-10,000 cells/cm ²
Upcyte [®] LSECs	5000-10,000 cells/cm ²	5000-10,000 cells/cm ²
Upcyte [®] /primary MSC	5000-10,000 cells/cm ²	5000-10,000 cells/cm ²

2.2.1.4 Cell counting and viability determination

The pellet was suspended in cell-specific culture medium and the cell suspension was diluted by 10-fold in PBS⁻ and counted using a Millipore Scepter[™]- handheld automated cell counter. Alternatively, the cell suspension was mixed with 0.05% Trypan blue solution (1:10 dilution of the stock Trypan blue solution in PBS⁻) and pipetted onto a Neubauer counting

MATERIALS & METHODS

chamber. The unstained (viable) and stained (non-viable) cells were counted. The PD was calculated as described in Equation 1.

$$PD = last\ PD + \frac{\ln \frac{cellcount\ yield}{cellcount\ seed}}{\ln 2} \quad \text{Equation 1}$$

Where “cellcount seed” is the number of cells initially seeded and “cellcount yield” is the number of cells harvested from the harvested cells after trypsinisation.

2.2.1.5 Cryopreservation

The cells were resuspended at an appropriate density in freezing medium. The optimal freezing densities and media for each cell type are summarized in Table 5. The cells were aliquoted into cryovials (1 ml/vial) and then placed in a pre-cooled (4°C) Nalgene® “Mr. Frosty” freezing container. The freezing container was then placed in a -70°C freezer for 16-24 h. After this time, the vials were placed in a liquid nitrogen tank for long-term storage.

Table 5. Freezing densities and media for different cell types.

Cell Type	Freezing Medium	Optimal freezing densities
upcyte® hepatocytes	70% upcyte® Hepatocyte Growth Medium (HGM) + 20%FBS +10%DMSO	1.0-5.0 x 10 ⁶ cells/ml
upcyte®/primary mvECs	vericyte® Endothelial Cell Growth Medium (ECGM) + 20%FBS +10%DMSO	1.0-3.0 x 10 ⁶ cells/ml
upcyte® LSECs	upcyte® LSECs Growth Medium + 20%FBS +10%DMSO	1.0-2.0 x 10 ⁶ cells/ml
upcyte®/ primary MSC	DMEM High glucose (4,5g/l) W/O L-glutamine w/o sodium pyruvate + 10% FBS + 20%FBS +10%DMSO	1.0-2.0 x 10 ⁶ cells/ml

2.2.2 Hepatic models – 3D Mimetix® scaffolds

2.2.2.1 Upcyte® hepatocyte in Mimetix® scaffolds

The Mimetix® scaffolds were removed from the packaging material and transferred to a sterile flow hood. The scaffolds were wetted with 20% ethanol. Ethanol was aspirated carefully from the edge of the scaffolds and washed twice with HGM. The scaffolds containing the medium were incubated for 30 min under standard culture conditions before seeding the cells.

MATERIALS & METHODS

2.2.2.2 Confocal analysis

Nuclei were stained with DAPI and analyzed for penetration into the scaffolds at the various time points using confocal microscopy. Optical z-stacks were obtained using a confocal microscope to generate side view images using the software ZEN 2012 (ZEN: Zeiss Efficient Navigation).

2.2.2.3 Metabolic activity in Mimetix[®] scaffolds

The upcyte[®] hepatocytes were seeded at a seeding density of 50,000 cells/well and pre-cultured in HGM up to Day 7. To determine the induction of CYP3A4 activity, after the pre-culture period, cells were cultured for an additional 3 days (day 7 to 10) in upcyte[®] hepatocyte high performance medium (HPM), during which time medium was replaced every day with fresh HPM containing 20 μ M of rifampicin. Control cells were cultured in 0.1% DMSO for 3 consecutive days in HPM. Measurement of CYP3A4 activities were carried out on Day 10 according to the method described in Section 2.2.5.3 using 250 μ M testosterone in KHB as substrate. CYP activities were normalised with respect to protein content and time (min).

2.2.2.4 Upcyte[®] hepatocyte culture viability and protein content

The viability of upcyte[®] hepatocyte cultures was measured using the MTS assay (CellTiter[®] 96 AQueous Non-Radioactive Cell kit), according to the supplier's protocol. Cells bioreduce MTS in the presence of phenazine methosulfate (PMS) into a formazan product that is soluble in tissue culture medium. The formazan product has an absorbance maximum at 490-500 nm. The amount of formazan product produced is directly proportional to the number of living cells in culture. The MTS stock solution was thawed and diluted in KHB (5-fold dilution) and a volume of 0.2 ml MTS solution was added per well. The cultures were incubated with MTS for 1 h under standard culture conditions. The absorbance was read at 490 nm against a background absorbance of 620 nm. After the MTS incubation, the cultures were washed twice with PBS⁻ and the proteins dissolved in 0.2 ml protein lysis buffer. The protein content was measured using the Pierce assay according to the manufacture's protocol.

2.2.3 Hepatic models – Liver organoids

2.2.3.1 Generation of liver organoids

Upcyte[®] and primary cells used to generate liver organoids were pre-cultured in 2D according to Section 2.2.1.2 in cell-specific growth medium. One day before the generation of the liver organoids, culture plates, *Quasi-vivo*[®] chambers (Kirkstall Ltd.) and pipette tips were cooled

MATERIALS & METHODS

to 4°C. Matrigel™ (BD) was thawed overnight at 4°C. On Day 1 of the generation of liver organoids, Matrigel™ was mixed to homogeneity using cooled pipettes and then diluted in a 1:1 ratio with upcyte® LSEC growth medium. For generation of one liver organoid in a 24-well format or in *Quasi-vivo*® System, 380 µl of diluted Matrigel™ was required (~200 µl/cm²) resulting in a thick layer of matrix. Using pre-cooled pipette tips, Matrigel™ was added to the plates/chambers and incubated at 37°C for 30 min to polymerize. The cells were trypsinized according to the method described in Section 2.2.1.3 and the cell pellets were re-suspended in liver organoid growth medium. Liver organoid growth medium was prepared by adding upcyte® HGM and upcyte® LSEC growth medium in 1:1 ratio. The liver organoid was prepared by mixing the cells mixture as shown in Table 6 and added to the plates/chambers containing the thick layer of Matrigel™. The cell mixture was incubated under standard culture conditions for the formation of liver organoids.

Table 6. Number of cells required to form organoids according to the cell type in a 24-well format.

Cell type	Cell number
upcyte® hepatocytes (Donor 422A-03)	1.0 x 10 ⁶
upcyte® / primary MSC	0.2 x 10 ⁶
upcyte® LSECs	1.0 x 10 ⁶

2.2.3.2 Liver organoids in *Quasi-vivo*® System

To create conditions that were more physiologically relevant, liver organoids were also cultured in a dynamic system, namely the *Quasi-vivo*® System (Kirkstall Ltd.). The basic building blocks of this system are QV500 chambers, which are made of poly-dimethylsiloxane (PDMS), a biocompatible silicone polymer with a surface area similar to that of a 24-well multi-well format. The liver organoids were generated in the *Quasi-vivo*® chambers under static conditions. After 24 h, chambers containing the liver organoids were connected to the dynamic system and cultured with a medium flow rate of 300 µl/min. The medium was changed every alternate day. Liver organoids were cultured for 7 days in liver organoid growth medium and then for 3 days in HPM. Liver organoids were incubated for 3 consecutive days (day 7 to 10) in HPM containing 20 µM rifampicin in order to determine the CYP3A4 induction response in these organoids. The medium was changed every day during the induction period. For basal activities, organoids were cultured for 3 days (day 7 to 10) in HPM containing 0.1% DMSO. Incubation of liver organoids with 500 µM in KHB of testosterone as a substrate metabolized by CYP3A4 were carried out on Day 10 according to the method described in Section 2.2.5.3 using 500 µM testosterone in KHB.

MATERIALS & METHODS

2.2.3.3 Scalability to different well formats

The scalability of liver organoids to 48-well formats and 96-well formats was achieved by reducing the cell numbers according to Table 7. In the static system, the organoids were cultured in liver organoid growth medium for 4 days with daily medium changes and then fixed with formalin for histological studies (see Section 2.2.3.5).

Table 7. Cell numbers required for different formats and different cell types.

Cell type	Cell number	
	48 well	96 well
upcyte [®] hepatocytes (Donor 422A-03)	0.5×10^6	0.25×10^6
upcyte [®] / primary MSC	0.1×10^6	0.05×10^6
upcyte [®] LSECs	0.5×10^6	0.25×10^6

2.2.3.4 Immunocytochemistry in 2D monolayer

Upcyte[®] hepatocytes/LSECs/MSCs and primary MSCs were seeded at a density of 10,000 cells/well in a 96-well plate and cultured for 2 days in cell-specific growth medium. Cells were washed twice with PBS⁻ and then fixed with 4% paraformaldehyde for 5 min. After washing three times with PBS⁻, cells were blocked using 3% BSA in PBS⁻ for 20 min to saturate unspecific binding sites. For detection of different markers, fixed cells were incubated with the respective primary antibodies. Cells were incubated for 45 min at 37°C with the primary antibody diluted in 0.2% BSA/PBS⁻ (washing buffer) to detect CD31 (1:300), vimentin (1:200) or cytokeratin 8/18 (1:50). Wells were washed again three times with washing buffer to remove unbound primary antibody and incubated for 45 min at 37°C with the respective secondary antibody. CyTM3-conjugated Affinity Pure Goat anti-Mouse IgG was used as a secondary antibody (at a dilution of 1:200 in 0.2% BSA in PBS⁻). The secondary antibody solution additionally contained DAPI (final concentration of 300 nM) in order to counterstain cell nuclei. After washing the cells three times in washing buffer, cells were analyzed using a fluorescence microscope. The immunocytochemical stainings were analyzed at a wavelength of 553 nm. This was compared with the cellular morphology of the culture observed using phase contrast microscopy.

2.2.3.5 Immunohistochemistry of 3D organoid

Immunoperoxidase-based immunohistochemistry was performed to stain 2 µm sections of paraffin-embedded liver organoids. The following primary antibodies were used: mouse anti human CK8/18 (monoclonal, concentrated, pH6), rabbit anti human vimentin (monoclonal,

MATERIALS & METHODS

1:400, pH 6), and mouse anti human CD31 (monoclonal, 1:500, pH 9). Immunohistochemistry was performed as described previously using the following: antigen retrieval in Novocastra antigen retrieval solution pH 6 or pH 9.0; blocking of endogenous peroxidase (DAKO blocking solution); detection of bound antibodies by the immunoperoxidase/DAB-based DAKO REAL detection system (DAKO).

2.2.3.6 *In situ* hybridization

Detection of mRNA transcripts in paraffin sections was performed. The protocol is based on the preparation of DNA *in vitro* transcription templates using PCR, with primers that include RNA polymerase promoter sequences and size-based purification of PCR fragments containing the target gene-specific cDNA and promoter elements for T7 and SP6 RNA polymerase. The primer sequences listed in Section 2.1.7 were used.

2.2.4 Hepatic models – Liver organoids/BioVaSc

2.2.4.1 Explantation of BioVaSc

The experiments on culturing of liver organoid in biological vascularized scaffold (BioVaSc) were carried out in collaboration with Holger Kirch (M.Sc.) from University of Würzburg. The porcine jejunal segment was from German landrace pigs from Sigmaringen. At the time of explantation the pigs were 8 to 9 weeks old and weighed up to 30 kg. Prior to sacrifice, the animals were administrated heparin. The performed organ harvesting was performed according to the third section of the Animal Welfare Act, "killing animals" (§ 4 para 3 of the Animal Welfare" killing of animals for scientific purposes"). Abdominal cavity was cut open to expose the intestinal section connected to stomach (duodenum, jejunum). This enabled the location of suitable artery and vein pairs (the associated lymph node tissue was removed to achieve this). Arteries and veins were cannulated with an IV catheter and the intestinal segment rinsed with 0.9% NaCl solution. A section of intestinal lumen of between 10-15 cm in length with preserved vascular system (arterial and venous inflow), was tied off for explanation. The harvested biological vascularized scaffold is called a BioVaSc (Figure 9 b). The BioVaSc was transported on ice in a sealed plastic container containing cold PBS⁻ with 1% gentamycin. The decellularization was carried out either directly on the day of surgery, or no later than one day after, provided the BioVaSc is sufficiently flushed with 0.9% NaCl solution (Figure 9 c).

MATERIALS & METHODS

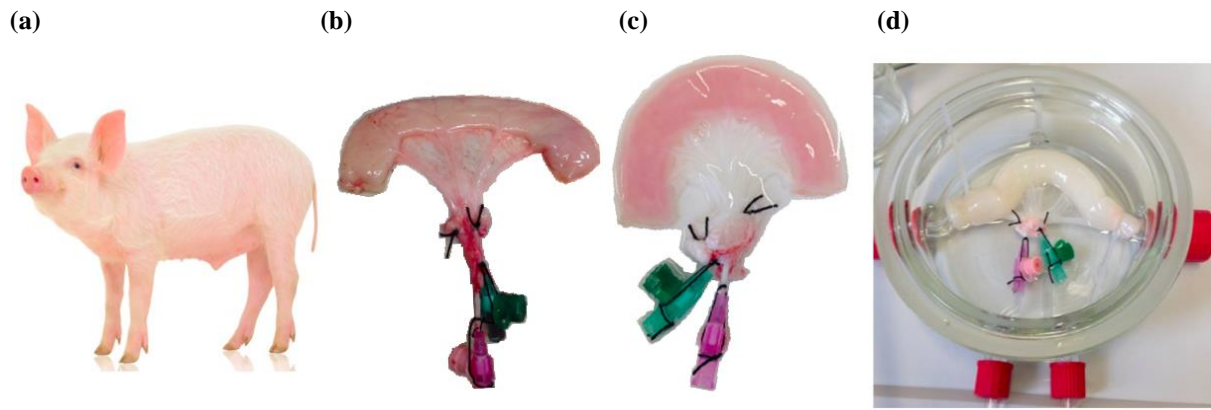


Figure 9: a) Pigs used were German landrace pigs from Sigmaringen, b) BioVaSc harvesting: 10–15 cm long segment of jejunum was harvested including its artery and vein outlets. c) Blood vessels and lumen portion of the BioVaSc was thoroughly flushed with PBS⁺ 1% gentamycin, streptomycin and penicillin at 4°C. d) Arterial vascular pedicle was connected to a bioreactor system and perfused with 500 ml of 3% sodium deoxycholate for chemical decellularization.

2.2.4.2 Decellularization of BioVaSc

Decellularization of the jejunal segment was carried out by a modified method of Meezan (Meezan et al. 1975). Decellularization solution was flushed into the BioVaSc via artery to remove blood. The BioVaSc was then transferred into a bioreactor and the arterial vascular pedicle of the BioVaSc was connected to the bioreactor system (Figure 8 d). A volume of 500 ml of pre-cooled decellularization solution was perfused through the BioVaSc at a rate of 1.8-2.8 ml/min for 60-90 min. The pressure was adjusted to 80 mm Hg, so as not to destroy the vascular system. In addition, the lumen of the tissue was rinsed with 500 ml of decellularization solution through the vascular system. The decellularized intestinal segment was flushed with 1000 ml PBS⁺ at a rate of 2.8-5 ml/min via arterial perfusion for 1-2 h. The pressure was adjusted to 100 mm Hg. The resulting tissue was white in colour and no longer pinkish-red. It was important to ensure no air bubbles were pumped through the vascular system. In the next step, decellularized scaffold was rinsed with 150 ml DNase I (60 mg in PBS⁺) with 1% gentamycin, and incubated at 4°C. In order to remove the sodium deoxycholate from the BioVaSc, it was transferred to a glass bottle and rinsed further with PBS⁺ containing 1% gentamycin for 3 consecutive days. For best washing results, rinsing was carried out using a rotator maintained at 4° C. The BioVaSc was sterilized overnight by irradiating it with 25 kGr in pre-cooled PBS⁺ containing 1% gentamycin. The resulting matrix could be stored at 4°C until used. Before populating with cells, BioVaSc was incubated overnight in the cell-specific medium.

MATERIALS & METHODS

2.2.4.3 Colonization of the BioVaSc

The vascular system of the BioVaSc was colonized with upcyte[®] mvECs in two steps. Upcyte[®] mvECs were cultured/passaged and harvested as described in Section 2.2.1.2/3. Cells were resuspended in the required amount of vericyte[®] endothelial cell growth medium (ECGM) to achieve a density of $1.5\text{-}3.5 \times 10^6$ cells/ml of medium. The BioVaSc was clamped in the bioreactor, which was then filled with vericyte[®] ECGM. In step 1, colonization of the vascular system was done by injecting upcyte[®] mvECs into the BioVaSc via the arterial inflow using a 10 ml syringe (2-3 times with 2 ml of cell suspension with 45 minute break each time). To allow the cells to adhere to BioVaSc, the tissue was perfused with minimal media flow (1.26 ml/min) for 45-60 min. In step 2, the same method of injection was used via arterial inflow. On Day 1, the cells were incubated with a pulsating pressure of 20 mm Hg (\pm 10 mm Hg). The next day, the pressure was gradually increased to 100 mm Hg (\pm 20 mm Hg) over 7 h and the pressure was maintained throughout the culture period. The BioVaSc was cultured in vericyte[®] ECGM containing 1% gentamycin at 37°C, 5% CO₂ in a specially developed chamber for 10 to 14 days (Figure 10). A medium change was performed every 3-4 days. In order to ensure optimal culture conditions, parameters such as temperature, gas exchange, pumping power and pressure in the bioreactor was computer-controlled (Hewlett-Packard, Böblingen, software: Measure foundry, Data Translation, Bietigheim-Bissingen). After 10-14 days of culture, the lumen was colonized with liver organoids

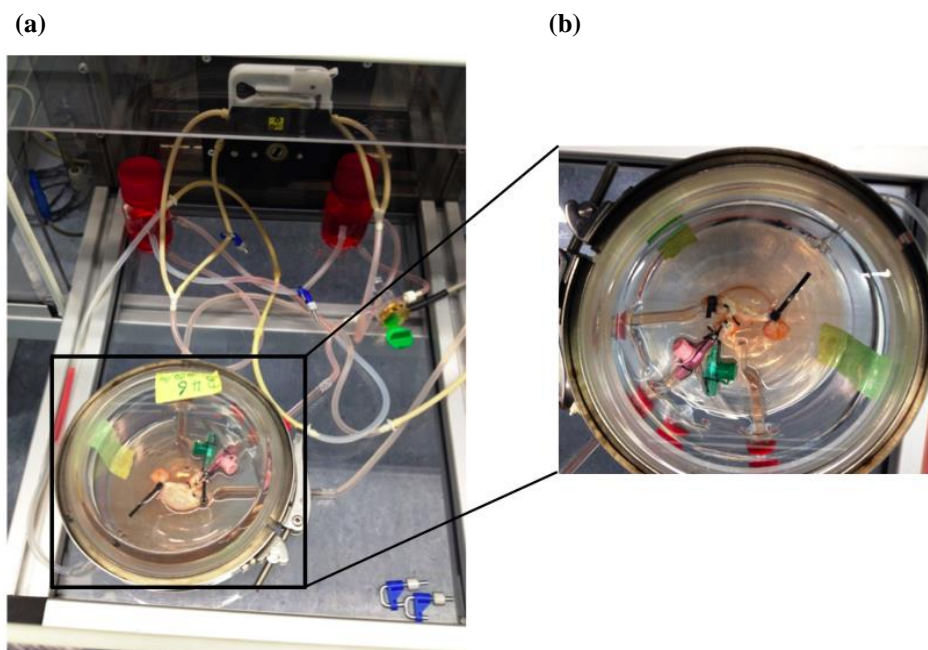


Figure 10: BioVaSc colonized with upcyte[®] mvECs and cultured in the bioreactor for 14 days

MATERIALS & METHODS

2.2.4.4 Liver organoids in BioVaSc

Generation of liver organoid was carried out in 48-well formats (Figure 11a) as described in Section 2.2.3.3 Bioreactors with the BioVaSc colonized with upcyte[®] mvECs were cultured for 14 days, after which time they were disconnected from the system and carefully transferred to a laminar airflow. Freshly generated liver organoids cultured in static conditions for 48 h were then placed in the BioVaSc using a sterile spatula (Figure 11b & c). The BioVaSc colonized with liver organoids was then returned to the bioreactor chamber. After 24 h, the dynamic flow was started and the pressure was adjusted to 80 mm Hg (reflecting physiological conditions). The liver organoids were cultured inside the BioVaSc for 30 days in liver organoid growth medium containing 1% gentamycin.

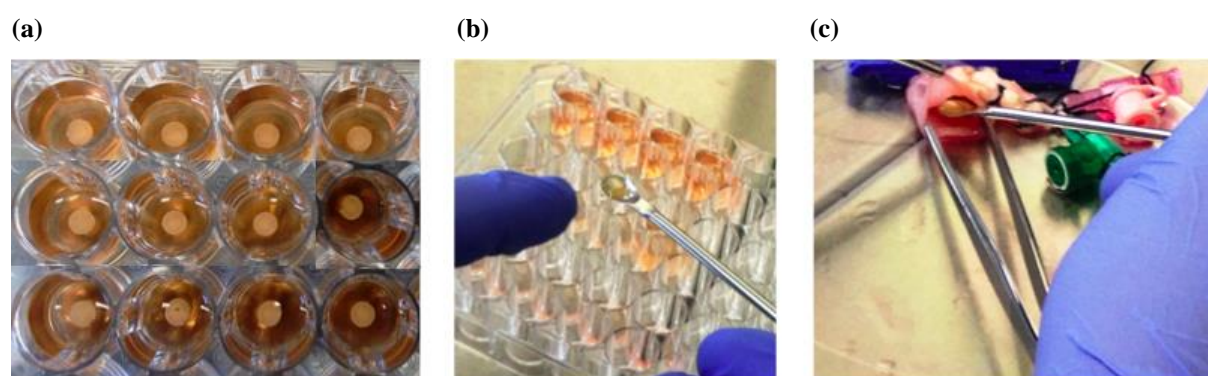


Figure 11: a) Liver organoids generated in 48-well multi-well plate b) & c) Liver organoids transferred from multi-well plate into BioVaSc for long-term culture.

2.2.5 Application of hepatic models - inhibition/induction study

2.2.5.1 Pre-culture conditions for inhibition/induction study

Two pre-culture durations were used: A standard pre-culture of 3 days, with a PD of one, or a longer 6-7 day pre-culture with a PD of 3.5. Standard pre-cultures were used for testing the induction of all 4 CYPs by a single concentration of inducer (as part of the quality control of the cell batch). All other inhibition and induction assays were conducted using a 6-7 day pre-culture period. Standard pre-culture involved seeding the cells at 75,000 cells/cm² in HPM medium (0.5 ml/well) in collagen Type I-coated 48-well plates. The cells were cultured for 3 days without a medium change, after which time, the medium was replaced with fresh HPM with the respective control and inducer compounds. For the longer pre-culture period, upcyte[®] hepatocytes were seeded at 5,000 cells/cm² in collagen Type I-coated T150 flasks in HGM and pre-cultured for up to 1 week or until they reached 70-80% confluence. The medium was changed every 2-3 days. The cells were then trypsinized and re-seeded into 48-well plates at 150,000 cells/cm² (confluence) in HPM (0.5 ml per well).

MATERIALS & METHODS

2.2.5.2 Upcyte[®] hepatocyte inhibition assays

For inhibition assays, after the cells had attached (2-4 h), the medium was replaced with either HGM or HPM containing either 0.1% or 0.5% DMSO. The cells were cultured for a further 3 days during which time the medium was replaced daily with the appropriate medium. Cultures that were subsequently used for CYP1A2 inhibition assays were treated daily for 3 days with 100 μM omeprazole to pre-induce this CYP. After this time, the cells were used for inhibition assays. The cells were washed twice with PBS⁺ and pre-incubated with 0.1 ml of an appropriate CYP inhibitor dissolved in KHB. α -naphthoflavone (0.1 to 10 μM), miconazole (0.01 to 50 μM) and ketoconazole (0.01 to 20 μM) were pre-incubated for 5 min and ticlopidine (0.01 to 50 μM) was pre-incubated for 30 min (since this is a mechanism based inhibitor). CYP activities were measured by adding 0.1 ml of the CYP-selective substrate in KHB and incubating for 1 h (final concentrations were: 26 μM phenacetin, 500 μM bupropion, 75 μM tolbutamide and 250 μM testosterone).

2.2.5.3 Upcyte[®] hepatocyte induction assays measuring CYP activities

There were two types of induction assays carried out: (1) standard induction assays in which a single concentration of prototypical CYP inducer was tested to determine CYP1A2, CYP2B6, CYP2C9 and CYP3A4 induction and (2) calibration induction assays in which a range of concentrations of test compounds were incubated to determine their potential to induce CYP2B6 and CYP3A4 only. For both assays, after attachment of upcyte[®] hepatocytes in 48-well plates, the medium was replaced with HPM and the cells were cultured for 24 h. After this time, the cells were treated daily for 3 days with the test compound/prototypical inducer. For standard induction assays, the prototypical inducers were 50 μM omeprazole (CYP1A2 inducer), 1 mM phenobarbital (CYP2B6 inducer) and 20 μM rifampicin (CYP2C9 and CYP3A4 inducer). At the end of the induction period, the cells were washed with PBS⁺ and CYP activities were measured by adding 0.2 ml KHB containing final concentrations of CYP substrate: 26 μM phenacetin, 500 μM bupropion, 75 μM tolbutamide and 250 μM testosterone and incubating for 30 min (testosterone) or 1 h (phenacetin, bupropion and tolbutamide). After incubation, the supernatant was transferred to a fresh 96-well plate and processed for HPLC analysis. For induction assays generating dose response curves for CYP3A4 and CYP2B6 and subsequent calibration curves relating to *in vivo* induction, the test compounds were rifampicin (0.05-40 μM), phenobarbital (20-2000 μM), phenytoin (1-1000 μM), carbamazepine (1-100 μM), troglitazone (0.5-50 μM), pioglitazone (0.5-40 μM),

MATERIALS & METHODS

dexamethasone (0.1-500 μM), nifedipine (0.05-100 μM), omeprazole (0.5-200 μM), flumazenil (0.05-100 μM), and quinidine (0.1-250 μM). At the end of the induction period, the cells were washed with PBS⁺ and a volume of 0.2 ml of 250 μM testosterone in KHB was added to each well and incubated for 30 min. The supernatant was transferred to a fresh standard cell culture 96-well plate and processed for HPLC analysis. The remaining cell cultures were again washed twice with PBS⁺ and then incubated with 500 μM bupropion in KHB for 1 h. The supernatant was transferred to a fresh standard cell culture 96-well plate and processed for HPLC analysis.

2.2.5.4 Calculation and curve fitting

Experiments were carried out in duplicate and each compound was tested in at least 2 different experiments. All curve-fitting was carried out using Prism Version 8.0 software. Dose response curves for test compounds from calibration induction assays (Section 2.2.2.4) were generated and the Ind_{max} and Ind_{50} values were determined by fitting the data to a three-parameter sigmoid (Hill) equation as described by Ripp (Ripp et al. 2006). Ind_{max} is the maximum fold induction of CYP activity induced by the compound and Ind_{50} is the concentration at which 50% maximal induction was achieved. The Relative Induction Score (RIS) was determined using Equation 2:

$$\text{RIS} = \frac{C_{\text{max,u}} \times \text{Ind}_{\text{max}}}{C_{\text{max,u}} + \text{Ind}_{50}} \quad \text{Equation 2}$$

The $C_{\text{max,u}}$ value for omeprazole was taken from Mostafavi and Tavakoli (Mostafavi & Tavakoli 2004); the $C_{\text{max,u}}$ value for all other compounds used for RIS determinations were taken from Ripp (Ripp et al. 2006) or Fahmi (Fahmi et al. 2008). (values for quinidine and flumazenil were not needed since they were the negative control compounds).

The relative induction of CYP3A4 and CYP2B6 by different compounds compared to the positive control was calculated using Equation 3:

$$\% \text{ Relative PC induction} = \frac{\text{Ind}_{50, \text{TC}} - 1}{\text{Ind}_{50, \text{PC}} - 1} \quad \text{Equation 3}$$

Where $\text{Ind}_{50, \text{TC}}$ is the Ind_{50} of the test compound and $\text{Ind}_{50, \text{PC}}$ is the Ind_{50} of the positive control (rifampicin for CYP3A4 and phenobarbital for CYP2B6).

MATERIALS & METHODS

2.2.5.5 Metabolite analysis by HPLC

All metabolites were analyzed using UV-HPLC.

Sample preparation

CYP1A2

After the substrate incubation, the supernatants (200 μ l) were transferred to fresh 96-well plates for extraction. To each 200 μ l sample, 10 μ l of the internal standard (1 mg/ml chlorpropamide) was added. The samples were then transferred to separate 10 ml glass tubes. To each of the glass tube containing samples, 3 ml diethyl ether was added. The samples were mixed by gentle vortexing for 4 seconds. The vortexing was repeated to maximize the extraction of the metabolites from the sample into the diethyl ether. The samples were allowed to settle so that the aqueous phase was separated from the diethyl ether. The lower aqueous phase was removed and discarded, leaving the diethyl ether phase. The samples were dried under a stream of nitrogen gas and then reconstituted in 30 μ l of 1:1 methanol:distilled water.

CYP3A4, CYP2B6 and CYP2C9

After the substrate incubation, the supernatants (200 μ l) were transferred to fresh 96-well plates for extraction. To each 200 μ l sample, 10 μ l of the internal standard was added. For testosterone and its metabolite, 0.5 mM cortexolone was used as internal standard. For tolbutamide and bupropion and their metabolites, 0.1 mg/ml chlorpropamide was used as internal standard. An Oasis[®] μ Elution plate was prepared by conditioning the wells/columns with 200 μ l 100% methanol. The solvent was pushed through the columns using the positive pressure manifold, according to the manufacturer's instructions. The wells/columns were washed with 200 μ l of 100% water. The water was pushed through the columns using the positive pressure manifold. The standards and samples were loaded into the wells and pushed them through the columns. A clean 96-well plate was paced below the plate separator so that the samples will be collected in this plate. To all the wells/columns containing sample or standard, 10 μ l of solvent (Solvent: 100% isopropanol for testosterone and 2% formic acid in methanol for tolbutamide and bupropion) was added and pushed through the columns using the positive pressure manifold. A second 10 μ l of the respective solvent was added to each well containing sample or standard and pushed through the columns using the positive pressure manifold. The collection 96-well plate was removed from the Positive Pressure

MATERIALS & METHODS

Manifold and 20 μ l of 100% water was added directly to each of the sample after the extraction process.

The samples were transferred to an HPLC glass insert inside the glass vial. Air bubbles were removed from the sample and the samples were transferred to the HPLC autosampler for analysis. All metabolites and their respective internal standards (chlorpropamide for phenacetin, bupropion and tolbutamide and cortexolone for testosterone) were separated on a SunFire C18 2.5 μ m 2.1 \times 20mm column (Waters, Munich, Germany). The substrates for each CYP and their metabolites are shown in Table 8, together with the UV detection wavelength.

Table 8. CYPs, substrates, metabolites and corresponding detection wavelengths.

CYP	Substrate	Metabolite	Detection wavelength (nm)
CYP1A2	Phenacetin (26 μ M)	Acetaminophen	240
CYP2B6	Bupropion (500 μ M)	4-Hydroxybupropion	200 229
CYP2C9	Tolbutamide (75 μ M)	4-Hydroxymethyl-tolbutamide	200 229
CYP3A4	Testosterone (250 μ M)	6 β -hydroxytestosterone	252

2.2.6 Application of hepatic models – Haemophilia Therapy

2.2.6.1 Cloning of FVIII gene

The full length FVIII gene was derived from pSP64-FVIII-FL [(Toole et al. 1984); ATCC: K01740]. As the B-domain of FVIII gene does not play a role in the coagulation cascade, nucleotides (2428-5067) corresponding to the B-domain were deleted as described by (Tonn et al. 2002). To mediate the Gateway[®] BP recombination reaction with a donor vector, the FVIII gene (B-domain deleted) was incorporated with *attB* sites using the cocktail (Table 9) and quantitative real-time (PCR) programme shown in Table 10.

Table 9. Cocktail used for the Gateway[®] BP recombination reaction.

Components	Amount 20 μ l rxn. vol.	Final Concentration
5X Phusion [®] reaction HF buffer or GC buffer	4 μ l	1X
10 mM dNTP-mix	0.4 μ l	200 μ M
Forward primer 10 μ M, FVIII- pENTR FWD	1.0 μ l	0.5 μ M

MATERIALS & METHODS

Reverse primer 10 uM FVIII-pENTR REV	1.0 µl	0.5 µM
Template DNA (100ng/ul), FVIII	1 µl (100 ng)	< 250 ng
Nuclease free H2O	to 20 µl	
Phusion polymerase (2.000 U/ml)	0.2 µl (0.4 U/20 µl)	1.0 U/50 µl PCR

Table 10. PCR programme used for the Gateway[®] BP recombination reaction.

Cycle step	Temperature	Time	Cycles
Initial denaturation	98°C	30 sec	1
Denaturation	98°C	7 sec	32
Annealing	65°C	20 sec	
Extension	72°C	2,5 min	
Final extension	72°C	7 min	1
Hold	4°C	Unlimited	

The PCR programme was performed using Qiagen rotor genes. The FVIII gene, flanked by the *attB* site, was purified using quick-start protocol from the QIAquick[®] PCR purification kit. The concentration and purity of the resulting DNA was determined by measuring the absorbance at 260 nm and 280 nm on a Nanodrop spectrophotometer.

2.2.6.2 Generation of entry clones using BP Reaction

The *attB*-flanked FVIII gene was used to create entry clone according to the protocol described in the BP Clonase[™] II enzyme kit. The cocktail for the BP reaction is shown in Table 11.

Table 11. Cocktail for the BP reaction.

<i>attB</i> - flanked FVIII gene (100 ng)	1 µl
pDONR-Donor vector (150 ng/µl)	1 µl
TE buffer, pH 8.0	6 µl
BP Clonase [™] II enzyme mix	2 µl

2.2.6.3 Transformation and plasmid extraction

A volume of 2 µl of BP reaction mix was added to 8 µl of Mega DH10B[™] T1^R electrocompetent *E.coli* cells and mixed gently. The Eppendorf tubes containing BP reaction mix and electrocompetent cells were transferred into a chilled electroporator cuvette and pulsed in an electroporator using Program EC-1. The cuvette was removed and 1 ml of 20°C

MATERIALS & METHODS

warm SOC medium was added immediately and the entire contents of the cuvette were transferred into a 2 ml Eppendorf tube. The bacteria were then incubated at 37°C for 1 h in a Thermomixer (150 xg). After this time, the samples were centrifuged at 150 ×g for 5 min. The supernatant was discarded, leaving behind a volume of approximately 100 µl. The pellet was re-suspended in the medium and streaked onto LB agar plates containing 100 µg/ml kanamycin. The plates were placed upside down and incubated at 37°C overnight for bacterial colony to grow. Nine colonies were randomly picked for replica plating and these were inoculated in 3 ml of LB agar broth containing 100 µg/ml kanamycin. The vials and replica plates were incubated at 37°C overnight to allow bacterial growth. The plasmid extraction was carried out according to the QIAprep[®] Spin Miniprep Kit protocol and the concentration and the purity of the DNA was determined by measuring the absorbance at 260 nm and 280 nm on a Nanodrop spectrophotometer.

2.2.6.4 Double restriction hydrolysis of entry clone

To check for the integration of the FVIII transgene into the entry clone, 1 µg of DNA was taken for double restriction hydrolysis using Bsa H1 and Spe 1. The quantity of ingredients is shown in Table 12.

Table 12. Ingredients for double restriction hydrolysis.

Composition	Volume
Bsa H1 (10,000 U/ml)	4 U
Spe 1 (10,000 U/ml)	4 U
10X NE buffer	5 µl (1X)
DNA	1 µg
Incubation time	1 h
Incubation temperature	37°C
Total Reaction volume	50 µl
Heat inactivation	80°C -20 min

2.2.6.5 Generation of expression clones using LR Reaction

The expression clones were generated using LR Reaction as described in the LR Clonase[™] II enzyme kit protocol. The cocktail for the LR reaction is shown in Table 13.

Table 13. Cocktail for the LR reaction.

Composition	Volume
Entry clone (120 ng/µl)	5 µl
Destination vector (150 ng/µl) pLenti6 V5 Dest	1 µl

MATERIALS & METHODS

TE buffer, pH 8.0	2 μ l
LR Clonase™ II enzyme mix	2 μ l

A volume of 2 μ l of LR reaction mix was added to 50 μ l ElectroMAX™ Stbl4™ electrocompetent *E.coli* and the cells, and the sample was then gently mixed. Electroporation and plasmid extraction was carried out as described in Section 2.2.6.3. As an antibiotic selection process, 100 μ g/ml ampicillin was added to the LB agar plates and incubated at 30°C overnight in order to prevent recombination.

2.2.6.6 Double restriction hydrolysis of expression clone

To check the presence of FVIII transgene in the expression clone, 1 μ g of DNA was taken for restriction hydrolysis using Spe 1. The corresponding composition for restriction hydrolysis is shown in Table 14

Table 14. Restriction hydrolysis solution composition.

Composition	Volume
Spe 1 (10,000 U/ml)	4 U
10X NE buffer	5 μ l (1X)
DNA	1 μ g
Incubation time	1 h
Incubation temperature	37°C
Total reaction volume	50 μ l
Heat inactivation	80°C -20 min

2.2.6.7 Midi preparation and sequencing of FVIII transgene

The expression clone that was positive for the presence of FVIII gene by double restriction hydrolysis was used to inoculate a starter culture. A volume of 2 ml starter culture was grown from the plate for 8 h in LB broth containing 100 μ g/ml of ampicillin at 30°C with a rotation of 200 rpm. The starter culture was used to inoculate 200 ml of culture to extract plasmid for sequencing. The flask was incubated at 30°C overnight with a rotation mixing at 200 rpm for the bacterial growth. The plasmid extraction was carried out according to the QIAprep® Spin Midiprep Kit protocol and the concentration of the DNA was determined by measuring the absorbance at 260 nm and 280 nm on a Nanodrop. Oligonucleotide primers were designed to analyse the FVIII gene in the expression vector. Approximately 2 μ g of DNA was sent to GATC Biotech for sequencing.

MATERIALS & METHODS

2.2.6.8 Lentiviral production and Transduction

The production of lentiviral particles was carried out according to a modified protocol of Scherr and colleagues (Scherr & Eder, 2002). For safety reasons, the production is based on a four-plasmid system. The day before transfection (Day 1), 3 ml poly-D-lysine (100 g/ml in PBS⁻) was added to coat the 10 cm petri dish, which was incubated at room temperature for 5 min. Poly-D-lysine was aspirated and the plates were rinsed with 5 ml of sterile water. 293 FT cells (5×10^6) were seeded in a 10 cm tissue culture plate to achieve a confluence of 90–95% on the day of transfection. The cells were cultured in DMEM medium containing 10% non-heat inactivated FBS, 6 mM L-glutamine, 0.1 mM MEM non-essential amino acids, and were incubated at 37°C under standard culture conditions. On day 2 of transfection, the culture medium was aspirated and 5 ml Opti-MEM[®] I medium containing 10% FBS was added to each plate. Plasmids (9 µg) from the ViraPower[™] Packaging Mix and pLenti FVIII expression vector (3 µg) were diluted in 1.5 ml serum-free Opti-MEM[®] I Medium and mixed gently. In a separate sterile tube, Lipofectamine[™] 2000 was prepared and combined with the diluted DNA. The contents were mixed gently and incubated at RT for 20 min to allow the DNA-Lipofectamine[™] 2000 complexes to form. DNA-Lipofectamine[™] 2000 complexes were added drop-wise to each plate of cells. The plates were mixed gently by rocking back and forth and incubated overnight.

The next day (Day 3), the DNA-Lipofectamine[™] 2000 complex medium was removed and replaced with 10 ml of complete culture medium (DMEM supplemented with 10% non-heat inactivated FBS, 6 mM L-glutamine, 0.1 mM MEM non-essential amino acids, 10 mM of sodium butyrate) and incubated further at 37°C under standard culture conditions. During this time, the expression of the VSV G glycoprotein causes 293FT cells to fuse, resulting in the appearance of large, multinucleated cells known as “syncytia”. After 4 to 5 h, the medium was discarded and fresh DMEM without any supplements was added to the plates and incubated under standard culture conditions. On Day 4, virus-containing supernatant was harvested and filtered through a 0.45 µm Whatman[®] filter. In order to concentrate the virus particle, a Vivaspin column with a molecular weight cutoff of 100,000 Da was used. After washing with 10 ml of PBS⁻, the supernatant was added to the top of the column, which was then centrifuged ($300 \times g$) until the supernatant was concentrated to 500-1000 µl). The concentrated virus supernatant was aliquoted in 50 µl volume and stored at -80 °C.

MATERIALS & METHODS

2.2.6.9 Titration of virus supernatant

The amount of virus particles per ml of solution was determined directly by titrating the amount of viral RNA using quantitative real-time PCR (qRT-PCR). qRT-PCR was performed using a modified protocol from Scherr (Scherr et al. 2001). The primer binding to the long terminal repeat (LTR) sequence of the viral vector backbone was used. A reference standard curve was prepared by diluting the vector from 1:10¹ to 1:10⁹. Plasmids that contained the LTR sequence were amplified with the primers. In addition, various dilutions of the virus suspension (1:100, 1:1000 and 1: 10,000) were made. All reactions were carried out in triplicate according to the reaction mixture summarized in Table 15.

Table 15. Reaction mixture for qPCR.

Mastermix	1x
2x QuantiFast SYBR Green	7.5 µl
LTR Primer Mix 1:20	1 µl
Nuclease free water	5.5 µl
Sample to be measured	1 µl
	15 µl

qRT-PCR measurement was performed using a Qiagen rotor genes according to the program shown in Table 16.

Table 16. qPCR program.

Cycle step	Temperature	Time
1	95°C	15 min
2	94°C	15 sec
3	55°C	30 sec
4	72°C	30 sec
5 Go to step 2		40x
6 Melting curve		

To determine the concentration of virus particles in the suspension, a standard curve was derived for the vector (correlation <0.99). For this, the concentration of the vector was plotted against the corresponding Ct value. Using a linear equation, Ct values of the virus suspension were assigned against the concentration of the vector (FVIII).

2.2.6.10 Transduction

Upcyte[®] endothelial cells (BOECs, mvECs and LSECs) and primary mvECs were seeded according to Section 2.2.1.2 After 24 h, the cells were transduced with lentiviral particles at three different multiplicity of infection (MOI 1000, 10,000 and 100,000) (Figure 12). The MOI reflects the ratio of the infectious viral particles into the target cell. For example, an MOI of 1000 means each of the transduced cells will receive 1000 times the FVIII gene. To enhance the lentiviral transduction, 6 µg/ml of hexadimethrine bromide (polybrene[®]) was added to the culture medium. The medium was changed with fresh medium without lentivirus after 8 h and cultured further. Before plating the cells for FVIII supernatant harvest, they were grown for 5 to 6 passages.

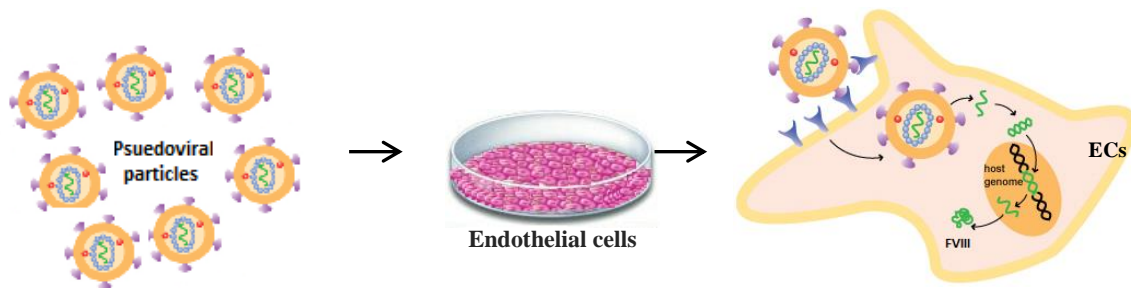


Figure 12: Schematic overview of lentiviral transduction into human endothelial cells (Picture source: www.invivogen.com - Modified)

2.2.6.11 Cytotoxicity curve analysis

In order to obtain a homogeneous population of FVIII secreting primary mvECs, it is important to select the transduced population from the non-transduced cells. The lentiviral construct used to transduce the FVIII gene also carries a gene for Blasticidine[®]. As an antibiotic selection process, the primary mvECs from same donor as upcyte[®] mvECs were transduced with three different MOIs (MOI 1000, 10,000 and 100,000) and selected using Blasticidine[®]. To determinate the optimal concentration of Blasticidine[®] required to eliminate non-transduced cells, a cytotoxicity curve was established over various concentrations. The concentration of blasticidine selected was the lowest concentration that killed 100% of the non-transduced cells and but resulted in maximal survival of transduced cells. To derive the cytotoxicity curve, cells were plated at approximately 25% confluence in 6-well plates and allowed to attach overnight. The next day, culture medium containing varying concentrations of blasticidine (i.e. 0, 2, 4, 6 and 8 µg/ml) was added to the wells. The medium was changed every 2 to 3 days, during which time, the percentage of surviving cells was observed. The appropriate concentration of blasticidine that was toxic to the cells within 10-14 days after addition of the antibiotic was determined. Therefore, the minimum antibiotic concentration

MATERIALS & METHODS

that eliminated all the non-transduced cells was used for cultures containing primary mvECs transduced with FVIII gene. During the 14-day culture period, a homogeneous population of primary mvECs carrying FVIII gene was selected (Figure 13).

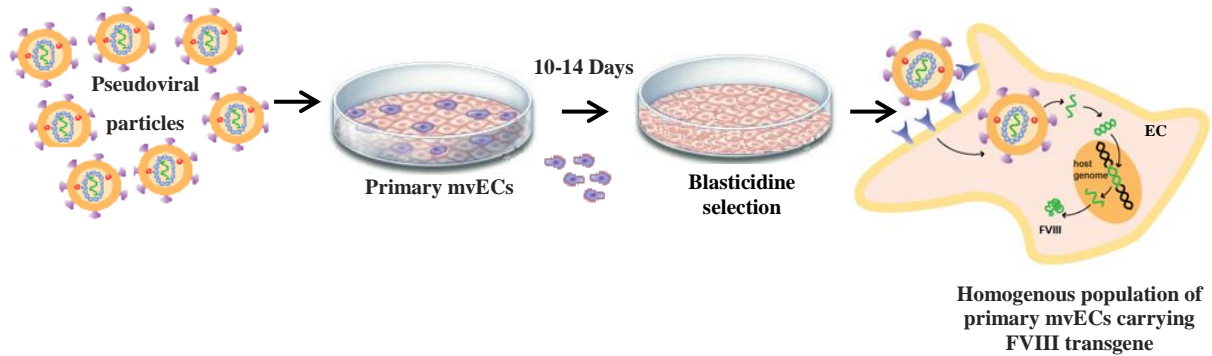


Figure 13: Pictorial representation of lentiviral transduction, followed by antibiotic selection to obtain uniform population of cells carrying FVIII gene (Picture source: www.invivogen.com - Modified)

2.2.6.12 Tube formation assay

The tube formation assay was used to study angiogenesis based on the method described by Arnaoutova (Arnaoutova et al. 2009). The assay was performed according to a modified protocol of Kubota (Kubota et al. 1988). A volume of 50 μl of MatrigelTM was pipetted onto a pre-cooled 96-well multi-well plate and incubated for 30 min at 37° C to polymerize. Thereafter, the cells were diluted in vericyte[®] ECGM and then plated onto the MatrigelTM at different densities (14,000 cells/cm² and 20,000 cells/cm²). The cultures were incubated for 6 h under standard culture conditions. The cells were then observed under light microscope for the formation of tubular networks.

2.2.6.13 FVIII analysis from different cell cultures

Primary LSECs

Freshly harvested and frozen supernatants from primary LSECs (sent frozen on dry ice) were received from Dr. Cristina Ionica Oie from the University in Tromsø (Vascular Biology Research Group, Department of Medical Biology, Faculty of Health Sciences, Tromsø, Norway) were provided by Bard Smedsrod and Cristina Ionica Oie from the University in Tromsø (Vascular Biology Research Group, Department of Medical Biology, Faculty of Health Sciences, Tromsø, Norway).

MATERIALS & METHODS

Upcyte[®] endothelial cells

To harvest the supernatant for FVIII analysis, different upcyte[®] endothelial cells (BOECs, mvECs and LSECs) transduced with lentiviral particles carrying a FVIII transgene were upcyte[®] BOECs, mvECs and LSECs transduced with FVIII gene were seeded at confluence (approximately 30,000 cells/cm²) in 6-well plates. Upcyte[®] BOECs and upcyte[®] mvECs were cultured for 2 to 3 days in vericyte[®] ECGM; whereas, upcyte[®] LSECs were cultured in upcyte[®] LSEC Growth Medium. After the initial culture period, the cells were cultured in 2 ml of the respective growth medium.

Primary mvECs

After antibiotic selection, an homogeneous population of primary mvECs carrying FVIII transgene was seeded and cultured in the same manner as that for upcyte[®] mvECs. After 24 h, 200 µl of the supernatant was harvested and centrifuged at 180 ×g for 20 min at 4°C to remove any cell debris. FVIII analysis was carried out according to the protocol by the supplier of the IMUBIND[®] Factor VIII ELISA Kit. The IMUBIND Factor VIII ELISA is a “sandwich” ELISA using a monoclonal antibody against human FVIII as the capture antibody. Samples were incubated in microwells coated with an anti-human FVIII monoclonal antibody and a second monoclonal antibody, horseradish peroxidase (HRP) conjugated, was used to detect the bound FVIII antigen. The addition of a perborate/3,3',5,5' – tetramethyl benzidine substrate, and its subsequent reaction with the HRP creates a blue colored solution. The sensitivity was enhanced by adding 0.5 M sulfuric acid, yielding a yellow color. FVIII levels were determined by measuring the absorbance at 450 nm and comparing the values to those of a standard curve and blank. Cell-specific Growth Medium was used as a blank.

RESULTS

3. Results

3.1 Hepatic models – 3D Mimetix[®] scaffolds

The hepatocytes were cultured in 3D synthetic scaffolds made of biodegradable polymers and generated using an electrospinning technique. Different fibre diameters and scaffold thicknesses were analyzed using upcyte[®] hepatocytes for optimal cell function and penetration into the scaffolds. The performance of upcyte[®] hepatocytes in 3D scaffolds was determined by measuring metabolic functions such as cytochrome P450 3A4 (CYP3A4) and MTS metabolism.

3.1.1 Effect of scaffold fibre thickness on cell penetration

Initial experiments were performed to study the ability of upcyte[®] hepatocytes (Donor 653-03) to penetrate the electrospun mesh, which was analyzed using confocal microscopy. Upcyte[®] hepatocytes were cultured in rhodamine-labelled, non-functionalized PLLA scaffolds (4 μm fibre diameter with 100 μm thickness) in HGM in a 12-well plate format. A seeding density of 300,000 cells/well was selected (confluence) and the penetration of the cells was analyzed over a period of 13 days. Upcyte[®] hepatocytes penetrated the scaffold to a depth of 40 μm on Day 1 and by Day 13, clusters were observed at a depth of 45 μm . There were very few clusters observed beyond the depth of 45 μm . The cells formed 3D islands or clusters, which were distributed horizontally throughout the scaffold (Figure 14), which were equivalent of 2 to 3 stacked cell layers. In order to determine whether a different fibre diameter (and therefore a larger pore size) resulted in deeper penetration of upcyte[®] hepatocytes, the subsequent experiment compared scaffolds (100 μm thickness) with fibres of 4 μm diameter (pore size ~ 15-31 μm) and 6 μm diameter (pore size ~ 18-42 μm). On Day 13, similar cell clusters were detected at a depth of 100 μm in 6 μm fibre diameter scaffolds i.e. they had reached the lower surface of the scaffold. There were no islands of cells observed in the middle of the scaffolds such that all the cells had moved through the scaffold to the lower surface of the scaffolds.

RESULTS

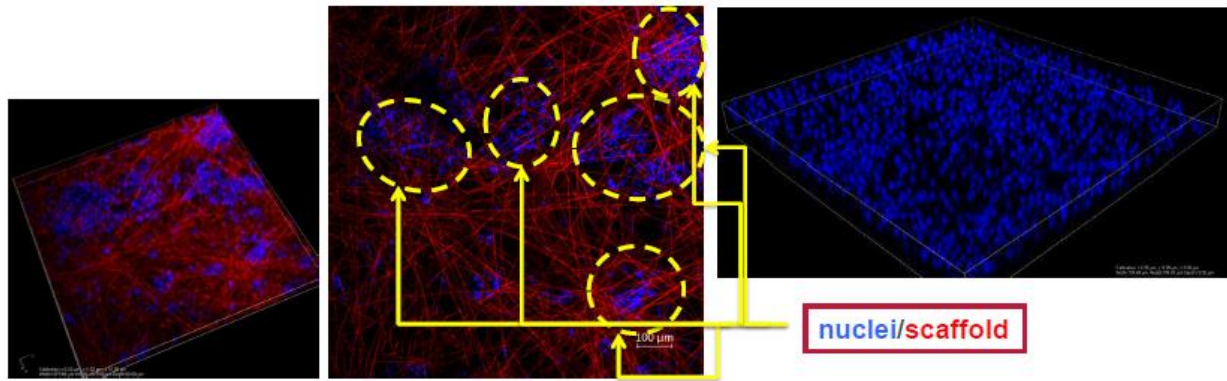


Figure 14: Visualization of the clusters of upcyte[®] hepatocytes (Donor 653-03 in 12-well rhodamine-labelled, non-functionalized PLLA scaffolds after 13 days of culture (100 μm thickness, 4 μm fibre diameter). Nuclei of the cells had been counter-stained using DAPI.

3.1.2 Viability and growth of upcyte[®] hepatocytes in 3D scaffolds

Having analyzed the penetration of upcyte[®] hepatocytes into electrospun scaffolds, the next step was to determine whether the cells could (a) proliferate within the scaffold and (b) whether the viability of the cells would be maintained over time, without necrosis. Confocal analysis showed that the penetration of the cells into and through the scaffolds was increased when the pore size was increased (by using 6 μm fibres); however, this technique did not show whether the cells were viable during the culture. Therefore, the viability of upcyte[®] hepatocytes (50,000 cells/well, i.e. confluence) in 96-well plates with electrospun, non-functionalized PLLA scaffolds was assessed by measuring MTS metabolism over a period of 7 days after seeding. MTS is a measure of both cell number and viability; an increase in the metabolism of MTS generally indicates proliferation has occurred (they were 93% viable at the start of the incubation); whereas, a decrease indicates detachment of cells or a loss in cell viability. In order to compare the effect of placing cells into 3D culture, concurrent 2D conventional cultures were cultured and analyzed in parallel. Two variables were assessed for their potential effects on cell viability, namely the scaffold thickness and the fibre diameter.

3.1.2.1 Scaffold thickness: 100 μm vs 50 μm

The viability and cell number within the scaffolds was determined over 7 days using MTS metabolism. The cells were also cultured in conventional 2D cultures in order to compare the effect on 3D scaffolds on the cell viability. Figure 15 shows the effect of scaffold thickness, using 4 μm fibre diameter on MTS metabolism. Two different scaffold thicknesses were tested, 100 μm and 50 μm , and the metabolism of MTS was measured after 4 h, Day 1, 3, 5

RESULTS

and 7. Cells cultured in 2D exhibited a higher MTS metabolism compared to cells grown in 3D scaffolds over the first 3 days of culture. However, after this time, the cells cultured in 2D showed a decrease in MTS metabolism after Day 5 and Day 7. In contrast to cells grown in 2D, upcyte[®] hepatocytes grown in scaffolds of both thicknesses continued to proliferate over the entire 7 days of culture period, evident as an increase in MTS metabolism.

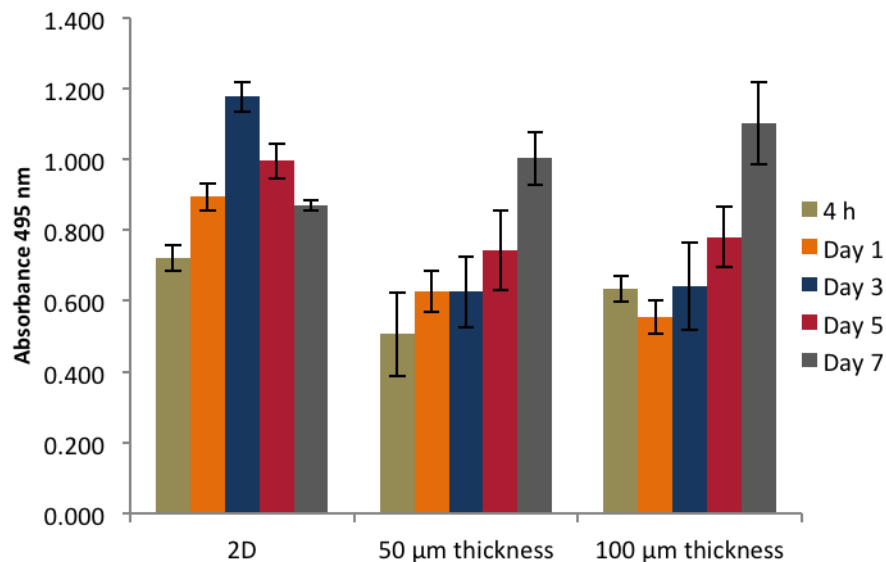


Figure 15: Effect of scaffold thickness on the viability of upcyte[®] hepatocytes (Donor 653-03) cultured in 2D monolayers and in 3D cultures in PLLA 4 µm fibre Ø scaffolds with a thickness of 100 and 50 µm. The viability/cell number of cells (MTS metabolism) was represented as green bars (4 h), orange bars (Day 1), blue bars (Day 3), red bars (Day 5) and grey bars (Day 7). Values are the mean \pm SD from 2 experiments, each with n=4 wells per condition.

3.1.2.2 Fibre thickness: 4 µm vs 6 µm

Figure 16 shows the MTS metabolism in the cultures of upcyte[®] hepatocytes in 2D culture and in non-functionalized PLLA scaffolds (50 µm thickness) with a fibre diameter of 4 and 6 µm. The growth rate of cells was initially similar in both the fibre diameters. However, on Days 3 and 5, the growth of the cells was marginally but significantly higher ($P < 0.05$) in PLLA scaffolds with 4 µm fibre diameter than with 6 µm fibre diameter. Based on the increase in MTS, the PD time for upcyte[®] hepatocytes grown in 2D was 4.7 days, compared to longer times of 8.2 (50 µm scaffolds) and 8.8 (100 µm) days in 3D cultures. On Day 7 there was no significant difference ($P = 0.08$) observed in the MTS metabolism in both the fibre diameters. Whereas in 2D monolayer, there was a significant difference ($P < 0.05$) observed in the growth of the cells on Day 3 compared with the two scaffold formats. But the viability of cells started to decline on Day 5 and Day 7. The decrease in MTS values in 2D

RESULTS

monolayer indicates detachment of cells or a loss in cell viability. The viability of cells in 2D monolayer correlated well with previous results (Figure 15).

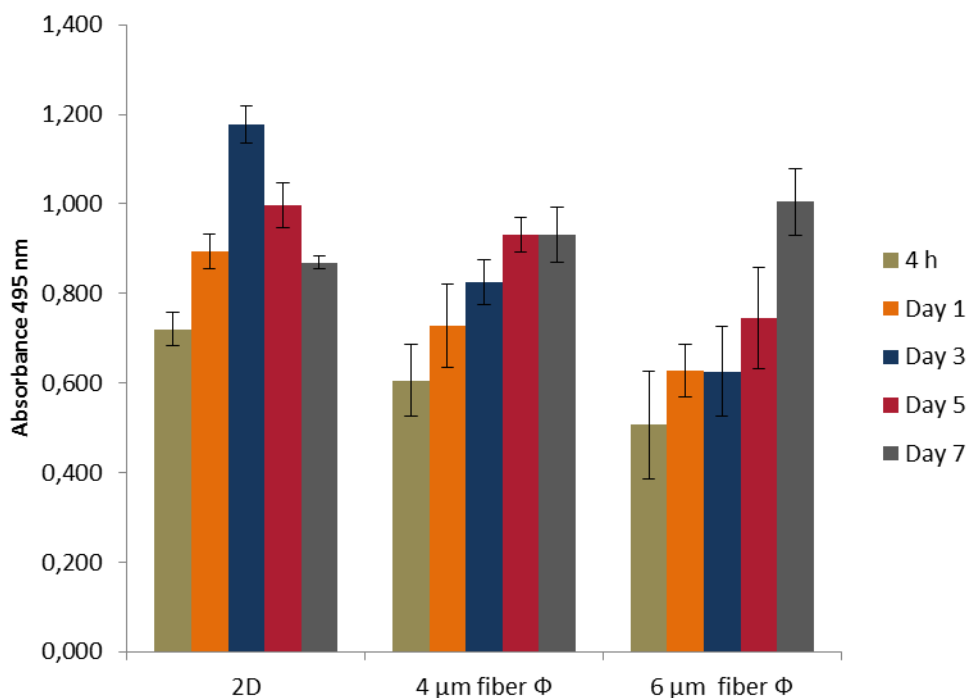


Figure 16: Effect of fibre thickness on the viability and growth of upcyte® hepatocytes (Donor 653-03) in 2D monolayers and in PLLA 50 μm thick scaffold with 4/6 μm fibre Ø in 96-well format. The viability/cell number of cells (MTS) is represented as green bars (4 h), orange bar (Day 1), blue bar (Day 3), red bar (Day 5) and grey bar (Day 7). Values are the mean ± SD from 2 experiments, each with n=4 wells per condition.

3.1.3 Functionality of upcyte® hepatocytes in Mimetix® scaffolds

The aim of these experiments was to analyze the influence of different parameters on the functionality of the cells. As there were no marked differences in terms of viability of upcyte® hepatocytes cultured in two different scaffold thickness and scaffolds with different fibre diameters, further investigations were carried out to determine whether these conditions also affect the metabolic function of the cells. The functionality of upcyte® hepatocytes was investigated by measuring the metabolism of a CYP3A4 substrate, testosterone, and the responsiveness of the cells to a CYP3A4 inducer, rifampicin. The cells were first cultured in 96-well plates with electrospun, non-functionalized PLLA scaffolds in HGM for 7 days and then incubated for another 3 days (day 7 to 10) in HPM containing either 20 μM rifampicin or 0.1 % DMSO (solvent control). During this induction period, medium was replaced daily with fresh HPM containing either inducer or DMSO. CYP activities were measured on day 10 according to Section 2.2.2.3.

RESULTS

3.1.3.1 Scaffold thickness: 100 μm vs 50 μm

The basal and induced CYP3A4 activities in upcyte[®] hepatocytes cultured on two different scaffold thickness were measured. The basal CYP3A4 activity in upcyte[®] hepatocytes cultured in non-functionalized PLLA 4 μm fibre scaffolds with a thickness of 50 μm thickness was 104 ± 3 pmol/mg/min and this was not significantly different ($P=0.63$) from that in the same cells cultured in 2D monolayers (119 ± 20 pmol/mg/min) (Figure 17). However, CYP3A4 activities in upcyte[®] hepatocytes cultured in thicker scaffolds of 100 μm were marginally higher (1.3-fold) than those cultures in the other two formats. Cells cultured in all formats were responsive to CYP3A4 induction by rifampicin. The fold induction values in 2D, 50 μm and 100 μm scaffolds were 2.6, 3.4 and 3.1 respectively. Induced activities in 50 μm thick scaffolds were 354 ± 26 pmol/mg/min and were not significantly different ($P=0.3$) from CYP activities in cells cultured in 2D monolayers (406 ± 32 pmol/mg/min) (Figure 17). Induced CYP3A4 activities in upcyte[®] hepatocytes cultured in 100 μm scaffolds were significantly higher ($P=0.003$) than those in 50 μm scaffolds but they were not significantly higher than those in cells cultured in 2D monolayers.

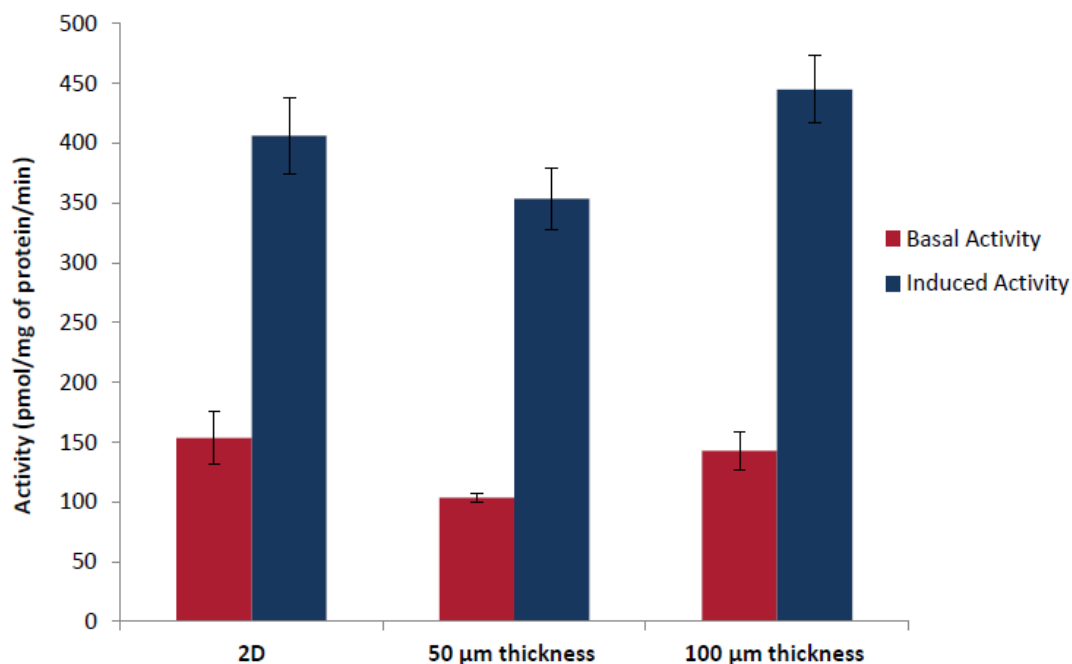


Figure 17: Basal and induced CYP3A4 activities in upcyte[®] hepatocytes (Donor 653-03) cultured in 2D monolayers and in PLLA 4 μm fibre scaffolds with a thickness of 50 and 100 μm . The CYP3A4 activity is shown as red bars (basal activity) and blue bar (induced activity). Values are the mean \pm SD from 2 experiments, each with $n=4$ wells per condition.

3.1.3.2 Fibre thickness: 4 μm vs 6 μm

Upcyte[®] hepatocytes cultured in 2D monolayer had basal activity of 119 ± 12 pmol/mg/min and the induced activity was 3.4 folds higher (406 ± 40 pmol/mg/min). Cells cultured in 50

RESULTS

μm thick scaffolds with a fibre diameter of $6 \mu\text{m}$ had basal and induced activity of 107 ± 4 pmol/mg/min and 354 ± 26 pmol/mg/min respectively. The fold induction is 3.3 times higher than the basal activity. However, upcyte[®] hepatocytes cultured in $50 \mu\text{m}$ thick scaffolds with a fibre diameter of $4 \mu\text{m}$ had higher basal (149 ± 9 pmol/mg/min) and induced CYP3A4 activities (487 ± 61 pmol/mg/min) compared to the cells cultured in 2D monolayers or $50 \mu\text{m}$ thick scaffolds with $6 \mu\text{m}$ fibre diameter (Figure 18).

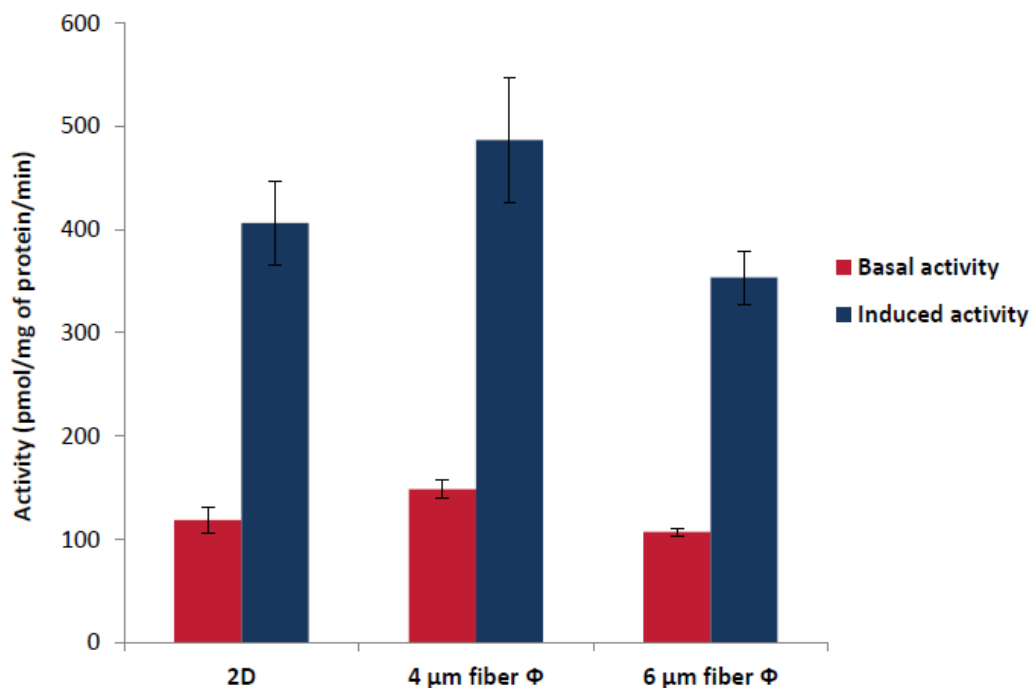


Figure 18: Basal and induced CYP3A4 activities in upcyte[®] hepatocytes (Donor 653-03) cultured in 2D monolayers and in PLLA $50 \mu\text{m}$ thickness scaffolds with a fibre Φ of 4 and $6 \mu\text{m}$. The CYP3A4 activity is represented as red bars (basal activity) and blue bar (induced activity). Values are the mean \pm SD from 2 experiments, each with $n=4$ wells per condition.

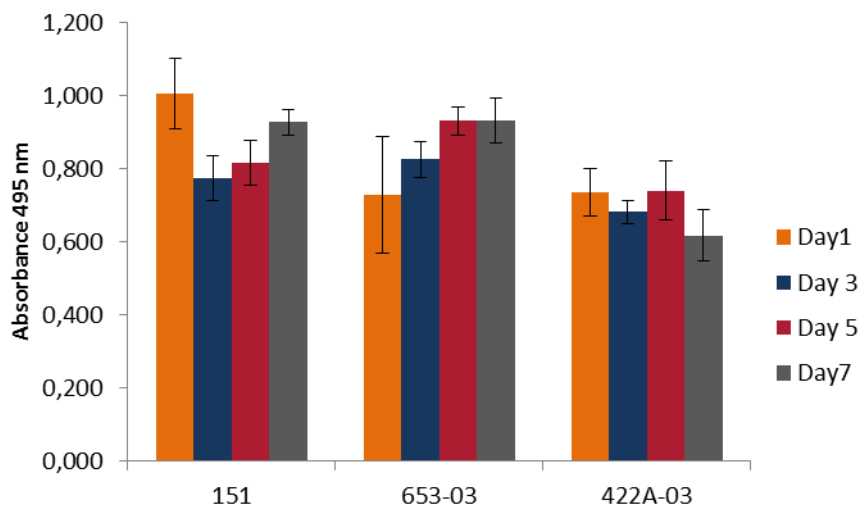
3.1.4 Viability: donor-to-donor variation

Since scaffolds with a thickness of $50 \mu\text{m}$ resulted in marginally higher basal and induced activities in upcyte[®] hepatocytes from Donor 653-03, the same scaffold thickness was used to investigate the viability and metabolic functions in upcyte[®] hepatocytes from two additional donors. In order to have the comparative study, Donor 653-03 was also cultured at the same time as the other two donors. Cells were seeded on non-functionalized, plain PLLA scaffolds with a fibre diameter of either 4 or $6 \mu\text{m}$. The three different donors of upcyte[®] hepatocytes from first and second-generation batches were used. Donor 151 a first generation upcyte[®] hepatocyte and Donors 653-03 and 422A-03 were second-generation upcyte[®] hepatocytes. Figure 19a & b shows the MTS metabolism by upcyte[®] hepatocytes from three different donors on non-functionalized plain PLLA scaffolds with $50 \mu\text{m}$ thickness and a fibre diameter of $4 \mu\text{m}$ and $6 \mu\text{m}$. For upcyte[®] hepatocytes from Donor 151 MTS metabolism on Day 1 was

RESULTS

initially higher in both the scaffold formats. However, there was a decline in MTS metabolism observed on Day 3 in both the scaffolds, followed by increase in the rate of viability on Day 5 and 7. The decline in MTS metabolism may be due to detachment of cells from the scaffolds. In contrast to upcyte[®] hepatocytes from Donor 151, the growth rate of upcyte[®] hepatocytes from Donor 653-03 continuously increased over time in both scaffold formats. The Donor 422A-03 showed almost no variation in MTS metabolism over time in both the scaffold formats.

(a) 4 μm fibre diameter



(b) 6 μm fibre diameter

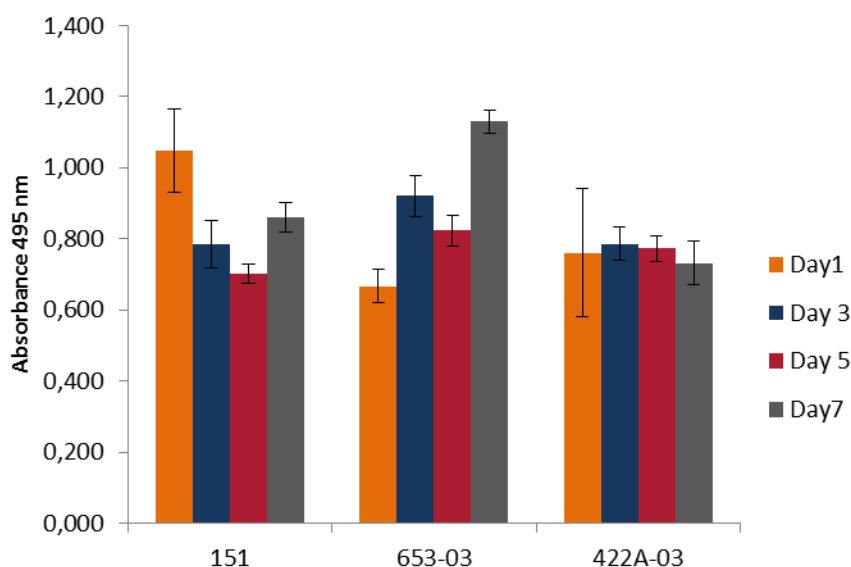


Figure 19: Three different donors of upcyte[®] hepatocytes were used to analyze the donor-to-donor variation on the cell viability and cellular growth rate when cultured in PLLA 50 μm thick scaffold with 4/6 μm fibre \varnothing in a 96-well format. Donor 151; Donor 653-03; Donor 422A-03 were used. The viability/cell number of cells (MTS) are shown as orange bar (Day 1), blue bar (Day 3), red bar (Day 5) and grey bar (Day 7). Values are the mean \pm SD from 2 experiments, each with n=4 wells per condition.

RESULTS

3.1.4.1 Functionality: donor-to-donor variation

The basal and induced CYP3A4 activities in the three different donors were analyzed in 2 different scaffold formats and the results were compared with 2D monolayer (Table 17). For upcyte[®] hepatocytes from Donor 151, the basal CYP3A4 activity in 4 μm and 6 μm fibre diameter was 13.7 ± 1 pmol/mg/min and 9.1 ± 1 pmol/mg/min, respectively. The fold induction upon culturing the cells with rifampicin in 4 μm and 6 μm fibre diameter was 5.1 and 7.9 respectively. Thus, for upcyte[®] hepatocytes from Donor 151, there was no significant difference ($P=0.69$) observed between the basal activities or responsiveness to rifampicin induction in the two scaffold formats. Likewise, for upcyte[®] hepatocytes from Donor 653-03, there was no difference observed in the fold induction when they were cultured in both the scaffold formats. However, the basal and induced activities in cells from this donor were significantly higher ($P < 0.05$) when cultured in scaffolds with fibres of 4 μm diameter than those with 6 μm thick fibres. This is in contrast to upcyte[®] hepatocytes from Donor 422A-03, for which the basal and induced CYP3A4 activities were significantly higher ($P < 0.05$) in scaffolds with 6 μm than 4 μm fibre diameters.

Table 17: Basal and induced CYP3A4 activities (pmol/mg of protein/min) in upcyte[®] hepatocytes (Donor 151; Donor 653-03; Donor 422A-03) cultured in PLLA 50 μm thickness scaffolds with a fibre diameter of 4 and 6 μm . Values are the mean \pm SD from 2 experiments, each with $n=4$ wells per condition.

	Donor 151			Donor 653-03			Donor 422A-03		
	Basal	Induced	Fold Induction	Basal	Induced	Fold Induction	Basal	Induced	Fold Induction
2D monolayer	3.5 ± 1	35 ± 4	10	118.7 ± 12	406.2 ± 40	3.4	199.64 ± 19	670.79 ± 67	3.4
4 μm fibre diameter	13.7 ± 1.1	69.9 ± 7.5	5.1	148.5 ± 8.78	486.7 ± 60.83	3.3	184.2 ± 12.99	676.13 ± 45	3.7
6 μm fibre diameter	9.1 ± 1	72.1 ± 7.7	7.9	107.04 ± 3.47	353.6 ± 25.6	3.3	277.60 ± 35.76	787.85 ± 24.63	2.8

3.2 Hepatic models – Liver organoids

When hepatocytes were cultured in 3D synthetic scaffolds, difference in functionality and viability of cells were observed in the Section 3.1. In order to reflect physiological situation, liver organoids were generated by co-culturing the upcyte[®] cell types namely, hepatocytes, LSECs and MSCs. A comparative study was performed to study the difference between static and dynamic system (*Quasi-vivo*[®] chambers). Functionality was investigated by measuring CYP3A4 activities. The organoids were also characterized using *in situ* hybridization for the expression of functional genes such as albumin and enzymes regulating glutamine and glucose levels.

RESULTS

3.2.1 Generation of liver organoids in static culture using upcyte[®] and primary cells

The morphology of primary and upcyte[®] cells, cultured in 2D and used for the generation of liver organoids were observed under light microscopy. The cells were initially cultured under static conditions i.e. no flow of medium over the cells. Upcyte[®] hepatocytes at sub-confluence were smooth with clear nuclei. Some cells were binucleated, suggesting they were in the process of cell division; whereas, other cells appeared to have recently gone through cytokinesis (Figure 20 a). Upcyte[®] LSECs are usually broad cells with extended cytoplasmic features having prominent nucleus at its centre. However, the cells become more compact when they reach confluence (as shown in Figure 20 b). Primary MSCs show fibroblast-like morphology, which is typical for the MSCs (Figure 20 c).

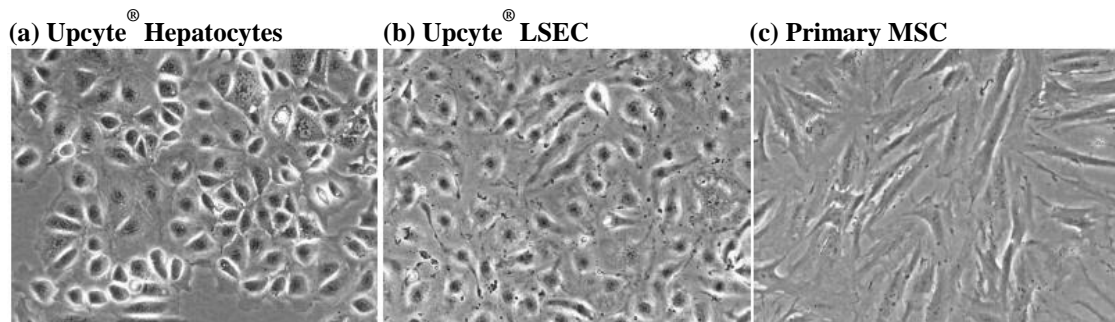


Figure 20: Morphology of (a) Upcyte[®] hepatocytes, (b) upcyte[®] LSECs and (c) primary MSCs observed under light microscopy (magnification: 100x).

All cells were harvested when they had reached 70-80% confluence. On Day 1, 1×10^6 upcyte[®] hepatocytes, 1×10^6 upcyte[®] LSECs and 0.2×10^6 primary MSC were mixed in liver organoid growth medium and cultured in 24-well format plates coated with a thick layer of Matrigel[™]. When all the three cell types were co-cultured, they interacted and moved towards each other (Figure 21- 8 h) and self-organized to form a single 3D liver organoid-like structure (Figure 21- 24 h). When cultured up to 72 h, this macroscopically visible 3D liver organoid-like structure became more compact and measured 2-3 mm in diameter (Figure 21- 48 h & 72 h).

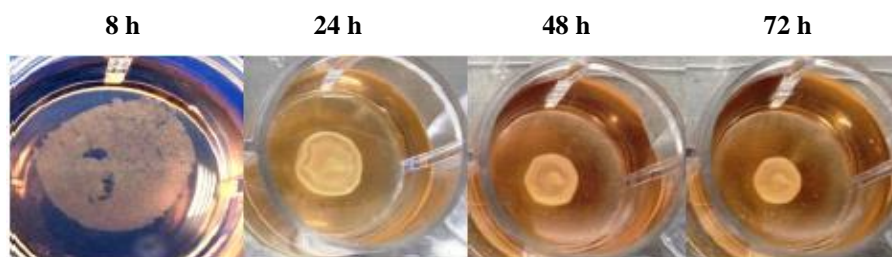


Figure 21: Self-organization and formation of liver organoid-like structures from upcyte[®] hepatocytes, upcyte[®] LSECs and primary MSCs. The cells move spontaneously towards each other (within 8 h) and formed liver organoid-like structure within 24 h. The organoid became more compact between 48 h and 72 h.

RESULTS

3.2.2 Generation of liver organoids in static culture using only upcyte[®] cells

As the generation of liver organoid-like structure was successful with upcyte[®] hepatocytes, LSECs and primary MSCs (Figure 21), the next step aimed to replace primary MSCs with upcyte[®] MSCs and evaluate the subsequent formation of liver organoid. Similar to primary MSCs (Figure 20 c), upcyte[®] MSCs also exhibited an elongated fibroblastic morphology (Figure 22) when observed under light microscopy.

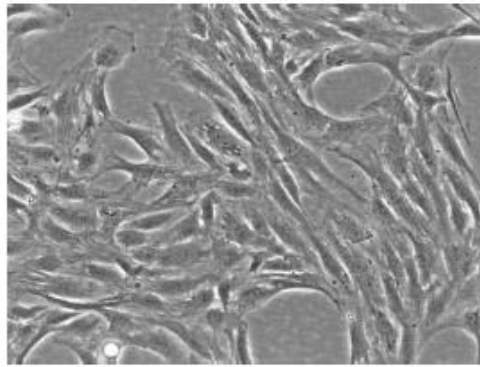


Figure 22: Morphology of upcyte[®] MSCs observed under light microscopy (magnification: 100x).

Figure 23 shows that it was possible to generate 3D liver organoid-like structure with all the three cell types as upcyte[®] (hepatocytes, LSECs and MSC) and the generation of organoids was reproducible. Also similar to initial experiments using primary MSCs, all the three cell types, when co-cultured in 24-well multiwells coated with a thick layer of Matrigel[™], self-organize to form an organoid-like structure within 24 h (Figure 23). When cultured up to 72 h, a compact structure (2-3 mm in diameter) was obtained.

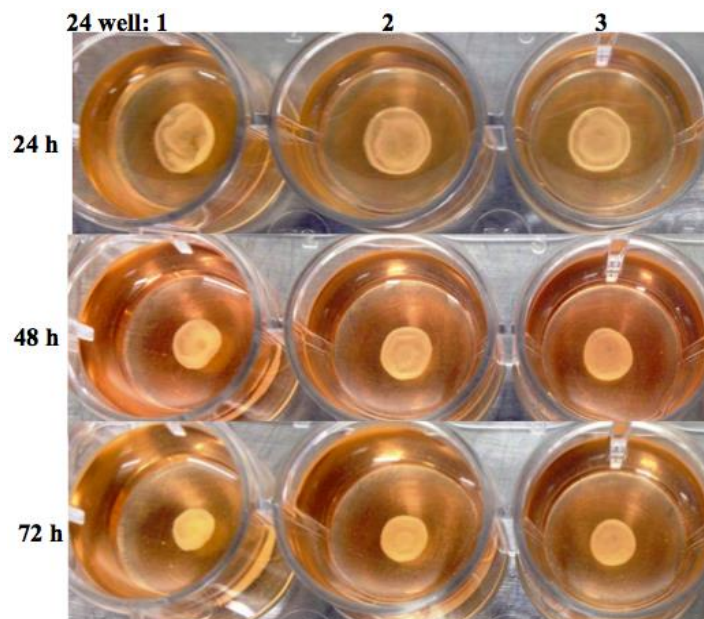


Figure 23: Formation of liver organoid-like structures from upcyte[®] hepatocytes, upcyte[®] LSECs and upcyte[®] MSCs within 24 h. The organoids became more compact between 48 h and 72 h.

RESULTS

3.2.3 Histology of organoids maintained in static culture

Liver organoids were cultured in a static system in liver organoid growth medium for 72 h, with a medium change every 24 h and then fixed with formalin for histological studies. The organization of cells in liver organoids maintained in static cultures for 72 h was visualized using HE staining. The static conditions may have prevented the nutrients and oxygen from the medium from reaching the inner part of the organoids. This was indicated by the presence of collapsed nuclei and cell debris accumulation (visualized as dark specks and indicated by a red arrow in Figure 24), which signify the presence of necrotic or dead cells.

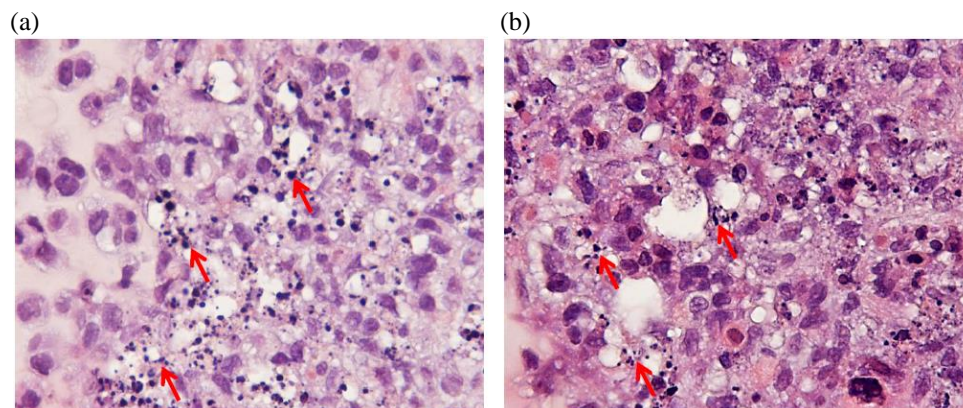


Figure 24: HE stainings of liver organoids maintained in static culture for 72 h. The presence of necrotic cells is denoted with a red arrow. The liver organoids were generated in a 24-well multiwell format using either (a) upcyte® hepatocytes, upcyte® LSECs and primary MSCs or (b) upcyte® forms of all three cell types (magnification: 400x).

3.2.4 Scalability

Downscaling of cell numbers was done according to Section 2.2.3.3 to generate liver organoids in smaller formats, such as the 96-well and 48-well multiwell formats, so that the smaller organoids can be adapted for other systems such as BioVaSc. When upcyte® hepatocytes, upcyte® LSECs and upcyte® MSCs were co-cultured on polymerized Matrigel™, as with cells cultured in the 24-well format, they form an organoid-like structure in 24 h (Figure 25).

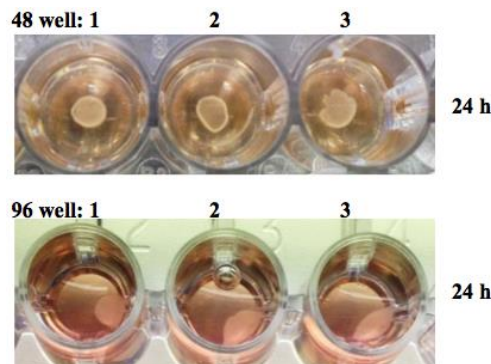


Figure 25: Formation of liver organoids within 24 h in static condition in 48-well and 96-well multiwell format using upcyte® Hepatocytes, upcyte® LSECs and upcyte® MSCs.

RESULTS

3.2.5 Adaptation of liver organoid in dynamic culture

The applicability of liver organoids generated from upcyte[®] cells (hepatocytes, LSECs and MSC) to dynamic culture conditions was investigated. Liver organoids were generated as described in Section 2.2.3.1 using *Quasi-Vivo*[®] chambers coated with a thick layer of Matrigel[™] instead of 24-well plates. As before, the cells self-organized to form liver organoid-like structures within 24 h (Figure 26 a). After 24 h, chambers containing the liver organoids were connected to the dynamic system (Figure 32 b) and perfused with liver organoid growth medium at a flow rate of 300 $\mu\text{l}/\text{min}$. The organoids were cultured for up to 10 days and during this time, the medium was changed every 2 to 3 days.

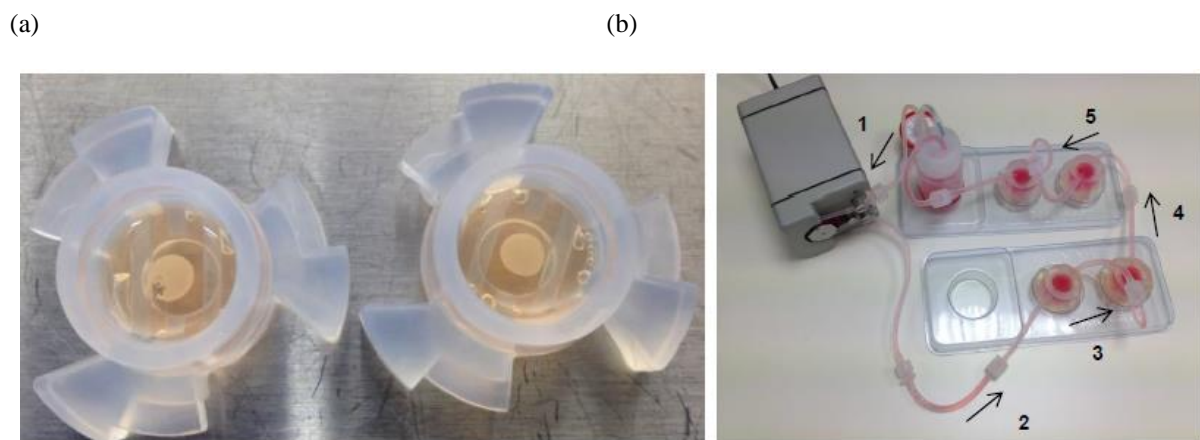


Figure 26: Formation of liver organoids in *Quasi-vivo*[®] chambers (QV500) under static conditions within 24 h (a). Once formed, the liver organoids were perfused with medium at a flow rate of 300 $\mu\text{l}/\text{min}$ (b). Arrows indicate the flow of medium from the reservoir bottle through the pump to the consecutively connected chambers.

3.2.6 Histology of liver organoids maintained in dynamic culture

Liver organoids in *Quasi-vivo*[®] chambers maintained in dynamic cultures were formalin fixed and paraffin embedded after 10 days. Under dynamic conditions, different cell types separated from each other and arranged into different layers (Figure 27 a). The number of necrotic cells was significantly reduced when liver organoids were maintained in dynamic culture compared to static culture (Figure 27 b). This suggests dynamic culture conditions help maintain the viability of the core cells, possibly by increasing the supply of nutrients and oxygen.

RESULTS

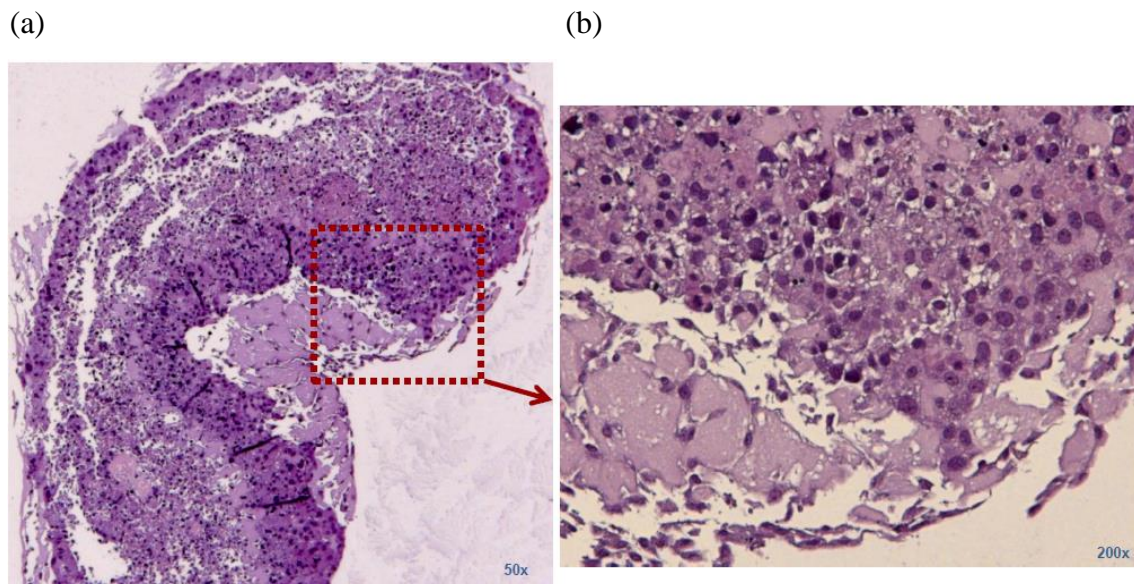


Figure 27: Histology of liver organoids maintained in dynamic culture for 10 days. Different cell types arrange in different layers (a) and very few necrotic cells were present (b). Liver organoids were generated using upcyte[®] forms of hepatocytes, LSECs and MSC (magnification: (a) 50x; (b) 200x).

3.2.7 Immunocytochemistry in 2D monolayers

2D monolayer cultures of upcyte[®] hepatocytes, upcyte[®] LSECs and upcyte[®] MSCs that were used for the generation of liver organoids were characterized for the presence of cell-specific markers. Similar to adult primary hepatocytes, upcyte[®] hepatocytes also expressed high levels of the differentiation marker, CK8 (Figure 28 a). Figure 28 b shows the presence of CD31 at cell-cell junctions in upcyte[®] LSECs which was similar to primary LSECs. Vimentin is a type III intermediate filament protein and also a major cytoskeletal component of MSCs. Figure 28 c shows that the MSCs were positive for vimentin staining.

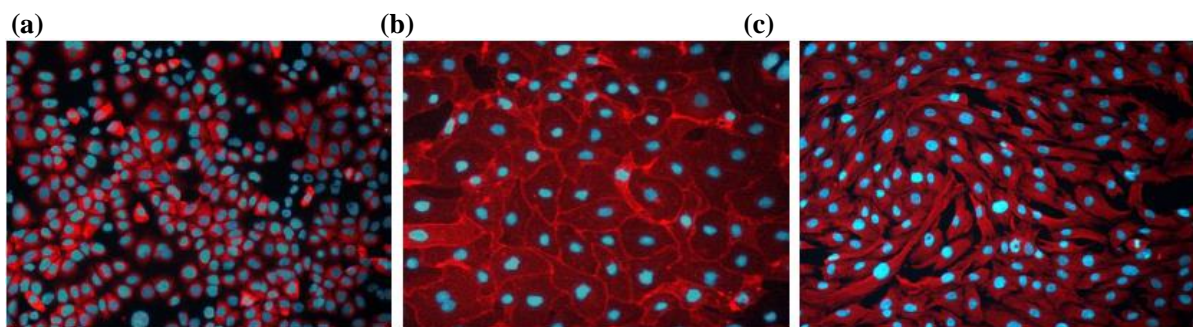


Figure 28: Immunocytochemistry staining for specific cell type markers in 2D monolayers. (a) upcyte[®] hepatocytes for CK8, (b) upcyte[®] LSECs for CD31 and (c) upcyte[®] MSCs for vimentin. The cell nuclei were stained blue with DAPI (magnification: 200x).

These specific markers were subsequently used to identify the different cells and their arrangement within the liver organoids.

RESULTS

3.2.8 Immunohistochemistry of 3D organoid

Liver organoids were generated using upcyte[®] cells (hepatocytes, LSECs and MSC) and maintained in in dynamic culture for 10 days. The arrangement of three different cells types inside the organoid was located using cell-specific immunostaining. Figure 29 b shows that upcyte[®] hepatocytes, which stained positive for CK8, were arranged in a closely adherent sheet and moved towards periphery of the liver organoid. Unlike the hepatocytes, upcyte[®] LSECs (Figure 29 c), which stained positive for CD31, occupied the inner part of the organoid. Upcyte[®] MSCs stained positive for vimentin and, in contrast to hepatocytes and LSECs, were distributed throughout the organoid (Figure 29 d). MSCs had a tendency to migrate easily; whereas; the epithelial cells or hepatocytes were polarized cells in an apical-basal orientation that lacked mobility and were organized into closely adherent sheets.

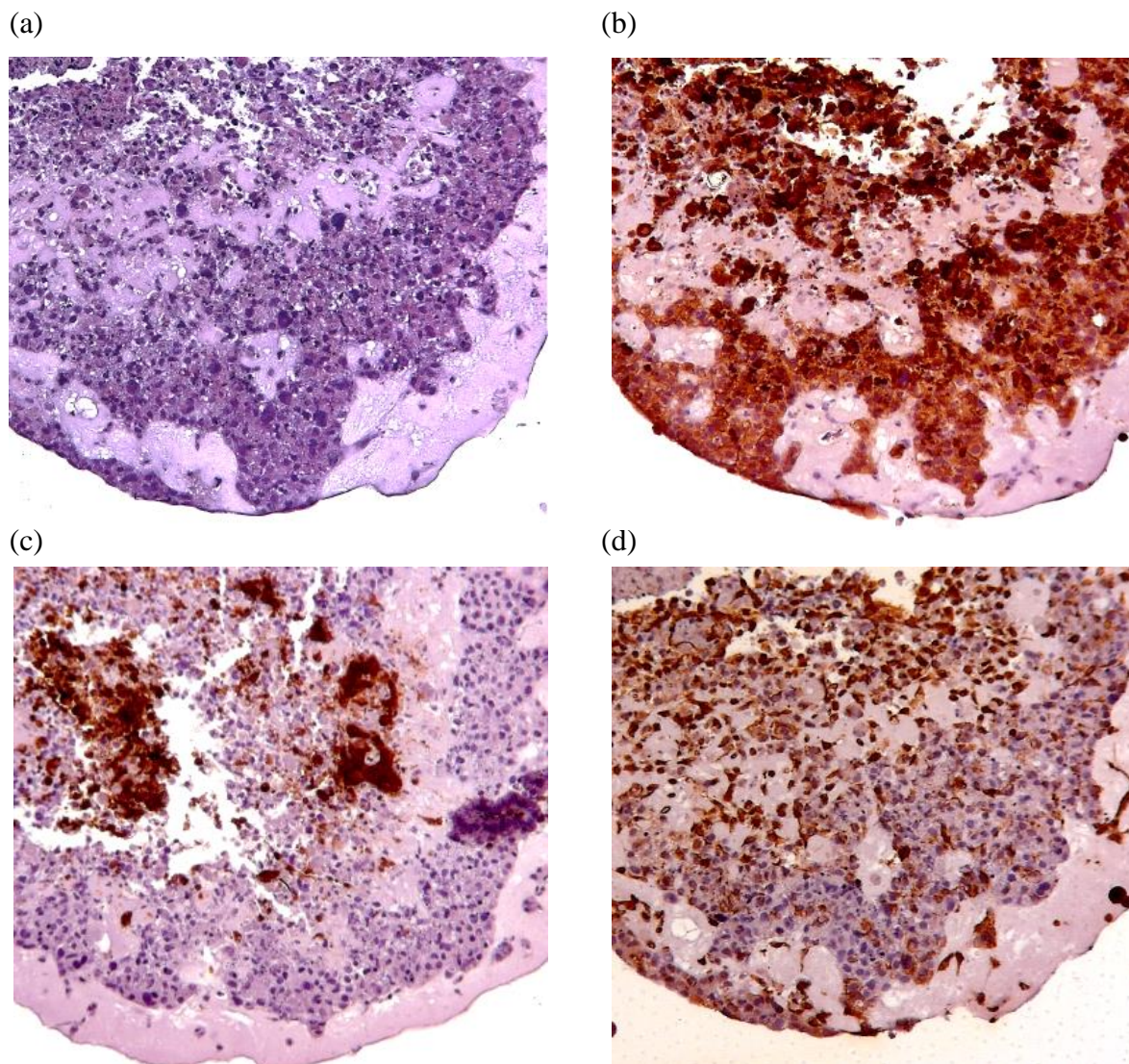
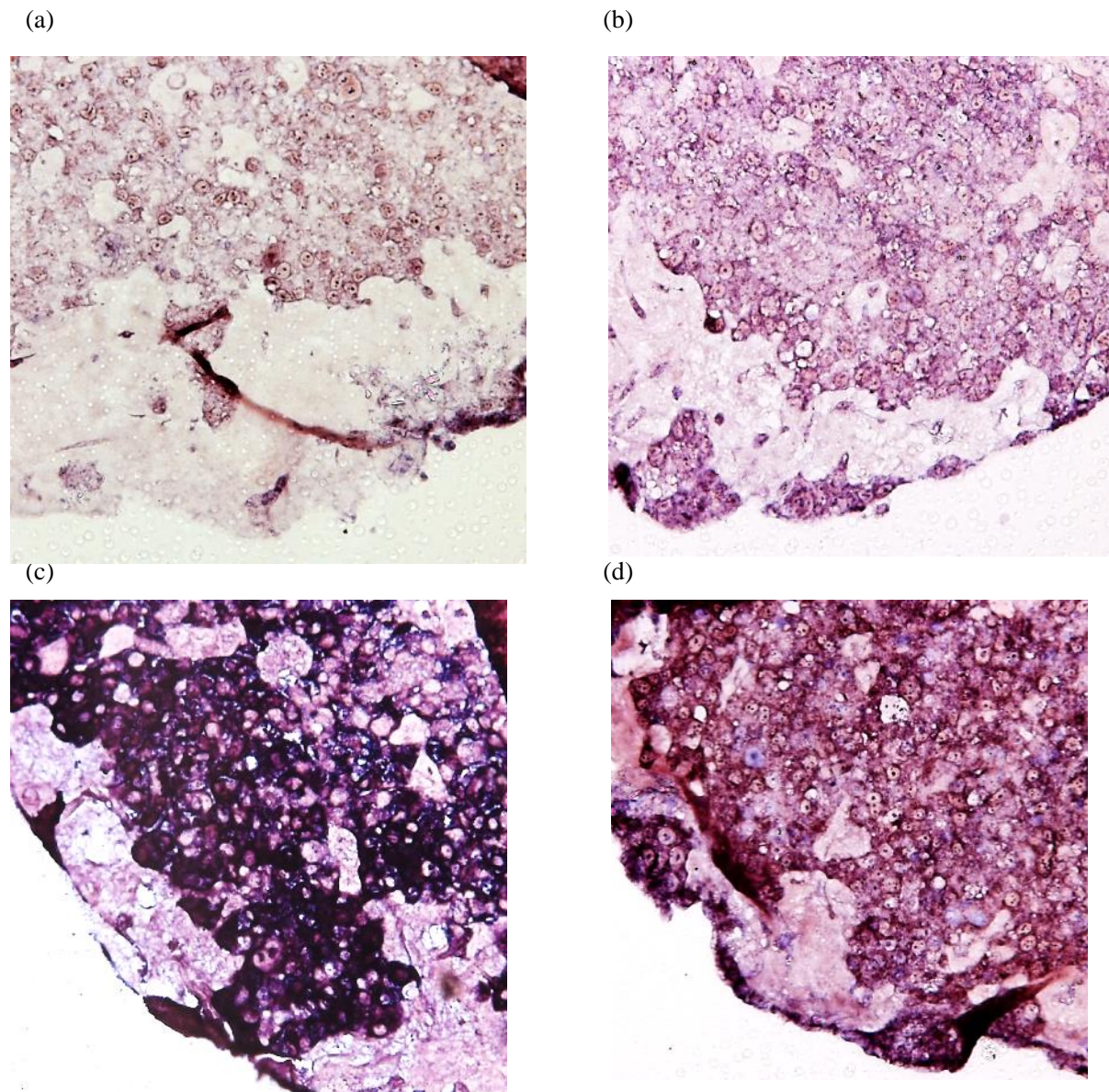


Figure 29: Liver organoids maintained for 10 days in dynamic cultures. (a) HE staining and immunostaining of cell-specific markers: (a) upcyte[®] hepatocytes expressing CK8, (b) upcyte[®] LSECs expressing CD31 and (c) upcyte[®] MSCs expressing vimentin (magnification: 200x).

RESULTS

3.2.9 *In situ* hybridizations

In an attempt to further characterize the functional status of the upcyte[®] hepatocytes within the organoids, *in situ* hybridization was performed on serial sections of organoids that were maintained for 10 days in dynamic culture. Upcyte[®] hepatocytes within the organoid retained a constitutive expression level of typical markers (e.g. CK8), as well as important functional genes such as albumin, enzymes regulating glutamine (such as glutaminase and glutamine synthase) and glucose (glucose-6-phosphate) and hypoxia-inducible factor 1- α (Hif1 α) (Figure 30).



RESULTS

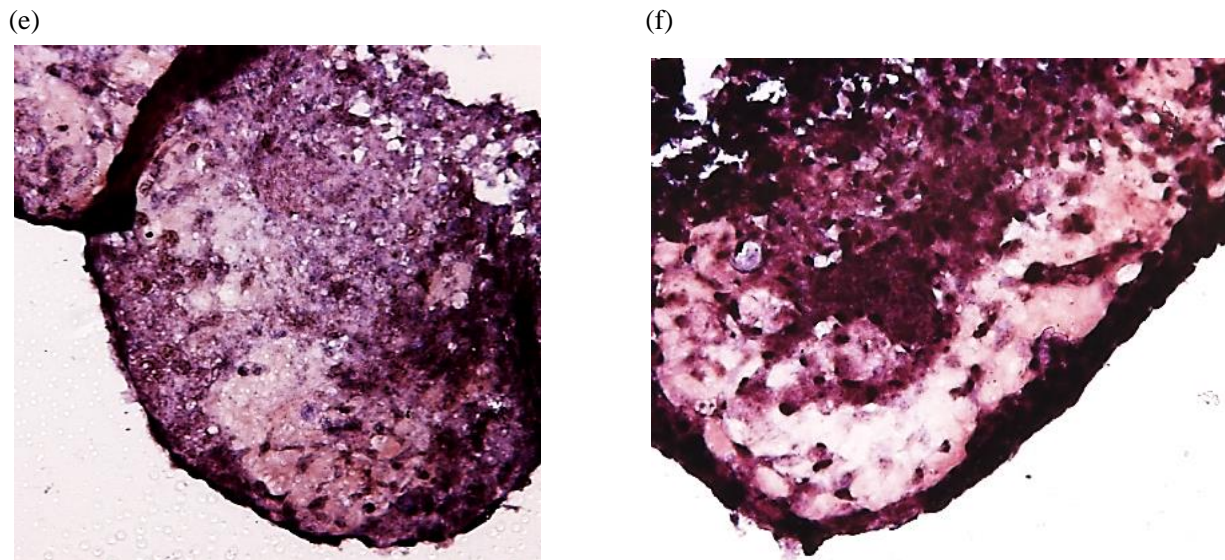
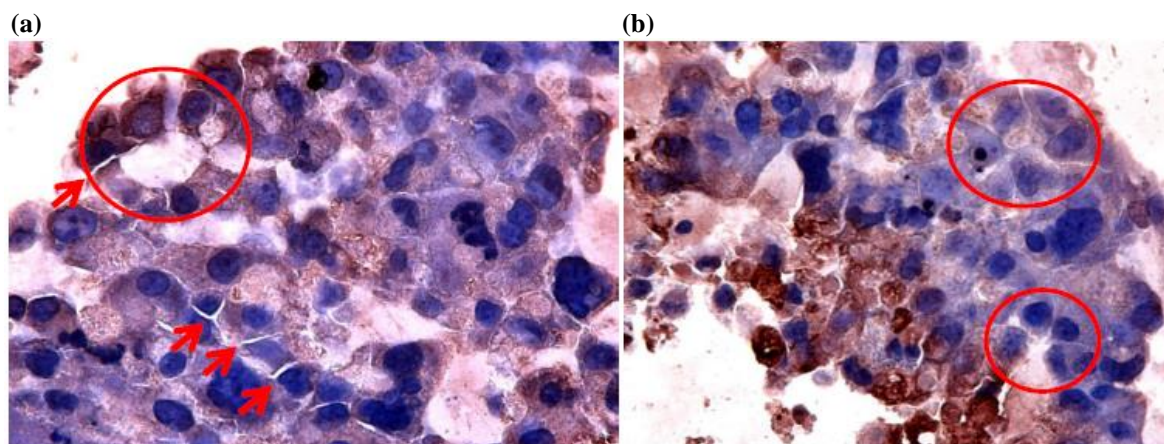


Figure 30: Detection of mRNA transcripts of genes in sections of liver organoids after 10 days of dynamic culture. a. Glutaminase, b. Hif1 α , c. albumin, d. CK 8/18, e. glutamine synthase f. glucose-6-phosphate.

3.2.10 Liver organoid architecture

Liver organoids that were maintained for 10 days in dynamic culture were stained for the expression of CK8 to detect upcyte[®] hepatocytes and the architecture were compared with that of intact liver slices. Figure 31 a shows that upcyte[®] hepatocytes are separated from the neighboring cells (indicated by a red arrow) by a space, which could be bile canaliculi-like structures. Similar to the normal adult liver Figure 31 a & b, upcyte[®] hepatocytes arrange themselves in a circle with a gap in the middle and form a sinusoidal lumen-like architecture similar to that observed in the differentiated adult liver (Figure 31 d). Hepatocytes in adult liver are arranged in a line to form a hepatic cord (Figure 31 d). Figure 31 c shows strings of upcyte[®] hepatocytes in the liver organoid that have arranged themselves to form hepatic cord-like structure.



RESULTS

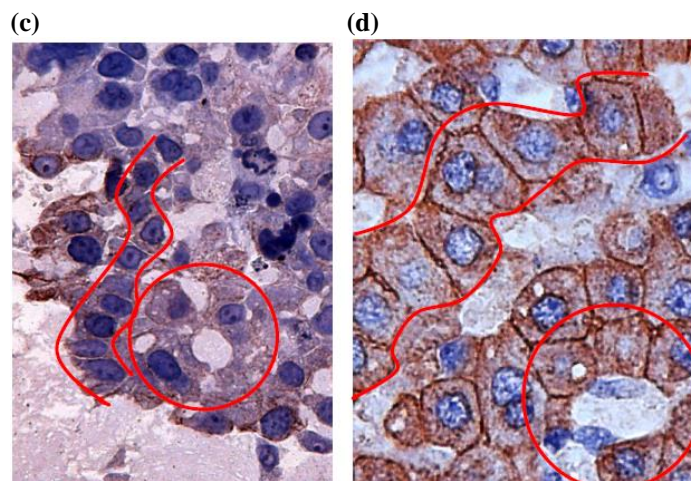


Figure 31: Arrangement of upcyte[®] hepatocytes expressing CK8 in 10-day liver organoids showing a (a) & (b) cellular arrangement surrounding circular openings, resembling bile canaliculi-like structures and (c) & (d) cord-like alignment of hepatocytes similar to the *in vivo* liver architecture (magnification: 400x).

3.2.11 Metabolic activity

Liver organoids were evaluated for the presence and induction of the major liver CYP, CYP 3A4. Organoids were cultured in liver organoid growth medium for 7 days and in HPM for 3 days, during which time some of the liver organoids were incubated with either vehicle control (0.1% DMSO) or a CYP3A4 inducer (rifampicin). The basal CYP3A4 activity in liver organoids was 47 ± 13 pmol/mg/min in experiment 1 and 70 ± 11 pmol/mg/min in experiment 2. When liver organoids were cultured in the presence of 20 μ M rifampicin from Day 7 to 10, CYP3A4 was induced by 3.4-fold (Experiment 1) and 2.2-fold (Experiment 2).

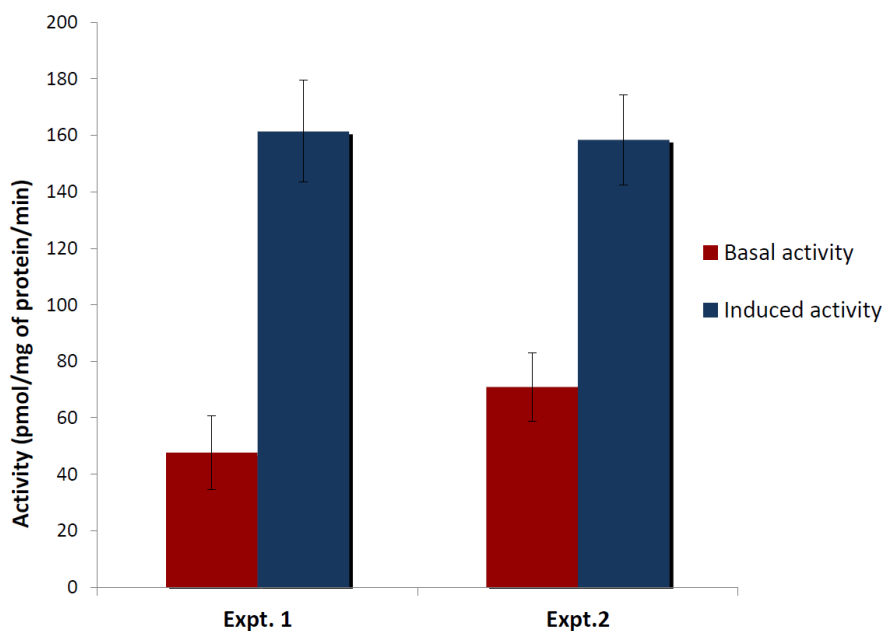


Figure 32: Basal and induced CYP 3A4 activities in liver organoid cultured for 10 days in a bioreactor. Values are the mean \pm SD from 2 experiments, each with n=3 organoids per condition.

RESULTS

3.3 Hepatic models – BioVaSc/Organoids

BioVaSc was prepared from the jejunum of the small intestine from pigs by chemical decellularization. The vascular system of the BioVaSc was retained which was repopulated with upcyte[®] mvECs. The BioVaSc was cultured in an *ex vivo* bioreactor. The lumen of the BioVaSc was used to culture the liver organoids generated using upcyte[®] hepatocytes, LSECs and MSCs. Immunohistochemical stainings were done to visualise the structural integrity of the different cell types within the organoid. After culturing the organoids inside the lumen of the BioVaSc for 30 days, CYP3A4 activities in the liver organoids were measured to evaluate their functionality.

3.3.1 Liver organoids in BioVaSc

Liver organoids were generated using upcyte[®] cells (hepatocytes, LSECs and MSCs) in static cultures in 48-well multiwell plates (using an appropriate cell number for this format) coated with a thick layer of Matrigel[™]. The liver organoids were cultured for a further 48 h under static conditions and then transferred to the luminal part of the repopulated BioVaSc. The vascular tree of the BioVaSc were repopulated with upcyte[®] mvECs and cultured for 14 days under dynamic conditions. The arterial vessel of the BioVaSc was perfused with endothelial cell growth medium to maintain the upcyte[®] mvECs, and the luminal vessels were perfused with liver bud growth medium. During this time, medium was changed every 3-4 days. The organoids inside the BioVaSc were maintained for 30 days under dynamic conditions. Figure 33 a shows the presence of organoids inside the lumen from the outer surface of the BioVaSc. The lumen was split to see the organization of liver organoids inside the lumen. After this time, the liver organoids were attached to the BioVaSc, albeit randomly distributed (Figure 33 b).

CYP3A4 activities in the liver organoids were measured to evaluate their functionality. To this end, individual liver organoids, together with the portion of the attached BioVaSc, were excised and incubated with testosterone. The basal CYP3A4 activity in liver organoids was 50.8 ± 5.5 pmol/mg/min in experiment 1, 48.6 ± 9.5 pmol/mg/min in experiment 2 and 48 ± 7.5 pmol/mg/min in experiment 3 which was reproducible across 3 experiments (Figure 40). The liver organoids expressed the average basal CYP 3A4 activity of 43.8 ± 3 pmol/mg/min in 60 min and 54 ± 1 pmol/mg/min in 90 min

RESULTS

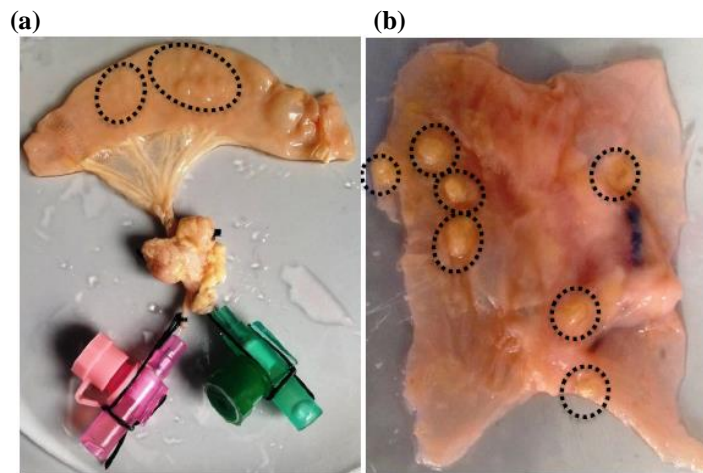


Figure 33: Liver organoids were cultured inside the lumen of the BioVaSc for 30 days. Distribution of organoids (a) from the outer surface of the lumen, (b) inside the lumen.

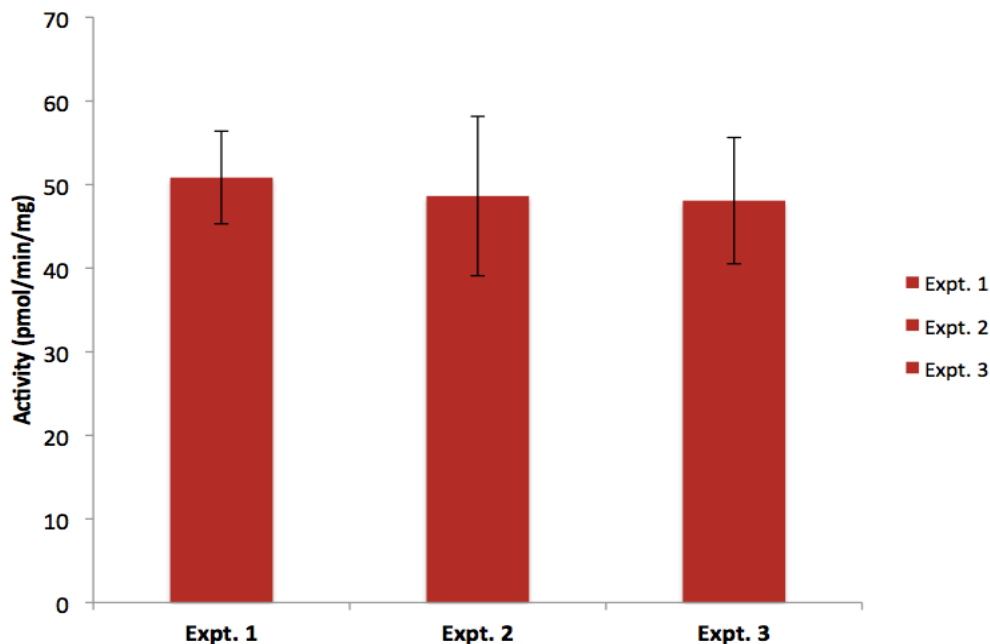


Figure 34: Basal CYP3A4 activities of liver organoids cultured in the lumen of BioVaSc for 30 days in the bioreactor. Values are the mean \pm SD from 3 experiments, each with n=4 organoids.

3.3.2 Immunostaining of organoids in BioVaSc

Liver organoids that had been cultured for 30 days in the lumen BioVaSc were analyzed for cell-specific markers to visualize the arrangement of the three different cells types in the organoid. CK8 was selected as a marker to denote upcyte[®] hepatocytes; whereas, CD31 and vimentin were selected to denote upcyte[®] LSECs and MSCs, respectively. As with liver organoids that had been maintained under dynamic culture (Figure 35), the three different cells types in the liver organoids cultured in the BioVaSc, also rearranged themselves into specific patterns. Upcyte[®] hepatocytes had a tendency to move towards the outer part of the liver organoid (Figure 35 b); whereas upcyte[®] LSECs were more localized in the central

RESULTS

regions (Figure 35 c), and upcyte[®] MSCs distributed evenly across the liver organoids, between hepatocytes and LSECs (Figure 35 d).

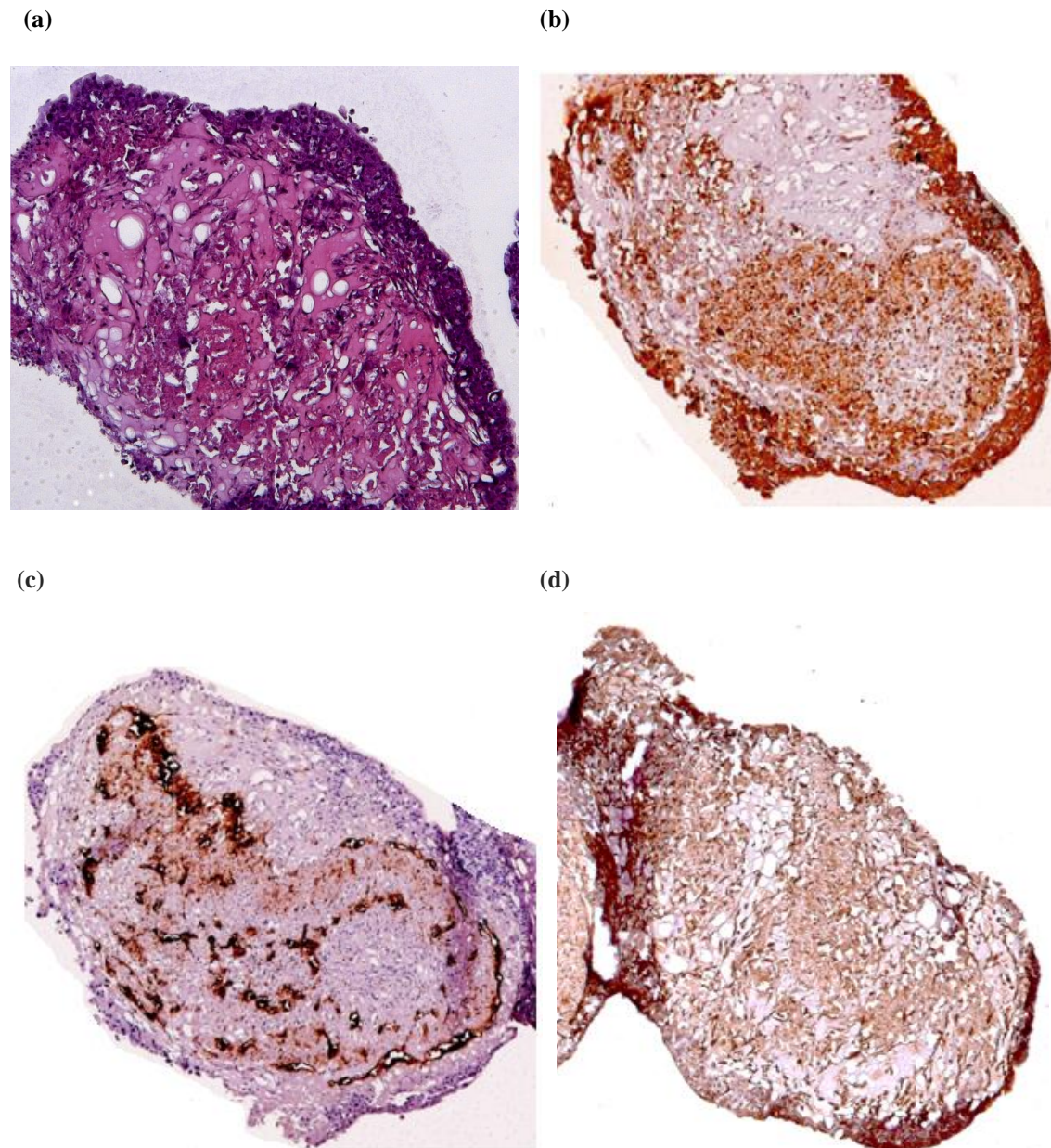


Figure 35: Architecture of liver organoids maintained in the lumen of the BioVaSc for 30 days in dynamic conditions. HE staining and immunostaining of cell specific markers:(a) upcyte[®] hepatocytes expressing CK8, (b) upcyte[®] LSECs expressing CD31 and (c) upcyte[®] MSC expressing vimentin (magnification: 200x).

3.3.3 Immunostaining for BioVaSc/organoid vascularization

Upcyte[®] mvECs were used to recolonize the vascular tree of the BioVaSc, as described in Section 2.2.4.3. As CD31 is one of the predominant markers expressed by endothelial cells, the vascular tree of the BioVaSc was examined for the expression of CD31. Sections of the liver organoids were analyzed to determine whether the capillaries from the BioVaSc had

RESULTS

reached the organoids. Figure 36 shows that circular opening inside the organoid was lined with endothelial cells since the upcyte[®] mvECs expressing CD31 were present in this area.

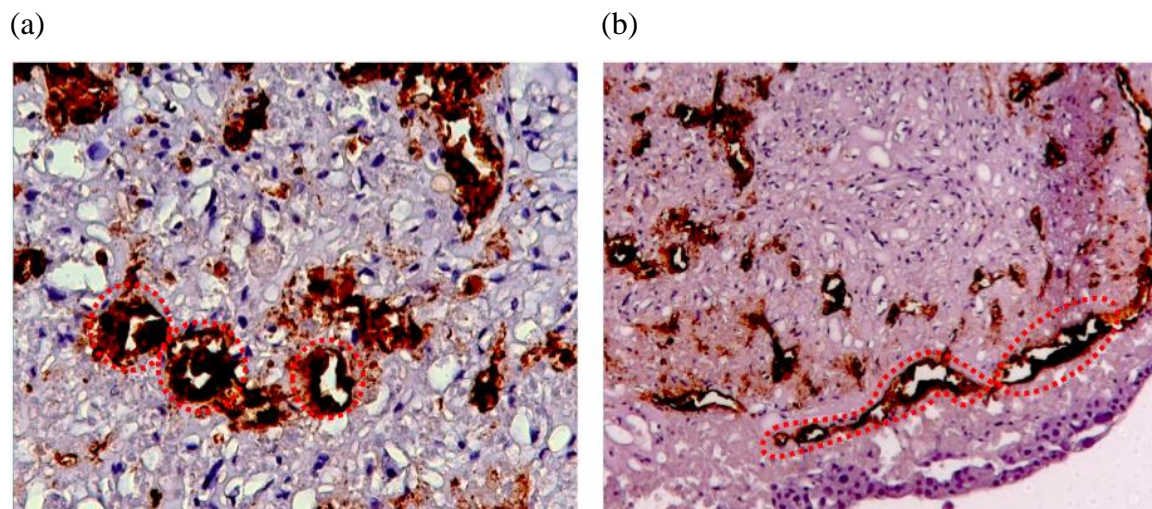


Figure 36: Section of a liver organoid. The openings of the blood vessel lined with upcyte[®] mvECs expressing CD31 are indicated with red circles (magnification: (a) 200x; (b) 100x).

3.4 Application of hepatic models - CYP inhibition

Second-generation upcyte[®] hepatocytes from 4 donors were used to perform inhibition assays, using a selection of reference inhibitors, under optimized culture conditions. CYP1A2, CYP2B6, CYP2C9 and CYP3A4 were reproducibly inhibited in a concentration-dependent manner and the calculated IC₅₀ values for each compound correctly classified them as potent inhibitors.

3.4.1 Culture optimisation for inhibition studies

Before starting inhibition studies, the culture conditions were modified to determine whether they could result in upcyte[®] hepatocyte cultures with higher CYP activities than were present using standard conditions i.e. seeding at 50% confluence with a 3-day pre-culture period (allowing for 1 PD) in HGM followed by a 3 day culture at confluence in HPM with daily refreshment of medium.

The main aspects investigated were:

- (1) The effect of DMSO in the pre-culture and conditioning medium.
- (2) The length of the pre-culture period (since previous studies using these cells in the *in vitro* micronucleus assay showed that there was less DNA damage to the cells when they were pre-cultured for 7 days prior to performing the assay (Nörenberg et al. 2013).
- (3) The type of basal medium used for the culture of cells at confluence (HGM versus HPM) and supplementing the pre-culture (during growth) and “conditioning” (i.e. at confluence) medium with DMSO.

RESULTS

Initial experiments were conducted to optimize the culture conditions for inhibition studies using Donor 422A-03. There was little difference observed in CYP activities when the pre-culture medium contained 0.25% or 0.5% DMSO (data not shown); therefore, in order to ensure maximal CYP activities, all subsequent experiments were conducted using 0.5% DMSO in the pre-culture HGM medium. The effect of DMSO on CYP2B6 and CYP3A4 activities in upcyte[®] hepatocytes from four donors (422A-03, 151-03, 653-01 and 10-03) was measured using a 7-day pre-culture followed by 3 daily treatments with HPM supplemented with a range of concentrations of DMSO (Figure 37). Activities of both CYPs in cells from all four donors were markedly induced in a concentration-dependent manner by DMSO and maximal effects were evident at 0.5-0.75% (v/v) DMSO. At higher concentrations of DMSO, there was a decrease in both CYP activities.

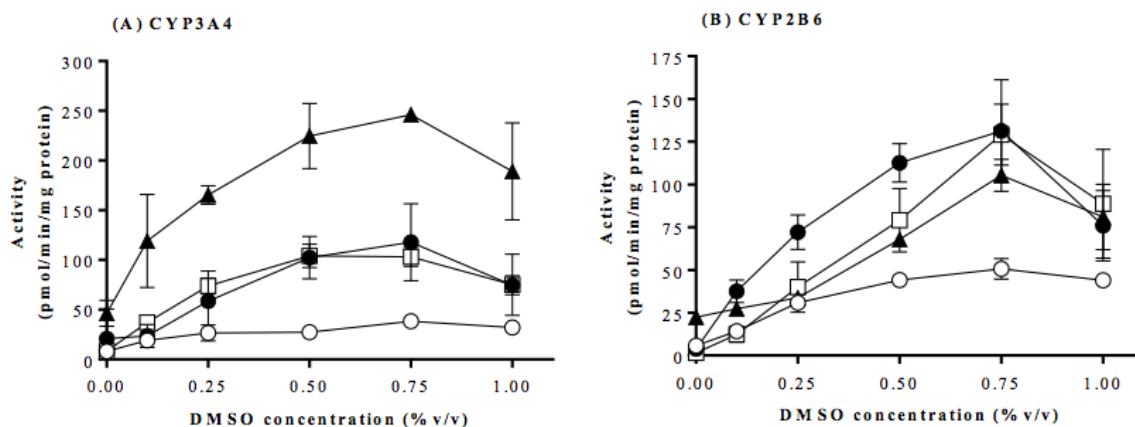


Figure 37: Effect of DMSO on CYP3A4 (A) and CYP2B6 (B) activities in upcyte[®] hepatocytes from different donors. Donor 10-03=○; Donor 151-03=●; Donor 422A-03=▲; Donor 653-03=□. Values are a mean of two experiments, each with n=2 wells per treatment

The influence of pre-culture conditions affected CYP2B6 and CYP3A4 activities in upcyte[®] hepatocytes from four donors is shown in Figure 38.

The conditions compared were:

- (1) Standard culture conditions (allowing for 1 PD)
- (2) Seeding at 3% confluence (5000 cells/cm²) in a T-flask with a 6-7-day pre-culture period (allowing for ~3.5 PDs) in HGM supplemented with 0.5% DMSO followed by trypsinisation, seeding at confluence (i.e. 150,000/cm²) and a 3 day culture in HGM with 0.5% DMSO with daily refreshment of medium
- (3) Seeding at 3% confluence in a T-flask with a 6-7-day pre-culture period in HGM supplemented with 0.5% DMSO followed by trypsinisation, seeding at confluence (i.e.

RESULTS

150,000/cm²) and a 3 day culture at confluence in HPM with 0.1% DMSO with daily refreshment of medium.

Increasing the pre-culture time from 3 days to 7 day did not increase the CYP3A4 activities but in three of the four donors, CYP2B6 activity was significantly increased. CYP3A4 activities were increased when the conditioning medium (used when the cells were at confluence) was changed from growth medium (HGM) to endpoint medium (HPM) with a lower concentration of DMSO (0.1% v/v). All further experiments were conducted using a 6-7 pre-culture period using HGM supplemented with 0.5% DMSO, trypsinisation, seeding at 5000 cells/cm² and conditioning for 3 days with HPM supplemented with 0.1% DMSO.

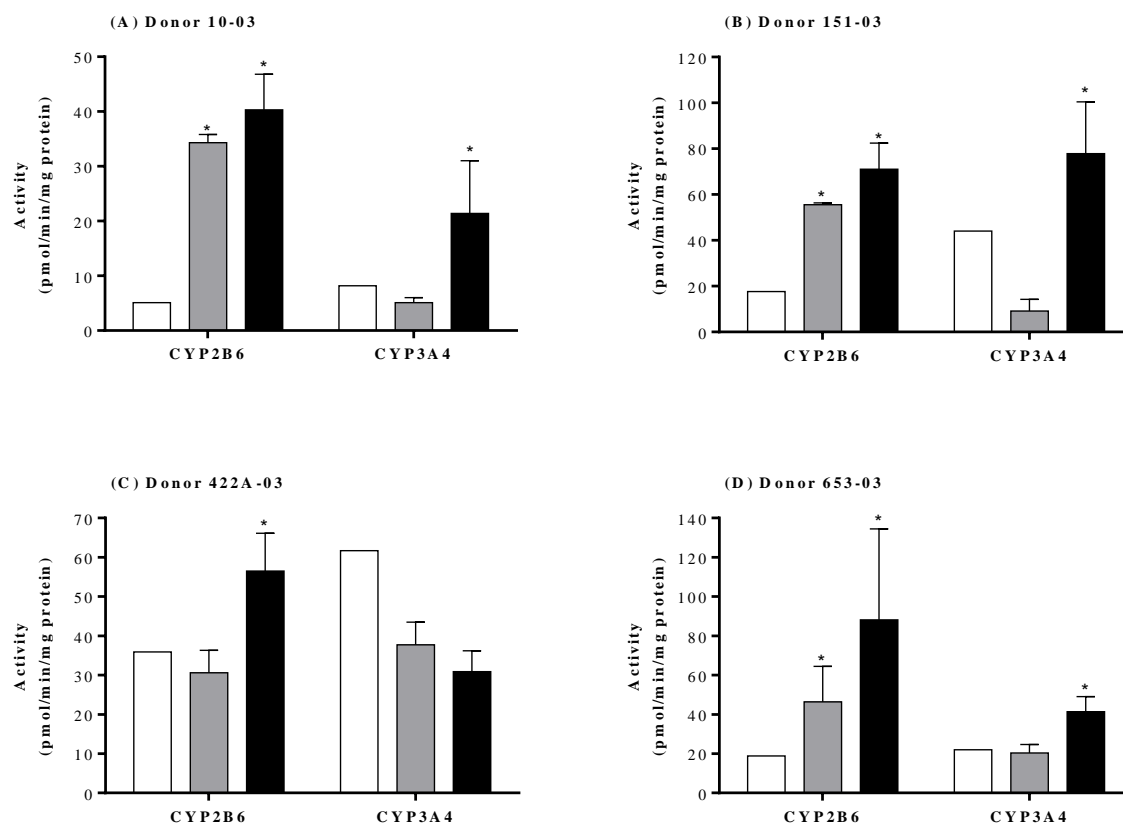


Figure 38: Effect of pre-culture time and DMSO treatment on CYP2B6 and CYP3A4 activities in upcyte[®] hepatocytes from different donors. White bars represent cells grown over a 3 day pre-culture and 3 days conditioning at confluence in GM+0.1% DMSO (standard conditions); grey bars represent cells grown over a 6-7-day pre-culture period followed by re-seeding at confluence and a 3 day conditioning in HGM+0.5% DMSO, and black bars represent cells grown over a 6-7-day pre-culture period followed by re-seeding at confluence and a 3 day conditioning in HPM + 0.1% DMSO. Values are a mean of two experiments, each with n=3 wells per treatment. * = significantly different from standard conditions (P< 0.05).

RESULTS

Having optimized the culture conditions, CYP activities in control incubations of upcyte[®] hepatocytes (using the optimized conditions) were compared with the corresponding primary human hepatocyte cultures from which they were derived (Table 18). As with primary hepatocytes, the CYP activities in upcyte[®] hepatocytes varied between donors. CYP1A2 activities were present in upcyte[®] hepatocytes from all four donors, although this activity in Donors 653-03 and 151-03 was only detected using 24 h incubations and analysis by LC-MS (data not shown), and all were lower than in corresponding paired donor hepatocytes. CYP2B6 mediated bupropion hydroxylation was markedly higher in upcyte[®] hepatocytes and were comparable to that in the original primary hepatocytes measured by the supplier (all donors). CYP2C9 activities were higher in upcyte[®] hepatocytes than the paired primary cells. As with CYP2B6 activities, CYP3A4 activities, measured using testosterone, were markedly higher in upcyte[®] hepatocytes than in their paired primary cells.

Table 18. Basal CYP activities (pmol/min/mg protein) in second-generation upcyte[®] hepatocytes and paired primary human hepatocytes were cultured. Values generated were compared with data provided by the supplier. Values for upcyte[®] hepatocytes are mean \pm SD, n=6-8 wells from 1-2 separate experiments. APAP = acetaminophen; OH-Bup = Hydroxybupropion; OH-Tolb = Hydroxytolbutamide; 6 β -OHT = 6 β -hydroxytestosterone; M = Medicyte, P = provider information on the cells, ND = not determined.

CYP	Metabolite	Donor 1		Donor 2		Donor 3		Donor 4	
		upcyte [®] Donor 10-03	Paired primary	upcyte [®] Donor 151-03	Paired primary	upcyte [®] Donor 422A-03	Paired primary	upcyte [®] Donor 653-03	Paired primary
1A2	APAP	3.3 \pm 0.4 (M)	ND (P)	0.7 \pm 1.4 (M)	2.0 (P)	2.3 \pm 0.1 (M)	4.5 (P) 0.1 \pm 0.0	0.0 \pm 0.0 (M)	13.4 (P)
2B6	OH-Bup	40.3 \pm 6.5 (M)	14.3 (P)	71.1 \pm 11.3 (M)	1.3 (P)	33.6 \pm 11.4 (M)	1.3 (P) 4.5 \pm 1.2	46.4 \pm 18.0 (M)	5.3 (P)
2C9	OH-Tolb	91.8 \pm 5.7 (M)	6.3 (P)	29.1 \pm 21.4 (M)	ND (P)	4.8 \pm 3.1 0.39 \pm 0.19 (M)	ND (P) 0.8 \pm 0.0	20.2 \pm 2.1 (M)	ND (P)
3A4	6 β -OHT	21.4 \pm 9.6 (M)	16.2 (P)	77.8 \pm 22.6 (M)	10.8 (P)	42.9 \pm 6.3 (M)	24.5 (P)	41.4 \pm 7.7 (M)	22.7 (P)

RESULTS

3.4.2 CYP inhibition studies

Inhibition studies were conducted using short-term incubation period of 1 h. Although the CYP1A2 activities that were present in upcyte[®] hepatocytes were measurable, cells incubated were pre-induced with 100 μ M omeprazole in order to obtain consistently high CYP1A2 activities for the inhibition studies using UV-HPLC as the analytical method. Two pre-induction regimens were investigated, namely a single treatment of 100 μ M omeprazole over 3 days and a daily treatment of 100 μ M omeprazole over the same period. Both induction regimens resulted in high CYP1A2 activities in upcyte[®] hepatocytes from Donors 422A-03 and 10-03 (>40 pmol/min/mg protein), suggesting both could be employed for CYP1A2 inhibition studies. In this study, daily treatments were used since this resulted in higher CYP1A2 activities than a single treatment. The induced activities were 57.1 ± 17.1 , 83.8 ± 21.7 , 205.0 ± 44.9 and 115.2 ± 30.2 pmol/min/mg protein in upcyte[®] hepatocytes from Donors 10-03, 151-03, 422A-03 and 653-03, respectively. CYP2B6, CYP2C9 and CYP3A4 did not require pre-induction with an inducer; therefore, conditioning medium included 100 μ M omeprazole for CYP1A2 assays only. Results for inhibition studies using upcyte[®] hepatocytes from Donor 422A-03 are shown in Figure 39. In these studies, CYPs were inhibited using competitive (α -naphthoflavone, miconazole and ketoconazole) and time-dependent (ticlopidine) inhibitors.

RESULTS

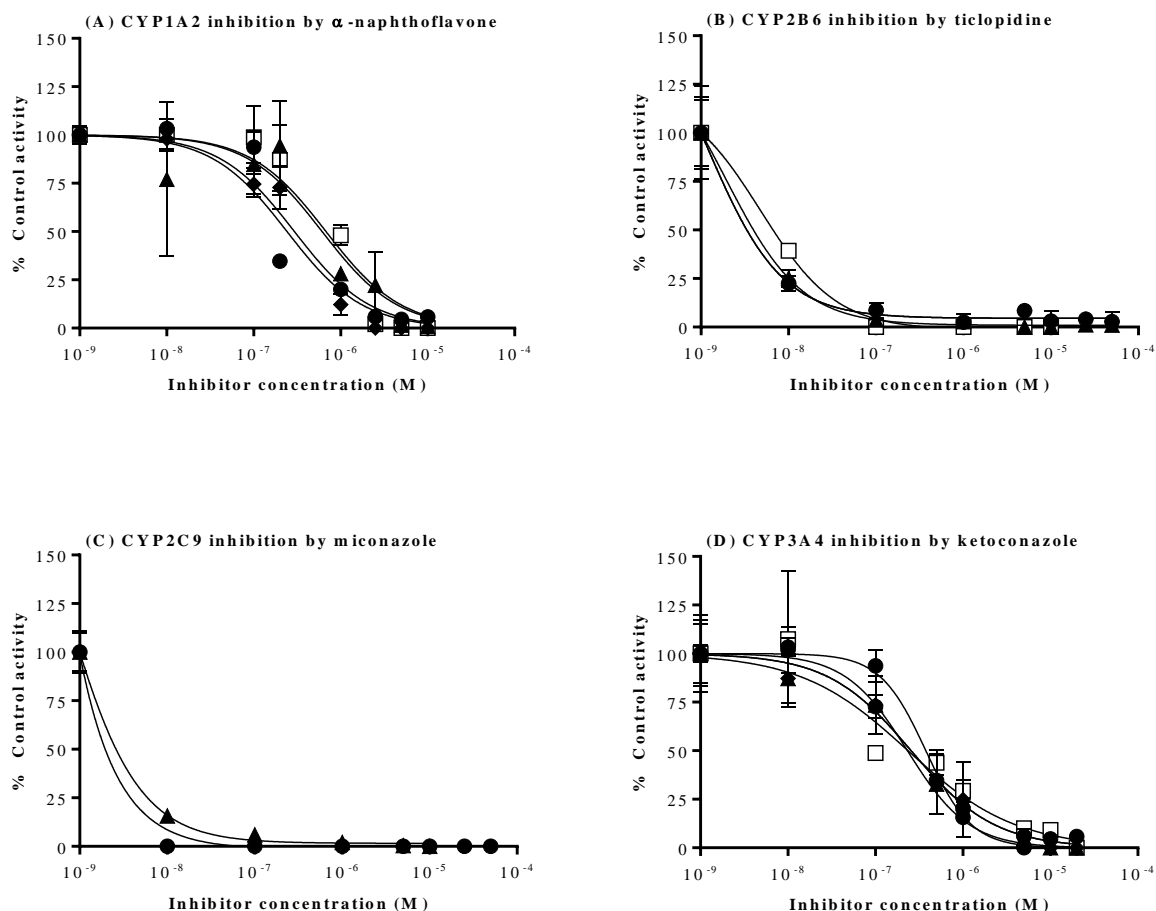


Figure 39: Inhibition of (A) CYP1A2 by \square -naphthoflavone, (B) CYP2B6 by ticlopidine, (C) CYP2C9 by miconazole and (D) CYP3A4 by ketoconazole in upcyte[®] hepatocytes from Donor 422A-03. Values are the mean \pm SD from triplicates in 2-4 experiments (denoted by different symbols).

The inhibition of different CYPs was reproducible across experiments (as shown for Donor 422A-03 in Figure 39) and in upcyte[®] hepatocytes from all four donors tested (Table 19). There was a concentration-dependent inhibition of CYP1A2, CYP2B6, CYP2C9 and CYP3A4, such that at the highest concentration all activities were completely inhibited. MTS analysis showed that inhibitors did not cause significant cytotoxicity at any concentration tested in upcyte[®] hepatocytes from all four donors (with the exception of ticlopidine, which caused ~10% cytotoxicity in upcyte[®] hepatocytes from Donor 151-03 at the highest concentration only). The IC_{50} values for each CYP tested also compared well with those reported in primary human hepatocytes or human liver microsomes (Table 19), such that all four CYP inhibitors were classified as potent inhibitors of the respective CYP. These results support the use of upcyte[®] hepatocytes in inhibition studies incubated in short-term assays to derive an IC_{50} value.

RESULTS

Table 19. IC₅₀ values of CYP inhibitors incubated with upcyte[®] hepatocytes from different donors. For comparison, literature values for microsomes and/or hepatocytes are also shown. Values for upcyte[®] hepatocytes are mean ± SD, n=6-8 wells from at least 2 separate experiments.

Donor	IC ₅₀ value							
	CYP1A2 by α-naphthoflavone μM		CYP2B6 by ticlopidine nM		CYP2C9 by miconazole nM		CYP3A4 by ketoconazole μM	
	upcyte [®]	Primary ^a	upcyte [®]	Microsome ^b	upcyte [®]	Primary ^c	upcyte [®]	Primary ^c
10-03	0.15, 0.04 (n=2)	0.1	8.1 ± 1.6 (n=4)	0.32	251, 95.8 (n=2)	2.12	0.30 ± 0.3 (n=4)	0.28 0.14
151-03	0.38, 0.19 (n=2)		36.1 ± 27.9 (n=4)		12, 6.6 (n=2)		0.15 ± 0.01 (n=4)	
422A- 03	0.46 ± 0.22 (n=4)		7.3 ± 1.6 (n=4)		3.1, 4.3 (n=2)		0.27 ± 0.06 (n=5)	
653-03	0.36, 0.12 (n=2)		27.5 ± 19.7 (n=4)		14.7, 4.1 (n=2)		0.23 ± 0.12 (n=4)	

Values are a = (Moeller et al. 2013); b = (Turpeinen et al. 2004) (microsomes); c = (Mao et al. 2012a; Moeller et al. 2013).

3.5 Application of hepatic models - CYP induction studies

Similar to the inhibition assays, induction assays were performed using second-generation upcyte[®] hepatocytes from 4 donors using a panel of 11 inducers classified as potent, moderate or non-inducers of CYP3A4 and CYP2B6. Upcyte[®] hepatocytes were responsive to prototypical CYP1A2, CYP2B6, CYP2C9 and CYP3A4 inducers, confirming that they have functional AhR, CAR and PXR mediated CYP regulation.. Three different predictive models for CYP3A4 induction, namely the Relative Induction Score (RIS), AUC_u/F₂ and C_{max,u}/Ind₅₀ were analyzed. In addition, PXR (rifampicin) and CAR-selective (carbamazepine and phenytoin) inducers of CYP3A4 and CYP2B6 induction, respectively, were also demonstrated.

3.5.1 CYP induction responses in upcyte[®] hepatocytes

Upcyte[®] hepatocytes from four donors (422A-03, 151-03, 653-03 and 10-03) using a 3 day pre-culture period were responsive to CYP1A2, CYP2B6, CYP2C9 and CYP3A4 induction by prototypical inducers (data from two donors are shown in Figure 40). In order to rule out false positive results from CYP3A4 induction studies, the FDA recommends including a negative control i.e. a non-inducer, in each induction assay. In these assays, two negative controls were included, namely quinidine (0.1-250 μM) and flumazenil (0.05 – 50μM), both of which did not induce CYP3A4 or CYP2B6 at any concentration tested (data not shown).

RESULTS

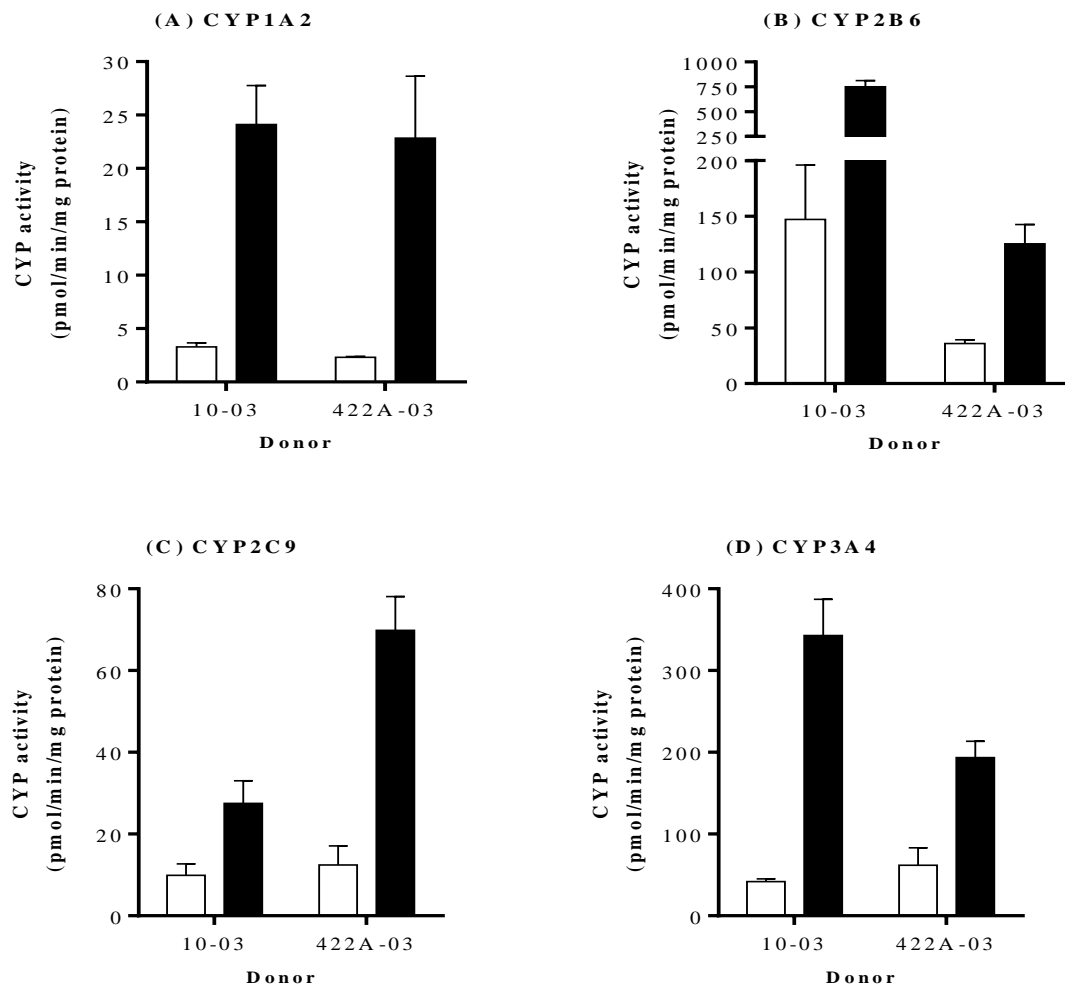


Figure 40: Induction of CYP1A2 (by 50 μ M omeprazole), CYP2B6 (by 2 mM phenobarbital), CYP2C9 (by 20 μ M rifampicin) and CYP3A4 (by 20 μ M rifampicin) in upcyte[®] hepatocytes from Donors 10-03 and 422A-03. White bars indicate control values and black bars indicate values for the prototypical inducers. Values are the mean \pm SD from triplicates.

3.5.2 Prediction models for *in vivo* CYP3A4 induction

Three main prediction models recommended by the FDA, EMA and PhARMA for CYP3A4 induction (Food and Drug Administration 2012; Chu et al. 2009; European Medicines Agency 2013), namely, the RIS, AUC_u/F_2 and $C_{max,u}/Ind_{50}$ were compared. Data from upcyte[®] hepatocytes from Donor 653 were used to compare the different models (Figure 41). Of the three, the fit was best when the RIS ($R^2 = 0.92$) and $C_{max,u}/Ind_{50}$ ($R^2 = 0.93$) were used; however, there was also a good correlation when the F_2 value ($R^2 = 0.89$), was used. The Ind_{max} and Ind_{50} values from all four donors were applied to the RIS model (values shown in Table 4) and, although the calibration curves were different across donors, they all exhibited a good fit of the data ($R^2 = 0.87$ to 0.94, Figure 41 C and Figure 42)

RESULTS

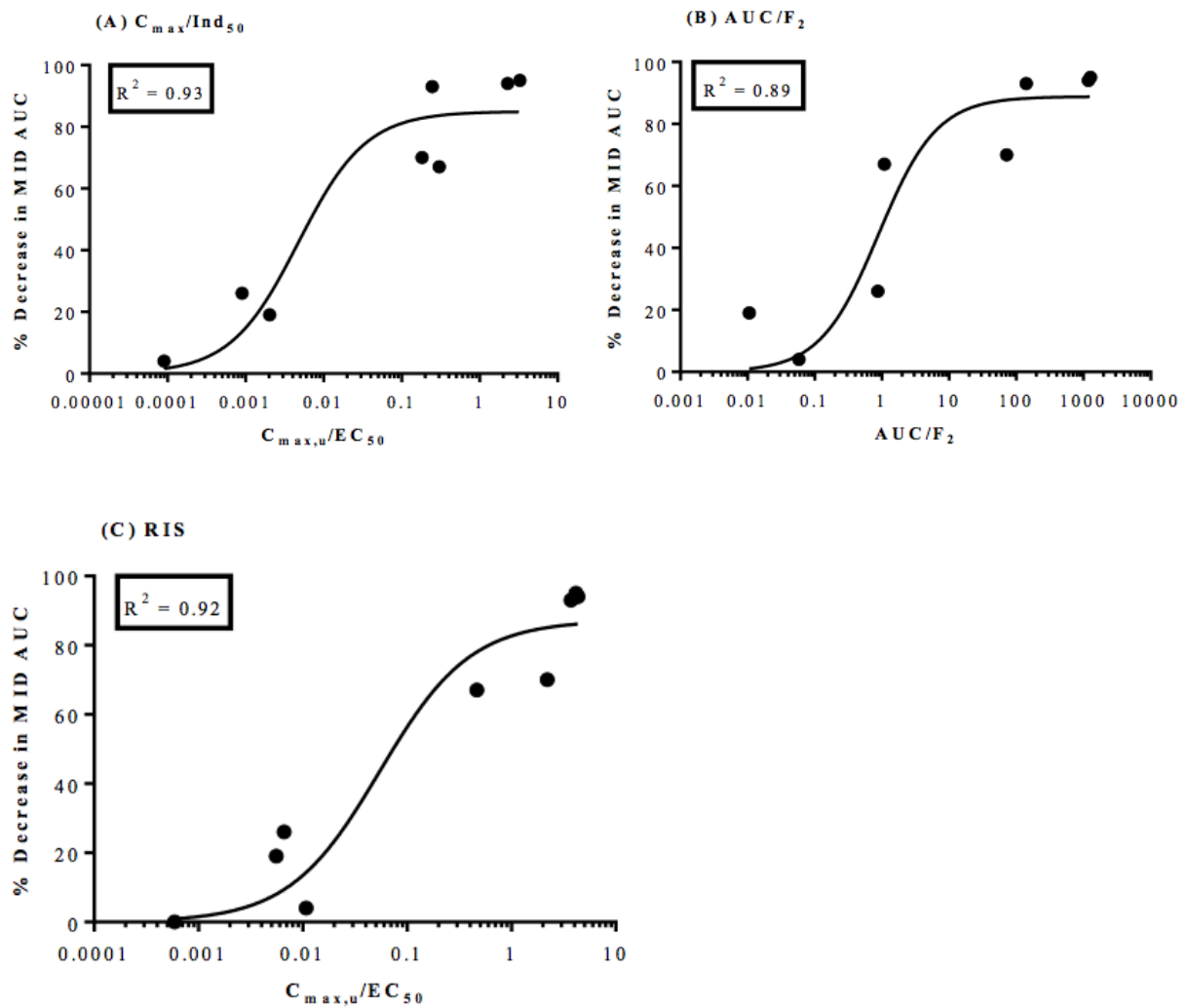
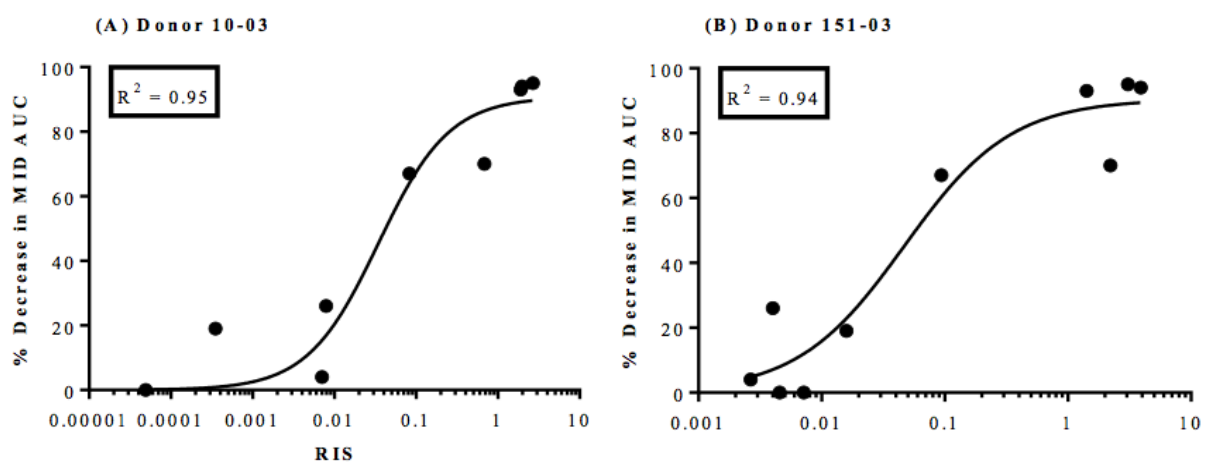


Figure 41: Comparison of calibration curves for RIS, AUC_u/F_2 and $C_{max,u}/Ind_{50}$ using upcyte[®] hepatocytes from Donor 653. Values are the mean from duplicate values of 2 experiments.



RESULTS

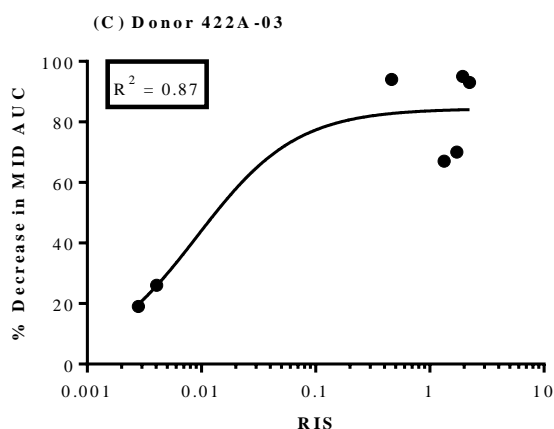


Figure 42: Comparison of calibration curves for RIS from three donors of upcyte[®] hepatocytes. Values are the mean from duplicate values of 2 experiments.

3.5.3 CAR and PXR selective induction of CYPs

The relative induction of CYP2B6 and CYP3A4 is known to be a result of selective activation of either the PXR or CAR receptors (Faucette et al. 2007); therefore, this attribute was investigated by treating upcyte[®] hepatocytes with different inducers and measuring CYP3A4 and CYP2B6 in same wells. Table 20 summarises the CYP3A4 and CYP2B6 induction responses of upcyte[®] hepatocytes from all donors to the same compounds tested for CYP3A4 induction. The unbound plasma concentrations (C_{max}) and *in vivo* induction values (expressed as a % decrease in the AUC of midazolam) used in the calculation of the RIS are shown for each compound.

RESULTS

Table 20. CYP3A4 induction responses of upcyte[®] hepatocytes from different donors to known inducers and non-inducers of CYP3A4. Values are from two experiments.

Compound	Donor 10-03			Donor 151-03			Donor 422A-03			Donor 653-03		
	Ind _{max}	Ind ₅₀	% Rif	Ind _{max}	Ind ₅₀	% Rif	Ind _{max}	Ind ₅₀	% Rif	Ind _{max}	Ind ₅₀	% Rif
Rifampicin	31	11	100	7.2	12	100	12	12	100	10	4.6	100
Phenobarbital	23	455	74	5.2	38	68	11	385	95	12	113	120
Phenytoin	15	46	45	4.7	1.1	60	16	225	137	6.3	2.4	59
Carbamazepine	4.8	6.2	13	3.8	2.0	45	4.0	11	28	5.7	3.1	52
Troglitazone	4.7	6.3	12	1.8	2.8	13	2.7	1.0	15	2.2	0.8	14
Pioglitazone	4.3	18	11	4.0	31	48	2.6	27	14	9.2	49	91
Dexamethasone	2.5	185	5	3.5	13	39	3.4	32	22	2.7	15	19
Nifedipine	2.1	0.4	4	4.6	5.6	58	Not determined			7.2	23	69
Omeprazole	2.3	36	4	3.1	22	34	Not determined			1.5	5.5	5
Flumazenil	No Induction			No Induction			No Induction			No Induction		
Quinidine	No Induction			No Induction			No Induction			No Induction		

The relative induction of both CYPs (compared to the maximal fold-induction by the positive controls, according to equation 3 in the Methods Section) by the PXR selective drug, rifampicin, the CAR-selective drugs, phenytoin and carbamazepine; and the mixed activator, phenobarbital was compared in Figure 43 in all four donors. The relative induction of CYP3A4 and CYP2B6 was compound-specific and donor-dependent. Rifampicin was a potent inducer of CYP3A4 in all upcyte[®] hepatocytes (Table 21), and only phenobarbital and phenytoin caused a higher induction (137% and 120% of rifampicin maximal induction in Donor 422A-03 and Donor 653-03, respectively (Figure 43 c and d, grey bars). Rifampicin was also a potent inducer of CYP2B6 in upcyte[®] hepatocytes from Donor 422A-03 (108% of the maximal PB response, Figure 43 c). By contrast, rifampicin was only a moderate inducer of CYP2B6 in upcyte[®] hepatocytes from Donors 10-03, 151-03 and 653-03 (between 14% and 34% of the maximal PB response). Phenobarbital was a potent inducer of both CYP3A4 and CYP2B6 and resulted in maximal induction of both CYPs in upcyte[®] hepatocytes from all four donors. Phenytoin was also a potent inducer of CYP3A4. This was reflected in these

RESULTS

studies by the predominance for CYP2B6 over CYP3A4 induction by this compound in three of the four donors (e.g. the induction of CYP2B6 and CYP3A4 in upcyte[®] hepatocytes from Donor 151-03 was 130% and 60% of the positive controls, respectively). Although carbamazepine was a moderate inducer of CYP3A4 and CYP2B6, the relative predominance for CYP2B6 induction was also evident for this CAR-selective compound in three of the four Donors.

Table 21. CYP2B6 induction responses of upcyte[®] hepatocytes from different donors to known inducers and non-inducers of CYP2B6. Values are from two experiments.

Compound	Donor 10-03			Donor 151-03			Donor 422A-03			Donor 653-03		
	Ind _{max}	Ind ₅₀	% PB	Ind _{max}	Ind ₅₀	% PB	Ind _{max}	Ind ₅₀	% PB	Ind _{max}	Ind ₅₀	% PB
Rifampicin	2.0	60	34	1.3	21	14	7.8	11	108	1.6	16	29
Phenobarbital	3.9	277	100	2.9	183	100	7.3	731	100	3.1	60	100
Phenytoin	3.6	99	88	2.7	5.8	89	4.0	5.4	48	2.8	5.9	85
Carbamazepine	2.0	48	33	2.3	6.6	68	4.3	20	52	1.4	50	17
Troglitazone	5.4	18	150	2.1	4.6	57	5.0	5.4	63	2.3	5.9	63
Pioglitazone	2.6	20	55	1.9	89	49	3.6	9.3	42	2.1	65	54
Dexamethasone	No induction			No Induction			No Induction			No Induction		
Nifedipine	3.9	12	98	No Induction			No Induction			No Induction		
Omeprazole	2.0	12	31	No Induction			Not determined			2.2	9.7	56
Flumazenil	No Induction			No Induction			No Induction			No Induction		
Quinidine	No Induction			No Induction			No Induction			No Induction		

RESULTS

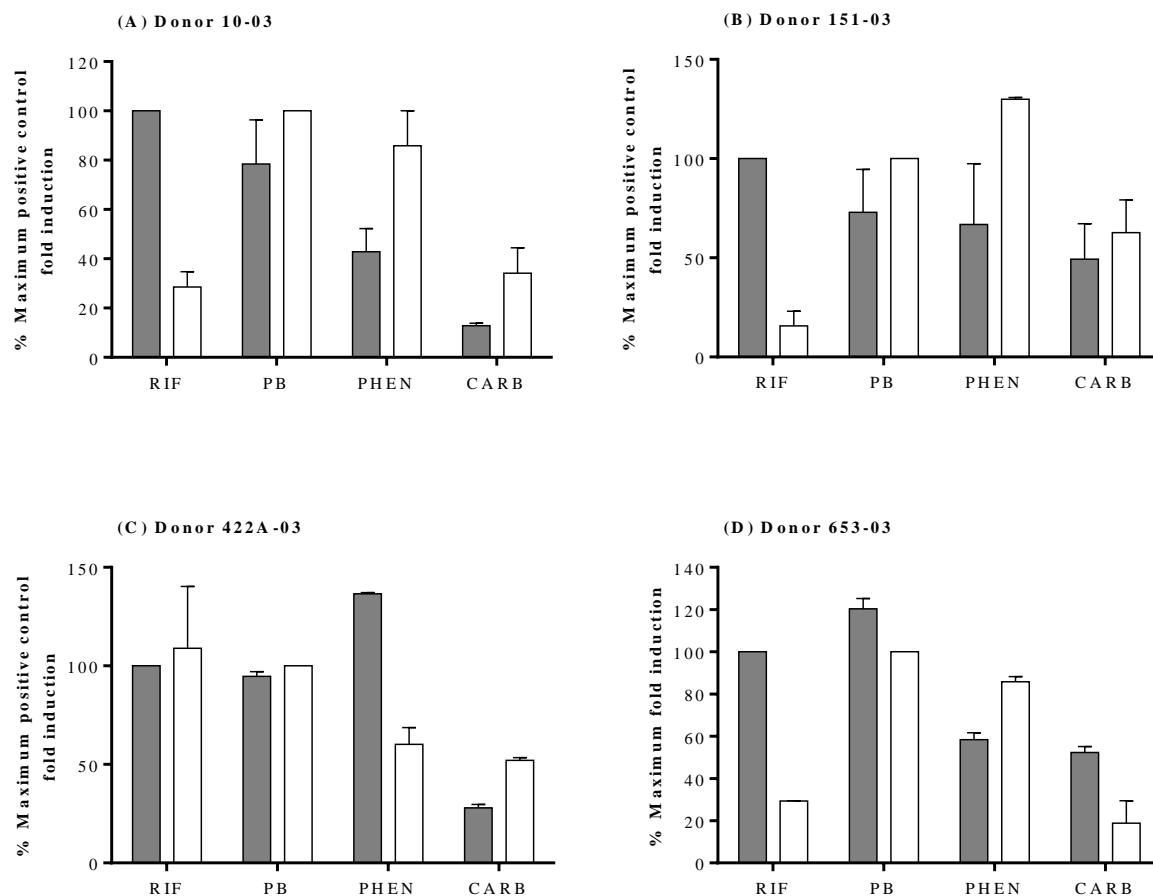


Figure 43. A comparison of % maximum fold induction by rifampicin, phenobarbital, phenytoin and carbamazepine in upcyte[®] hepatocytes from different donors. Black bars indicate values for CYP3A4 and white bars indicate values for CYP2B6. Values are the mean from duplicate values of 2 experiments.

3.6 Application of hepatic models – Haemophilia Therapy

As the primary LSECs are one of the predominant FVIII producing cells *in vivo*, the supernatant from primary LSECs were evaluated to detect the presence of functional FVIII. In order to increase the FVIII production, different upcyte[®] endothelial cells such as BOECs, LSECs and mvECs were transduced with lentiviral particles carrying a FVIII transgene. To duplicate the physiological situation, primary endothelial cells (primary mvECs) were used to transduce with FVIII lentivirus. The supernatant was harvested and evaluated for the secretion of functional FVIII.

RESULTS

3.6.1 FVIII expression in primary LSECs

Supernatants were harvested from cultures of primary LSECs and analyzed immediately or frozen and stored at -20°C before analysis. The concentration of FVIII in both medium samples was below the limit of detection of the assay; however, after concentrating them by 25-fold using an Amicon[®] Ultra-0.5 centrifugal filter device (30K MWCO) FVIII was detectable (Figure 44). The rate of production of FVIII was 27 ± 4 mU/ 10^6 cells/24 h and 23 ± 3 mU/ 10^6 cells/24 h in fresh (non-frozen) and frozen supernatant, respectively which is not significantly different ($P>0.05$). By extrapolating the concentration factor of 25, the non-concentrated samples expressed ~ 1 mU/ 10^6 cells/24 h.

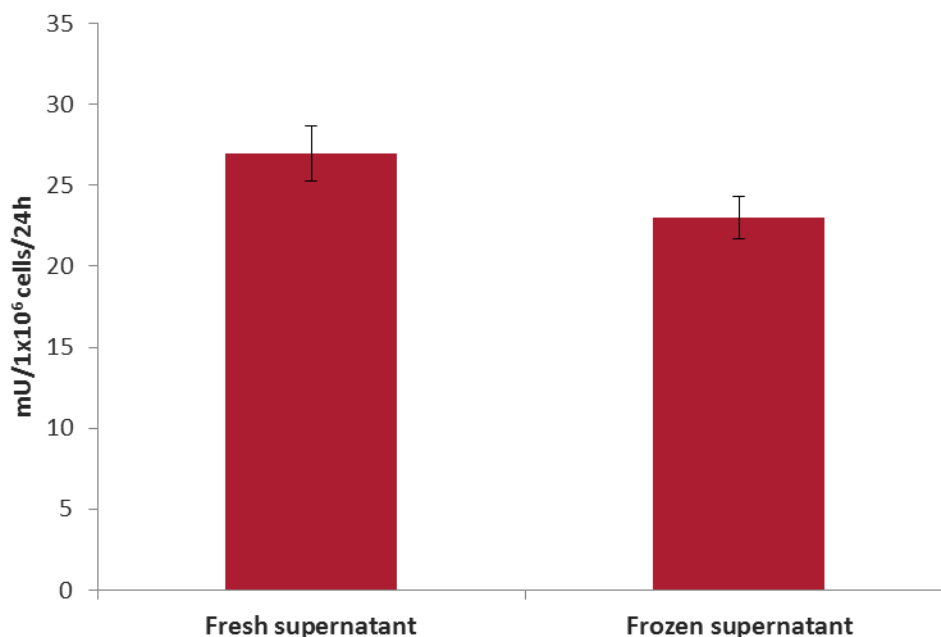


Figure 44: Comparison of the rate of secretion of FVII by LSECs and the effect of freezing and storing the media before analysis. Values are a mean of $n=3$ cultures \pm SD.

3.6.2 Generation of lentiviral FVIII construct

3.6.2.1 Cloning of entry clone

Figure 45 a shows the amplification of the FVIII gene flanked with *attB* sites using PCR and separated on 0.7% agarose gel. The expected size of the FVIII insert DNA is ~ 4 Kb. FVIII gene flanked with *attB* was used to generate an entry clone using BP Clonase[™] II enzyme kit (as described in 2.2.6.2). The entry clone was digested using the restriction enzymes, Bsa HI and SpeI, to verify the presence of FVIII gene. The expected size of the DNA fragment is ~ 1 Kb and 6 Kb. The double digestion confirmed the presence of FVIII gene in entry clone figure 45 b.

RESULTS

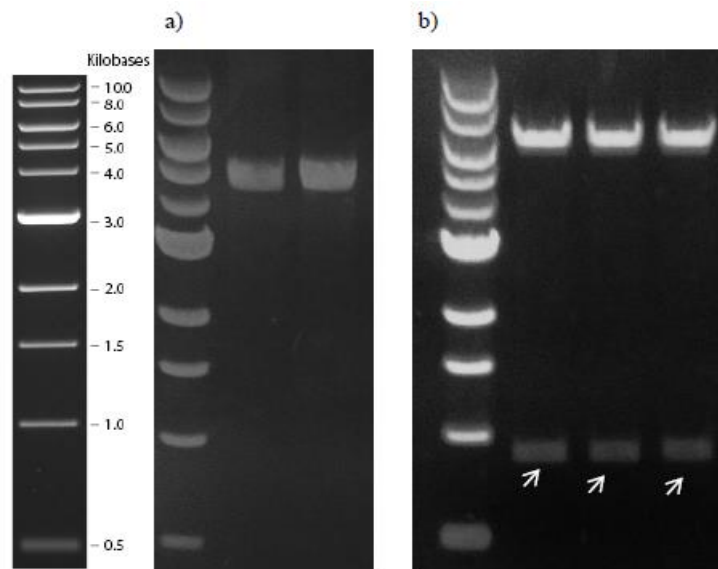


Figure 45: (a) Amplified FVIII gene fragment flanked with *attB*, (b) 1 μ g of entry clone plasmid was restricted digested using Bsa HI and SpeI to verify the presence of FVIII gene. Both the samples (a & b) were separated on 0.7 % agarose gel stained with gel red.

3.6.2.2 Cloning of expression clone

A recombination reaction occurs between the entry clones and destination vector, which results in generation of expression clone (LR reaction). The plasmid from the expression clone was digested as described in Section 2.2.6.5 with SpeI to verify the presence of FVIII gene. The expected size of the fragment DNA is ~ 685 bp and backbone construct is 11 kb. The double digestion confirmed the presence of FVIII gene in expression clone (Figure 46).

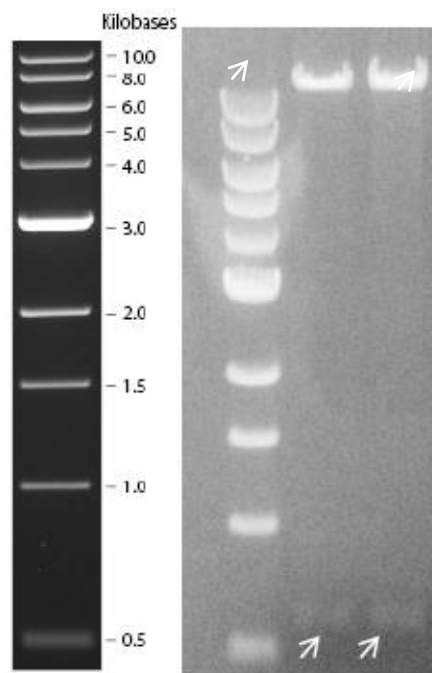


Figure 46: Expression clone plasmid (1 μ g) was restricted digested with SpeI and analyzed for the presence of FVIII gene after separation on a 0.7 % agarose gel and stained with gel red.

RESULTS

3.6.2.3 Sequencing of FVIII gene

DNA was sequenced at GATC Biotech and the results correlated 100% with the parental vector and NCBI sequence (Appendix no.6.1)

3.6.3 Viral titer determination

The titer of viral preparations is normally estimated from the number of infected cells expressing a transduced marker gene. This procedure is time-consuming step, and generally takes 4 to 5 days. To circumvent this, a protocol was established whereby the RNA of the lentiviral particle was directly measured by quantitative real-time PCR without a reverse transcription step. Each individual viral vector with similar backbone can be measured using primers binding at the LTR sequence. Titration of virus-containing supernatant was carried as described in Section 2.2.6.9, which resulted in 7.51×10^{10} viral particles per ml of solution carrying the FVIII gene.

3.6.4 FVIII expression in upcyte[®] mvECs

Upcyte[®] LSECs, upcyte[®] mvECs and upcyte[®] BOECs were transduced as described in Section 2.2.6.10 with three different MOIs (MOI 1000, 10,000 and 100,000). Figure 47 shows that the upcyte[®] endothelial cells (BOECs/LSECs/mvECs) exhibited cobble stone morphology which is typical for the endothelial cells.

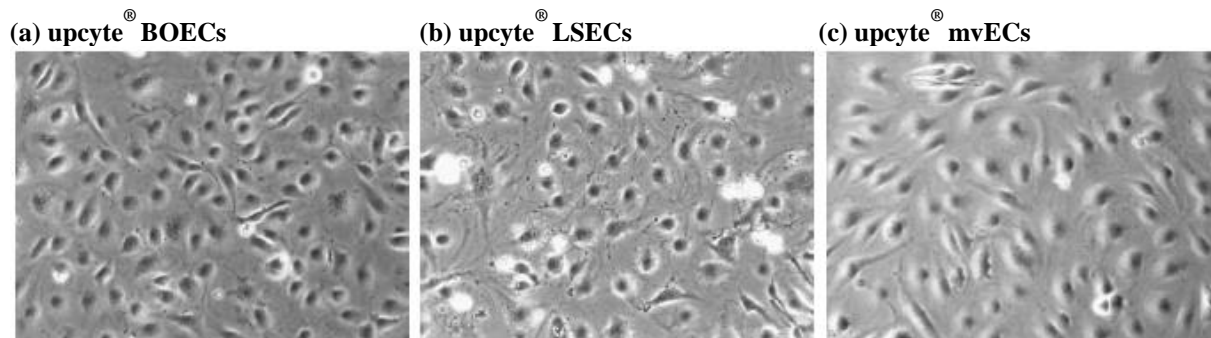


Figure 47: Morphology of (a) upcyte[®] BOECs, (b) upcyte[®] LSECs and (c) upcyte[®] mvECs observed under light microscopy (magnification: 100x).

To analyze FVIII production, upcyte[®] endothelial cells were transduced as described in Section 2.2.6.10. FVIII was not detected in the supernatant harvested from upcyte[®] BOECs and LSECs. However, upcyte[®] mvECs transduced with FVIII lentiviral particles (MOI 1000) yielded 6.9 mU/ 10^6 cells/24 h (Figure 48). Upcyte[®] mvECs transduced with MOIs of 10,000 and 100,000 produced 15.3 mU and 15.7 mU of FVIII per 10^6 cells in 24 h, respectively.

RESULTS

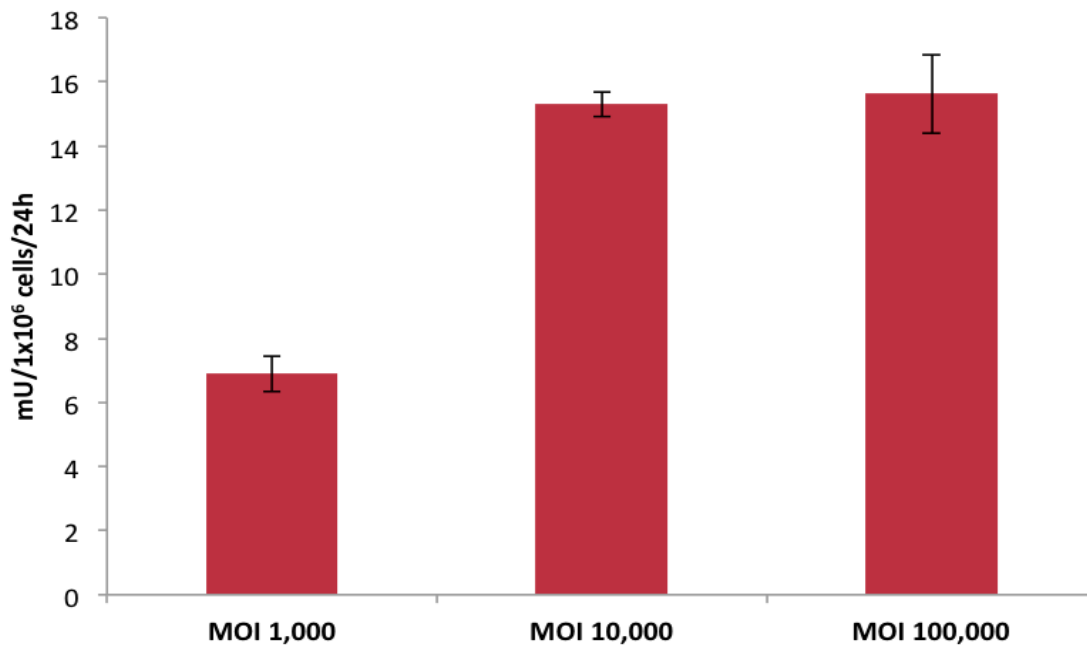


Figure 48: FVIII production in upcyte[®] mvECs transduced with different MOIs of lentiviral particles carrying FVIII gene. Values are the mean \pm SD from 2 experiments, each with n=3 wells.

3.6.5 Transduction of primary mvECs

As the proof-of-principle experiment demonstrated that upcyte[®] mvECs could produce FVIII after transduction with this specific gene, the next step was to transduce primary mvECs with lentiviral particles carrying FVIII gene in order to reflect *in vivo* situation, i.e. using primary cells (mvECs). Primary mvECs transduced as described in 2.2.6.10 were used for antibiotic selection process as described in Section 2.2.6.11. Using the blasticidine application, primary mvECs carrying FVIII gene were selected. The number of primary mvECs carrying the FVIII gene was relatively higher (30%) in cells transduced with a MOIs of 100,000 and MOI 10,000 than with a MOI of 1000. The islands of cells that were selected using blasticidine were cultured until they reached confluence before collecting the supernatant for FVIII analysis. Throughout the selection process each of the MOIs maintained the cobble stone morphology, which is typical for endothelial cells (Figure 49).

RESULTS

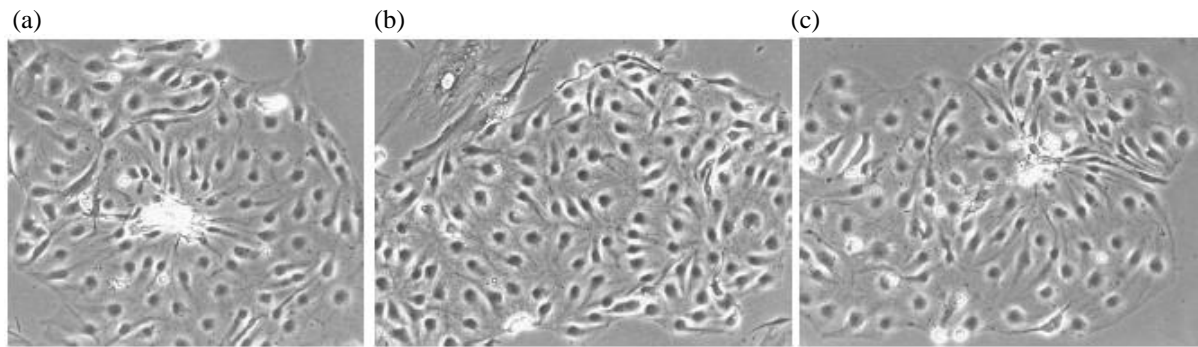


Figure 49: A comparison of the morphology of primary endothelial cells, seeded at 20,000 cells/cm² and 24 h after transduction with lentiviral particles with different MOIs (a. MOI 1000, b. MOI 10,000 and c. 100,000) (magnification: 100x).

3.6.5.1 Characterization of primary mvECs

Tube formation is an important endothelial cell character in the process of angiogenesis in *in vivo*. Primary mvECs transduced and selected for FVIII gene construct were analyzed for their ability to form tubes in Matrigel™. The cells were seeded at densities of 14,000 cells/cm² and 20,000 cells/cm² and then assessed for tube formation. The cells began to form tube-like structures after 2 h and, after 6 h of incubation. A complete network of capillaries was formed. A seeding density of 14,000 cells/cm² was found to be optimal for tube formation, since these primary mvECs formed tubes from single cells, as shown in Figure 50 a. At higher seeding densities, tubes were formed from more than one cell Figure 50 b.

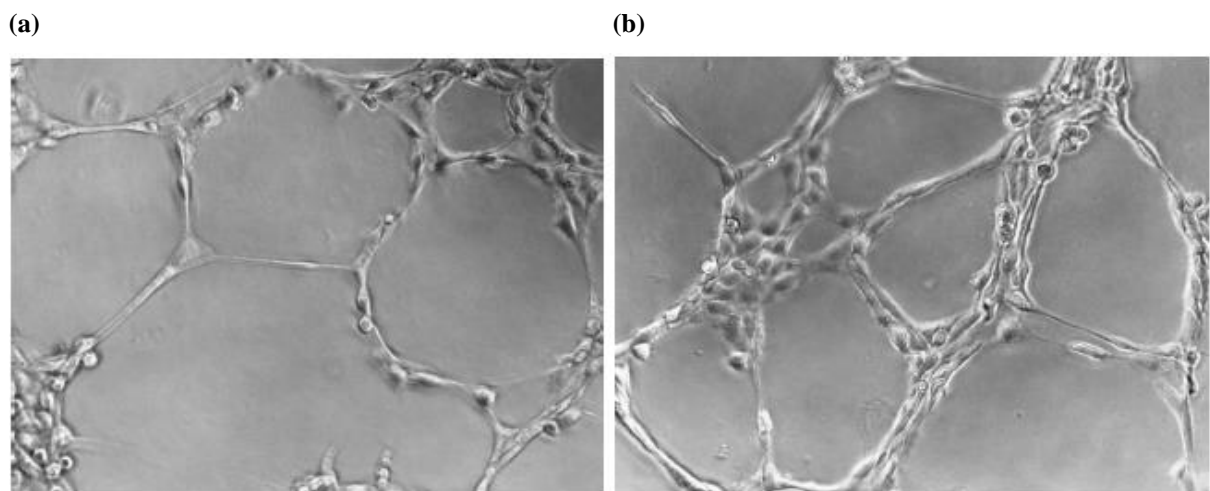


Figure 50: Tube formation after 6h by primary mvECs seeded at different densities (a) 14,000 cells/cm² and (b) 20,000 cells/cm².

RESULTS

3.6.5.2 FVIII expression in primary mvECs

The rate of formation of FVIII in primary mvECs transduced with lentiviral particles (MOI 1000) carrying FVIII gene was 160 mU/10⁶cells/24 h. The rate of FVIII expression in cells transduced with higher MOIs of 10,000 and 100,000 was 220.4 and 245.5 mU/10⁶/24 h, respectively. Primary mvECs transduced with FVIII lentiviral particles and selected using blasticidine produced FVII at a rate that was ~14 fold higher than the non-selected upcyte[®] mvECs .

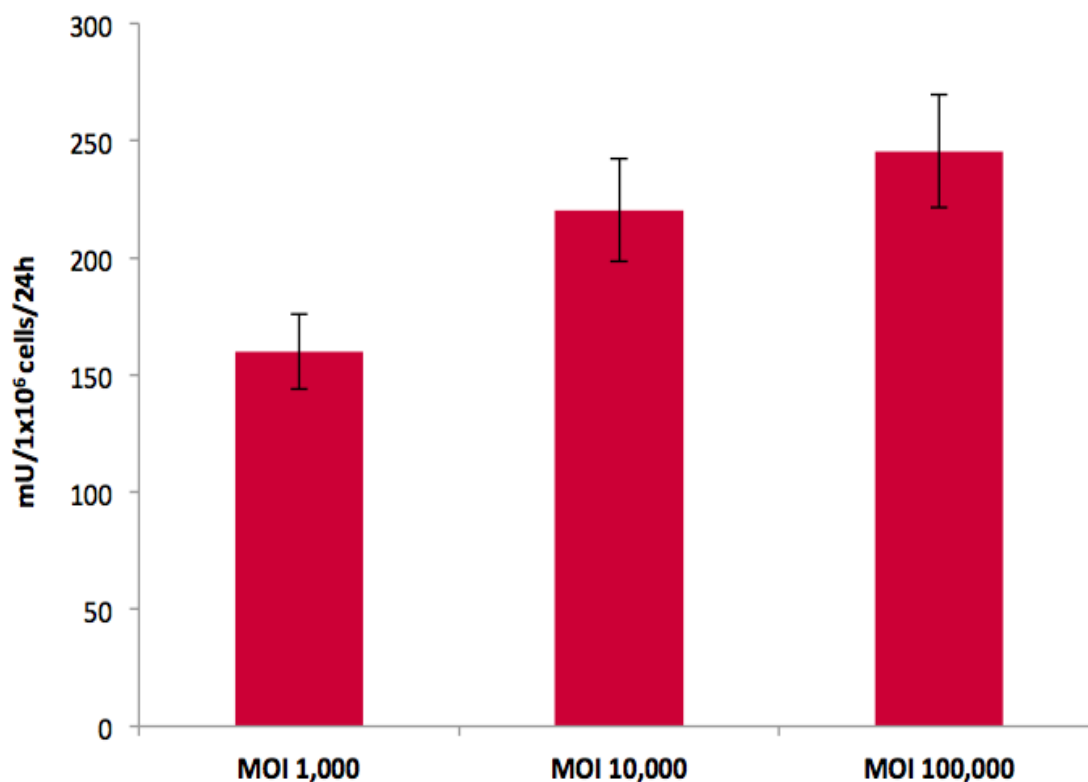


Figure 51: FVIII production in primary mvECs transduced with different MOIs of lentiviral particles carrying FVIII gene. Values are the mean \pm SD from 2 experiments, each with n=3 wells.

DISCUSSION

4. Discussion

Primary human cells are the gold standard for many *in vitro* liver-based assays, as they reflect the cell types present *in vivo* (Hewitt et al. 2007). However, the availability of primary cells is a limiting factor and there are different levels of quality of the cells due to the nature of the biopsy material (from healthy or diseased tissue) as well as different isolation techniques (Godoy et al. 2013). Donor-to-donor variation adds to complexity in interpreting the outcome of assays. This thesis mainly deals with hepatocytes and endothelial cells, namely mvECs and LSECs. Alternative models to replace and/or complement the use of freshly isolated primary hepatocytes have mainly focussed on hepatic cell lines, such as HepG2 (which are genetically unstable) and HepaRG (Castell et al. 2006) and also they express very low CAR and PXR activated pathways. Compared to primary hepatocytes, the phase I and phase II enzyme expression is low in hepatic cell lines (Wilkening et al. 2003). Human upcyte[®] hepatocytes are proliferating hepatocytes which retain many characteristics of primary human hepatocytes (Burkard et al. 2012) (Levy et al-Manuscript submitted). They therefore represent a promising cell type for use in higher throughput assays, such as metabolism and drug-drug interaction (DDI) assays, since they address the need for large quantities of metabolically competent cells from multiple donors. Primary endothelial cells such as mvECs and LSECs have certain limitations including: (1) They de-differentiate rapidly, evident as a loss of their endothelial cell markers when placed in *in vitro* culture (Unger et al. 2002; Richard et al. 1998; Fodor 2003). (2) Establishing standardized *in vitro* test systems is difficult due to donor-to-donor variation (Unger et al. 2002). (3) They have a limited proliferative capacity, for example, primary LSECs have a short life span in *in vitro* culture (2-3 population doublings) (Kim & von Recum 2008; Karasek 1989). (4) Similar to other primary cells, obtaining high purity and high yields of primary LSECs is also challenging. Additionally, compared to other cell types such as hepatocytes or mvECs, the published research regarding LSECs is limited and a full characterization of these cells is still lacking (Smedsrød et al. 1994). To overcome these limitations, upcyte[®] mvECs and upcyte[®] LSECs were generated employing the upcyte[®] technology. Upcyte[®] mvECs and upcyte[®] LSECs exhibit enhanced proliferative capacity and also retain their endothelial cell-specific markers when cultured *in vitro* (Scheller et al. 2012; Nörenberg 2013). As it is possible to obtain a large quantity of cells using upcyte[®] technology, *in vitro* test systems can be established. Multiple donors can also be obtained which makes it easier to study the donor-to-donor variations in cell responses and characteristics.

DISCUSSION

4.1 Hepatic models – 3D Mimetix[®] scaffolds

4.1.1 Confocal analysis of upcyte[®] hepatocytes

When seeded into Mimetix[®] scaffolds the cells formed a 3D architecture within the scaffolds and the upcyte[®] hepatocytes were able to penetrate to a depth of 42 μm . Cells that remained on the surface of the scaffolds also formed a multi-layered architecture similar to *in vivo*. Cells penetrated and colonized only halfway of the whole scaffold (100 μm thickness). This could be due to a difference in concentration gradient for the availability of nutrients and oxygen i.e. limited access of oxygen and nutrients at greater depths than on the top level (Goldstein et al. 2001). This might have influenced the cells to remain in middle of the scaffolds rather than colonizing the whole scaffold. Furthermore, upcyte[®] hepatocytes reached deeper layers of the scaffolds when cultured in an insert format in Alvetex[®] Strata scaffolds (Manuscript in progress), rather than when the scaffold was located at the bottom of the well (standard format). This could be due to the availability of higher volume of medium in the insert format (7 ml) than in the standard format (1 ml). The pore size of the scaffold influences the rate at which cells can penetrate; therefore, over the same time, cells would be expected to penetrate further when larger pore sizes are used. Indeed, upcyte[®] hepatocytes cultured in scaffolds with a larger pore size of ~18-42 μm (achieved when using scaffolds generated with fibres of 6 μm diameter) resulted in 100% penetration of the scaffold. However, culturing upcyte[®] hepatocytes in scaffolds with a bigger pore size resulted in all the cells migrating down to the bottom layer of the scaffolds in multiple stacks, which is less representative of liver sections or slices (Olinga et al. 1998). This is also in contrast to the observations of others who showed that cells migrated throughout the scaffolds (Zajicek et al. 1985; Arber et al. 1988) due to passive movement (Fabrikant 1967). Based on this result, it was decided to use 4 μm fibre diameter scaffolds with 50 μm thickness for future experiments.

4.1.2 Scaffold thickness and fiber diameter

Comparison of cell viability and functionality between two different thicknesses of electrospun scaffolds were conducted. Results from confocal microscopy shows that the cells were able to migrate up to a depth of 42 μm in scaffolds with a 4 μm fiber diameter compared to 6 μm fiber diameter, where the cells merely settle down to the bottom of the scaffolds. It may be expected that proliferating cells like upcyte[®] hepatocytes would grow into and fill the scaffold over time upon culturing, since this is observed for proliferating tumour-derived cells such as HepG2 (Bokhari et al. 2007). Although upcyte[®] hepatocytes proliferate, they also

DISCUSSION

exhibit contact inhibition (Burkard et al. 2012) and therefore do not infiltrate the scaffold in the same way as tumour cells. The number of viable cells increases with time in both 50 μm and 100 μm PLLA scaffolds but the initial rate of increase was lower than those cultured in 2D cultures. Cells cultured in 3D have a slower proliferation rate than the cells cultured in 2D, especially when they are sub-confluent (Stangegaard et al. 2006). However, the number of viable cells starts to decline in 2D cultures after Day 3 (day 5 and 7). The decline may be due to detachment of cells or loss of cell viability. On day 7, number of viable cells was significantly higher when they were cultured in both the formats of PLLA scaffolds (50 and 100 μm scaffold thickness) compared cells cultured in 2D. This signifies that 3D scaffold formats are more appropriate for long-term culture of upcyte[®] hepatocytes, a finding also observed using primary hepatocytes (Larson et al. 2014). Although the basal CYP3A4 activity is marginally higher in 100 μm thickness scaffold, similar to cell viability/growth, there was no significant difference observed for basal CYP3A4 activity in upcyte[®] hepatocytes cultured in the two different scaffold formats compared to those cultured in 2D monolayers. Unlike the nanofibrous scaffolds in which higher cell proliferation has been shown in thicker scaffolds (Ghasemi-Mobarakeh et al. 2009), increasing the thickness of electrospun scaffolds does not influence the cell growth and functionality. Results from confocal analysis and functional data (CYP3A4) signify that scaffolds of 50 μm thickness can be selected for future experiments.

Using scaffolds with an optimal thickness of 50 μm , two different fiber diameters were used to investigate their influence on the number of viable cells and functionality. As observed with the two different scaffold thicknesses, the growth of viable cells was initially higher in the 2D environment compared with that in scaffolds of both fiber diameters. This may be due to a slower proliferation time in 3D than in 2D (Stangegaard et al. 2006). However on Day 7, the number of viable cells present in both the scaffold formats (4 and 6 μm fiber diameter) increased and was higher than that in 2D cultures. Although there was no difference observed in the number of viable cells between the two scaffold formats, basal and induced CYP3A4 activities were higher in 50 μm scaffolds with 4 μm fibres than with 6 μm fibres. In conclusion, confocal analysis and CYP3A4 data suggests that upcyte[®] hepatocytes from Donor 653-03 can be optimally cultured in 50 μm thick scaffolds with 4 μm diameter fibres.

4.1.3 Donor-to-donor variation

Donor-to-donor variation was also investigated using 50 μm thick scaffolds with two different fiber diameters. Donor 151 was a first generation batch of cells and Donors 653-03 and

DISCUSSION

422A-03 were generated employing a refined upcyte[®] technology resulting in a second generation of upcyte[®] hepatocytes. Cells from first and second-generation batches were selected to determine if cells with lower metabolic activity play a role in cell functionality within the scaffolds. Regardless of the scaffold format used, the number of viable cells from Donor 653-03 increased over time. By contrast, the number of viable cells from Donor 422A-03 remained constant between Days 1 to 7 in scaffolds with both 4 μm and 6 μm fiber diameters. The PD time of upcyte[®] hepatocytes from Donor 653-03 in 2D monolayer was less than 48 h; whereas, the PD of upcyte[®] hepatocytes from Donor 422A-03 was between 55 to 60 h. The combined effects of the 3D environment and a slower proliferation rate of upcyte[®] hepatocytes from Donor 422A-03 may have resulted in slower proliferation throughout the culture period in 3D scaffolds. For upcyte[®] hepatocytes from Donor 151, the number of viable cells was markedly lower between Day 1 and 2, possibly due to detachment of cells. However, the initial drop was followed by a gradual increase in the number of viable cells over the remaining 5 days, suggesting the remaining cells were functional and did undergo proliferation. To analyze an additional functionality of the cells in different scaffold formats and also to know the donor-to-donor variation, CYP3A4 activity was also measured. Upcyte[®] hepatocytes from each donor were cultured in two different scaffold formats and CYP3A4 activities were compared with those in the same cells cultured in conventional 2D formats. Second-generation cells (Donors 653-03 and 422A-03) exhibited significantly higher CYP3A4 activities in both scaffold formats compared to the first generation cells (Donor 151). For upcyte[®] hepatocytes from Donor 653-03, the CYP3A4 activity was highest when they were cultured in scaffolds generated with 4 μm fibre diameter. By contrast, the CYP3A4 activity in upcyte[®] hepatocytes from Donor 422A-03 was highest when they were cultured in scaffolds with 6 μm diameter fibres. There were no differences observed in CYP3A4 activities in upcyte[®] hepatocytes from Donor 151 cultured in scaffolds with the two fiber diameters, which signifies that either of the scaffold formats can be used for this donor. In contrast to the second generation upcyte[®] hepatocytes, CYP3A4 activities in first generation upcyte[®] hepatocytes (Donor 151) were 3-fold higher when they were cultured in a 3D environment compared to 2D monolayers. An increase in CYP3A4 enzyme activity upon 3D culture has also been observed using primary hepatocytes (Hammond et al. 2006; Ohashi et al. 2007), thus, supporting the use of this more *in vivo* like culture format. In order to improve the scaffolds, surface functionalization of scaffolds with sugar residues such as galactose (Yin et al. 2003) or polymer coating (Philippart et al. 2015) can also enhances the cell growth and functionality.

DISCUSSION

4.2 Hepatic models – Liver organoids and in BioVaSc

4.2.1 3D liver model- Liver organoid

A shortage of livers for organ transplantation to treat end-stage liver disease and the lengthy waiting list of organ recipients emphasizes the importance of developing an *ex vivo* functional liver through tissue engineering (Rai 2013). Moreover, the intention to reduce animal experiments is of high priority and animal models can never fully reflect the human cell interactions (Martignoni et al. 2006; Liang et al. 1993; Rippin et al. 2001). Conventional *in vitro* systems often lack the necessary cellular cross-talk and cells (hepatocytes) in these systems often have lost major properties (Gómez-Lechón et al. 1998) of the corresponding primary cells, which profoundly limit their possible applications. The main focus is to exploit the *in vivo* physiological mechanism that occurs during an organ development and to implement the similar principles to develop a functional tissue *in vitro*. Apart from this, other applications can be use of 3D liver-like structures, e.g. in order to meet the needs of pharmacological and toxicological industry for drug screening. Takebe and his colleagues (Takebe et al. 2013) have generated three-dimensional liver bud-like structure. When human induced pluripotent stem cells (iPSCs) differentiated to hepatic cells were co-cultured with HUVECs and MSCs on Matrigel™, they self-organized to form liver bud-like structure. Such pre-formed liver buds were transplanted into the cranial window of mice where they have engrafted and rapidly have been vascularized (Takebe et al. 2013).

The principal, functional cell type within the liver is the hepatocyte that contributes to 60% of parenchymal volume. The remaining volume is occupied by non-parenchymal cells such as LSECs, Kupffer cells (hepatic macrophages), hepatic stellate cells (Gu & Manautou 2012). It is not only hepatocytes by themselves but also non-parenchymal cells that have a direct impact on the development of functional hepatocytes (Lammert et al. 2003). During early organogenesis, signals from the heart induce the endoderm for liver bud formation (Jung et al. 1999). Emergence of the liver bud requires transition of hepatic endodermal cells from the columnar epithelium. As soon as the liver bud emerges from the columnar epithelium, endothelial cells surround it and migrate rapidly through the mesenchyme (Matsumoto et al. 2001). Studies revealed that when there is a lack of mature endothelial cells, the liver bud fails to expand and migration through the septum transverse mesenchyme was also affected (Matsumoto et al. 2001). Failure to invade the septum transverse mesenchyme results in development of liver lobes but devoid of hepatocytes (Sosa-Pineda et al. 2000). The mesenchymal part of the liver is essential for hepatoblast proliferation (Houssaint 1980).

DISCUSSION

Therefore, hepatic architecture requires certain morphogenetic cues from the endodermal/mesenchymal component (Zhao & Duncan 2005). In addition, MSCs secrete multiple growth factors that play a role in MSC migration to promote angiogenesis and also to decrease apoptosis (Boomsma & Geenen 2012). Not only during embryogenesis but also in adult tissue, cell-cell interaction plays an important role. For example: endothelial cells and hepatocytes signal during liver regeneration to establish sinusoidal liver architecture (Yamane et al. 1994). In conclusion, hepatocytes, endothelial cells and mesenchymal cells play vital roles in controlling the growth of the hepatic primodium (Davis et al. 1996).

4.2.2 Generation of liver organoid

A modified protocol of Takebe (Takebe et al. 2013) has been used for the generation of liver organoids. Human iPSCs differentiated to hepatic cells were replaced with adult differentiated upcyte[®] hepatocytes (Donor 422A-03) to reflect the parenchymal cells of the adult liver. In order to depict hepatic, physiological conditions, HUVECs were replaced with upcyte[®] LSECs, as LSECs are the native endothelial cells of the liver that are highly specialized to facilitate the selective transport of molecules into hepatocytes (Braet et al. 2001). Primary MSCs co-cultured with upcyte[®] LSECs and upcyte[®] hepatocytes on Matrigel[™], self-organized to form liver organoids. MSCs are multipotent, self-renewing, adult stem cells, which can also differentiate into hepatocytes (Volarevic et al. 2014). Such differentiation can be induced by addition of growth factors like HGF or bFGF (Shu et al. 2004) or by co-culturing the cells with hepatocytes (Lange et al. 2005; Luk et al. 2005).

HE staining of the formalin-fixed organoid revealed the presence of collapsed nuclei and cell debris, which signifies necrotic cells in the liver organoid after a static culture period of 72 h. Though the medium was changed every 24 h, culturing nearly 2.2×10^6 cells in 1 ml of medium (24 well format) for 24 h most certainly resulted in deficiency of nutrients from the medium and also oxygen might not have reached the inner part of the liver organoid (3-4mm in diameter). This is similar to the retinal organotypic *in vitro* model, where disintegrated cytoarchitecture was observed in static culture (Kobuch et al. 2008). When the cells are cultured in 2D surface, nutrient reaches the cell by simple diffusion (van den Dolder et al. 2003). However, when the cells are cultured in 3D environment, sufficient oxygen delivery and waste removal from the cell from inner part of the organoid will not be met by simple diffusion process, whereas the outer surface of the 3D structure will be nourished (Sikavitsas et al. 2002). In order to overcome the hypoxia condition in the static culture, bioreactors were

DISCUSSION

introduced in tissue engineering applications such as bone and cartilage to increase the nutrient availability for the 3D tissue and enhanced waste removal (Martin & Vermette 2005; Abousleiman & Sikavitsas 2006). Apart from nutrient deficiency, limited availability of quality of primary MSCs posed another challenge for liver organoid generation. Because, self-renewal capacity of MSCs which includes proliferation and differentiation function of MSCs decreases with increase in the age of donor (Stolzing et al. 2008; He et al. 2009; Li et al. 2011). In addition, primary cells can be expanded only to a limited extent, the so-called “Hayflick limit”, before reaching senescence (Hayflick 1965). The primary cells show a highly unstable phenotype in culture and produce very variable results due to donor differences (Stolzing et al. 2008) and/or varying effectiveness of the isolation process. Structures that resemble the 3D architecture such as hepatospheres is better than conventional monolayer cultures but consists of hepatoma cell lines (HepG2) (Chang & Hughes-Fulford 2009) which is far from physiological conditions. Upcyte[®] cell strains which exhibit primary cell phenotypes (Scheller et al. 2012; Burkard et al. 2012; Levy et al. Manuscript submitted) can be obtained in large amounts from the same or different donor, which meets the demand for comprehensive sets of experiments. Therefore, primary MSCs were replaced with upcyte[®] MSCs for liver organoid development. HE staining of the liver organoids generated using exclusively upcyte[®] cells and cultured in a dynamic cell culture system, i.e. a bioreactor, showed that the presence of necrotic cells in the liver organoid has been considerably reduced compared to the organoids cultured in the static system. Very few nuclear fragmentations were present in liver organoids cultured in a dynamic system due to apoptosis, which represents the regular cell cycle. Liver organoids can also be stained for apoptotic markers such as caspase-1 to identify the cells entering apoptosis.

4.2.3 Organoids cultured in a dynamic system

Cell viability and synthesis of extra cellular matrix in the core of 3D organoid would be challenging to obtain in a static culture (Ishaug-Riley et al. 1998). Though culturing of liver organoids in a dynamic system such as the *Quasi-Vivo*[®] system provides advantages over the static culture, it is still far from physiological conditions. In the *Quasi-Vivo*[®] system, multiple chambers (5 to 6) are connected linearly each holding one liver organoid. The flow of medium from the reservoir bottle to the *Quasi-Vivo*[®] chambers is linear. Therefore, there would be a number parameters varying between the different organoids. For example: the nutrient availability to the first organoid (No.1), which is connected immediately to the reservoir bottle is high, compared the last chamber containing the last organoid (No.6).

DISCUSSION

Whereas, the cytokines and other signaling molecules secreted by the organoids will be available in higher amount to the last organoid (No.6) compared to the first organoid (No.1) due to linear flow of medium. Although the medium is mixed in the reservoir bottle, the condition in which the organoids were cultured is not uniform due to linear flow of medium. So it would be highly desirable to culture these organoids in an *in vivo*-like microenvironment. Hence, more sophisticated systems such as BioVaSc were used to culture the organoids using the computer-controlled bioreactor system (Mertsching & Hansmann 2009). Briefly, nearly 10-15 cm of porcine small intestine with intact vascular system is excised from a sacrificed animal. The matrix is chemically treated to remove the native porcine cells that retain an intact vascular and capillary network (Mertsching et al. 2005; Schultheiss et al. 2005). The vascular system was re-populated with upcyte[®] mvECs (Scheller et al. 2012) and the lumen of the BioVaSc was used for culturing the liver organoids for a period of 30 days.

4.2.4 Immunostainings of liver organoid and in BioVaSc

Cell-type specific immunostaining was performed on 2D monolayers to confirm the expression of cell-specific markers, i.e. their proper cellular identity and also for the 3D liver organoid to assess the arrangement of the three different cell types inside the organoid. The upcyte[®] hepatocytes are differentiated adult hepatocytes (Burkard et al. 2012) and were stained for CK8. CD31 is a transmembrane glycoprotein present predominantly along the cell-cell contacts and also the most common endothelial marker present in different endothelial cells (Jaffe et al. 1973) which was also detected in upcyte[®] LSECs (Nörenberg 2013) and upcyte[®] mvECs (Scheller et al. 2012). MSCs were stained for vimentin, which is an intermediate filament protein. Vimentin is the most commonly used marker of mesenchymal-derived cells or cells that undergo EMT i.e. epithelial to mesenchymal transition (Chen et al. 2012). Immunohistochemistry can help to identify the arrangement of three different cell types in the organoid. Liver organoids cultured in the *Quasi-Vivo*[®] system and in the BioVaSc showed similar type of cell arrangements i.e. different cell types arrange in different layers. Upcyte[®] hepatocytes positive for CK8 organized in different compartments as closely adherent sheets and move towards the periphery of the liver organoid by surrounding the endothelial cells in its center. Compared to 2D monolayer, liver-specific functions, interaction with ECM (Berthiaume et al. 1996; Dunn et al. 1989) and cell density (Sudo et al. 2005; Hamilton et al. 2001) are maintained better in 3D environment. mRNA expression indicative of differentiated hepatic functionality such as albumin, enzymes regulating glutamine and

DISCUSSION

glucose as well as hypoxia-inducible factor 1- α (Hif1 α) was detectable using *in situ* hybridization. In conclusion, these findings suggest that upcyte[®] hepatocytes inside the organoids possess functional gene expression typical for hepatocytes without having faced gross changes such as epithelial to mesenchymal transition (EMT). In contrast to the upcyte[®] hepatocytes, upcyte[®] LSECs were stained for CD31 in order to trace the presence of organization of endothelial cells in the inner part of liver organoid. Unlike the hepatocytes and endothelial cells, which followed specific patterns to organize in the liver organoids, MSCs that stained positive for vimentin were distributed throughout the organoid. Also during embryogenesis, construction of liver parenchyma depends on the complex signalling between epithelial cells (hepatocytes) themselves and between epithelial-mesenchymal cells (Zhao & Duncan 2005). MSC-derived hepatocytes acquired the ability to express hepatocyte marker genes like albumin, which makes it difficult to distinguish between the original hepatocytes and MSC-derived hepatocytes in the liver organoid. Therefore it is not possible to exclude the probability that some of the hepatocytes in the organoids might be derived from MSCs. However, direct differentiation of MSCs into hepatocytes might not represent the major mechanism of hepatocytes itself and how MSCs support the survival of liver tissue.

It has been shown that intravenous bolus of conditioned medium from MSCs can already provide a significant survival benefit in rats with fulminant liver failure (Parekkadan et al. 2007). The hepatoprotective effect of MSCs seems to be mainly based on the secretion of factors, which on the one side may modulate cells of the immune system but also exert direct anti-apoptotic effects on hepatocytes (Xagorari et al. 2013). The exact nature of these MSC-derived factors those are essential for organoid formation are yet to be explored. However, Takebe and colleagues have already described that application of inhibitors directed against bone morphogenetic proteins (BMPs) or fibroblast growth factor (FGF) effectively prevented the structure formation in their experimental set-up (Takebe et al. 2013). Sections of liver organoid can also be stained for proliferation marker such as Ki-67 to check if the cells undergo proliferation. E-cadherin is a calcium-dependent cell-cell adhesion molecule that plays a pivotal role in epithelial cell junctions. E-cadherin was well known to be expressed in differentiated cell types (Shino et al. 1995) and is widely expressed in most of the normal epithelial tissue (Takeichi 1990). As hepatocytes organize in asymmetrical orientation with its basolateral, apical and lateral domain, staining the hepatocytes for E-cadherin can be used to analyze the cell-cell junction.

DISCUSSION

4.2.5 Liver organoid architecture

The network of bile canalicular structures (~1µm diameter) joins to form the bile-secretory unit, which is formed between adjacent hepatocytes (Boyer 2013). As bile acid causes detergent effects on the cell membrane, excretion of bile acid is considered as one of the primary detoxification mechanisms in liver (Tamai et al. 2013). The morphological architecture of the liver organoid cultured for 10 days was compared to normal adult liver slices. Bile canaliculi-like structures were observed between the neighboring upcyte[®] hepatocytes that stained positive for CK8. However, these organoids could be stained for hepatic bile canaliculus markers such as CD25, EP-1 to exactly confirm the presence of bile canaliculus structure in the organoid. The bulk of liver consists of hepatocytes, which organize to form linear or branched hepatic cords. These hepatic cords are one of the major characteristic features of mature liver, an arrangement of cells that happens during embryogenesis and also during regeneration of liver (Treyer & Müsch 2013).

Similar to the adult liver slice, single-cell thick plates of hepatocytes arranged linearly to form hepatic cord-like structure in the organoid. As the upcyte[®] hepatocytes used for the liver organoid generation are adult and differentiated cells, the organoid generated also retained characteristic features of mature liver. Liver lobules consist of intact sinusoidal lumen formed by hepatocytes in a circular manner with endothelial lining (Braet et al. 2004). The sinusoids lined with endothelial cells (LSECs) contain Kupffer cells, lymphocytes (pit cells) and immature dendritic cells (Crispe 2003). Similar to sinusoidal lumen in normal liver, the organoids also show circular arrangement of hepatocytes. However, lining of the lumen with endothelial cells could not be detected. Ongoing experiments aim at further optimizing the parameters for long-term culture and growth of liver organoids. Integration of further liver cell types like Kupffer cells and hepatic stellate cells is planned in order to generate bioartificial liver-like structures which come more close to the *in vivo* conditions. Though the circular arrangement of hepatocytes in liver organoid lacks endothelial lining, these structure resembled “*Muralium*” structures. During early embryogenesis, the hepatoblast that develops from the endoderm forms plates that are five to six cell thick known as *Muralium multiplex*. During the gestation week of 8th -10th, *muralium multiplex* is reduced to two-cell thick structures known as *muralium duplex*. From the age of 6, a sheet of one-cell thick adult and differentiated hepatocytes forms the *Muralium simplex* architecture (Erwin Kuntz 2008). As the organoids were generated using adult, differentiated upcyte[®] hepatocytes, the structure formed in the liver organoid could be *Muralium simplex-like* architecture.

DISCUSSION

4.2.6 Metabolic activity

To further investigate if hepatocytes inside the organoids that have been cultured for 10 days in the *Quasi-Vivo*[®] system show functional properties of liver parenchymal cells, liver organoids were analyzed for basal and induced CYP3A4 enzyme activity. CYP3A4 is an enzyme that metabolizes a large number of clinically important substrates. Induced activity of this enzyme was 2.8 fold higher than the basal activity that correlates with the FDA guidelines, which suggest that *in vitro* induction results should be 2 to 5 fold higher than the basal activity (Food and Drug Administration 2012). Whereas the liver organoids cultured for 30 days inside the lumen of BioVaSc expressed the basal CYP3A4 activity of 49 pmol/mg/min. This further supports the conclusion that hepatocytes within the organoids possess functional cells allowing the use of these structures to analyze e.g. hepatic toxicity of certain substances or drugs. Apart from CYP3A4 enzyme activities, upcyte[®] hepatocytes when cultured in 2D monolayer also express functional CYPs such as CYP2B6, CYP1A2, CYP2C9 (Section 3.4) (Burkard et al. 2012). So these organoids could also be analyzed for larger panels of CYPs in future experiments. The detoxification function such as urea synthesis or the albumin secretion can also be evaluated in future studies. As the organoids were viable and functional for 30 days in culture, long-term culture such as 90 days can be planned to generate a model for chronic toxicity testing.

4.2.7 Vascularization

In the *in vivo* situation, mvECs line the lumen of the blood vessels and are naturally exposed to mechanical shear stress due to blood flow. mvECs are responsible for a wide number of functions such as regulating the blood pressure by vasodilation or vasoconstriction (Cosentino & Volpe 2005), regulating the exchange of substances between blood and tissue cells by para- and transcellular transport of molecules, contributing to the blood coagulation processes (Wiel et al. 2006; Chen & López 2005), harbouring Weibel palade bodies that store growth factors, cytokines and hormones (Hannah et al. 2002; Michaux & Cutler 2004; van Mourik et al. 2002), play a vital role in vascular biology (Wiel et al. 2006) and angiogenesis (Scheller et al. 2012). The native vascular system in the BioVaSc has been re-populated with dermal derived human upcyte[®] mvECs and cultured in a bioreactor under systolic and diastolic pressure which is similar to the physiological condition. Sprouting of new capillaries from the existing blood vessel was also observed (Scheller et al. 2012). The decellularized BioVaSc contains mainly collagen I and III (Mertsching et al. 2005; Schanz et al. 2010). and these collagen components help the endothelial cells for adhesion and migration.

DISCUSSION

Studies show that the collagen gel would provide physiological microenvironment for microvessel formation (Hoying et al. 1996; Pepper et al. 1991). A scaffold derived from biological source (BioVaSc) together with an intact vascular system that has been repopulated with human derived upcyte[®] mvECs provides a much more *in vivo-like* environment to culture liver organoids than the other two systems such as common 2D cell culture or a bioreactor, i.e. *Quasi-Vivo*[®] system. Unlike the endothelial cells, which are exposed to shear stress, the hepatocytes are sensitive. Henceforth, liver organoids generated in 48-well format using upcyte[®] hepatocytes, LSECs and MSC (1.2×10^6 cells/organoid) were cultured in the luminal part of the BioVaSc for 30 days. Collagen present in the mucosal part of the intestine enabled the organoids to adhere to the intestinal wall. HE staining of the liver organoid showed opening of blood vessel-like structure, which has been lined with cells. To explore further, when the sections of the liver organoids were stained for cell-specific immunostaining (CD31), the cells lining the blood vessel-like structures were positive for this endothelial cell specific marker. The upcyte[®] mvECs expressed CD31 after culturing in the vascular tree of the BioVaSc for 30 days (Scheller et al. 2012). In conclusion, the capillaries of the BioVaSc might have reached the organoid after 30 days of culturing in the bioreactor. VEGF is one of the most important growth factors for the neoangiogenesis (Ferrara et al. 2003) and also plays a central role in liver regeneration (Bockhorn et al. 2007). Though VEGF is already present in the liver organoid growth medium, further optimization of medium composition together with other growth factors such as FGF, EGF and OSM can enable the organoid for increase in mass and also to produce their own ECM. The ECM contains a wide range of complex, tissue-specific proteins and polysaccharides that play a vital role in cellular function. Together with collagen that is already present in the BioVaSc, the ECM niche would improve the assessment of cell behavior in the areas of research such as drug development applications (DeQuach et al. 2010).

4.3 Application of hepatic models - CYP inhibition

4.3.1 Culture optimisation

In order to carry out CYP inhibition assays, the cells require sufficient levels of CYP enzyme activities such that they can be inhibited in a concentration-dependent manner, i.e. there should be a sufficient dynamic range. Therefore, different (pre-) culture conditions such as the effect of DMSO, length of pre-culture period and type of basal medium were analyzed (HGM and HPM). DMSO is known to induce CYP3A4 activities in primary human hepatocytes (LeCluyse 2001) and CYP3A4 and CYP2B6 activities in HepaRG cells (Anthérieu et al.

DISCUSSION

2010) by activating PXR and/or CAR, although, CYP1A2 is not induced over the same concentration of DMSO (LeCluyse 2001). Therefore, the effect of DMSO was determined for CYP3A4 and CYP2B6 only. For the Donor 422A-03, there was negligible difference detectable between the two different DMSO concentrations, i.e. pre-culture medium contained 0.25% or 0.5%. Moreover, a maximum CYP2B6 and 3A4 activity is observed for all the donors at 0.5-0.75% (v/v) DMSO whereas at higher concentrations of DMSO, there was a decrease in both CYP activities. These data confirmed that supplementing the medium with DMSO was beneficial to the overall DME (drug metabolizing enzyme) properties of the cells. Among the different culture conditions tested to analyse the effect on CYP3A4 and CYP2B6, CYP3A4 activity did not increase significantly in all the four donors. Increasing the pre-culture time (3 days to 7 days), significantly increased the CYP2B6 activity. Also for CYP3A4 activity, when the conditioning medium is changed from HGM to HPM with a lower concentration of DMSO (0.1% v/v), an increase in CYP3A4 activity was observed. The reason for this effect may be due to a down-regulation of CYPs when the DMSO concentration is maintained at the higher concentration and/or that factors in the growth medium may not be suitable for differentiating the cells once they reach confluence. These results suggest that 6-7 days of pre-culture time using HGM supplemented with 0.5% DMSO followed by conditioning the cells at confluence for 3 days with HPM supplemented with 0.1% DMSO result in sufficiently high CYP activities that can be inhibited. This concentration of DMSO in the conditioning medium was considered acceptable since it is the standard solvent and concentration for many test compound control incubations.

4.3.2 CYP activities in different donors of upcyte[®] hepatocytes

Similar to primary hepatocytes, the CYP activities in upcyte[®] hepatocytes varied between donors. Except for the Donor 653-03 in which the CYP1A2 activity was only detected using LC-MS (data not shown), all the other CYPs (CYP2B6, CYP2C9, CYP3A4) were expressed in varying levels in upcyte[®] hepatocytes from all four donors (422A-03, 653-03, 151-03, 10-03) compared to that in the original primary hepatocytes measured by the supplier (all donors). These results demonstrate that upcyte[®] hepatocytes exhibit functional phase 1 and 2 activities and, with the exception of CYP1A2, the CYP activities were generally higher than in their corresponding primary human hepatocyte cultures. Despite the low CYP1A2 activities demonstrated in short-term incubations of 1 h, longer incubations of 24 h showed that CYP1A2 substrates were also metabolized. Moreover, in the case of CYP2B6 and CYP3A4, activities in upcyte[®] hepatocytes were 5 to 10-fold higher than paired primary cultures. The

DISCUSSION

CYP activities in upcyte[®] hepatocytes which were comparable to their corresponding primary hepatocytes demonstrated that these cells can serve as a suitable model for both metabolic identification, clearance and inhibition studies, which all require XMEs higher than that present in short-term cultures of primary human hepatocytes. These studies demonstrated that refinement of the upcyte[®] technology, together with optimized culture conditions, resulted in hepatocyte cultures expressing sufficient levels of CYP activities equivalent or higher than in those in paired primary cell cultures from the same donor. The sustained levels of CYPs makes them ideal for longer-term clearance studies (lasting 24-72 h) for metabolically stable compounds, since they can be used over days in culture without a medium change. Upcyte[®] hepatocytes therefore offer an advantage over liver microsomes and hepatocytes which generally do not metabolise test compounds sufficiently in short-term assays (< 24 h) to determine an area under the curve measurement (Di et al. 2012).

4.3.3 Inhibition and induction studies

CYPs were inhibited using competitive inhibitors such as α -naphthoflavone for CYP1A2 (induced with 100 μ M of omeprazole), miconazole for CYP2C9 and ketoconazole for CYP3A4. For CYP2B6, a time-dependent inhibitor, ticlopidine was used. There was a concentration-dependent inhibition of CYP1A2, CYP2B6, CYP2C9 and CYP3A4, such that at the highest concentration all corresponding enzyme activities were completely inhibited. These results support the use of upcyte[®] hepatocytes in inhibition studies incubated in longer-term assays to determine clearance in the presence and absence of selected inhibitors. In conclusion, the data shows that upcyte[®] hepatocytes can also be used in CYP inhibition studies, which require sufficient metabolic activities to ensure a good dynamic range. For CYP1A2, inhibition assays can be conducted using a 24 h incubation period to ensure higher control activities; whereas, incubations of 1 h require booting of CYP activity by pre-inducing CYP1A2 (e.g. with omeprazole). All four CYPs were inhibited in a concentration-dependent manner and the calculated IC₅₀ values were comparable to those reported in primary human hepatocytes. Upcyte[®] hepatocytes from all four donors (422A-03, 151-03, 653-03 and 10-03) tested using a 3 day pre-culture period were responsive to CYP1A2, CYP2B6, CYP2C9 and CYP3A4 induction by prototypical inducers. This was a significant finding since induction CYP2B6 in upcyte[®] hepatocyte using previous technology was only evident at the mRNA level (Burkard et al. 2012). This suggests the responsiveness of these cells, especially via CAR, was improved by the refined upcyte[®] process. Likewise, upcyte[®] hepatocytes demonstrated functional AhR and PXR mediated CYP induction since CYP1A2 and CYP3A4

DISCUSSION

were also induced by omeprazole and rifampicin, respectively. So, upcyte[®] hepatocytes from all four donors were responsive to prototypical CYP1A2, CYP2B6, CYP2C9 and CYP3A4 inducers, confirming that they have functional AhR, CAR and PXR mediated CYP regulation.

4.3.4 Prediction models for *in vivo* CYP3A4 induction

Among the three prediction model used namely, the RIS, AUC_u/F_2 and $C_{max,u}/Ind_{50}$, best fit was obtained from RIS ($R^2 = 0.92$) and $C_{max,u}/Ind_{50}$ ($R^2 = 0.93$); however, the F_2 value ($R^2 = 0.89$) may also be used when compounds are too toxic or insoluble to reach a maximal induction response. Moreover, there was a good fit of data from these studies when they were applied to three different predictive models for CYP3A4 induction, namely the Relative Induction Score, AUC_u/F_2 and $C_{max,u}/Ind_{50}$. Importantly, there was a very good intra- and inter experimental reproducibility of the measurements for all end points measured in these studies. For researchers employing the RIS calibration curve as part of their screening process, the robust nature of these cells means that the calibration curve would not need to be repeated once established (although a yearly check would be advisable). By contrast, those who employ cryopreserved human hepatocytes for the same assay need to re-establish a new calibration curve for each batch once the previous batch is depleted. Since billions of upcyte[®] hepatocytes from a number of donors are available, results over a period of years can be compared.

4.3.5 CAR and PXR selective induction of CYPs

The relative induction of CYP3A4 and CYP2B6 was compared between a PXR selective drug (rifampicin), the CAR-selective drugs (phenytoin and carbamazepine) and the mixed activator (phenobarbital). Rifampicin in general is a potent CYP3A4 inducer which was clearly seen in all the donors of upcyte[®] hepatocytes (Section 3.5.3). However, rifampicin can also induce the CAR pathway, which results in increased expression of CYP2B6. Except for the Donor 422A-03, for all the other three donors (10-03, 151-03 and 653-03), rifampicin was a moderate inducer of CYP2B6. This explains why the relative induction potential of different CYPs varies between donors. Phenobarbital which is a mixed activator, was a potent inducer of both CYPs in all the donors of upcyte[®] hepatocytes. Though phenytoin is a CAR-selective drug, the induction potential is higher only in two of the four donors used. The relative induction potential of carbamazepine is higher for CYP2B6 in three of the four Donors. However, similar to rifampicin, carbamazepine is a moderate inducer of both CYP3A4 and CYP2B6. These data correspond to the findings of Faucette and colleagues (Faucette et al. 2004) who

DISCUSSION

reported phenytoin, phenobarbital and rifampicin to be classified as strong inducers, and carbamazepine as a moderate inducer of CYP2B6 (based on mean fold induction values).

By contrast, dexamethasone - a known PXR selective activator - did not induce CYP2B6 in upcyte[®] hepatocytes from any of the donors (Table 4) but it were a weak inducer of CYP3A4 (Table 3). Troglitazone is a mixed PXR/CAR activator and induced both CYP3A4 and CYP2B6. This drug is known to cause *in vivo* CYP3A4 induction; whereas, pioglitazone is a weak inducer (Sahi et al. 2003; Ripp et al. 2006). In upcyte[®] hepatocytes, troglitazone was a more potent inducer of both CYP3A4 and CYP2B6 than pioglitazone, either due to a higher fold induction or a lower Ind₅₀ (i.e. the efficiency ratio was higher). Like primary human hepatocytes, there were differences in the responsiveness of upcyte[®] hepatocytes to CYP inducers. There were also differences in the CYP3A4 and CYP2B6 induction responses in the same cultures of upcyte[®] hepatocytes to different inducers. For example, phenytoin preferentially activates CAR over PXR, evident in these cells as a more potent induction of CYP2B6 than CYP3A4 at the same concentration. By contrast, rifampicin was a more potent inducer of CYP3A4 than phenytoin, indicative of the preferential activation of PXR by this potent inducer.

4.4 Application of hepatic models – Haemophilia Therapy

Deficiency of functional coagulation FVIII causes hemophilia A, which is due to a X-linked recessive disorder that affects 1 in 5000 males (Antonarakis et al. 1995). By a complete liver transplant a sub-hemophiliac phenotype arises (50% of FVIII is produced in extra hepatic sources). In case of bleeding, e.g. during surgery, FVIII is quickly exhausted. Therefore, FVIII is given to these patients prophylactically before OPs. According to Morbi-RSA (based on the “Risikostrukturausgleich” (Morbi-RSA)) the average cost of the treatment for one hemophilia patient ranges between € 180,000 to € 220,000 in 2011/2012 (Prof. Oldenburg, personal communication). Liver transplantation may not be an appropriate alternative treatment for hemophilia A due to the dependency of immunosuppression drugs after the surgery. Since hemophilia A is treatable, the consequential damages or costs due to immunosuppression drugs during treatment (leading to renal failure that results in dialysis) are very high. Hemophilia A can also be treated using recombinant FVIII (rFVIII) therapy. However, rFVIII is expensive due to the cost of production, purification and formulation (Mannucci 2003). An average of 280,000 (range 70 to 700,000) rFVIII units are used for a patient per year, where 1 unit costs ~1 €. The Experimental Hematology and Transfusion

DISCUSSION

Medicine (EHT) in Bonn charges 75 CT / unit of rFVIII and 45 CT / unit of plasma-derived FVIII. Nevertheless the cost of treatment is still expensive. Also, rFVIII has to be infused through intravenous access; otherwise an increase in bioavailability of FVIII cannot be achieved using other delivery routes. *In vitro* production of FVIII was analyzed from the supernatant of primary LSECs. Primary LSECs were analyzed because the hepatic source is one of the major sites (50%) for FVIII production (Stel et al. 1983).

4.4.1 Calculation for FVIII dosage

$$\text{FVIII dose (U)} = [\text{body weight (BW) (kg)} \times \text{desired FVIII increase (\%)}] / 2$$

1U FVIII per kg of bodyweight increases FVIII plasma levels by ~2%

The primary LSECs produced only negligible amount of FVIII i.e., non-concentrated samples expressed 1mU/1x10⁶ cells/24 h. This may be due to lose of functional characters of LSECs in *in vitro* culture (Smedsrød et al. 1994). In severe hemophiliacs, spontaneous bleeding episodes occur often in their joints and muscles. When the blood plasma level is maintained above 2% (moderate hemophilia A - 5% of FVIII in blood plasma), this can effectively prevent most severe hemorrhages (Tusell & Pérez-Bianco 2002). This makes hemophilia A an attractive target for gene therapy applications. If the blood plasma concentration of the severe haemophilia A is increased from 0% to 5%, the quality of life of a severe hemophilia A patient will be significantly improved. Assuming the fact that the haemophilia A patient whose body mass is 70 kg has severe hemophiliac condition i.e., 0% of FVIII level in blood plasma and in order to raise the blood plasma concentration from 0% to 5%, using the above mentioned calculation for FVIII dosage, 175x10⁹ primary LSECs are required. As the cell volume required to treat the patient is too high for any kind of practical handling, genetic modification of cells is required to increase the FVIII expression per unit per cell. As hemophiliacs already face severe problems with bleeding episodes, it was decided to choose other cell types than LSECs that can be harvested using minimal invasive methods for the proof-of-principle study.

4.4.2 Proof-of-Principle

Primary cells are sporadic in availability and are difficult to obtain which can be overcome by using upcyte[®] cells (Burkard et al. 2012; Scheller et al. 2012). So as a proof-of-principle concept, three different upcyte[®] endothelial cells were chosen for genetic modification. BOECs are one such cell type that can be harvested with minimal injury. From the initially

DISCUSSION

isolated BOECs, an overall 3.4×10^{12} fold expansion can be achieved (Lin et al. 2002) which provides a sufficient source of cells for genetic modification during therapeutic application. Next to BOECs, mvECs can be harvested from skin graft. Together with BOECs and mvECs, LSECs were also included for genetic modification using a B-domain deleted (BDD) FVIII lentiviral construct, as LSECs are one of the primary cell types that produce FVIII *in vivo*. Full-length mature FVIII comprises of 2332 aminoacids, which is one of the large plasma proteins (Vehar et al. 1984). The B domain within the FVIII molecule does not play a pivotal role in the coagulation activity (Toole et al. 1986). Therefore, starting from serine 743 to glutamine 1638, the B-domain was excised from the full length FVIII molecule that results in significant decrease in the size of protein molecule (38% reduction). Compared to the full-length FVIII molecule, BDD-FVIII results in 17 folds increase in mRNA expression, which eventually results in 30%, increased protein secretion in eukaryotic cells (Pittman et al. 1993). Biological activity of B-domain deleted (BDD) version of the FVIII molecule in the coagulation cascade is comparable with full length FVIII (Miao et al. 2004).

4.4.3 Cloning of FVIII gene

B-domain deleted FVIII gene construct was cloned using Gateway[®] Technology. Upon sequencing the cloned FVIII construct showed 100% homology when compared against parental vector and also with nucleotide database (NCBI). The expression of FVIII is driven by a CMV (Cytomegalovirus) promoter sequence. The CMV promoter is a constitutive RNA polymerase II promoter, which is active in wide range of eukaryotic cell types. RNA polymerase II is mainly responsible for *in vivo* transcription of mRNA within the cell. CMV is a strong promoter compared to other widely used RNA pol II promoters including Simian virus-40 (SV40) and Rous sarcoma virus (RSV) (Foecking & Hofstetter 1986). As FVIII is already a large glycoprotein, using a strong promoter like CMV can enhance the protein secretion. The FVIII gene construct driven by the CMV promoter also contains a gene conferring resistance towards blasticidine, which can be used as a selection marker. Blasticidine is an efficient selective antibiotic that was used to eliminate all the non-transduced cells. When the transduced cells were cultured in medium containing antibiotic, it prevented the proliferation of untransduced cells (Bloor & Cranenburgh 2006), which resulted in a homogeneous population of cells harboring FVIII gene.

DISCUSSION

4.4.4 Lentiviral Transduction

Lentiviral particles harboring FVIII gene were generated for transient transduction. Lentiviral vector, which is a modified version of retrovirus, is the most commonly used tool for the gene introduction into the cells. Lentivirus has the potential to get through the intact membrane of both dividing and non-dividing cells. However, the lentiviral particle cannot enter the cells that are in the G0 stage as this blocks the reverse transcription step (Amado & Chen 1999). Though there is an advantage of gene integration and long-term expression of the transferred gene, the risk of insertional mutagenesis is higher. Lentiviral systems have the potential for random gene integration into the host system, which may activate e.g. oncogenes or degenerate the cells (Pauwels et al. 2009; Gray 1991). For the *in vitro* proof-of-principle study to analyze the functionality of cloned FVIII vector, the lentiviral construct was used to transduce different endothelial cells. For the *in vivo* gene therapy application for hemophilia, alternative sources such as adenovirus that does not integrate the gene into host genome (Nagabhushan Kalburgi et al. 2013) or AAV (adeno-associate virus) can be investigated. There are a number of promising adenoviral gene therapy applications which are in phase III clinical trials such as for malignant glioma (European union), cancer gene therapy (U.S and China) (Shirakawa 2009).

4.4.5 FVIII production in upcyte[®] cells

Upcyte[®] endothelial cells (mvECs, BOECs and LSECs) were transduced with three different MOIs. Viral titer values for lentiviral vector that are packed with FVIII gene were measured by quantitative PCR. As the measurement is based on quantification of viral RNA, it is not possible to obtain information on the number of functional viral particles. Also in order to increase the integration of more number of gene copies per cell for increased FVIII secretion, higher MOIs (MOI 1000, 10,000 and 100,000) were chosen. Among the three endothelial cells used, FVIII secretion was detected only from the upcyte[®] mvECs supernatant. Compared to upcyte[®] mvECs transduced with MOI 10,000 and 100,000; the amount of FVIII secreted from cells that had been transduced with MOI 1000 was 2.2-fold less. This result explains that the amount of FVIII secreted is directly proportional to the MOI used, which means the number of gene copies integrated into the host system from MOI 1000 was significantly lower than the other two MOIs. However, there was no difference observed in the amount of FVIII secreted from cells that has been transduced with MOI 10,000 and 100,000, this may be due to the possibility of maximum levels of FVIII secretion might have already been reached in these cells.

DISCUSSION

Compared to primary LSECs, FVIII secretion by upcyte[®] mvECs was increased by an average of 15-fold. Taking the same parameters such as body weight into consideration and to increase the blood plasma concentration of the severe hemophiliacs from 0% to 5%, the number of upcyte[®] mvECs required still would be 12×10^9 cells. As the amount of cells required for treatment would still be high, it is necessary to increase the FVIII production (unit/cell). To select homogeneous population of FVIII producing cells, antibiotic selection process was included. The backbone vector construct used for upcyte[®] process and also for FVIII transduction were same. This means that upcyte[®] cells already carries gene for blasticidine resistance. So it was not possible to select the FVIII transduced upcyte[®] population from the non-transduced cells. To circumvent this issue, two approaches could be performed. The first approach could be to replace the gene conferring blasticidine resistance in the FVIII construct with hygromycin or neomycin resistance gene.

The second approach could be to use primary endothelial cells for FVIII transduction. As the final aim of the work is to launch it for therapeutic application using primary autologous cells, it was decided to transduce primary mvECs using lentiviral particles carrying FVIII. As the lentiviral system incorporate the gene into the host genome, the cells were cultured further for 3-5 passages to increase the number of cells carrying FVIII gene. At 80% confluence, the transduced cells were selected using blasticidine (7 $\mu\text{g/ml}$). The primary mvECs transduced with the lentiviral FVIII construct were selected and subsequently analyzed for their tube formation capacity, a major indicator of endothelial cell specific functionality. Endothelial cells play an important role in the process of angiogenesis by formation of new blood vessels *in vivo* (Ausprunk & Folkman 1977; Folkman 1971). This property of endothelial cells is mimicked *in vitro* by tube formation assay. Also, if these cells are transplanted in intracorporeal devices like the Cell Pouch System[™] then formation of tubes to connect to the host vascular system is an important feature. The half-life of FVIII molecules is between 7.4 h and 20.4 h (van Dijk et al. 2005), so to increase the availability of the secreted FVIII molecule, it has to reach the blood circulation faster. As mvECs facilitate neovascularization (Scheller et al. 2012), therapeutic cells producing FVIII can be connected to the blood stream enabling the circulation of FVIII. This potentially protects hemophiliacs from severe episodes of excessive bleeding and greatly reduces annual therapy costs.

DISCUSSION

4.4.6 FVIII production in primary mvECs

When compared with cells that have been transduced with MOI 10,000 and 100,000 of the FVIII lentiviral construct; the number of cells surviving the selection process employing a MOI 1000 was 10-fold less. As it was possible to select the cells, a homogeneous population of primary mvECs could be obtained, which resulted in higher FVIII secretion of those cells (220mU/1x10⁶cells/24 h). Compared with non-selected upcyte[®] mvECs, while using the same MOIs nearly a 14.6-fold increase in production of FVIII was detected in transduced primary mvECs. Therefore the amount of cells required to treat a patient (same parameters) will be reduced by 14.6-fold i.e., 0.8 x10⁹ cells. The FVIII molecule is stabilized by the carrier protein VWF (Kaufman et al. 1989). Therefore, in order to increase the FVIII secretion (unit/cells), one future approach could be to co-transduce the primary cells with lentiviral particles carrying the FVIII gene and additionally the VWF gene.

The generated FVIII producing primary mvECs are in the process of being evaluated by Sernova[™] in its subcutaneous device (Cell Pouch System[™]) in small animal studies from a safety and efficacy perspective.

DISCUSSION

5. Summary

In summary this thesis deals with two major topics. First, the *in vitro* generation of three different hepatic models. Second, optimization of the hepatic models to drug development and therapy.

Optimization of 3D Mimetix[®] scaffolds for growth and viability of upcyte[®] hepatocytes (Donor 653-03) was achieved using confocal microscopy. By modifying the fiber diameter (pore size) and thickness of scaffold, the penetration of upcyte[®] hepatocytes and their metabolic functions, such as CYP3A4 activities, was optimized. Two additional donors, namely 422A-03 and 151, were also studied for the cell growth and CYP3A4 activity to analyze the donor-to-donor variation. Upcyte[®] hepatocytes, LSECs and MSCs were co-cultured to generate live organoids. The liver organoids were cultured for 10 days in *Quasi-vivo*[®] chambers and analyzed for cell organization within the organoids (HE staining, cell type specific immunohistochemistry), metabolic activity (CYP3A4), expression of functional genes such as albumin, as well as enzymes regulating glutamine and glucose (*in situ* hybridization). Organoids generated using upcyte[®] hepatocytes, LSECs and MSCs were cultured in biologically derived de-cellularized scaffold (BioVaSc) in an *ex vivo* bioreactor for a period of 30 days. The vascular tree of the BioVaSc that has been re-populated with upcyte[®] mvECs also undergoes angiogenesis to connect the liver organoids to the host blood vessel system. CYP3A4 activity and cell-specific immunohistochemical analysis were also performed. The application of four donors of second generation upcyte[®] hepatocytes (653-03, 422A-03, 151-03 and 10-03) for CYP induction and inhibition study under optimized culture conditions was established. The CYPs (CYP1A2, CYP2B6, CYP2C9 and CYP3A4) were inhibited in a concentration-dependent manner and the calculated IC₅₀ values correlated with the classification of inhibitors. CYP3A4 and CYP2B6 activities are induced by a panel of inducers of all categories such as potent, moderate and non-inducer. For CYP3A4 induction, three different predictive models, namely the Relative Induction Score (RIS), AUC_u/F₂ and C_{max,u}/Ind₅₀ were analyzed. Supernatant obtained from primary LSEC cultures, upcyte[®] endothelial cells (mvECs, BOECs and LSECs) that have been transduced with lentiviral particles carrying a FVIII-BDD gene were analyzed for the expression of FVIII protein using FVIII-ELISA. Primary mvECs were also transduced using FVIII lentiviral particles followed by antibiotic selection after which the secreted amount of FVIII increased compared to all the other endothelial cells such as primary LSECs and non-selected upcyte[®] cells.

6. Appendix

6.1 Sequence of FVIII

FVIII DNA was sequenced at GATC Biotech and the sequence is shown below:

TCACCTTTTCAACATCGCTAAGCCAAGGCCACCCTGGATGGGTCTGCTAGGTCCT
ACCATCCAGGCTGAGGTTTATGATACAGTGGTCATTACACTTAAGAACATGGCCT
CCCATCCTGTCAGTCTTCATGCTGTTGGTGTATCCTACTGGAAAGCTTCTGAGGGA
GCTGAATATGATGATCAGACCAGTCAAAGGGAGAAAGAAGATGATAAAGTCTTC
CCTGGTGGAAAGCCATACATATGTCTGGCAGGTCTGAAAGAGAATGGTCCAATGG
CCTCTGACCCACTGTGCCTTACCTACTCATATCTTTCTCATGTGGACCTGGTAAAA
GACTTGAATTCAGGCCTCATTGGAGCCCTACTAGTATGTAGAGAAGGGAGTCTGG
CCAAGGAAAAGACACAGACCTTGCACAAATTTATACTACTTTTTGCTGTATTTGA
TGAAGGGAAAAGTTGGCACTCAGAAACAAAGAACTCCTTGATGCAGGATAGGGA
TGCTGCATCTGCTCGGGCCTGGCCTAAAATGCACACAGTCAATGGTTATGTAAC
AGGTCTCTGCCAGGTCTGATTGGATGCCACAGGAAATCAGTCTATTGGCATGTGA
TTGGAATGGGCACCACTCCTGAAGTGCCTCAATATTCCTCGAAGGTCACACATT
TCTTGTGAGGAACCATCGCCAGGCGTCCTTGGAATCTCGCCAATAACTTTCCTTA
CTGCTCAAACACTCTTGATGGACCTTGGACAGTTTCTACTGTTTTGTCATATCTCT
TCCCACCAACATGATGGCATGGAAGCTTATGTCAAAGTAGACAGCTGTCCAGAGG
AACCCCAACTACGAATGAAAAATAATGAAGAAGCGGAAGACTATGATGATGATC
TACTGATTCTGAAATGGATGTGGTCAGGTTTGATGATGACAACTCTCCTTCCTTT
ATCCAAATTCGCTCAGTTGCCAAGAAGCATCCTAAAACCTTGGGTACATTACATTG
CTGCTGAAGAGGAGGACTGGGACTATGCTCCCTTAGTCCTCGCCCCCGATGACAG
AAGTTATAAAAGTCAATATTTGAACAATGGCCCTCAGCGGATTGGTAGGAAGTAC
AAAAAAGTCCGATTTATGGCATAACAGATGAAACCTTTAAGACTCGTGAAGCT
ATTCAGCATGAATCAGGAATCTTGGGACCTTTACTTTATGGGGAAAGTTGGAGACA
CACTGTTGATTATATTTAAGAATCAAGCAAGCAGACCATATAACATCTACCCTCA
CGGAATCACTGATGTCCGTCCTTTGTATTCAAGGAGATTACCAAAGGTGTAAAA
CATTGAAAGGATTTTCCAATTCTGCCAGGAGAAATATTCAAATATAAATGGACAG
TGACTGTAGAAGATGGGCCAACTAAATCAGATCCTCGGTGCCTGACCCGCTATTA
CTCTAGTTTCGTTAATATGGAGAGAGATCTAGCTTCAGGACTCATTGGCCCTCTCC
TCATCTGCTACAAAGAATCTGTAGATCAAAGAGGAAACCAGATAATGTCAGACA
AGAGGAATGTCATCCTGTTTTCTGTATTTGATGAGAACCGAAGCTGGTACCTCAC
AGAGAATATAACAACGCTTTCTCCCCAATCCAGCTGGAGTGCAGCTTGAGGATCCA
GAGTTCCAAGCCTCCAACATCATGCACAGCATCAATGGCTATGTTTTTGATAGTTT
GCAGTTGTCAGTTTGTGTTGCATGAGGTGGCATACTGGTACATTCTAAGCATTGGA
GCACAGACTGACTTCCTTTCTGTCTTCTCTCTGGATATACCTTCAAACCAAATG
GTCTATGAAGACACACTCACCCTATTCCCATTCTCAGGAGAACTGTCTTCATGTC
GATGGAAAACCCAGGTCTATGGATTCTGGGGTGCCACAACCTCAGACTTTCGGAAC
AGAGGCATGACCGCCTTACTGAAGGTTTCTAGTTGTGACAAGAACACTGGTGATT
ATTACGAGGACAGTTATGAAGATATTTACGCATACTTGCTGAGTAAAAACAATGC
CATTGAACCAAGAGAAATAGAAGTCACCTGGGCAAAGCAAGGTAGGACTGAAAG
GCTGTGCTCTCAAACCCACCAGTCTTGAAACGCCATCAACGGGAAATAACTCGT
ACTACTCTTCAGTCAGATCAAGAGGAAATTGACTATGATGATACCATATCAGTTG
AAATGAAGAAGGAAGATTTTGACATTTATGATGAGGATGAAAATCAGAGCCCCC
GCAGCTTTCAAAGAAAACACGACACTATTTTATTGCTGCAGTGGAGAGGCTCTG
GGATTATGGGATGAGTAGCTCCCCACATGTTCTAAGAAACAGGGCTCAGAGTGGC
AGTGTCCCTCAGTTCAAGAAAGTTGTTTTCCAGGAATTTACTGATGGCTCCTTTAC
TCAGCCCTTATACCGTGGAGAACTAAATGAACATTTGGGACTCCTGGGGCCATAT
ATAAGAGCAGAAGTTGAAGATAATATCATGGTAACTTTCAGAAATCAGGCCTCTC

GTCCCTATTCCTTCTATTCTAGCCTTATTTCTTATGAGGAAGATCAGAGGCAAGGA
GCAGAACCTAGAAAAAACTTTGTCAAGCCTAATGAAACCAAACTTACTTTTGGA
AAGTGCAACATCATATGGCACCCACTAAAGATGAGTTTGACTGCAAAGCCTGGGC
TTATTTCTCTGATGTTGACCTGGAAAAAGATGTGCACTCAGGCCTGATTGGACCC
CTTCTGGTCTGCCACACTAACACACTGAACCCTGCTCATGGGAGACAAGTGACAG
TACAGGAATTTGCTCTGTTTTTACCATCTTTGATGAGACCAAAAGCTGGTACTTC
ACTGAAAATATGGAAAGAACTGCAGGGCTCCCTGCAATATCCAGATGGAAGAT
CCCACTTTTAAAGAGAATTATCGCTTCCATGCAATCAATGGCTACATAATGGATA
CACTACCTGGCTTAGTAATGGCTCAGGATCAAAGGATTCGATGGTATCTGCTCAG
CATGGGCAGCAATGAAAACATCCATTCTATTTCAGTGGACATGTGTTCACT
GTACGAAAAAAGAGGAGTATAAAATGGCACTGTACAATCTCTATCCAGGTGTTT
TTGAGACAGTGGAAATGTTACCATCCAAAGCTGGAATTTGGCGGGTGGAATGCCT
TATTGGCGAGCATCTACATGCTGGGATGAGCACACTTTTTCTGGTGTACAGCAAT
AAGTGTCAGACTCCCCTGGGAATGGCTTCTGGACACATTAGAGATTTTCAGATTA
CAGCTTCAGGACAATATGGACAGTGGGCCCCAAAGCTGGCCAGACTTCATTATTC
CGGATCAATCAATGCCTGGAGCACCAAGGAGCCCTTTTTCTTGGATCAAGGTGGAT
CTGTTGGCACCAATGATTATTCACGGCATCAAGACCCAGGGTGCCCGTCAGAAGT
TCTCCAGCCTCTACATCTCTCAGTTTATCATCATGTATAGTCTTGATGGGAAGAAG
TGGCAGACTTATCGAGGAAATCCACTGGAACCTTAATGGTCTTCTTTGGCAATG
TGGATTCATCTGGGATAAAACACAATATTTTTAACCCCTCCAATTATTGCTCGATAC
ATCCGTTTGCACCCAACCTCATTATAGCATTTCGCAGCACTCTTCGCATGGAGTTGAT
GGGCTGTGATTTAAATAGTTGCAGCATGCCATTGGGAATGGAGAGTAAAGCAAT
ATCAGATGCACAGATTACTGCTTCATCCTACTTTACCAATATGTTTGCCACCTGGT
CTCCTTCAAAGCTCGACTTCACCTCCAAGGGAGGAGTAATGCCTGGAGACCTCA
GGTGAATAATCCAAAAGAGTGGCTGCAAGTGGACTTCCAGAAGACAATGAAAGT
CACAGGAGTAACTACTCAGGGAGTAAAATCTCTGCTTACCAGCATGTATGTGAAG
GAGTTCCTCATCTCCAGCAGTCAAGATGGCCATCAGTGGACTCTCTTTTTTCAGAA
TGGCAAAGTAAAGGTTTTTCAGGGAAATCAAGACTCCTTCACACCTGTGGTGAAC
TCTCTAGACCCACCGTACTGACTCGCTACCTTCGAATTCACCCCCAGAGTTGGGT
GCACCAGATTGCCCTGAGGATGGAGGTTCTGGGCTGCGAGGCACAGGACCTCTAC
TGA

REFERENCES

6.2 References

- Abousleiman, R.I. & Sikavitsas, V.I., 2006. Bioreactors for tissues of the musculoskeletal system. *Advances in experimental medicine and biology*, 585, pp.243–59.
- Aird, W.C., 2007. Phenotypic heterogeneity of the endothelium: II. Representative vascular beds. *Circulation research*, 100(2), pp.174–90.
- Altman, G.H. et al., 2002. Cell differentiation by mechanical stress. *FASEB journal : official publication of the Federation of American Societies for Experimental Biology*, 16(2), pp.270–2.
- Amado, R.G. & Chen, I.S., 1999. Lentiviral vectors--the promise of gene therapy within reach? *Science (New York, N.Y.)*, 285(5428), pp.674–6.
- Anthérieu, S. et al., 2010. Stable expression, activity, and inducibility of cytochromes P450 in differentiated HepaRG cells. *Drug metabolism and disposition: the biological fate of chemicals*, 38(3), pp.516–25.
- Antonarakis, S.E. et al., 1995. Factor VIII gene inversions in severe hemophilia A: results of an international consortium study. *Blood*, 86(6), pp.2206–12.
- Arber, N., Zajicek, G. & Ariel, I., 1988. The streaming liver. II. Hepatocyte life history. *Liver*, 8(2), pp.80–7.
- Arnaoutova, I. et al., 2009. The endothelial cell tube formation assay on basement membrane turns 20: state of the science and the art. *Angiogenesis*, 12(3), pp.267–74.
- Ausprunk, D.H. & Folkman, J., 1977. Migration and proliferation of endothelial cells in preformed and newly formed blood vessels during tumor angiogenesis. *Microvascular research*, 14(1), pp.53–65.
- Bader, A. et al., 1998. Tissue engineering of heart valves--human endothelial cell seeding of detergent acellularized porcine valves. *European journal of cardio-thoracic surgery : official journal of the European Association for Cardio-thoracic Surgery*, 14(3), pp.279–84.
- Bao, J. et al., 2011. Construction of a portal implantable functional tissue-engineered liver using perfusion-decellularized matrix and hepatocytes in rats. *Cell transplantation*, 20(5), pp.753–66.
- Batouli, S. et al., 2003. Comparison of stem-cell-mediated osteogenesis and dentinogenesis. *Journal of dental research*, 82(12), pp.976–81.
- Bell, E. et al., 1981. Living tissue formed in vitro and accepted as skin-equivalent tissue of full thickness. *Science (New York, N.Y.)*, 211(4486), pp.1052–4.

REFERENCES

- Bergers, G. & Benjamin, L.E., 2003. Tumorigenesis and the angiogenic switch. *Nature reviews. Cancer*, 3(6), pp.401–10.
- Berthiaume, F. et al., 1996. Effect of extracellular matrix topology on cell structure, function, and physiological responsiveness: hepatocytes cultured in a sandwich configuration. *FASEB journal : official publication of the Federation of American Societies for Experimental Biology*, 10(13), pp.1471–84.
- Bertolino, P., McCaughan, G.W. & Bowen, D.G., 2002. Role of primary intrahepatic T-cell activation in the “liver tolerance effect”. *Immunology and cell biology*, 80(1), pp.84–92.
- Bhardwaj, N. & Kundu, S.C., 2010. Electrospinning: a fascinating fiber fabrication technique. *Biotechnology advances*, 28(3), pp.325–47.
- Bissell, D.M. et al., 1987. Support of cultured hepatocytes by a laminin-rich gel. Evidence for a functionally significant subendothelial matrix in normal rat liver. *The Journal of clinical investigation*, 79(3), pp.801–12.
- Bloor, A.E. & Cranenburgh, R.M., 2006. An efficient method of selectable marker gene excision by Xer recombination for gene replacement in bacterial chromosomes. *Applied and environmental microbiology*, 72(4), pp.2520–5.
- Bockhorn, M. et al., 2007. VEGF is important for early liver regeneration after partial hepatectomy. *The Journal of surgical research*, 138(2), pp.291–9.
- Bokhari, M. et al., 2007. Culture of HepG2 liver cells on three dimensional polystyrene scaffolds enhances cell structure and function during toxicological challenge. *Journal of anatomy*, 211(4), pp.567–76.
- Bontempo, F.A. et al., 1987. Liver transplantation in hemophilia A. *Blood*, 69(6), pp.1721–4.
- Boomsma, R.A. & Geenen, D.L., 2012. Mesenchymal stem cells secrete multiple cytokines that promote angiogenesis and have contrasting effects on chemotaxis and apoptosis. *PloS one*, 7(4), p.e35685.
- Boyer, J.L., 2013. Bile formation and secretion. *Comprehensive Physiology*, 3(3), pp.1035–78.
- Braet, F. et al., 2001. Endothelial and pit cells. *The Liver: Biology and Pathobiology*, pp.437–453.
- Braet, F. et al., 2004. Liver sinusoidal endothelial cell modulation upon resection and shear stress in vitro. *Comparative hepatology*, 3(1), p.7.
- Braet, F. & Wisse, E., 2002. Structural and functional aspects of liver sinusoidal endothelial cell fenestrae: a review. *Comparative hepatology*, 1, p.1.

REFERENCES

- Branch, M.J. et al., 2012. Mesenchymal stem cells in the human corneal limbal stroma. *Investigative ophthalmology & visual science*, 53(9), pp.5109–16.
- Brighton, C.T. et al., 1992. The pericyte as a possible osteoblast progenitor cell. *Clinical orthopaedics and related research*, (275), pp.287–99.
- Brighton, C.T. & Hunt, R.M., 1991. Early histological and ultrastructural changes in medullary fracture callus. *The Journal of bone and joint surgery. American volume*, 73(6), pp.832–47.
- Brown, J.R. et al., 1998. Fos family members induce cell cycle entry by activating cyclin D1. *Molecular and cellular biology*, 18(9), pp.5609–19.
- Burkard, A. et al., 2012. technology: characterisation and applications in induction and cytotoxicity assays. *Xenobiotica*, 42, pp.939–956.
- Burnouf, T., 2011. Recombinant plasma proteins. *Vox sanguinis*, 100(1), pp.68–83.
- Cai, J. et al., 2007. Directed differentiation of human embryonic stem cells into functional hepatic cells. *Hepatology (Baltimore, Md.)*, 45(5), pp.1229–39.
- Cao, Y. et al., 2005. Human adipose tissue-derived stem cells differentiate into endothelial cells in vitro and improve postnatal neovascularization in vivo. *Biochemical and biophysical research communications*, 332(2), pp.370–9.
- Cartmell, S.H. et al., 2003. Effects of medium perfusion rate on cell-seeded three-dimensional bone constructs in vitro. *Tissue engineering*, 9(6), pp.1197–203.
- Casademunt, E. et al., 2012. The first recombinant human coagulation factor VIII of human origin: human cell line and manufacturing characteristics. *European journal of haematology*, 89(2), pp.165–76.
- Castell, J. V et al., 2006. Hepatocyte cell lines: their use, scope and limitations in drug metabolism studies. *Expert opinion on drug metabolism & toxicology*, 2(2), pp.183–212.
- Chang, T.T. & Hughes-Fulford, M., 2009. Monolayer and spheroid culture of human liver hepatocellular carcinoma cell line cells demonstrate distinct global gene expression patterns and functional phenotypes. *Tissue engineering. Part A*, 15(3), pp.559–67.
- Charalambous, C. et al., 2005. Interleukin-8 differentially regulates migration of tumor-associated and normal human brain endothelial cells. *Cancer research*, 65(22), pp.10347–54.
- Chen, J. & López, J.A., 2005. Interactions of platelets with subendothelium and endothelium. *Microcirculation (New York, N.Y. : 1994)*, 12(3), pp.235–46.

REFERENCES

- Chen, Y.S. et al., 2012. Small molecule mesengenic induction of human induced pluripotent stem cells to generate mesenchymal stem/stromal cells. *Stem cells translational medicine*, 1(2), pp.83–95.
- Chu, V. et al., 2009. In vitro and in vivo induction of cytochrome p450: a survey of the current practices and recommendations: a pharmaceutical research and manufacturers of america perspective. *Drug metabolism and disposition: the biological fate of chemicals*, 37(7), pp.1339–54.
- Clayton, D.F. & Darnell, J.E., 1983. Changes in liver-specific compared to common gene transcription during primary culture of mouse hepatocytes. *Molecular and cellular biology*, 3, pp.1552–1561.
- Cosentino, F. & Volpe, M., 2005. Hypertension, stroke, and endothelium. *Current hypertension reports*, 7(1), pp.68–71.
- Crispe, I.N., 2003. Hepatic T cells and liver tolerance. *Nature reviews. Immunology*, 3(1), pp.51–62.
- Davis, S. et al., 1996. Isolation of angiopoietin-1, a ligand for the TIE2 receptor, by secretion-trap expression cloning. *Cell*, 87(7), pp.1161–9.
- DeLeve, L.D. et al., 2004. Rat liver sinusoidal endothelial cell phenotype is maintained by paracrine and autocrine regulation. *American journal of physiology. Gastrointestinal and liver physiology*, 287(4), pp.G757–63.
- DeQuach, J.A. et al., 2010. Simple and high yielding method for preparing tissue specific extracellular matrix coatings for cell culture. *PloS one*, 5(9), p.e13039.
- Di, L. et al., 2012. Mechanistic insights from comparing intrinsic clearance values between human liver microsomes and hepatocytes to guide drug design. *European journal of medicinal chemistry*, 57, pp.441–8.
- Van Dijk, K. et al., 2005. Factor VIII half-life and clinical phenotype of severe hemophilia A. *Haematologica*, 90(4), pp.494–8.
- Do, H. et al., 1999. Expression of factor VIII by murine liver sinusoidal endothelial cells. *The Journal of biological chemistry*, 274(28), pp.19587–92.
- Van den Dolder, J. et al., 2003. Flow perfusion culture of marrow stromal osteoblasts in titanium fiber mesh. *Journal of biomedical materials research. Part A*, 64(2), pp.235–41.
- Dunn, J.C. et al., 1989. Hepatocyte function and extracellular matrix geometry: long-term culture in a sandwich configuration. *FASEB journal : official publication of the Federation of American Societies for Experimental Biology*, 3(2), pp.174–7.

REFERENCES

- Dunn, J.C., Tompkins, R.G. & Yarmush, M.L., 1991. Long-term in vitro function of adult hepatocytes in a collagen sandwich configuration. *Biotechnology progress*, 7(3), pp.237–45.
- Elaut, G. et al., 2006. Molecular mechanisms underlying the dedifferentiation process of isolated hepatocytes and their cultures. *Current drug metabolism*, 7, pp.629–660.
- Elder, B., Lakich, D. & Gitschier, J., 1993. Sequence of the murine factor VIII cDNA. *Genomics*, 16(2), pp.374–9.
- Erwin Kuntz, H.-D.K., 2008. Hepatology: Textbook and Atlas: 3rd Edition. Available at: <http://www.amazon.com/Hepatology-Textbook-Atlas-Erwin-Kuntz/dp/3540768386> [Accessed February 2, 2015].
- European Medicines Agency, 2013. Guideline on the Investigation of Drug Interactions Guideline on the Investigation of Drug Interactions Table of contents. , 1(6).
- Fabrikant, J.I., 1967. The spatial distribution of parenchymal cell proliferation during regeneration of the liver. *The Johns Hopkins medical journal*, 120(3), pp.137–47.
- Fahmi, O.A. et al., 2008. Prediction of drug-drug interactions from in vitro induction data: application of the relative induction score approach using cryopreserved human hepatocytes. *Drug metabolism and disposition: the biological fate of chemicals*, 36, pp.1971–1974.
- Faucette, S.R. et al., 2004. Regulation of CYP2B6 in primary human hepatocytes by prototypical inducers. *Drug metabolism and disposition: the biological fate of chemicals*, 32(3), pp.348–58.
- Faucette, S.R. et al., 2007. Relative activation of human pregnane X receptor versus constitutive androstane receptor defines distinct classes of CYP2B6 and CYP3A4 inducers. *The Journal of pharmacology and experimental therapeutics*, 320(1), pp.72–80.
- Faustman, D.L. et al., 2002. Cells for repair: breakout session summary. *Annals of the New York Academy of Sciences*, 961, pp.45–7.
- Fay, P., Haidaris, P. & Smudzin, T., 1991. Human factor VIIIa subunit structure. Reconstruction of factor VIIIa from the isolated A1/A3-C1-C2 dimer and A2 subunit. *J. Biol. Chem.*, 266(14), pp.8957–8962.
- Fay, P.J., 1988. Reconstitution of human factor VIII from isolated subunits. *Archives of biochemistry and biophysics*, 262(2), pp.525–31.
- Ferrara, N., Gerber, H.-P. & LeCouter, J., 2003. The biology of VEGF and its receptors. *Nature medicine*, 9(6), pp.669–76.

REFERENCES

- Figueiredo, M.S. & Brownlee, G.G., 1995. cis-acting elements and transcription factors involved in the promoter activity of the human factor VIII gene. *The Journal of biological chemistry*, 270(20), pp.11828–38.
- Fodor, W.L., 2003. Tissue engineering and cell based therapies, from the bench to the clinic: the potential to replace, repair and regenerate. *Reproductive biology and endocrinology : RB&E*, 1, p.102.
- Foecking, M.K. & Hofstetter, H., 1986. Powerful and versatile enhancer-promoter unit for mammalian expression vectors. *Gene*, 45(1), pp.101–5.
- Folkman, J., 1971. Tumor angiogenesis: therapeutic implications. *The New England journal of medicine*, 285(21), pp.1182–6.
- Food and Drug Administration, 2012. Guidance for industry. Drug interaction studies study design, data analysis, implications for dosing, and labeling recommendations. , (February), p.79.
- Freed, L.E. & Vunjak-Novakovic, G., 1997. Microgravity tissue engineering. *In vitro cellular & developmental biology. Animal*, 33(5), pp.381–5.
- Fulcher, C.A., Roberts, J.R. & Zimmerman, T.S., 1983. Thrombin proteolysis of purified factor viii procoagulant protein: correlation of activation with generation of a specific polypeptide. *Blood*, 61(4), pp.807–11.
- Gebhardt, R., 1992. Metabolic zonation of the liver: Regulation and implications for liver function. *Pharmacology and Therapeutics*, 53, pp.275–354.
- Gerhardt, H. & Betsholtz, C., 2005. How do endothelial cells orientate? *EXS*, (94), pp.3–15.
- Germain, L. et al., 2002. Engineering human tissues for in vivo applications. *Annals of the New York Academy of Sciences*, 961, pp.268–70.
- Ghasemi-Mobarakeh, L. et al., 2009. The thickness of electrospun poly (epsilon-caprolactone) nanofibrous scaffolds influences cell proliferation. *The International journal of artificial organs*, 32(3), pp.150–8.
- Ghodsizadeh, A. et al., 2010. Generation of liver disease-specific induced pluripotent stem cells along with efficient differentiation to functional hepatocyte-like cells. *Stem cell reviews*, 6(4), pp.622–32.
- Godoy, P. et al., 2013. *Recent advances in 2D and 3D in vitro systems using primary hepatocytes, alternative hepatocyte sources and non-parenchymal liver cells and their use in investigating mechanisms of hepatotoxicity, cell signaling and ADME.*,
- Goldstein, A.S. et al., 2001. Effect of convection on osteoblastic cell growth and function in biodegradable polymer foam scaffolds. *Biomaterials*, 22(11), pp.1279–88.

REFERENCES

- Gómez-Lechón, M.J. et al., 1998. Long-term expression of differentiated functions in hepatocytes cultured in three-dimensional collagen matrix. *Journal of Cellular Physiology*, 177, pp.553–562.
- Grau, G.E. et al., 1997. Haemostatic properties of human pulmonary and cerebral microvascular endothelial cells. *Thrombosis and haemostasis*, 77(3), pp.585–90.
- Gray, D.A., 1991. Insertional mutagenesis: neoplasia arising from retroviral integration. *Cancer investigation*, 9(3), pp.295–304.
- Griffith, L.G. & Naughton, G., 2002. Tissue engineering--current challenges and expanding opportunities. *Science (New York, N.Y.)*, 295(5557), pp.1009–14.
- Groth, C.G. et al., 1974. Correction of coagulation in the hemophilic dog by transplantation of lymphatic tissue. *Surgery*, 75(5), pp.725–33.
- Gu, X. & Manautou, J.E., 2012. Molecular mechanisms underlying chemical liver injury. *Expert Reviews in Molecular Medicine*, 14.
- Guguen-Guillouzo, C. et al., 1983. Maintenance and reversibility of active albumin secretion by adult rat hepatocytes co-cultured with another liver epithelial cell type. *Experimental cell research*, 143(1), pp.47–54.
- Guguen-Guillouzo, C. & Guillouzo, A., 2010. General review on in vitro hepatocyte models and their applications. *Methods in molecular biology (Clifton, N.J.)*, 640, pp.1–40.
- Hamilton, G.A. et al., 2001. Regulation of cell morphology and cytochrome P450 expression in human hepatocytes by extracellular matrix and cell-cell interactions. *Cell and tissue research*, 306(1), pp.85–99.
- Hammond, J.S., Beckingham, I.J. & Shakesheff, K.M., 2006. Scaffolds for liver tissue engineering. *Expert review of medical devices*, 3(1), pp.21–7.
- Hannah, M.J. et al., 2002. Biogenesis of Weibel-Palade bodies. *Seminars in cell & developmental biology*, 13(4), pp.313–24.
- Hariparsad, N. et al., 2008. Comparison of immortalized Fa2N-4 cells and human hepatocytes as in vitro models for cytochrome P450 induction. *Drug metabolism and disposition: the biological fate of chemicals*, 36, pp.1046–1055.
- Hayflick, L., 1965. The limited in vitro lifetime of human diploid cell strains. *Experimental cell research*, 37, pp.614–36.
- He, S., Nakada, D. & Morrison, S.J., 2009. Mechanisms of stem cell self-renewal. *Annual review of cell and developmental biology*, 25, pp.377–406.

REFERENCES

- Hewitt, N.J., Lecluyse, E.L. & Ferguson, S.S., 2007. Induction of hepatic cytochrome P450 enzymes: methods, mechanisms, recommendations, and in vitro in vivo correlations. *Xenobiotica*, 37, pp.1196–1224.
- High, K.A., 2007. Update on progress and hurdles in novel genetic therapies for hemophilia. *Hematology / the Education Program of the American Society of Hematology. American Society of Hematology. Education Program*, pp.466–72.
- Hirschi, K.K. et al., 2002. Vascular assembly in natural and engineered tissues. *Annals of the New York Academy of Sciences*, 961, pp.223–42.
- Holy, C.E., Shoichet, M.S. & Davies, J.E., 2000. Engineering three-dimensional bone tissue in vitro using biodegradable scaffolds: investigating initial cell-seeding density and culture period. *Journal of biomedical materials research*, 51(3), pp.376–82.
- Houssaint, E., 1980. Differentiation of the mouse hepatic primordium. I. An analysis of tissue interactions in hepatocyte differentiation. *Cell differentiation*, 9(5), pp.269–79.
- Hoying, J.B., Boswell, C.A. & Williams, S.K., 1996. Angiogenic potential of microvessel fragments established in three-dimensional collagen gels. *In vitro cellular & developmental biology. Animal*, 32(7), pp.409–19.
- Hutmacher, D.W. & Singh, H., 2008. Computational fluid dynamics for improved bioreactor design and 3D culture. *Trends in biotechnology*, 26(4), pp.166–72.
- Hwa, A.J. et al., 2007. Rat liver sinusoidal endothelial cells survive without exogenous VEGF in 3D perfused co-cultures with hepatocytes. *FASEB journal : official publication of the Federation of American Societies for Experimental Biology*, 21(10), pp.2564–79.
- Iorio, A. et al., 2010. Rate of inhibitor development in previously untreated hemophilia A patients treated with plasma-derived or recombinant factor VIII concentrates: a systematic review. *Journal of thrombosis and haemostasis : JTH*, 8(6), pp.1256–65.
- Ishaug-Riley, S.L. et al., 1998. Three-dimensional culture of rat calvarial osteoblasts in porous biodegradable polymers. *Biomaterials*, 19(15), pp.1405–12.
- Jacquemin, M. et al., 2006. FVIII production by human lung microvascular endothelial cells. *Blood*, 108(2), pp.515–7.
- Jaffe, E.A. et al., 1973. Culture of human endothelial cells derived from umbilical veins. Identification by morphologic and immunologic criteria. *The Journal of clinical investigation*, 52(11), pp.2745–56.
- Jiang, Y. et al., 2002. Multipotent progenitor cells can be isolated from postnatal murine bone marrow, muscle, and brain. *Experimental hematology*, 30(8), pp.896–904.
- Jung, J. et al., 1999. Initiation of mammalian liver development from endoderm by fibroblast growth factors. *Science (New York, N.Y.)*, 284(5422), pp.1998–2003.

REFERENCES

- Jungermann, K. & Kietzmann, T., 1996. Zonation of parenchymal and nonparenchymal metabolism in liver. *Annual review of nutrition*, 16, pp.179–203.
- Kadhom, N. et al., 1988. Factor VIII procoagulant antigen in human tissues. *Thrombosis and haemostasis*, 59(2), pp.289–94.
- Kanebratt, K.P. & Andersson, T.B., 2008. HepaRG cells as an in vitro model for evaluation of cytochrome P450 induction in humans. *Drug metabolism and disposition: the biological fate of chemicals*, 36, pp.137–145.
- Karasek, M.A., 1989. Microvascular endothelial cell culture. *The Journal of investigative dermatology*, 93(2 Suppl), p.33S–38S.
- Kaufman, R.J., 1992. Biological regulation of factor VIII activity. *Annual review of medicine*, 43, pp.325–39.
- Kaufman, R.J. et al., 1989. Effect of von Willebrand factor coexpression on the synthesis and secretion of factor VIII in Chinese hamster ovary cells. *Molecular and cellular biology*, 9(3), pp.1233–42.
- Kaufman, R.J., Wasley, L.C. & Dorner, A.J., 1988. Synthesis, processing, and secretion of recombinant human factor VIII expressed in mammalian cells. *The Journal of biological chemistry*, 263(13), pp.6352–62.
- Kelley, K., Verma, I. & Pierce, G.F., 2002. Gene therapy: reality or myth for the global bleeding disorders community? *Haemophilia : the official journal of the World Federation of Hemophilia*, 8(3), pp.261–7.
- Kim, K. et al., 2010. Epigenetic memory in induced pluripotent stem cells. *Nature*, 467(7313), pp.285–90.
- Kim, S. & von Recum, H., 2008. Endothelial stem cells and precursors for tissue engineering: cell source, differentiation, selection, and application. *Tissue engineering. Part B, Reviews*, 14(1), pp.133–47.
- Klugewitz, K. et al., 2002. Immunomodulatory effects of the liver: deletion of activated CD4+ effector cells and suppression of IFN-gamma-producing cells after intravenous protein immunization. *Journal of immunology (Baltimore, Md. : 1950)*, 169(5), pp.2407–13.
- Kobuch, K. et al., 2008. Maintenance of adult porcine retina and retinal pigment epithelium in perfusion culture: characterisation of an organotypic in vitro model. *Experimental eye research*, 86(4), pp.661–8.
- Kubota, Y. et al., 1988. Role of laminin and basement membrane in the morphological differentiation of human endothelial cells into capillary-like structures. *The Journal of cell biology*, 107(4), pp.1589–98.

REFERENCES

- Kuo, T.K. et al., 2008. Stem cell therapy for liver disease: parameters governing the success of using bone marrow mesenchymal stem cells. *Gastroenterology*, 134(7), pp.2111–21, 2121.e1–3.
- Van der Kwast, T.H. et al., 1986. Localization of factor VIII-procoagulant antigen: an immunohistological survey of the human body using monoclonal antibodies. *Blood*, 67(1), pp.222–7.
- Lammert, E., Cleaver, O. & Melton, D., 2003. Role of endothelial cells in early pancreas and liver development. *Mechanisms of development*, 120(1), pp.59–64.
- Lange, C. et al., 2005. Liver-specific gene expression in mesenchymal stem cells is induced by liver cells. *World journal of gastroenterology : WJG*, 11(29), pp.4497–504.
- Larson, B., Instruments, B. & Hunt, S., 2014. *Applicatio note: The Effect of Cell Culture Method on Long-Term Primary Hepatocyte Cell Health*,
- LeCluyse, E.L., 2001. Human hepatocyte culture systems for the in vitro evaluation of cytochrome P450 expression and regulation. *European journal of pharmaceutical sciences : official journal of the European Federation for Pharmaceutical Sciences*, 13(4), pp.343–68.
- Legaz, M.E. et al., 1973. Isolation and characterization of human Factor VIII (antihemophilic factor). *The Journal of biological chemistry*, 248(11), pp.3946–55.
- Lenting, P.J., van Mourik, J.A. & Mertens, K., 1998. The life cycle of coagulation factor VIII in view of its structure and function. *Blood*, 92(11), pp.3983–96.
- Levinson, B. et al., 1990. A transcribed gene in an intron of the human factor VIII gene. *Genomics*, 7(1), pp.1–11.
- Levinson, B. et al., 1992. Evidence for a third transcript from the human factor VIII gene. *Genomics*, 14(3), pp.585–9.
- Levy, G. et al Genetic induction of metabolically functional, polarized cultures of proliferating human hepatocytes (submitted to Nature Biotechnology)
- Li, A.P. & Jurima-Romet, M., 1997. Applications of primary human hepatocytes in the evaluation of pharmacokinetic drug-drug interactions: evaluation of model drugs terfenadine and rifampin. *Cell biology and toxicology*, 13(4-5), pp.365–74.
- Li, Z. et al., 2011. Epigenetic dysregulation in mesenchymal stem cell aging and spontaneous differentiation. *PloS one*, 6(6), p.e20526.
- Liang, D. et al., 1993. Parallel decrease of Na(+)-taurocholate cotransport and its encoding mRNA in primary cultures of rat hepatocytes. *Hepatology (Baltimore, Md.)*, 18(5), pp.1162–6.

REFERENCES

- Liang, D., Hsiao, B.S. & Chu, B., 2007. Functional electrospun nanofibrous scaffolds for biomedical applications. *Advanced drug delivery reviews*, 59(14), pp.1392–412.
- Liddle, C. et al., 1998. Separate and interactive regulation of cytochrome P450 3A4 by triiodothyronine, dexamethasone, and growth hormone in cultured hepatocytes. *The Journal of clinical endocrinology and metabolism*, 83(7), pp.2411–6.
- Limmer, A. et al., 2000. Efficient presentation of exogenous antigen by liver endothelial cells to CD8+ T cells results in antigen-specific T-cell tolerance. *Nature medicine*, 6(12), pp.1348–54.
- Limmer, A. & Knolle, P.A., 2001. Liver sinusoidal endothelial cells: a new type of organ-resident antigen-presenting cell. *Archivum immunologiae et therapeuticae experimentalis*, 49 Suppl 1, pp.S7–11.
- Lin, C.Y., Kikuchi, N. & Hollister, S.J., 2004. A novel method for biomaterial scaffold internal architecture design to match bone elastic properties with desired porosity. *Journal of biomechanics*, 37(5), pp.623–36.
- Lin, Y. et al., 2002. Use of blood outgrowth endothelial cells for gene therapy for hemophilia A. *Blood*, 99(2), pp.457–62.
- Luk, J.M. et al., 2005. Hepatic potential of bone marrow stromal cells: development of in vitro co-culture and intra-portal transplantation models. *Journal of immunological methods*, 305(1), pp.39–47.
- M, M., a, F. & Y, T., 2011. Mesenchymal Stem Cells as Muscle Reservoir. *Journal of Stem Cell Research & Therapy*, 01(2), pp.1–9.
- Macchiarini, P. et al., 2004. First human transplantation of a bioengineered airway tissue. *The Journal of thoracic and cardiovascular surgery*, 128(4), pp.638–41.
- Manco-Johnson, M., 2007. Comparing prophylaxis with episodic treatment in haemophilia A: implications for clinical practice. *Haemophilia : the official journal of the World Federation of Hemophilia*, 13 Suppl 2, pp.4–9.
- Manning, F., O Fágáin, C. & O’Kennedy, R., 1993. Factor VIII: structure, function and analysis. *Biotechnology advances*, 11(1), pp.79–114.
- Mannucci, P.M., 2003. Hemophilia: treatment options in the twenty-first century. *Journal of thrombosis and haemostasis : JTH*, 1(7), pp.1349–55.
- Mao, J. et al., 2012. Predictions of Cytochrome P450-Mediated Drug-Drug Interactions Using Cryopreserved Human Hepatocytes: Comparison of Plasma and Protein-Free Media Incubation Conditions. *Drug metabolism and disposition: the biological fate of chemicals*, 40, pp.706–716.

REFERENCES

- March, S. et al., 2009. Microenvironmental regulation of the sinusoidal endothelial cell phenotype in vitro. *Hepatology (Baltimore, Md.)*, 50(3), pp.920–8.
- Marchioro, T.L. et al., 1969. Hemophilia: role of organ homografts. *Science (New York, N.Y.)*, 163(3863), pp.188–90.
- Marsell, R. & Einhorn, T.A., 2011. The biology of fracture healing. *Injury*, 42(6), pp.551–5.
- Martignoni, M., Groothuis, G.M.M. & de Kanter, R., 2006. Species differences between mouse, rat, dog, monkey and human CYP-mediated drug metabolism, inhibition and induction. *Expert opinion on drug metabolism & toxicology*, 2(6), pp.875–94.
- Martin, Y. & Vermette, P., 2005. Bioreactors for tissue mass culture: design, characterization, and recent advances. *Biomaterials*, 26(35), pp.7481–503.
- Matsumoto, K. et al., 2001. Liver organogenesis promoted by endothelial cells prior to vascular function. *Science (New York, N.Y.)*, 294(5542), pp.559–63.
- Mazariegos, G. V et al., 2001. Safety observations in phase I clinical evaluation of the Excorp Medical Bioartificial Liver Support System after the first four patients. *ASAIO journal (American Society for Artificial Internal Organs : 1992)*, 47(5), pp.471–5.
- Meezan, E. et al., 1975. A simple, versatile, nondisruptive method for the isolation of morphologically and chemically pure basement membranes from several tissues. *Life sciences*, 17(11), pp.1721–32.
- Meili, E.O., 2004. [Congenital deficiencies of coagulation factors and acquired inhibitors leading to bleeding disorders]. *Hämostaseologie*, 24(4), pp.221–33.
- Meirelles, L. da S. et al., 2009. Mechanisms involved in the therapeutic properties of mesenchymal stem cells. *Cytokine & growth factor reviews*, 20(5-6), pp.419–27.
- Mertsching, H. et al., 2005. Engineering of a vascularized scaffold for artificial tissue and organ generation. *Biomaterials*, 26(33), pp.6610–7.
- Mertsching, H. et al., 2009. Generation and transplantation of an autologous vascularized bioartificial human tissue. *Transplantation*, 88(2), pp.203–10.
- Mertsching, H. & Hansmann, J., 2009. Bioreactor technology in cardiovascular tissue engineering. *Advances in biochemical engineering/biotechnology*, 112, pp.29–37.
- Mertsching, H. & Walles, T., 2009. Europe's advanced therapy medicinal products: chances and challenges. *Expert review of medical devices*, 6(2), pp.109–10.
- Miao, H.Z. et al., 2004. Bioengineering of coagulation factor VIII for improved secretion. *Blood*, 103(9), pp.3412–9.

REFERENCES

- Michaux, G. & Cutler, D.F., 2004. How to roll an endothelial cigar: the biogenesis of Weibel-Palade bodies. *Traffic (Copenhagen, Denmark)*, 5(2), pp.69–78.
- Moeller, T. et al., 2013. Comparison of Inhibition of CYP1A2 , 2C9 and 3A4 using Human Liver Microsomes and Hepatocytes. In *ISSX Toronto*. ISSX Toronto, p. 50.
- Moghe, P. V. et al., 1997. Cell-cell interactions are essential for maintenance of hepatocyte function in collagen gel but not on matrigel. *Biotechnology and Bioengineering*, 56, pp.706–711.
- Moll, C. et al., 2013. Tissue engineering of a human 3D in vitro tumor test system. *Journal of visualized experiments : JoVE*, (78).
- Mostafavi, S.A. & Tavakoli, N., 2004. Relative bioavailability of omeprazole capsules after oral dosing. *Daru*, 12(4), pp.146–150.
- Van Mourik, J.A., Romani de Wit, T. & Voorberg, J., 2002. Biogenesis and exocytosis of Weibel-Palade bodies. *Histochemistry and cell biology*, 117(2), pp.113–22.
- Nagabhushan Kalburgi, S., Khan, N.N. & Gray, S.J., 2013. Recent gene therapy advancements for neurological diseases. *Discovery medicine*, 15(81), pp.111–9.
- Nichols, T.C. et al., 2009. Protein replacement therapy and gene transfer in canine models of hemophilia A, hemophilia B, von willebrand disease, and factor VII deficiency. *ILAR journal / National Research Council, Institute of Laboratory Animal Resources*, 50(2), pp.144–67.
- Niklason, L.E. et al., 2002. Bioreactors and bioprocessing: breakout session summary. *Annals of the New York Academy of Sciences*, 961, pp.220–2.
- Nörenberg, A. et al., 2013. Optimization of upcyte® human hepatocytes for the in vitro micronucleus assay. *Mutation Research - Genetic Toxicology and Environmental Mutagenesis*, 758, pp.69–79.
- Nörenberg, A. b, 2013. *Generation of proliferating hepatocytes , liver sinusoidal endothelial cells and stellate cells and establishment of a genotoxicity assay based on proliferating hepatocytes .*
- Oda, M., Yokomori, H. & Han, J.-Y., 2003. Regulatory mechanisms of hepatic microcirculation. *Clinical hemorheology and microcirculation*, 29, pp.167–182.
- Ogu, C.C. & Maxa, J.L., 2000. Drug interactions due to cytochrome P450. *Proceedings (Baylor University. Medical Center)*, 13(4), pp.421–3.
- Ohashi, K. et al., 2007. Engineering functional two- and three-dimensional liver systems in vivo using hepatic tissue sheets. *Nature medicine*, 13(7), pp.880–5.

REFERENCES

- Ohi, Y. et al., 2011. Incomplete DNA methylation underlies a transcriptional memory of somatic cells in human iPS cells. *Nature cell biology*, 13(5), pp.541–9.
- Olinga, P. et al., 1998. Effect of human liver source on the functionality of isolated hepatocytes and liver slices. *Drug metabolism and disposition: the biological fate of chemicals*, 26(1), pp.5–11.
- Owen, C.A., Bowie, E.J. & Fass, D.N., 1979. Generation of factor VIII coagulant activity by isolated, perfused neonatal pig livers and adult rat livers. *British journal of haematology*, 43(2), pp.307–15.
- Pampaloni, F., Stelzer, E.H.K. & Masotti, A., 2009. Three-dimensional tissue models for drug discovery and toxicology. *Recent patents on biotechnology*, 3(2), pp.103–17.
- Parekkadan, B. et al., 2007. Mesenchymal stem cell-derived molecules reverse fulminant hepatic failure. *PloS one*, 2(9), p.e941.
- Parenteau, N.L. & Hardin-Young, J., 2002. The use of cells in reparative medicine. *Annals of the New York Academy of Sciences*, 961, pp.27–39.
- Patrick, C. W., Jr., Mikos, A. G., and McIntire, L., V., 1998. *Prospectus of Tissue Engineering*. In “*Frontiers in Tissue Engineering*,” Elsevier.
- Pauwels, K. et al., 2009. State-of-the-art lentiviral vectors for research use: risk assessment and biosafety recommendations. *Current gene therapy*, 9(6), pp.459–74.
- Pepper, M.S. et al., 1991. Chondrocytes inhibit endothelial sprout formation in vitro: evidence for involvement of a transforming growth factor-beta. *Journal of cellular physiology*, 146(1), pp.170–9.
- Pfeifer, A. & Verma, I.M., 2001. Gene therapy: promises and problems. *Annual review of genomics and human genetics*, 2, pp.177–211.
- Philippart, A. et al., 2015. Toughening and functionalization of bioactive ceramic and glass bone scaffolds by biopolymer coatings and infiltration: a review of the last 5 years. *Expert review of medical devices*, 12(1), pp.93–111.
- Pipe, S.W. & Kaufman, R.J., 1997. Characterization of a genetically engineered inactivation-resistant coagulation factor VIIIa. *Proceedings of the National Academy of Sciences of the United States of America*, 94(22), pp.11851–6.
- Pittman, D.D. et al., 1993. Biochemical, immunological, and in vivo functional characterization of B-domain-deleted factor VIII. *Blood*, 81(11), pp.2925–35.
- Powell, J.S. et al., 2003. Phase 1 trial of FVIII gene transfer for severe hemophilia A using a retroviral construct administered by peripheral intravenous infusion. *Blood*, 102(6), pp.2038–45.

REFERENCES

- Przyborski, S.A., 2005. Differentiation of human embryonic stem cells after transplantation in immune-deficient mice. *Stem cells (Dayton, Ohio)*, 23(9), pp.1242–50.
- Rai, R., 2013. Liver transplantatation- an overview. *The Indian journal of surgery*, 75(3), pp.185–91.
- Ranucci, C.S. et al., 2000. Control of hepatocyte function on collagen foams: sizing matrix pores toward selective induction of 2-D and 3-D cellular morphogenesis. *Biomaterials*, 21(8), pp.783–93.
- Rashid, S.T. et al., 2010. Modeling inherited metabolic disorders of the liver using human induced pluripotent stem cells. *The Journal of clinical investigation*, 120(9), pp.3127–36.
- Reneker, D.H. & Chun, I., 1996. Nanometre diameter fibres of polymer, produced by electrospinning. *Nanotechnology*, 7(3), pp.216–223.
- Richard, L., Velasco, P. & Detmar, M., 1998. A simple immunomagnetic protocol for the selective isolation and long-term culture of human dermal microvascular endothelial cells. *Experimental cell research*, 240(1), pp.1–6.
- Richter, T. et al., 2004. Potent mechanism-based inhibition of human CYP2B6 by clopidogrel and ticlopidine. *The Journal of pharmacology and experimental therapeutics*, 308, pp.189–197.
- Ripp, S.L. et al., 2006. Use of immortalized human hepatocytes to predict the magnitude of clinical drug-drug interactions caused by CYP3A4 induction. *Drug metabolism and disposition: the biological fate of chemicals*, 34(10), pp.1742–8.
- Rippin, S.J. et al., 2001. Cholestatic expression pattern of sinusoidal and canalicular organic anion transport systems in primary cultured rat hepatocytes. *Hepatology (Baltimore, Md.)*, 33(4), pp.776–82.
- Robotin-Johnson, M.C. et al., 1998. An experimental model of small intestinal submucosa as a growing vascular graft. *The Journal of thoracic and cardiovascular surgery*, 116(5), pp.805–11.
- Rosenberg, J.B., Greengard, J.S. & Montgomery, R.R., 2000. Genetic induction of a releasable pool of factor VIII in human endothelial cells. *Arteriosclerosis, thrombosis, and vascular biology*, 20(12), pp.2689–95.
- Roth, D.A. et al., 2001. Nonviral transfer of the gene encoding coagulation factor VIII in patients with severe hemophilia A. *The New England journal of medicine*, 344(23), pp.1735–42.
- Ruiz, S. et al., 2012. Identification of a specific reprogramming-associated epigenetic signature in human induced pluripotent stem cells. *Proceedings of the National Academy of Sciences of the United States of America*, 109(40), pp.16196–201.

REFERENCES

- Saenko, E.L. et al., 1994. A role for the C2 domain of factor VIII in binding to von Willebrand factor. *The Journal of biological chemistry*, 269(15), pp.11601–5.
- Sahi, J. et al., 2003. Comparative effects of thiazolidinediones on in vitro P450 enzyme induction and inhibition. *Drug metabolism and disposition: the biological fate of chemicals*, 31(4), pp.439–46.
- Schanz, J. et al., 2009. Experimental tracheal patching using extracellular matrix scaffolds. *The Annals of thoracic surgery*, 87(4), pp.1321–2; author reply 1322–3.
- Schanz, J. et al., 2010. Vascularised human tissue models: a new approach for the refinement of biomedical research. *Journal of biotechnology*, 148(1), pp.56–63.
- Scheller, K. et al., 2012. Microvascular Endothelial Cells Repopulate Decellularized Scaffold. *Tissue Engineering Part C: Methods*, p.120913061739004.
- Scherr, M. et al., 2001. Quantitative determination of lentiviral vector particle numbers by real-time PCR. *BioTechniques*, 31(3), pp.520, 522, 524, passim.
- Schultheiss, D. et al., 2005. Biological vascularized matrix for bladder tissue engineering: matrix preparation, reseeding technique and short-term implantation in a porcine model. *The Journal of urology*, 173(1), pp.276–80.
- Scott, P.A. & Bicknell, R., 1993. The isolation and culture of microvascular endothelium. *Journal of cell science*, 105 (Pt 2, pp.269–73.
- Sefton, M. V, 2002. Functional considerations in tissue-engineering whole organs. *Annals of the New York Academy of Sciences*, 961, pp.198–200.
- Shaw, E. et al., 1979. Synthesis of procoagulant factor VIII, factor VIII related antigen and other coagulation factors by the isolated perfused rat liver. *British journal of haematology*, 41(4), pp.585–96.
- Shi, Q. et al., 2006. Factor VIII ectopically targeted to platelets is therapeutic in hemophilia A with high-titer inhibitory antibodies. *The Journal of clinical investigation*, 116(7), pp.1974–82.
- Shi, X.-L. et al., 2011. Protective effects of ACLF sera on metabolic functions and proliferation of hepatocytes co-cultured with bone marrow MSCs in vitro. *World journal of gastroenterology : WJG*, 17(19), pp.2397–406.
- Shimizu, K. et al., 2005. Gene regulation of a novel angiogenesis inhibitor, vasohibin, in endothelial cells. *Biochemical and biophysical research communications*, 327(3), pp.700–6.
- Shino, Y. et al., 1995. Clinicopathologic evaluation of immunohistochemical E-cadherin expression in human gastric carcinomas. *Cancer*, 76(11), pp.2193–201.
- Shirakawa, T., 2009. Clinical trial design for adenoviral gene therapy products. *Drug news & perspectives*, 22(3), pp.140–5.

REFERENCES

- Shu, S.-N. et al., 2004. Hepatic differentiation capability of rat bone marrow-derived mesenchymal stem cells and hematopoietic stem cells. *World journal of gastroenterology : WJG*, 10(19), pp.2818–22.
- Si-Tayeb, K., Duclos-Vallée, J.-C. & Petit, M.-A., 2012. Hepatocyte-like cells differentiated from human induced pluripotent stem cells (iHLCs) are permissive to hepatitis C virus (HCV) infection: HCV study gets personal. *Journal of hepatology*, 57(3), pp.689–91.
- Sikavitsas, V.I., Bancroft, G.N. & Mikos, A.G., 2002. Formation of three-dimensional cell/polymer constructs for bone tissue engineering in a spinner flask and a rotating wall vessel bioreactor. *Journal of biomedical materials research*, 62(1), pp.136–48.
- Singh, S., Wu, B.M. & Dunn, J.C.Y., 2011. The enhancement of VEGF-mediated angiogenesis by polycaprolactone scaffolds with surface cross-linked heparin. *Biomaterials*, 32(8), pp.2059–69.
- Sinz, M., Wallace, G. & Sahi, J., 2008. Current industrial practices in assessing CYP450 enzyme induction: preclinical and clinical. *The AAPS journal*, 10(2), pp.391–400.
- Sivertsson, L. et al., 2010. CYP3A4 catalytic activity is induced in confluent Huh7 hepatoma cells. *Drug metabolism and disposition: the biological fate of chemicals*, 38(6), pp.995–1002.
- Smedsrød, B. et al., 1994. Cell biology of liver endothelial and Kupffer cells. *Gut*, 35(11), pp.1509–16.
- Smedsrød, B. et al., 1990. Scavenger functions of the liver endothelial cell. *The Biochemical journal*, 266(2), pp.313–27.
- Smith, T.O. et al., 2011. Diagnostic accuracy of ultrasound for rotator cuff tears in adults: a systematic review and meta-analysis. *Clinical radiology*, 66(11), pp.1036–48.
- Sosa-Pineda, B., Wigle, J.T. & Oliver, G., 2000. Hepatocyte migration during liver development requires Prox1. *Nature genetics*, 25(3), pp.254–5.
- Stangegaard, M. et al., 2006. Whole genome expression profiling using DNA microarray for determining biocompatibility of polymeric surfaces. *Molecular bioSystems*, 2(9), pp.421–8.
- Stel, H. V, van der Kwast, T.H. & Veerman, E.C., 1983. Detection of factor VIII/coagulant antigen in human liver tissue. *Nature*, 303(5917), pp.530–2.
- Stolzing, A. et al., 2008. Age-related changes in human bone marrow-derived mesenchymal stem cells: consequences for cell therapies. *Mechanisms of ageing and development*, 129(3), pp.163–73.
- Sudo, R. et al., 2005. Reconstruction of 3D stacked-up structures by rat small hepatocytes on microporous membranes. *FASEB journal : official publication of the Federation of American Societies for Experimental Biology*, 19(12), pp.1695–7.

REFERENCES

- Sutherland, R.M. et al., 1986. Oxygenation and differentiation in multicellular spheroids of human colon carcinoma. *Cancer research*, 46(10), pp.5320–9.
- Szekanecz, Z. & Koch, A.E., 2005. Endothelial cells in inflammation and angiogenesis. *Current drug targets. Inflammation and allergy*, 4(3), pp.319–23.
- Takebe, T. et al., 2013. Vascularized and functional human liver from an iPSC-derived organ bud transplant. *Nature*, 499(7459), pp.481–4.
- Takeichi, M., 1990. Cadherins: a molecular family important in selective cell-cell adhesion. *Annual review of biochemistry*, 59, pp.237–52.
- Tamai, M., Adachi, E. & Tagawa, Y., 2013. Characterization of a liver organoid tissue composed of hepatocytes and fibroblasts in dense collagen fibrils. *Tissue engineering. Part A*, 19(21-22), pp.2527–35.
- Taylor, D.A., 2002. Is in vivo remodeling necessary or sufficient for cellular repair of the heart? *Annals of the New York Academy of Sciences*, 961, pp.315–8.
- Tengborn, L., 2012. Fibrinolytic Inhibitors in the Management of Bleeding Disorders. *World Federation of Haemophilia*, (42), pp.1–10.
- Thomas D. Boyer, Theresa L. Wright, M.P.M., 2011. *Zakim and Boyer's Hepatology: A Textbook of Liver Disease - Expert Consult: Online and Print, 6e (Hepatology (Zakim))*: Arun J. Sanyal MD: 9781437708813: Amazon.com: Books,
- Thude, S. et al., 2008. Testsysteme für die Entwicklung von Tumordiagnoseverfahren. *Endoskopie heute*, 21(03), pp.191–194.
- Tonn, T. et al., 2002. Generation and characterization of human hematopoietic cell lines expressing factor VIII. *Journal of hematology & stem cell research*, 11(4), pp.695–704.
- Toole, J.J. et al., 1986. A large region (approximately equal to 95 kDa) of human factor VIII is dispensable for in vitro procoagulant activity. *Proceedings of the National Academy of Sciences of the United States of America*, 83(16), pp.5939–42.
- Toole, J.J. et al., 1984. Molecular cloning of a cDNA encoding human antihemophilic factor. *Nature*, 312(5992), pp.342–7.
- Treyer, A. & Müsch, A., 2013. Hepatocyte polarity. *Comprehensive Physiology*, 3(1), pp.243–87.
- Truett, M.A. et al., 1985. Characterization of the polypeptide composition of human factor VIII:C and the nucleotide sequence and expression of the human kidney cDNA. *DNA (Mary Ann Liebert, Inc.)*, 4(5), pp.333–49.
- Turner, R.R. et al., 1987. Endothelial cell phenotypic diversity. In situ demonstration of immunologic and enzymatic heterogeneity that correlates with specific morphologic subtypes. *American journal of clinical pathology*, 87(5), pp.569–75.

REFERENCES

- Turpeinen, M. et al., 2004. Selective inhibition of CYP2B6-catalyzed bupropion hydroxylation in human liver microsomes in vitro. *Drug metabolism and disposition: the biological fate of chemicals*, 32, pp.626–631.
- Turpeinen, M., Raunio, H. & Pelkonen, O., 2006. The functional role of CYP2B6 in human drug metabolism: substrates and inhibitors in vitro, in vivo and in silico. *Current drug metabolism*, 7(7), pp.705–14.
- Tusell, J. & Pérez-Bianco, R., 2002. Prophylaxis in developed and in emerging countries. *Haemophilia : the official journal of the World Federation of Hemophilia*, 8(3), pp.183–8.
- Unger, R.E. et al., 2002. In vitro expression of the endothelial phenotype: comparative study of primary isolated cells and cell lines, including the novel cell line HPMEC-ST1.6R. *Microvascular research*, 64(3), pp.384–97.
- Vehar, G.A. et al., 1984. Structure of human factor VIII. *Nature*, 312(5992), pp.337–42.
- Veltkamp, J.J. et al., 1974. Extrahepatic factor VIII synthesis. Lung transplants in hemophilic dogs. *Transplantation*, 18(1), pp.56–62.
- Volarevic, V. et al., 2014. Concise review: Therapeutic potential of mesenchymal stem cells for the treatment of acute liver failure and cirrhosis. *Stem cells (Dayton, Ohio)*, 32(11), pp.2818–23.
- Wang, J. et al., 2011. The effect of scaffold architecture on odontogenic differentiation of human dental pulp stem cells. *Biomaterials*, 32(31), pp.7822–30.
- Wang, L. et al., 2013. Identification of a clonally expanding haematopoietic compartment in bone marrow. *The EMBO journal*, 32(2), pp.219–30.
- Westerink, W.M. & Schoonen, W.G., 2007. Cytochrome P450 enzyme levels in HepG2 cells and cryopreserved primary human hepatocytes and their induction in HepG2 cells. *Toxicol In Vitro*, 21, pp.1581–1591.
- Wiel, E. et al., 2006. Activated protein C increases sensitivity to vasoconstriction in rabbit Escherichia coli endotoxin-induced shock. *Critical care (London, England)*, 10(2), p.R47.
- Wilcox, D.A. et al., 2003. Induction of megakaryocytes to synthesize and store a releasable pool of human factor VIII. *Journal of thrombosis and haemostasis : JTH*, 1(12), pp.2477–89.
- Wilkening, S., Stahl, F. & Bader, A., 2003. Comparison of primary human hepatocytes and hepatoma cell line Hepg2 with regard to their biotransformation properties. *Drug metabolism and disposition: the biological fate of chemicals*, 31(8), pp.1035–42.
- Williams, R., Schuldt, B. & Müller, F.-J., 2011. A guide to stem cell identification: progress and challenges in system-wide predictive testing with complex biomarkers. *BioEssays : news and reviews in molecular, cellular and developmental biology*, 33(11), pp.880–90.

REFERENCES

- Wion, K.L. et al., 1985. Distribution of factor VIII mRNA and antigen in human liver and other tissues. *Nature*, 317(6039), pp.726–729.
- Wion, K.L. et al., 1985. Distribution of factor VIII mRNA and antigen in human liver and other tissues. *Nature*, 317(6039), pp.726–9.
- Wise, R.J. et al., 1991. The role of von Willebrand factor multimers and propeptide cleavage in binding and stabilization of factor VIII. *The Journal of biological chemistry*, 266(32), pp.21948–55.
- Xagorari, A. et al., 2013. Protective effect of mesenchymal stem cell-conditioned medium on hepatic cell apoptosis after acute liver injury. *International journal of clinical and experimental pathology*, 6(5), pp.831–40.
- Yamane, A. et al., 1994. A new communication system between hepatocytes and sinusoidal endothelial cells in liver through vascular endothelial growth factor and Flt tyrosine kinase receptor family (Flt-1 and KDR/Flk-1). *Oncogene*, 9(9), pp.2683–90.
- Yarovoi, H. V et al., 2003. Factor VIII ectopically expressed in platelets: efficacy in hemophilia A treatment. *Blood*, 102(12), pp.4006–13.
- Yin, C. et al., 2003. High density of immobilized galactose ligand enhances hepatocyte attachment and function. *Journal of biomedical materials research. Part A*, 67(4), pp.1093–104.
- Youdim, K.A. et al., 2007. Induction of cytochrome P450: assessment in an immortalized human hepatocyte cell line (Fa2N4) using a novel higher throughput cocktail assay. *Drug metabolism and disposition: the biological fate of chemicals*, 35(2), pp.275–82.
- Youjin, S. & Jun, Y., 2009. The treatment of hemophilia A: from protein replacement to AAV-mediated gene therapy. *Biotechnology letters*, 31(3), pp.321–8.
- Zajicek, G., Oren, R. & Weinreb, M., 1985. The streaming liver. *Liver*, 5(6), pp.293–300.
- Zatloukal, K. et al., 1994. In vivo production of human factor VII in mice after intrasplenic implantation of primary fibroblasts transfected by receptor-mediated, adenovirus-augmented gene delivery. *Proceedings of the National Academy of Sciences of the United States of America*, 91(11), pp.5148–52.
- Zhao, R. & Duncan, S.A., 2005. Embryonic development of the liver. *Hepatology (Baltimore, Md.)*, 41(5), pp.956–67.
- Zhou, S.-F. et al., 2007. Clinically important drug interactions potentially involving mechanism-based inhibition of cytochrome P450 3A4 and the role of therapeutic drug monitoring. *Therapeutic drug monitoring*, 29, pp.687–710.
- Zylber-Katz, E., 1995. Multiple drug interactions with cyclosporine in a heart transplant patient. *The Annals of pharmacotherapy*, 29(2), pp.127–31.

6.3 Figures

Figure 1	Basic structure of hexagonal liver lobe	1
Figure 2	Differentiating ability of MSCs	5
Figure 3	Upcytes controlled cell multiplication technology	8
Figure 4	Schematic diagram of the set up of electrospinning apparatus	12
Figure 5	Schematic representation of phase I und phase II metabolism.	15
Figure 6	Spontaneous bleeding occurs in joints and soft tissues of sever haemophilia-A	18
Figure 7	Organization of FVIII domain	19
Figure 8	Schematic representation of coagulation cascade involving FVIII molecule	21
Figure 9	BioVaSc harvested and decellularized using sodium deoxycholate	41
Figure 10	BioVaSc colonized with upcyte [®] mvECs and cultured in the bioreactor for 14 days	42
Figure 11	Liver organoids generated and transferred to BioVaSc	43
Figure 12	Schematic overview of lentiviral transduction into human endothelial cells	53
Figure 13	Pictorial representation of lentiviral transduction, followed by antibiotic selection	54
Figure 14	Visualization of the clusters of upcyte [®] hepatocytes (Donor -653-03; PD= 36) in 12-well rhodamine-labelled non-functionalized PLLA scaffolds	57
Figure 15	Effect of scaffold thickness on the viability of upcyte [®] hepatocytes (Donor 653-03)	58
Figure 16	Effect of fibre thickness on the viability and growth of upcyte [®] hepatocytes (Donor 653-03)	59
Figure 17	Effect of scaffold thickness on the basal and induced CYP3A4 activities of upcyte [®] hepatocytes (Donor 653-03)	60
Figure 18	Effect of fibre thickness on the basal and induced CYP3A4 activities and growth of upcyte [®] hepatocytes (Donor 653-03)	61
Figure 19	Analyzing the donor-to-donor variation on the cell viability in PLLA 50 µm thick scaffold with 4/6 µm fibre Ø.	62
Figure 20	Morphology of upcyte [®] hepatocytes, upcyte [®] LSECs and primary MSCs	64
Figure 21	Formation of liver organoid-like structures from upcyte [®] hepatocytes, upcyte [®] LSECs and primary MSCs	64
Figure 22	Morphology of upcyte [®] MSCs	65
Figure 23	Formation of liver organoid-like structures from upcyte [®] cells	65
Figure 24	HE stainings of liver organoids maintained in static culture for 72 h.	66
Figure 25	Scalability of organoids in 48-well and 96-well formats	66
Figure 26	Formation of liver organoids in <i>Quasi-vivo</i> [®] chambers (QV500)	67
Figure 27	HE stainings of liver organoids maintained in <i>Quasi-vivo</i> [®] system for 10 days.	68

Figure 28	Immunocytochemistry in 2D monolayers of upcyte [®] cells	68
Figure 29	Immunocytochemistry of liver organoid cultured for 10 days in dynamic cultures	69
Figure 30	<i>in situ</i> hybridizations of liver organoid cultured for 10 days in dynamic cultures	70/71
Figure 31	Comparison of liver organoid architecture to normal liver slice	71/72
Figure 32	Basal and induced CYP 3A4 activities in liver organoid cultured for 10 days in a bioreactor	72
Figure 33	Liver organoids cultured inside the lumen of the BioVaSc for 30 days.	74
Figure 34	Basal CYP3A4 activities of liver organoids cultured in the lumen of BioVaSc for 30 days	74
Figure 35	Immunocytochemistry of liver organoid cultured for 30 days in the lumen of BioVaSc.	75
Figure 36	Immunostaining to trace upcyte [®] mvECs (CD31) to detect organoid vascularization	76
Figure 37	Effect of DMSO on CYP3A4 and CYP2B6 activities in upcyte [®] hepatocytes	77
Figure 38	Effect of pre-culture time and DMSO treatment on CYP2B6 and CYP3A4 activities	78
Figure 39	Inhibition of CYP1A2 , CYP2B6 ,CYP2C9, CYP3A4 by respective inhibitors in upcyte [®] hepatocytes (Donor 422A-03)	81
Figure 40	Induction of CYP1A2, CYP2B6, CYP2C9 and CYP3A4 in upcyte [®] hepatocytes	83
Figure 41	Comparison of calibration curves for RIS, AUC _u /F ₂ and C _{max,u} /Ind ₅₀ using upcyte [®] hepatocytes from Donor 653	84
Figure 42	Comparison of calibration curves for RIS from three donors of upcyte [®] hepatocytes	84/85
Figure 43	Comparison of % maximum fold induction by rifampicin, phenobarbital, phenytoin and carbamazepine in upcyte [®] hepatocytes	88
Figure 44	Comparison of FVIII secretion by LSECs and the effect of freezing and storing the media before analysis	89
Figure 45	Amplified FVIII gene fragment flanked with <i>attB</i> and restriction digestion of entry clone	90
Figure 46	Restriction digestion of expression clone	90
Figure 47	Morphology of upcyte [®] BOECs, upcyte [®] LSECs and upcyte [®] mvECs	91
Figure 48	FVIII production in upcyte [®] mvECs transduced with different MOIs	92
Figure 49	Morphology of primary mvECs transduced with different MOIs	93
Figure 50	Tube formation after 6h by primary mvECs transduced with FVIII lentiviral particles	93
Figure 51	FVIII production in primary mvECs transduced with different MOIs	94

6.4 Tables

Table 1	Summarizes <i>in vitro</i> hepatic models, its advantages and disadvantages.	6
Table 2	Centrifugation parameters used for different cell types.	34
Table 3	Cell-specific stop solutions	35
Table 4	Cell-specific seeding density.	35
Table 5	Freezing densities and media for different cell types.	36
Table 6	Number of cells required to form organoids according to the cell type in a 24-well format.	38
Table 7	Cell numbers required for different formats and different cell types.	39
Table 8	CYPs, substrates, metabolites and corresponding detection wavelengths.	47
Table 9	Cocktail used for the Gateway [®] BP recombination reaction.	47
Table 10	PCR programme used for the Gateway [®] BP recombination reaction.	48
Table 11	Cocktail for the BP reaction.	48
Table 12	Ingredients for double restriction hydrolysis.	49
Table 13	Cocktail for the LR reaction.	49
Table 14	Restriction hydrolysis solution composition.	50
Table 15	Reaction mixture for qPCR.	52
Table 16	qPCR program to titrate the viral particles	52
Table 17	Analyzing the donor-to-donor variation on the basal and induced CYP3A4 activities in PLLA 50 µm thick scaffold with 4/6 µm fibre Ø.	63
Table 18	Basal CYP activities in upcyte [®] hepatocytes and paired primary human hepatocytes were cultured	79
Table 19	IC ₅₀ values of CYP inhibitors incubated with upcyte [®] hepatocytes from different donors	82
Table 20	CYP3A4 induction responses of upcyte [®] hepatocytes from different donors to known inducers and non-inducers.	86
Table 21	CYP2B64 induction responses of upcyte [®] hepatocytes from different donors to known inducers and non-inducers.	87

6.5 Publications

Submitted to Plos-one

1. *In vitro* generation of functional liver organoid-like structures using adult human cells

Sarada Devi Ramachandran¹, Katharina Schirmer², Bernhard Müntst¹, Stefan Heinz¹, Shahrouz Ghafoory³, Stefan Wölfl³, Katja Simon-Keller⁴, Alexander Marx⁴, Cristina Ionica Øie⁵, Matthias P. Ebert², Heike Walles⁶, Joris Braspenning^{1,§}, and Katja Breilkopf-Heinlein^{2,§,*}

¹Medicyte GmbH, Im Neuenheimer Feld 581, 69120 Heidelberg, Germany, ²Department of Medicine II, Faculty of Medicine at Mannheim, Heidelberg University, Mannheim, Germany.

³Institute of Pharmacy and Molecular Biotechnology, Heidelberg University, Heidelberg, Germany. ⁴Institute of Pathology, University Medical Centre Mannheim, Heidelberg University, Mannheim, Germany.

⁵Vascular Biology Research Group, Department of Medical Biology, Faculty of Health Sciences, University of Tromsø, Sykehusgt. 44, N-9037, Tromsø, Norway.

⁶Tissue Engineering and Regenerative Medicine, University Wuerzburg, Roentgenring 11, D-97070 Wuerzburg, Germany.

Manuscripts ready for submission

2. Applicability of second generation upcyte[®] human hepatocytes for use in CYP inhibition and induction studies

Sarada Devi Ramachandran¹, Aurélie Vivarès², Sylvie Klieber², Nicola J. Hewitt³, Bernhard Muenst¹, Stefan Heinz¹, Heike Walles⁴ and Joris Braspenning¹,

¹Medicyte GmbH, Im Neuenheimer Feld 581, D-69120 Heidelberg, Germany; ²Sanofi - DSAR Drug Disposition – In Vitro models, 371, rue du Pr. Blayac 34000 Montpellier, France, ³SWS, Wingertstrasse, D- 64390 Erzhausen, Germany, ⁴Tissue Engineering and Regenerative Medicine, University Wuerzburg, Roentgenring 11, D-97070 Wuerzburg, Germany

3. Three dimensional architecture and CYP induction responses of upcyte[®] human hepatocytes cultured in Alvetex[®] and Mimetix[®] scaffolds

Sarada Devi Ramachandran¹, Vera Sonntag-Buck¹, Anne Zutavern¹, Bernard Münst¹, Stefan Heinz¹, Daniel Maltman², Adam Hayward³, Elena Heister⁵, Ann Kramer⁵, Stefan Przyborski^{2,3}, Heike Walles⁶, Nicola J. Hewitt⁴, Joris Braspenning¹

¹Medicyte GmbH, Im Neuenheimer Feld 581, D-69120 Heidelberg, Germany; ²Reinnervate Limited, NETPark Incubator, Sedgefield TS21 3FD, UK; ³School of Biological and Biomedical Science, Durham University, South Road, Durham DH1 3LE, UK; ⁴SWS, Wingertstrasse 25, Erzhausen, Germany; ⁵The Electrospinning Company Ltd., R70 Rutherford, Appleton Laboratory Harwell, Oxford, Didcot, OX11 0QX, UK; ⁶Tissue Engineering and Regenerative Medicine, University Wuerzburg, Roentgenring 11, D-97070 Wuerzburg, Germany

6.6 Curriculum Vitae

Name: Sarada Devi Ramachandran
Date of Birth: 16th March 1986 in Salem, Tamilnadu, India
Citizen: Indian
Beruf: M.Sc. Pharmaceutical Biotechnology

Education and Professional Experience

07/2012– Present **PhD student**, under Prof. Dr. Heike Walles,
Department of Tissue Engineering and Regenerative
Medicine, Würzburg and
Implementation at the company Medicyte GmbH,
Heidelberg.

02/2011– 03/2012 **Biotechnologist**, Supervisor: Dr. Stephen Fullerton,
In vitro protein binding assays using micro scale
thermophoresis (MST) and thermofluor.

11/2008-01/2011 **Research Assistant**, Supervisor: Prof. Dr. Birgit Dräger
Martin-Luther-Universität Halle-Wittenberg, Germany.

10/2008– 01/2011 **M.Sc. Pharmaceutical Biotechnology**,
Thesis: Alkaloid production in plant system
Martin-Luther-Universität Halle-Wittenberg, Germany.

05/2007-08/2007 **On-Site Trainee**,
Jain Institute of Vocational and Advanced Studies,
Bangalore, India.
Work description: Performed polymorphism analysis in
Gaillardia sp., by DNA finger printing

05/2006- 06/2006 **Summer Intern Trainee**, E.I.D Parry, Chennai, India.
Work description: Worked in Bio-pesticide division to
learn HPLC and GC.

07/2004-04/2008 **Bachelor in Biotechnology**,
Thesis: Isolation and characterization of gene(s)
governing the fiber quality in *Gossypium* species.
Tamil Nadu Agricultural University, Coimbatore, India.

6.7 Affidavit

I hereby confirm that my thesis entitled “**Development Of Three-Dimensional Liver Models For Drug Development And Therapeutical Applications**” is the result of my own work. I did not receive any help or support from commercial consultants. All sources and / or materials applied are listed and specified in the thesis.

Furthermore, I confirm that this thesis has not yet been submitted as part of another examination process neither in identical nor in similar form.

Heidelberg, 16.02.2015

Place, Date

Sarada Devi Ramachandran

Signature

6.8 Acknowledgement

I acknowledge my deep sense of gratitude to my supervisor and guide Prof. Dr. Heike Walles for providing me the guidance with all the valuable advices and constant encouragement during my entire PhD.

I would like to offer my sincere thanks to Dr. Joris Braspenning for offering me the possibilities to perform my thesis at Medicyte. Also, thank you very much for providing me an independent working atmosphere with guidance and also for exploring the real-science world in many congresses and consortiums.

My wholehearted thanks to Dr. Bernhard Müntst (Berni), for all the valuable suggestions throughout my lab work and thesis. I cannot just stop here without mentioning your multifarious helps or advices and friendly nature throughout my PhD.

I express my heartfelt thanks to Dr. Nicola Hewitt (Nicky). All those help that you did are incredible and ofcourse, without you my thesis wouldn't get its perfect shape. Thank you so much for spending your valuable time for my thesis, all the publications and ofcourse our superbusy DDI experiments.

I would like to take this opportunity to thank Dr. Stefan Heinz for helping me in various aspects of my research work esp. the Hemophilia part. Big thanks also to the research group of Prof. Dr. Heike Walles at the Department of Tissue Engineering and Regenerative Medicine in Würzburg, esp. Holger Kirsch who helped me to conduct all the BioVaSc experiments.

I am pleased to place my sincere thanks to all the technical staffs, Vera, Renate, Melanie for the helpful technical assistance during various experiments and all our awesome coffee/lunch breaks together. Also I would like to take this opportunity to thank GSLS members and all the Re-liver consortium partners for their support. Many thanks to PD Dr. Katja Breitkopf-Heinlein for all the histological data and a big thanks to everyone at Medicyte, esp. Dr. Astrid Nörenberg (Astrid) for all the fun time together.

Words cannot express much of my profound gratitude to all my great friends and my loving dad, Ramachandran and my sweet mom, Renuga Ramachandran who always helped me to chase my dreams and sole responsible for being what I am. Also, a special thanks to my brother, Raja Ramachandran who is always my moral support throughout my life.

Finally, to my caring, loving, and supportive husband, Vijayakumar: my deepest gratitude. Your encouragement when the times got rough are much appreciated and duly noted. It was a great comfort and relief to know that you were willing to help me in many aspects while I completed my work. My heartfelt thanks.

- The work leading to these results has received funding from the European Union Seventh Framework Program (FP7/2007–2013) under the grant agreement no. 304961.